Mathematics of Signal Processing:
A First Course

Charles L. Byrne
Department of Mathematical Sciences
University of Massachusetts Lowell
Lowell, MA 01854

March 31, 2013

(Text for 92.548   Mathematics of Signal Processing)
(The most recent version is available as a pdf file at
http://faculty.uml.edu/cbyrne/cbyrne.html)

Contents

V   Nonlinear Models   173

VII   Estimation and Detection   259

24 The BLUE and The Kalman Filter   261

25 Signal Detection and Estimation   271

VIII   Appendices   279

26 Appendix: Inner Products   281

Part I

Introduction

Chapter 1

Preface

1.1   Chapter Summary

In a course in signal processing it is easy to get lost in the details and lose sight of the big picture. The main goals of this first course are to present the most important ideas, techniques and methods, to describe how they relate to one another, and to illustrate their uses in several applications. For signal processing, the most important mathematical tools are Fourier series and related notions, matrices, and probability and statistics. Most students with a solid mathematical background have probably encountered each of these topics in previous courses, and therefore already know some signal processing, without realizing it.

Our discussion here will involve primarily functions of a single real variable, although most of the concepts will have multi-dimensional versions. It is not our objective to treat each topic with the utmost mathematical rigor, and we shall seek to avoid issues that are primarily of mathematical concern.

1.2   Course Aims and Topics

The term *signal processing* has broad meaning and covers a wide variety of applications. In this course we focus on those applications of signal processing that can loosely be called *remote sensing*, although the mathematics we shall study is fundamental to all areas of signal processing.

There are a wide variety of problems in which what we want to know about is not directly available to us and we need to obtain information by more indirect methods.

1.2.1   Some Examples of Remote Sensing

Here are several examples of remote sensing.

Full-Body Scanners

Recently there has been much discussion about the use of full-body scanners in airports. What we really want to know about the passenger can only be completely determined by methods that are completely impractical, particularly if we want to discover explosive material that may be carried within the body. Instead, we use these low-energy back-scatter scanners that penetrate only clothing.

CAT Scans and MRI

Someone who has been hit in the head may have a concussion or a fractured skull. To know with perfect confidence is impossible. Instead, we perform an x-ray CAT scan or take a magnetic-resonance image (MRI).

Cosmic Ray Tomography

Because of their ability to penetrate granite, cosmic rays are being used to obtain transmission-tomographic three-dimensional images of the interiors of active volcanos. Where magma has replaced granite there is less attenuation of the rays, so the image can reveal the size and shape of the magma column. It is hoped that this will help to predict the size and occurrence of eruptions.

Spectral Analysis

Scientists want to know what elements are in the outer layers of the sun and other stars. We cannot travel there to find out, but we can perform *spectral analysis* on the electro-magnetic radiation coming from the sun and look for spectral lines that indicate the presence of particular elements.

Seismic Exploration

Oil companies want to know if it is worth their while drilling in a particular place. If they go ahead and drill, they will find out, but they would like to know what is the chance of finding oil without actually drilling. Instead, they set off explosions and analyze the signals produced by the seismic waves, which will tell them something about the materials the waves encountered.

Astronomy

Astronomers know that there are radio waves, visible-light waves, and other forms of electro-magnetic radiation coming from distant regions of space, and they would like to know precisely what is coming from which regions. They cannot go there to find out, so they set up large telescopes and antenna arrays and process the signals that they are able to measure.

Radar

Those who predict the weather use radar to help them see what is going on in the atmosphere. Radio waves are sent out and the returns are analyzed and turned into images. The location of airplanes is also determined by radar. The radar returns from different materials are different from one another and can be analyzed to determine what materials are present. Synthetic-aperture radar is used to obtain high-resolution images of regions of the earth's surface. The radar returns from different geometric shapes also differ in strength; by avoiding right angles in airplane design *stealth* technology attempts to make the plane invisible to radar.

Sonar

Features on the bottom of the ocean are imaged with sonar, in which sound waves are sent down to the bottom and the returning waves are analyzed. Sometimes near or distant objects of interest in the ocean emit their own sound, which is measured by sensors. The signals received by the sensors are processed to determine the nature and location of the objects. Even changes in the temperature at different places in the ocean can be determined by sending sound waves through the region of interest and measuring the travel times.

Gravity Maps

The pull of gravity varies with the density of the material. Features on the surface of the earth, such as craters from ancient asteroid impacts, can be imaged by mapping the variations in the pull of gravity, as measured by satellites.

Echo Cancelation

In a conference call between locations A and B, what is transmitted from A to B can get picked up by microphones in B, transmitted back to speakers in A and then retransmitted to B, producing an echo of the original transmission. Signal processing performed at the transmitter in A can reduce the strength of the second version of the transmission and decrease the echo effect.

Hearing Aids

Makers of digital hearing aids include signal processing to enhance the quality of the received sounds, as well as to improve localization, that is, the ability of the hearer to tell where the sound is coming from. When a hearing aid is used, sounds reach the ear in two ways: first, the usual route directly into the ear, and second, through the hearing aid. Because that part that passes through the hearing aid is processed, there is a slight delay. In order for the delay to go unnoticed, the processing must be very fast. When hearing aids are used in both ears, more sophisticated processing can be used.

1.2.2   A Role for Mathematics

The examples just presented look quite different from one another, but the differences are often more superficial than real. As we begin to use mathematics to model these various situations we often discover a common core of mathematical tools and ideas at the heart of each of these applications.

1.2.3   Limited Data

As we shall see, it is often the case that the data we measure is not sufficient to provide a single unique answer to our problem. There may be many, often quite different, answers that are consistent with what we have measured. In the absence of prior information about what the answer should look like, we do not know how to select one solution from the many possibilities. For that reason, I believe that to get information out we must put information in. How to do this is one of the main topics of the course. The example at the end of this chapter will illustrate this point.

1.2.4   Course Emphasis

This text is designed to provide the necessary mathematical background to understand and employ signal processing techniques in an applied environment. The emphasis is on a small number of fundamental problems and essential tools, as well as on applications. Certain topics that are commonly included in textbooks are touched on only briefly or in exercises or not mentioned at all. Other topics not usually considered to be part of signal processing, but which are becoming increasingly important, such as matrix theory and linear algebra, are included.

   The term *signal* is not meant to imply a specific context or a restriction to functions of time, or even to functions of a single variable; indeed, most of what we discuss in this text applies equally to functions of one and several variables and therefore to image processing. However, there are special problems that arise in image processing, such as edge detection,

and special techniques to deal with such problems; we shall not consider such techniques in this text.

1.2.5 Course Topics

Topics discussed include the following: Fourier series and transforms in one and several variables; applications to acoustic and EM propagation models, transmission and emission tomography, and image reconstruction; sampling and the limited data problem; matrix methods, singular value decomposition, and data compression; optimization techniques in signal and image reconstruction from projections; autocorrelations and power spectra; high-resolution methods; detection and optimal filtering; eigenvector-based methods for array processing and statistical filtering.

1.3 Applications of Interest

The applications of interest to us here can be summarized as follows: the data has been obtained through some form of sensing; physical models, often simplified, describe how the data we have obtained relates to the information we seek; there usually isn't enough data and what we have is corrupted by noise and other distortions. Although applications differ from one another in their details they often make use of a common core of mathematical ideas; for example, the Fourier transform and its variants play an important role in many areas of signal and image processing, as do the language and theory of matrix analysis, iterative optimization and approximation techniques, and the basics of probability and statistics. This common core provides the subject matter for this course. Applications of the core material to tomographic medical imaging, optical imaging, and acoustic signal processing are included.

1.4 Sensing Modalities

1.4.1 Active and Passive Sensing

In some signal and image processing applications the sensing is *active*, meaning that we have initiated the process, by, say, sending an x-ray through the body of a patient, injecting a patient with a radionuclide, transmitting an acoustic signal through the ocean, as in sonar, or transmitting a radio wave, as in radar. In such cases, we are interested in measuring how the system, the patient, the quiet submarine, the ocean floor, the rain cloud, will respond to our probing. In many other applications, the sensing is *passive*, which means that the object of interest to us provides its own signal of some sort, which we then detect, analyze, image,

or process in some way. Certain sonar systems operate passively, listening for sounds made by the object of interest. Optical and radio telescopes are passive, relying on the object of interest to emit or reflect light, or other electromagnetic radiation. Night-vision instruments are sensitive to lower-frequency, infrared radiation.

From Aristotle and Euclid until the middle ages there was an ongoing debate concerning the active or passive nature of human sight [162]. Those, like Euclid, whose interests were largely mathematical, believed that the eye emitted rays, the *extramission theory*. Aristotle and others, more interested in the physiology and anatomy of the eye than in mathematics, believed that the eye received rays from observed objects outside the body, the *intromission theory*. Finally, around 1000 AD, the Arabic mathematician and natural philosopher Alhazen demolished the extramission theory by noting the potential for bright light to hurt the eye, and combined the mathematics of the extramission theorists with a refined theory of intromission.

1.4.2   A Variety of Modalities

Although acoustic and electromagnetic sensing are the most commonly used methods, there are other modalities employed in remote sensing.

Radiation

In transmission tomography x-rays are transmitted along line segments through the object and the drop in intensity along each line is recorded. In emission tomography radioactive material is injected into the body of the living subject and the photons resulting from the radioactive decay are detected and recorded outside the body.

Cosmic-Ray Scattering

In addition to mapping the interior of volcanos, cosmic rays can also be used to detect the presence of shielding around nuclear material in a cargo container. The shielding can be sensed by the characteristic scattering by it of muons from cosmic rays; here neither we nor the objects of interest are the sources of the probing. This is about as "remote" as sensing can be.

Variations in Gravity

Gravity, or better, changes in the pull of gravity from one location to another, was used in the discovery of the crater left behind by the asteroid strike in the Yucatan that led to the extinction of the dinosaurs. The rocks and other debris that eventually filled the crater differ in density from the

surrounding material, thereby exerting a slightly different gravitational pull on other masses. This slight change in pull can be detected by sensitive instruments placed in satellites in earth orbit. When the intensity of the pull, as a function of position on the earth's surface, is displayed as a two-dimensional image, the presence of the crater is evident.

Seismic Exploration

In seismic oil exploration, explosive charges create waves that travel through the ground and are picked up by sensors. The waves travel at different speeds through different materials. Information about the location of different materials in the ground is then extracted from the received signals.

Spectral Analysis

In our detailed discussion of transmission and remote sensing we shall, for simplicity, concentrate on signals consisting of a single frequency. Nevertheless, there are many important applications of signal processing in which the signal being studied has a *broad spectrum*, indicative of the presence of many different frequencies. The purpose of the processing is often to determine which frequencies are present, or not present, and to determine their relative strengths. The hotter inner body of the sun emits radiation consisting of a continuum of frequencies. The cooler outer layer absorbs the radiation whose frequencies correspond to the elements present in that outer layer. Processing these signals reveals a spectrum with a number of missing frequencies, the so-called *Fraunhofer lines*, and provides information about the makeup of the sun's outer layers. This sort of *spectral analysis* can be used to identify the components of different materials, making it an important tool in many applications, from astronomy to forensics.

Back-Scatter Detectors

There is considerable debate at the moment about the use of so-called *full-body scanners* at airports. These are not scanners in the sense of a CAT-scan; indeed, if the images were skeletons there would probably be less controversy. These are images created by the returns, or *backscatter*, of millimeter-wavelength (MMW) radio-frequency waves, or sometimes low-energy x-rays, that penetrate only the clothing and then reflect back to the machine. The controversies are not really about safety to the passenger being imaged. The MMW imaging devices use about $10,000$ times less energy than a cell phone, and the x-ray exposure is equivalent to two minutes of flying in an airplane. At present, the images are fuzzy and faces are intentionally blurred, but there is some concern that the images will get sharper, will be permanently stored, and eventually end up on the net.

Given what is already available on the net, the market for these images will almost certainly be non-existent.

Near-Earth Asteroids

An area of growing importance is the search for potentially damaging near-earth asteroids. These objects are initially detected by passive optical observation, as small dots of reflected sunlight; once detected, they are then imaged by active radar to determine their size, shape, rotation, path, and other important parameters.

1.5 Inverse Problems

Many of the problems we study in applied mathematics are *direct problems.* For example, we imagine a ball dropped from a building of known height h and we calculate the time it takes for it to hit the ground and the impact velocity. Once we make certain simplifying assumptions about gravity and air resistance, we are able to solve this problem easily. Using his inverse-square law of universal gravitation, Newton was able to show that planets move in ellipses, with the sun at one focal point. Generally, direct problems conform to the usual flow of time and seek the effects due to known causes. Problems we call *inverse problems* go the other way, seeking the causes of observed effects; we measure the impact velocity to determine the height h of the building. Newton solved an inverse problem when he determined that Kepler's empirical laws of planetary motion follow from an inverse-square law of universal gravitation.

In each of the examples of remote sensing just presented, we have measured some of the effects and want to know the causes. In x-ray tomography, for example, we observe that the x-rays that passed through the body of the patient come out weaker than when they went in. We know that they were weakened, or *attenuated*, because they were partially absorbed by the material they had to pass through; we want to know precisely where the attenuation took place. This is an inverse problem; we are trying to go back in time, to uncover the causes of the observed effects.

Direct problems have been studied for a long time, while the theory of inverse problems is still being developed. Generally speaking, direct problems are easier than inverse problems. Direct problems, at least those corresponding to actual physical situations, tend to be *well-posed* in the sense of Hadamard, while inverse problems are often *ill-posed*. A problem is said to be *well-posed* if there is a unique solution for each input to the problem and the solution varies continuously with the input; roughly speaking, small changes in the input lead to small changes in the solution. If we vary the height of the building slightly, the time until the ball hits the

ground and its impact velocity will change only slightly. For inverse problems, there may be many solutions, or none, and slight changes in the data can cause the solutions to differ greatly. In [14] Bertero and Boccacci give a nice illustration of the difference between direct and inverse problems, using the heat equation.

Suppose that $u(x,t)$ is the temperature distribution for x in the interval $[0, a]$ and $t \geq 0$. The function $u(x,t)$ satisfies the heat equation

$$\frac{\partial^2 u}{\partial x^2} = \frac{1}{D} \frac{\partial u}{\partial t},$$

where $D > 0$ is the thermal conductivity. In addition, we adopt the boundary conditions $u(x,0) = f(x)$, and $u(0,t) = u(a,t) = 0$, for all t. By separating the variables, and using Fourier series, we find that, if

$$f(x) = \sum_{n=1}^{\infty} f_n \sin(\frac{n\pi x}{a}),$$

where

$$f_n = \frac{2}{a} \int_0^a f(x) \sin(\frac{n\pi x}{a}) dx,$$

then

$$u(x,t) = \sum_{n=1}^{\infty} f_n e^{-D(\frac{\pi n}{a})^2 t} \sin(\frac{n\pi x}{a}).$$

The direct problem is to find $u(x,t)$, given $f(x)$. Suppose that we know $f(x)$ with some finite precision, that is, we know those Fourier coefficients f_n for which $|f_n| \geq \epsilon > 0$. Because of the decaying exponential factor, fewer Fourier coefficients in the expansion of $u(x,t)$ will be above this threshold, and we can determine $u(x,t)$ with the same precision or better. The solution to the heat equation tends to be smoother than the input distribution.

The inverse problem is to determine the initial distribution $f(x)$ from knowledge of $u(x,t)$ at one or more times $t > 0$. As we just saw, for any fixed time $t > 0$, the Fourier coefficients of $u(x,t)$ will die off faster than the f_n do, leaving fewer coefficients above the threshold of ϵ. This means we can determine fewer and fewer of the f_n as t grows larger. For t beyond some point, it will be nearly impossible to say anything about $f(x)$.

1.6 Using Prior Knowledge

An important point to keep in mind when doing signal processing is that, while the data is usually limited, the information we seek may not be lost. Although processing the data in a reasonable way may suggest otherwise,

other processing methods may reveal that the desired information is still available in the data. Figure 1.1 illustrates this point.

The original image on the upper right of Figure 1.1 is a discrete rectangular array of intensity values simulating a slice of a head. The data was obtained by taking the two-dimensional discrete Fourier transform of the original image, and then discarding, that is, setting to zero, all these spatial frequency values, except for those in a smaller rectangular region around the origin. The problem then is under-determined. A minimum-norm solution would seem to be a reasonable reconstruction method.

The minimum-norm solution is shown on the lower right. It is calculated simply by performing an inverse discrete Fourier transform on the array of modified discrete Fourier transform values. The original image has relatively large values where the skull is located, but the minimum-norm reconstruction does not want such high values; the norm involves the sum of squares of intensities, and high values contribute disproportionately to the norm. Consequently, the minimum-norm reconstruction chooses instead to conform to the measured data by spreading what should be the skull intensities throughout the interior of the skull. The minimum-norm reconstruction does tell us something about the original; it tells us about the existence of the skull itself, which, of course, is indeed a prominent feature of the original. However, in all likelihood, we would already know about the skull; it would be the interior that we want to know about.

Using our knowledge of the presence of a skull, which we might have obtained from the minimum-norm reconstruction itself, we construct the prior estimate shown in the upper left. Now we use the same data as before, and calculate a minimum-weighted-norm reconstruction, using as the weight vector the reciprocals of the values of the prior image. This minimum-weighted-norm reconstruction is shown on the lower left; it is clearly almost the same as the original image. The calculation of the minimum-weighted norm solution can be done iteratively using the ART algorithm [204].

When we weight the skull area with the inverse of the prior image, we allow the reconstruction to place higher values there without having much of an effect on the overall weighted norm. In addition, the reciprocal weighting in the interior makes spreading intensity into that region costly, so the interior remains relatively clear, allowing us to see what is really present there.

When we try to reconstruct an image from limited data, it is easy to assume that the information we seek has been lost, particularly when a reasonable reconstruction method fails to reveal what we want to know. As this example, and many others, show, the information we seek is often still in the data, but needs to be brought out in a more subtle way.
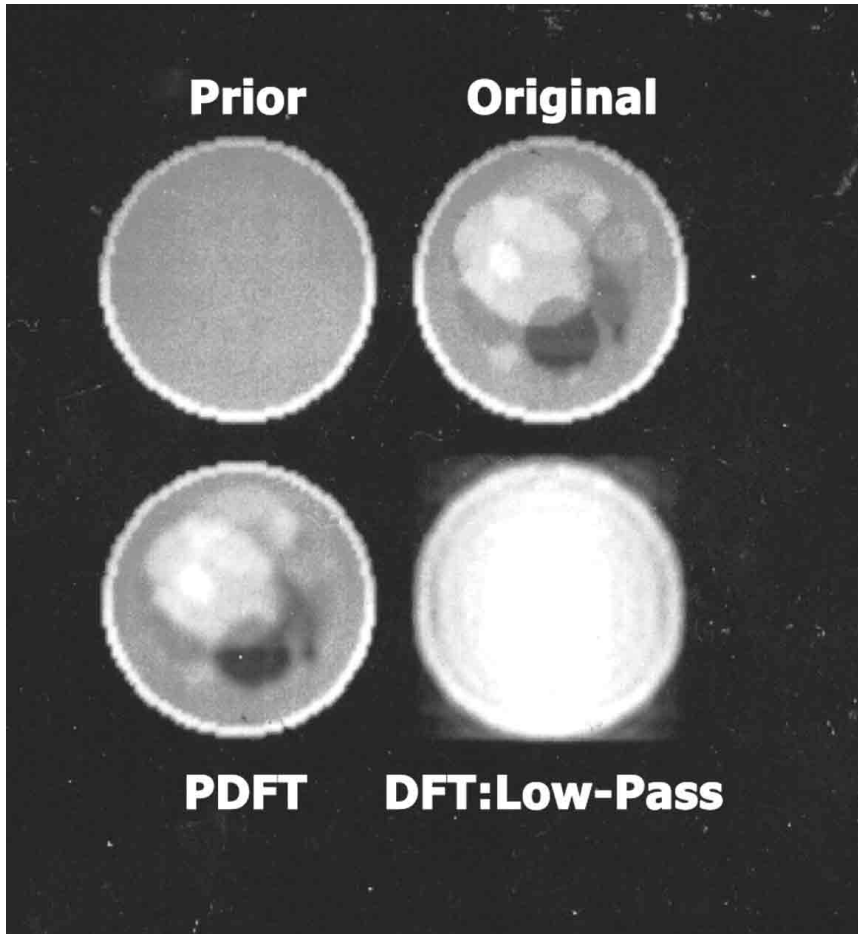
Figure 1.1: Extracting information in image reconstruction.

Chapter 2

Urn Models in Remote Sensing

2.1 Chapter Summary

Most of the signal processing that we shall discuss in this book is related to the problem of *remote sensing*, which we might also call *indirect measurement*. In such problems we do not have direct access to what we are really interested in, and must be content to measure something else that is related to, but not the same as, what interests us. For example, we want to know what is in the suitcases of airline passengers, but, for practical reasons, we cannot open every suitcase. Instead, we x-ray the suitcases. A recent paper [197] describes progress in detecting nuclear material in cargo containers by measuring the scattering, by the shielding, of cosmic rays; you can't get much more *remote* than that. Before we get into the mathematics of signal processing, it is probably a good idea to consider a model that, although quite simple, manages to capture many of the important features of remote sensing applications. To convince the reader that this is indeed a useful model, we relate it to the problem of image reconstruction in *single-photon computed emission tomography* (SPECT).

2.2 The Urn Model

There seems to be a tradition in physics of using simple models or examples involving urns and marbles to illustrate important principles. In keeping with that tradition, we have here two examples, to illustrate various aspects of remote sensing.

Suppose that we have J urns numbered $j = 1, ..., J$, each containing marbles of various colors. Suppose that there are I colors, numbered $i =$

$1, ..., I$. Suppose also that there is a box containing a large number of small pieces of paper, and on each piece is written the number of one of the J urns. Assume that I know the precise contents of each urn. My objective is to determine the precise contents of the box, that is, to estimate, for each $j = 1, ..., J$, the probability of selecting the jth urn, which is the relative number of pieces of paper containing the number j.

Out of my view, my assistant removes one piece of paper from the box, takes one marble from the indicated urn, announces to me the color of the marble, and then replaces both the piece of paper and the marble. This action is repeated N times, at the end of which I have a long list of colors, $\mathbf{i} = \{i_1, i_2, ..., i_N\}$, where i_n denotes the color of the nth marble drawn. This list $\mathbf{i}$ is my data, from which I must determine the contents of the box.

This is a form of remote sensing; what we have access to is related to, but not equal to, what we are interested in. What I wish I had is the list of urns used, $\mathbf{j} = \{j_1, j_2, ..., j_N\}$; instead I have $\mathbf{i}$, the list of colors. Sometimes data such as the list of colors is called "incomplete data", in contrast to the "complete data", which would be the list $\mathbf{j}$ of the actual urn numbers drawn from the box.

Using our urn model, we can begin to get a feel for the *resolution problem*. If all the marbles of one color are in a single urn, the problem is trivial; when I hear a color, I know immediately which urn contained that marble. My list of colors is then a list of urn numbers; I have the complete data now. My estimate of the number of pieces of paper containing the urn number j is then simply the proportion of draws that resulted in urn j being selected.

At the other extreme, suppose two urns have identical contents. Then I cannot distinguish one urn from the other and I am unable to estimate more than the total number of pieces of paper containing either of the two urn numbers. If the two urns have nearly the same contents, we can distinguish them only by using a very large N. This is the resolution problem.

Generally, the more the contents of the urns differ, the easier the task of estimating the contents of the box. In remote sensing applications, these issues affect our ability to resolve individual components contributing to the data.

2.3   Some Mathematical Notation

To introduce some mathematical notation, let us denote by x_j the proportion of the pieces of paper that have the number j written on them. Let P_{ij} be the proportion of the marbles in urn j that have the color i. Let y_i be the proportion of times the color i occurs in the list of colors. The expected proportion of times i occurs in the list is $E(y_i) = \sum_{j=1}^{J} P_{ij} x_j = (Px)_i$,

where P is the I by J matrix with entries P_{ij} and x is the J by 1 column vector with entries x_j. A reasonable way to estimate x is to replace $E(y_i)$ with the actual y_i and solve the system of linear equations $y_i = \sum_{j=1}^{J} P_{ij} x_j$, $i = 1, ..., I$. Of course, we require that the x_j be nonnegative and sum to one, so special algorithms may be needed to find such solutions. In a number of applications that fit this model, such as medical tomography, the values x_j are taken to be parameters, the data y_i are statistics, and the x_j are estimated by adopting a probabilistic model and maximizing the likelihood function. Iterative algorithms, such as the expectation maximization (EMML) algorithm are often used for such problems.

2.4 An Application to SPECT Imaging

In *single-photon computed emission tomography* (SPECT) the patient is injected with a chemical to which a radioactive tracer has been attached. Once the chemical reaches its destination within the body the photons emitted by the radioactive tracer are detected by gamma cameras outside the body. The objective is to use the information from the detected photons to infer the relative concentrations of the radioactivity within the patient.

We discretize the problem and assume that the body of the patient consists of J small volume elements, called *voxels*, analogous to *pixels* in digitized images. We let $x_j \geq 0$ be the unknown amount of the radioactivity that is present in the jth voxel, for $j = 1, ..., J$. There are I detectors, denoted $\{i = 1, 2, ..., I\}$. For each i and j we let P_{ij} be the known probability that a photon that is emitted from voxel j is detected at detector i. We denote by i_n the detector at which the nth emitted photon is detected. This photon was emitted at some voxel, denoted j_n; we wish that we had some way of learning what each j_n is, but we must be content with knowing only the i_n. After N photons have been emitted, we have as our data the list $\mathbf{i} = \{i_1, i_2, ..., i_N\}$; this is our *incomplete data*. We wish we had the *complete data*, that is, the list $\mathbf{j} = \{j_1, j_2, ..., j_N\}$, but we do not. Our goal is to estimate the frequency with which each voxel emitted a photon, which we assume, reasonably, to be proportional to the unknown amounts x_j, for $j = 1, ..., J$.

This problem is completely analogous to the urn problem previously discussed. Any mathematical method that solves one of these problems will solve the other one. In the urn problem, the colors were announced; here the detector numbers are announced. There, I wanted to know the urn numbers; here I want to know the voxel numbers. There, I wanted to estimate the frequency with which the jth urn was used; here, I want to estimate the frequency with which the jth voxel is the site of an emission. In the urn model, two urns with nearly the same contents are hard to distinguish unless N is very large; here, two neighboring voxels will be

very hard to distinguish (i.e., to resolve) unless N is very large. But in the SPECT case, a large N means a high dosage, which will be prohibited by safety considerations. Therefore, we have a built-in resolution problem in the SPECT case.

Both problems are examples of probabilistic mixtures, in which the mixing probabilities are the x_j that we seek. The *maximum likelihood* (ML) method of statistical parameter estimation can be used to solve such problems. The interested reader should consult the text [48].

2.5   Hidden Markov Models

In the urn model we just discussed, the order of the colors in the list is unimportant; we could randomly rearrange the colors on the list without affecting the nature of the problem. The probability that a green marble will be chosen next is the same, whether a blue or a red marble was just chosen the last time. This independence from one selection to another is fine for modeling certain physical situations, such as emission tomography. However, there are other situations in which this independence does not conform to reality.

In written English, for example, knowing the current letter helps us, sometimes more, sometimes less, to predict what the next letter will be. We know that if the current letter is a "q", then there is a high probability that the next one will be a "u" . So what the current letter is affects the probabilities associated with the selection of the next one.

Spoken English is even tougher. There are many examples in which the pronunciation of a certain sound is affected, not only by the sound or sounds that preceded it, but by the sound or sounds that will follow. For example, the sound of the "e" in the word "bellow" is different from the sound of the "e" in the word "below" ; the sound changes, depending on whether there is a double "l" or a single "l" following the "e" . Here the entire context of the letter affects its sound.

Hidden Markov models (HMM) are increasingly important in speech processing, optical character recognition and DNA sequence analysis. They allow us to incorporate dependence on the past into our model. In this section we illustrate HMM using a modification of the urn model.

Suppose, once again, that we have J urns, indexed by $j = 1, ..., J$ and I colors of marbles, indexed by $i = 1, ..., I$. Associated with each of the J urns is a box, containing a large number of pieces of paper, with the number of one urn written on each piece. My assistant selects one box, say the j_0th box, to start the experiment. He draws a piece of paper from that box, reads the number written on it, call it j_1, goes to the urn with the number j_1 and draws out a marble. He then announces the color. He then draws a piece of paper from box number j_1, reads the next number,

say j_2, proceeds to urn number j_2, etc. After N marbles have been drawn, the only data I have is a list of colors, $\mathbf{i} = \{i_1, i_2, ..., i_N\}$.

The *transition probability* that my assistant will proceed from the urn numbered k to the urn numbered j is b_{jk}, with $\sum_{j=1}^{J} b_{jk} = 1$. The number of the current urn is the current *state*. In an ordinary *Markov chain* model, we observe directly a sequence of states governed by the transition probabilities. The Markov chain model provides a simple formalism for describing a system that moves from one state into another, as time goes on. In the hidden Markov model we are not able to observe the states directly; they are hidden from us. Instead, we have indirect observations, the colors of the marbles in our urn example.

The probability that the color numbered i will be drawn from the urn numbered j is a_{ij}, with $\sum_{i=1}^{I} a_{ij} = 1$, for all j. The colors announced are the *visible states*, while the unannounced urn numbers are the *hidden states*.

There are several distinct objectives one can have, when using HMM. We assume that the data is the list of colors, $\mathbf{i}$.

- **Evaluation:** For given probabilities a_{ij} and b_{jk}, what is the probability that the list $\mathbf{i}$ was generated according to the HMM? Here, the objective is to see if the model is a good description of the data.

- **Decoding:** Given the model, the probabilities and the list $\mathbf{i}$, what list $\mathbf{j} = \{j_1, j_2, ..., j_N\}$ of urns is most likely to be the list of urns actually visited? Now, we want to infer the hidden states from the visible ones.

- **Learning:** We are told that there are J urns and I colors, but are not told the probabilities a_{ij} and b_{jk}. We are given several data vectors $\mathbf{i}$ generated by the HMM; these are the *training sets*. The objective is to learn the probabilities.

Once again, the ML approach can play a role in solving these problems [102]. The *Viterbi algorithm* is an important tool used for the decoding phase (see [209]).

Part II

Fundamental Examples

Chapter 3

Transmission and Remote Sensing- I

3.1 Chapter Summary

In this chapter we illustrate the roles played by Fourier series and Fourier coefficients in the analysis of signal transmission and remote sensing, and use these examples to motivate several of the problems we shall consider in detail later in the text.

3.2 Fourier Series and Fourier Coefficients

We suppose that $f(x)$ is defined for $-L \leq x \leq L$, with Fourier series representation

$$f(x) = \frac{1}{2}a_0 + \sum_{n=1}^{\infty} a_n \cos(\frac{n\pi}{L}x) + b_n \sin(\frac{n\pi}{L}x). \qquad (3.1)$$

To find the Fourier coefficients a_n and b_n we make use of *orthogonality*.

For any m and n we have

$$\int_{-L}^{L} \cos(\frac{m\pi}{L}x) \sin(\frac{n\pi}{L}x)dx = 0,$$

and for $m \neq n$ we have

$$\int_{-L}^{L} \cos(\frac{m\pi}{L}x) \cos(\frac{n\pi}{L}x)dx = 0,$$

and

$$\int_{-L}^{L} \sin(\frac{m\pi}{L}x)\sin(\frac{n\pi}{L}x)dx = 0.$$

Therefore, to find the a_n and b_n we multiply both sides of Equation (3.1) by $\cos(\frac{m\pi}{L}x)$, or $\sin(\frac{m\pi}{L}x)$ and integrate. We find that the Fourier coefficients are

$$a_n = \frac{1}{L}\int_{-L}^{L} f(x)\cos(\frac{n\pi}{L}x)dx, \qquad (3.2)$$

and

$$b_n = \frac{1}{L}\int_{-L}^{L} f(x)\sin(\frac{n\pi}{L}x)dx. \qquad (3.3)$$

In the examples in this chapter, we shall see how Fourier coefficients can arise as data obtained through measurements. However, we shall be able to measure only a finite number of the Fourier coefficients. One issue that will concern us is the effect on the representation of $f(x)$ if we use some, but not all, of its Fourier coefficients.

Suppose that we have a_n and b_n for $n = 0, 1, 2, ..., N$. It is not unreasonable to try to estimate the function $f(x)$ using the *discrete Fourier transform* (DFT) estimate, which is

$$f_{DFT}(x) = \frac{1}{2}a_0 + \sum_{n=1}^{N} a_n \cos(\frac{n\pi}{L}x) + b_n \sin(\frac{n\pi}{L}x). \qquad (3.4)$$

In Figure 3.1 below, the function $f(x)$ is the solid-line figure in both graphs. In the bottom graph, we see the true $f(x)$ and a DFT estimate. The top graph is the result of *band-limited extrapolation*, a technique for predicting missing Fourier coefficients that we shall discuss later.

3.3   The Unknown Strength Problem

In this example, we imagine that each point x in the interval $[-L, L]$ is sending a sine function signal at the frequency ω, each with its own strength $f(x)$; that is, the signal sent by the point x is

$$f(x)\sin(\omega t). \qquad (3.5)$$

In our first example, we imagine that the strength function $f(x)$ is unknown and we want to determine it. It could be the case that the signals originate at the points x, as with light or radio waves from the sun, or are simply reflected from the points x, as is sunlight from the moon or radio waves in radar. Later in this chapter, we shall investigate a related example, in which the points x transmit known signals and we want to determine what is received elsewhere.

3.3.1 Measurement in the Far-Field

Now let us consider what is received by a point P on the circumference of a circle centered at the origin and having large radius D. The point P corresponds to the angle θ as shown in Figure 3.2; we use θ in the interval $[0, \pi]$. It takes a finite time for the signal sent from x at time t to reach P, so there is a delay.

We assume that c is the speed at which the signal propagates. Because D is large relative to L, we make the *far-field assumption*, which allows us to approximate the distance from x to P by $D - x \cos(\theta)$. Therefore, what P receives at time t from x is approximately what was sent from x at time $t - \frac{1}{c}(D - x \cos(\theta))$.

Exercise 3.1 *Show that, for any point P on the circle of radius D and any $x \neq 0$, the distance from x to P is always greater than or equal to the far-field approximation $D - x \cos(\theta)$, with equality if and only if $\theta = 0$ or $\theta = \pi$.*

At time t, the point P receives from x the signal

$$f(x) \sin \left(\omega(t - \frac{D}{c}) + \frac{\omega \cos \theta}{c} x \right) =$$

$$f(x) \left(\sin(\omega(t - \frac{D}{c})) \cos(\frac{\omega \cos(\theta)}{c} x) + \cos(\omega(t - \frac{D}{c})) \sin(\frac{\omega \cos(\theta)}{c} x) \right), (3.6)$$

and the point Q corresponding to the angle $\theta + \pi$ receives

$$f(x) \left(\sin(\omega(t - \frac{D}{c})) \cos(\frac{\omega \cos(\theta)}{c} x) - \cos(\omega(t - \frac{D}{c})) \sin(\frac{\omega \cos(\theta)}{c} x) \right). (3.7)$$

Because P and Q receive signals from all the x, not just from one x, what P and Q receive at time t involves integrating over all x. Therefore, from our measurements at P and Q, we obtain the quantities

$$\int_{-L}^{L} f(x) \left(\sin(\omega(t - \frac{D}{c})) \cos(\frac{\omega \cos(\theta)}{c} x) + \cos(\omega(t - \frac{D}{c})) \sin(\frac{\omega \cos(\theta)}{c} x) \right) dx, (3.8)$$

and

$$\int_{-L}^{L} f(x) \left(\sin(\omega(t - \frac{D}{c})) \cos(\frac{\omega \cos(\theta)}{c} x) - \cos(\omega(t - \frac{D}{c})) \sin(\frac{\omega \cos(\theta)}{c} x) \right) dx. (3.9)$$

Adding the quantities in (3.8) and (3.9), we obtain

$$2 \left(\int_{-L}^{L} f(x) \cos(\frac{\omega \cos(\theta)}{c} x) dx \right) \sin(\omega(t - \frac{D}{c})), \qquad (3.10)$$

while subtracting the latter from the former, we get

$$2\Big(\int_{-L}^{L} f(x)\sin(\frac{\omega\cos(\theta)}{c}x)dx\Big)\cos(\omega(t-\frac{D}{c})). \tag{3.11}$$

Evaluating the signal in Equation (3.10) at the time when

$$\omega(t-\frac{D}{c}) = \frac{\pi}{2},$$

and dividing by 2, we get

$$\int_{-L}^{L} f(x)\cos(\frac{\omega\cos(\theta)}{c}x)dx,$$

while evaluating the signal in Equation (3.11) at the time when

$$\omega(t-\frac{D}{c}) = 2\pi$$

and dividing by 2 gives us

$$\int_{-L}^{L} f(x)\sin(\frac{\omega\cos(\theta)}{c}x)dx.$$

If we can select an angle θ for which

$$\frac{\omega\cos(\theta)}{c} = \frac{n\pi}{L}, \tag{3.12}$$

then we have a_n and b_n.

3.3.2   Limited Data

Note that we will be able to solve Equation (3.12) for θ only if we have

$$n \le \frac{L\omega}{\pi c}. \tag{3.13}$$

This tells us that we can measure only finitely many of the Fourier coefficients of $f(x)$. It is common in signal processing to speak of the *wavelength* of a sinusoidal signal; the wavelength associated with a given ω and c is

$$\lambda = \frac{2\pi c}{\omega}. \tag{3.14}$$

Therefore the number N of Fourier coefficients we can measure is the largest integer not greater than $\frac{2L}{\lambda}$, which is the length of the interval $[-L, L]$, measured in units of wavelength λ. We get more Fourier coefficients when the product $L\omega$ is larger; this means that when L is small, we want ω to be large, so that λ is small and N is large. As we saw previously, using these finitely many Fourier coefficients to calculate the DFT reconstruction of $f(x)$ can lead to a poor estimate of $f(x)$, particularly when N is small.

3.3.3   Can We Get More Data?

As we just saw, we can make measurements at any points P and Q in the far-field; perhaps we do not need to limit ourselves to just those angles that lead to the a_n and b_n. It may come as somewhat of a surprise, but from the theory of complex analytic functions we can prove that there is enough data available to us here to reconstruct $f(x)$ perfectly, at least in principle. The drawback, in practice, is that the measurements would have to be free of noise and impossibly accurate. All is not lost, however.

3.3.4   The Fourier Cosine and Sine Transforms

As we just saw, if θ is chosen so that

$$\frac{\omega \cos(\theta)}{c} = \frac{n\pi}{L}, \tag{3.15}$$

then our measurements give us the Fourier coefficients a_n and b_n. But we can select any angle θ and use any P and Q we want. In other words, we can obtain the values

$$\int_{-L}^{L} f(x) \cos\left(\frac{\omega \cos(\theta)}{c} x\right) dx, \tag{3.16}$$

and

$$\int_{-L}^{L} f(x) \sin\left(\frac{\omega \cos(\theta)}{c} x\right) dx \tag{3.17}$$

for any angle θ. With the change of variable

$$\gamma = \frac{\omega \cos(\theta)}{c},$$

we can obtain the values of the functions

$$F_c(\gamma) = \int_{-L}^{L} f(x) \cos(\gamma x) dx \tag{3.18}$$

and

$$F_s(\gamma) = \int_{-L}^{L} f(x) \sin(\gamma x) dx, \tag{3.19}$$

for any γ in the interval $[-\frac{\omega}{c}, \frac{\omega}{c}]$. The functions $F_c(\gamma)$ and $F_s(\gamma)$ are the *Fourier cosine transform* and *Fourier sine transform* of $f(x)$, respectively.

We are free to measure at any P and Q and therefore to obtain values of $F_c(\gamma)$ and $F_s(\gamma)$ for any value of γ in the interval $[-\frac{\omega}{c}, \frac{\omega}{c}]$. We need to be careful how we process the resulting data, however.

3.3.5   Over-Sampling

Suppose, for the sake of illustration, that we measure the far-field signals at points P and Q corresponding to angles θ that satisfy

$$\frac{\omega \cos(\theta)}{c} = \frac{n\pi}{2L}, \tag{3.20}$$

instead of

$$\frac{\omega \cos(\theta)}{c} = \frac{n\pi}{L}.$$

Now we have twice as many data points and from our new measurements we can obtain

$$c_n = \int_{-L}^{L} f(x) \cos(\frac{n\pi}{2L}x)dx,$$

and

$$d_n = \int_{-L}^{L} f(x) \sin(\frac{n\pi}{2L}x)dx,$$

for $n = 0, 1, ..., 2N$. We say now that our data is *twice over-sampled*. Note that we call it *over-sampled* because the rate at which we are sampling is higher, even though the distance between samples is lower.

Since $f(x) = 0$ for $L < |x| \le 2L$, we can say that we have

$$A_n = \frac{1}{2L}c_n = \frac{1}{4L}\int_{-2L}^{2L} g(x) \cos(\frac{n\pi}{2L}x)dx, \tag{3.21}$$

and

$$B_n = \frac{1}{2L}d_n = \frac{1}{4L}\int_{-2L}^{2L} g(x) \sin(\frac{n\pi}{2L}x)dx, \tag{3.22}$$

for $n = 0, 1, ..., 2N$, which are Fourier coefficients for the function $g(x)$ that equals $f(x)$ for $|x| \le L$, and equals zero for $L < |x| \le 2L$.

We have twice the number of Fourier coefficients that we had previously, but for the function $g(x)$. A DFT reconstruction using this larger set of Fourier coefficients will reconstruct $g(x)$ on the interval $[-2L, 2L]$. This will give us a reconstruction of $f(x)$ itself over the interval $[-L, L]$, but will also give us a reconstruction of the rest of $g(x)$, which we already know to be zero. So we are wasting the additional data by reconstructing $g(x)$ instead of $f(x)$. We need to use our prior knowledge that $g(x) = 0$ for $L < |x| \le 2L$.

Later, we shall describe in detail the use of prior knowledge about $f(x)$ to obtain reconstructions that are better than the DFT. In the example we are now considering, we have prior knowledge that $f(x) = 0$ for $L < |x| \le 2L$. We can use this prior knowledge to improve our reconstruction.

Suppose that we take as our reconstruction the *modified DFT* (MDFT), which is a function defined only for $|x| \leq L$ and having the form

$$f_{MDFT}(x) = \frac{1}{2}u_0 + \sum_{n=1}^{2N} u_n \cos(\frac{n\pi}{2L}x) + v_n \sin(\frac{n\pi}{2L}x), \qquad (3.23)$$

where the u_n and v_n are unknowns to be determined. Then we calculate the u_n and v_n by requiring that it be possible for the function $f_{MDFT}(x)$ to be the correct answer; that is, we require that $f_{MDFT}(x)$ be consistent with the measured data. Therefore, we must have

$$\int_{-L}^{L} f_{MDFT}(x) \cos(\frac{n\pi}{2L}x)dx = c_n, \qquad (3.24)$$

and

$$\int_{-L}^{L} f_{MDFT}(x) \sin(\frac{n\pi}{2L}x)dx = d_n, \qquad (3.25)$$

for $n = 0, 1, ..., 2N$. It is important to note now that the u_n and v_n are not the A_n and B_n; this is because we no longer have orthogonality. For example, when we calculate the integrals

$$\int_{-L}^{L} \cos(\frac{n\pi}{2L}x) \cos(\frac{m\pi}{2L}x)dx, \qquad (3.26)$$

for $m \neq n$, we do not get zero. To find the u_n and v_n we need to solve a system of linear equations in these unknowns.

The top graph in Figure (3.1) illustrates the improvement over the DFT that can be had using the MDFT. In that figure, we took data that was thirty times over-sampled, not just twice over-sampled, as in our previous discussion. Consequently, we had thirty times the number of Fourier coefficients we would have had otherwise, but for an interval thirty times longer. To get the top graph, we used the MDFT, with the prior knowledge that $f(x)$ was non-zero only within the central thirtieth of the long interval. The bottom graph shows the DFT reconstruction using the larger data set, but only for the central thirtieth of the full period, which is where the original $f(x)$ is non-zero.

3.3.6   Other Forms of Prior Knowledge

As we just showed, knowing that we have over-sampled in our measurements can help us improve the resolution in our estimate of $f(x)$. We may have other forms of prior knowledge about $f(x)$ that we can use. If

we know something about large-scale features of $f(x)$, but not about finer details, we can use the PDFT estimate, which is a generalization of the MDFT. In an earlier chapter, the PDFT was compared to the DFT in a two-dimensional example of simulated head slices. There are other things we may know about $f(x)$.

For example, we may know that $f(x)$ is non-negative, which we have not assumed explicitly previously in this chapter. Or, we may know that $f(x)$ is approximately zero for most x, but contains very sharp peaks at a few places. In more formal language, we may be willing to assume that $f(x)$ contains a few Dirac delta functions in a flat background. There are non-linear methods, such as the maximum entropy method, the indirect PDFT (IPDFT), and eigenvector methods that can be used to advantage in such cases; these methods are often called *high-resolution methods*.

3.4   Estimating the Size of Distant Objects

Suppose, in the previous example of the unknown strength problem, we assume that $f(x) = B$, for all x in the interval $[-L, L]$, where $B > 0$ is the unknown *brightness* constant, and we don't know L. More realistic, two-dimensional versions of this problem arise in astronomy, when we want to estimate the diameter of a distant star.

In this case, the measurement of the signal at the point P gives us

$$\int_{-L}^{L} f(x) \cos\left(\frac{\omega \cos\theta}{c} x\right) dx$$

$$= B \int_{-L}^{L} \cos\left(\frac{\omega \cos\theta}{c} x\right) dx = \frac{2Bc}{\omega \cos(\theta)} \sin(\frac{L\omega \cos(\theta)}{c}), \qquad (3.27)$$

when $\cos\theta \neq 0$, whose absolute value is then the strength of the signal at P. Notice that we have zero signal strength at P when the angle θ associated with P satisfies the equation

$$\sin(\frac{L\omega \cos(\theta)}{c}) = 0,$$

without

$$\cos(\theta) = 0.$$

But we know that the first positive zero of the sine function is at π, so the signal strength at P is zero when θ is such that

$$\frac{L\omega \cos(\theta)}{c} = \pi.$$

If

$$\frac{L\omega}{c} \geq \pi,$$

then we can solve for L and get

$$L = \frac{\pi c}{\omega \cos(\theta)}.$$

When $L\omega$ is too small, there will be no angle θ for which the received signal strength at P is zero. If the signals being sent are actually *broadband*, meaning that the signals are made up of components at many different frequencies, not just one ω, which is usually the case, then we might be able to filter our measured data, keep only the component at a sufficiently high frequency, and then proceed as before.

But even when we have only a single frequency ω and $L\omega$ is too small, there is something we can do. The received strength at $\theta = \frac{\pi}{2}$ is

$$F_c(0) = B \int_{-L}^{L} dx = 2BL.$$

If we knew B, this measurement alone would give us L, but we do not assume that we know B. At any other angle, the received strength is

$$F_c(\gamma) = \frac{2Bc}{\omega \cos(\theta)} \sin(\frac{L\omega \cos(\theta)}{c}).$$

Therefore,

$$F_c(\gamma)/F_c(0) = \frac{\sin(A)}{A},$$

where

$$A = \frac{L\omega \cos(\theta)}{c}.$$

From the measured value $F_c(\gamma)/F_c(0)$ we can solve for A and then for L. In actual optical astronomy, atmospheric distortions make these measurements noisy and the estimates have to be performed more carefully. This issue is discussed in more detail in a later chapter, in the section on the Two-Dimensional Fourier Transform.

There is a wonderful article by Eddington [104], in which he discusses the use of signal processing methods to discover the properties of the star Algol. This star, formally Algol (Beta Persei) in the constellation Perseus, turns out to be three stars, two revolving around the third, with both of the first two taking turns eclipsing the other. The stars rotate around their own axes, as our star, the sun, does, and the speed of rotation can be estimated by calculating the Doppler shift in frequency, as one side of the star comes toward us and the other side moves away. It is possible to measure one side at a time only because of the eclipse caused by the other revolving star.

3.5   The Transmission Problem

3.5.1   Directionality

Now we turn the table around and suppose that we are designing a broadcasting system, using transmitters at each x in the interval $[-L, L]$. At each x we will transmit $f(x)\sin(\omega t)$, where both $f(x)$ and ω are chosen by us. We now want to calculate what will be received at each point P in the far-field. We may wish to design the system so that the strengths of the signals received at the various P are not all the same. For example, if we are broadcasting from Los Angeles, we may well want a strong signal in the north and south directions, but weak signals east and west, where there are fewer people to receive the signal. Clearly, our model of a single-frequency signal is too simple, but it does allow us to illustrate several important points about directionality in array processing.

3.5.2   The Case of Uniform Strength

For concreteness, we investigate the case in which $f(x) = 1$ for $|x| \leq L$. Since this function is even, we need only the a_n. In this case, the measurement of the signal at the point P gives us

$$F(P) = \int_{-L}^{L} f(x) \cos\left(\frac{\omega \cos\theta}{c}x\right) dx$$

$$= \int_{-L}^{L} \cos\left(\frac{\omega \cos\theta}{c}x\right) dx = \frac{2c}{\omega \cos(\theta)} \sin(\frac{L\omega \cos(\theta)}{c}), \qquad (3.28)$$

when $\cos\theta \neq 0$. The absolute value of $F(P)$ is then the strength of the signal at P.

In the figures below we see the plots of the function $\frac{1}{2L}F(P)$, for various values of the aperture

$$A = \frac{L\omega}{\pi c} = \frac{2L}{\lambda}.$$

Beam-Pattern Nulls

Is it possible for the strength of the signal received at some P to be zero? As we saw in the previous section, to have zero signal strength, that is, to have $F(P) = 0$, we need

$$\sin(\frac{L\omega \cos(\theta)}{c}) = 0,$$

without

$$\cos(\theta) = 0.$$

Therefore, we need

$$\frac{L\omega\cos(\theta)}{c} = n\pi, \tag{3.29}$$

for some positive integers $n \geq 1$. Notice that this can happen only if

$$n \leq \frac{L\omega\pi}{c} = \frac{2L}{\lambda}. \tag{3.30}$$

Therefore, if $2L < \lambda$, there can be no P with signal strength zero. The larger $2L$ is, with respect to the wavelength λ, the more angles at which the signal strength is zero.

Local Maxima

Is it possible for the strength of the signal received at some P to be a local maximum, relative to nearby points in the farfield? We write

$$F(P) = \frac{2c}{\omega\cos(\theta)} \sin(\frac{L\omega\cos(\theta)}{c}) = 2L\text{sinc}\,(A(\theta)),$$

where

$$A(\theta) = \frac{L\omega\cos(\theta)}{c}$$

and

$$\text{sinc}\,(A(\theta)) = \frac{\sin A(\theta)}{A(\theta)},$$

for $A(\theta) \neq 0$, and equals one for $A(\theta) = 1$. The value of A used previously is then $A = A(0)$.

Local maxima or minima of $F(P)$ occur when the derivative of $\text{sinc}\,(A(\theta))$ equals zero, which means that

$$A(\theta)\cos A(\theta) - \sin A(\theta) = 0,$$

or

$$\tan A(\theta) = A(\theta).$$

If we can solve this equation for $A(\theta)$ and then for θ, we will have found angles corresponding to local maxima of the received signal strength. The largest value of $F(P)$ occurs when $\theta = \frac{\pi}{2}$, and the peak in the plot of $F(P)$ centered at $\theta = \frac{\pi}{2}$ is called the *main lobe*. The smaller peaks on either side are called the *grating lobes*. We can see grating lobes in some of the polar plots.

3.6   Remote Sensing

A basic problem in remote sensing is to determine the nature of a distant object by measuring signals transmitted by or reflected from that object. If the object of interest is sufficiently remote, that is, is in the *farfield*, the data we obtain by sampling the propagating spatio-temporal field is related, approximately, to what we want by *Fourier transformation*. The problem is then to estimate a function from finitely many (usually noisy) values of its *Fourier transform*. The application we consider here is a common one of remote-sensing of transmitted or reflected waves propagating from distant sources. Examples include optical imaging of planets and asteroids using reflected sunlight, radio-astronomy imaging of distant sources of radio waves, active and passive sonar, radar imaging using micro-waves, and infra-red (IR) imaging to monitor the ocean temperature .

3.7   One-Dimensional Arrays

Now we imagine that the points P are the sources of the signals and we are able to measure the transmissions at points x in $[-L, L]$. The P corresponding to the angle θ sends $F(\theta)\sin(\omega t)$, where the absolute value of $F(\theta)$ is the strength of the signal coming from P. In narrow-band passive sonar, for example, we may have hydrophone sensors placed at various points x and our goal is to determine how much acoustic energy at a specified frequency is coming from different directions. There may be only a few directions contributing significant energy at the frequency of interest.

3.7.1   Measuring Fourier Coefficients

To simplify notation, we shall introduce the variable $u = \cos(\theta)$. We then have

$$\frac{du}{d\theta} = -\sin(\theta) = -\sqrt{1 - u^2},$$

so that

$$d\theta = -\frac{1}{\sqrt{1 - u^2}}du.$$

Now let $G(u)$ be the function

$$G(u) = \frac{F(\arccos(u))}{\sqrt{1 - u^2}},$$

defined for u in the interval $[-1, 1]$.

Measuring the signals received at x and $-x$, we can obtain the integrals

$$\int_{-1}^{1} G(u)\cos(\frac{x\omega}{c}u)du, \qquad (3.31)$$

and

$$\int_{-1}^{1} G(u) \sin(\frac{x\omega}{c} u) du. \tag{3.32}$$

The Fourier coefficients of $G(u)$ are

$$\frac{1}{2} \int_{-1}^{1} G(u) \cos(n\pi u) du, \tag{3.33}$$

and

$$\frac{1}{2} \int_{-1}^{1} G(u) \sin(n\pi u) du. \tag{3.34}$$

Therefore, in order to have our measurements match Fourier coefficients of $G(u)$ we need

$$\frac{x\omega}{c} = n\pi, \tag{3.35}$$

for some positive integer n. Therefore, we need to take measurements at the points x and $-x$, where

$$x = n\frac{\pi c}{\omega} = n\frac{\lambda}{2} = n\Delta, \tag{3.36}$$

where $\Delta = \frac{\lambda}{2}$ is the *Nyquist spacing*. Since x is restricted to $[-L, L]$, there is an upper limit to the n we can use; we must have

$$n \leq \frac{L}{\lambda/2} = \frac{2L}{\lambda}. \tag{3.37}$$

The upper bound $\frac{2L}{\lambda}$, which is the length of our array of sensors, in units of wavelength, is often called the *aperture* of the array.

Once we have some of the Fourier coefficients of the function $G(u)$, we can estimate $G(u)$ for $|u| \leq 1$ and, from that estimate, obtain an estimate of the original $F(\theta)$.

As we just saw, the number of Fourier coefficients of $G(u)$ that we can measure, and therefore the resolution of the resulting reconstruction of $F(\theta)$, is limited by the aperture, that is, the length $2L$ of the array of sensors, divided by the wavelength λ. One way to improve resolution is to make the array of sensors longer, which is more easily said than done. However, *synthetic-aperture radar* (SAR) effectively does this. The idea of SAR is to mount the array of sensors on a moving airplane. As the plane moves, it effectively creates a longer array of sensors, a *virtual array* if you will. The one drawback is that the sensors in this virtual array are not

all present at the same time, as in a normal array. Consequently, the data must be modified to approximate what would have been received at other times.

As in the examples discussed previously, we do have more measurements we can take, if we use values of x other than those described by Equation (3.36). The issue will be what to do with these *over-sampled* measurements.

3.7.2   Over-sampling

One situation in which over-sampling arises naturally occurs in sonar array processing. Suppose that an array of sensors has been built to operate at a *design frequency* of ω_0, which means that we have placed sensors at the points x in $[-L, L]$ that satisfy the equation

$$x = n\frac{\pi c}{\omega_0} = n\frac{\lambda_0}{2} = n\Delta_0, \tag{3.38}$$

where λ_0 is the wavelength corresponding to the frequency ω_0 and $\Delta_0 = \frac{\lambda_0}{2}$ is the Nyquist spacing for frequency ω_0. Now suppose that we want to operate the sensing at another frequency, say ω. The sensors cannot be moved, so we must make due with sensors at the points x determined by the design frequency.

Consider, first, the case in which the second frequency ω is less than the design frequency ω_0. Then its wavelength λ is larger than λ_0, and the Nyquist spacing $\Delta = \frac{\lambda}{2}$ for ω is larger than Δ_0. So we have over-sampled.

The measurements taken at the sensors provide us with the integrals

$$\frac{1}{2K} \int_{-1}^{1} G(u) \cos(\frac{n\pi}{K}u) du, \tag{3.39}$$

and

$$\frac{1}{2K} \int_{-1}^{1} G(u) \sin(\frac{n\pi}{K}u) du, \tag{3.40}$$

where $K = \frac{\omega_0}{\omega} > 1$. These are Fourier coefficients of the function $G(u)$, viewed as defined on the interval $[-K, K]$, which is larger than $[-1, 1]$, and taking the value zero outside $[-1, 1]$. If we then use the DFT estimate of $G(u)$, it will estimate $G(u)$ for the values of u within $[-1, 1]$, which is what we want, as well as for the values of u outside $[-1, 1]$, where we already know $G(u)$ to be zero. Once again, we can use the modified DFT, the MDFT, to include the prior knowledge that $G(u) = 0$ for u outside $[-1, 1]$ to improve our reconstruction of $G(u)$ and $F(\theta)$. In the over-sampled case the interval $[-1, 1]$ is called *the visible region* (although *audible region* seems more appropriate for sonar), since it contains all the values of u that can correspond to actual angles of arrival of acoustic energy.

3.7.3 Under-sampling

Now suppose that the frequency ω that we want to consider is greater than the design frequency ω_0. This means that the spacing between the sensors is too large; we have *under-sampled*. Once again, however, we cannot move the sensors and must make due with what we have.

Now the measurements at the sensors provide us with the integrals

$$\frac{1}{2K} \int_{-1}^{1} G(u) \cos(\frac{n\pi}{K}u) du, \tag{3.41}$$

and

$$\frac{1}{2K} \int_{-1}^{1} G(u) \sin(\frac{n\pi}{K}u) du, \tag{3.42}$$

where $K = \frac{\omega_0}{\omega} < 1$. These are Fourier coefficients of the function $G(u)$, viewed as defined on the interval $[-K, K]$, which is smaller than $[-1, 1]$, and taking the value zero outside $[-K, K]$. Since $G(u)$ is not necessarily zero outside $[-K, K]$, treating it as if it were zero there results in a type of error known as *aliasing*, in which energy corresponding to angles whose u lies outside $[-K, K]$ is mistakenly assigned to values of u that lie within $[-K, K]$. Aliasing is a common phenomenon; the strobe-light effect is aliasing, as is the apparent backward motion of the wheels of stage-coaches in cowboy movies. In the case of the strobe light, we are permitted to view the scene at times too far apart for us to sense continuous, smooth motion. In the case of the wagon wheels, the frames of the film capture instants of time too far apart for us to see the true rotation of the wheels.
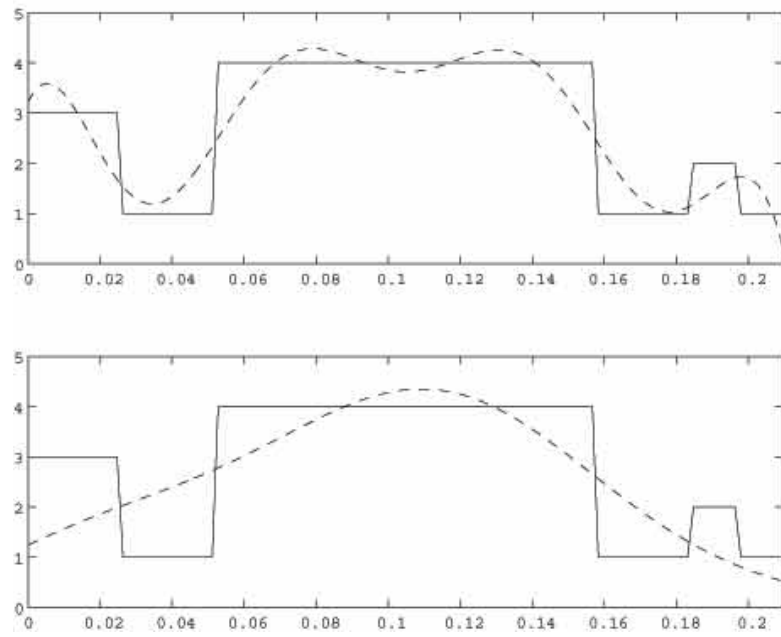
Figure 3.1: The non-iterative band-limited extrapolation method (MDFT) (top) and the DFT (bottom) for $N = 64$, 30 times over-sampled data.
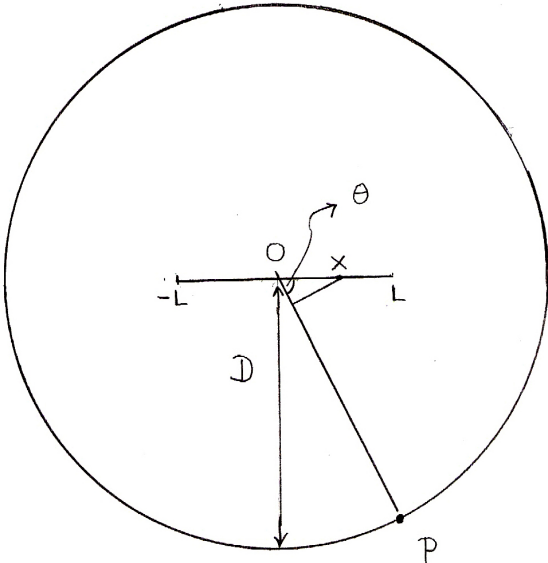
Figure 3.2: Farfield Measurements.
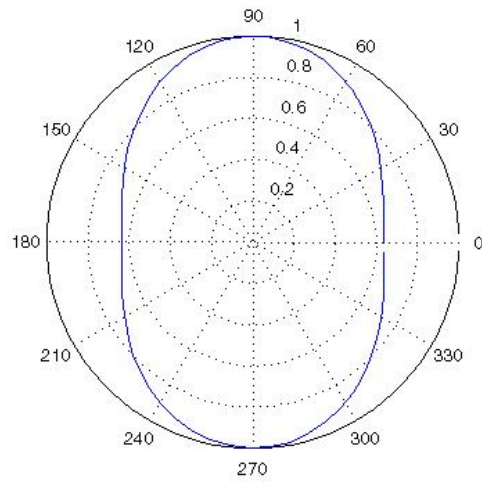
Figure 3.3: Relative strength at P for $A = 0.5$.
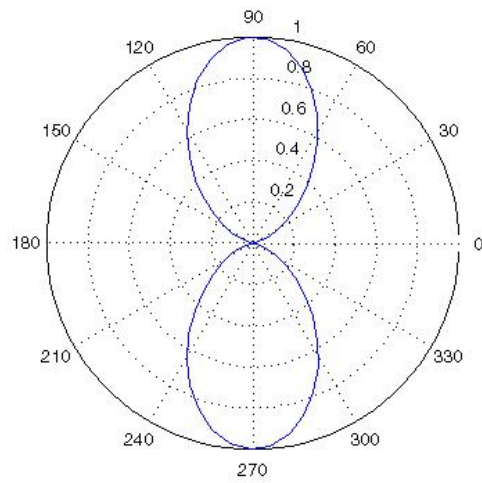
Figure 3.4: Relative strength at P for $A = 1.0$.
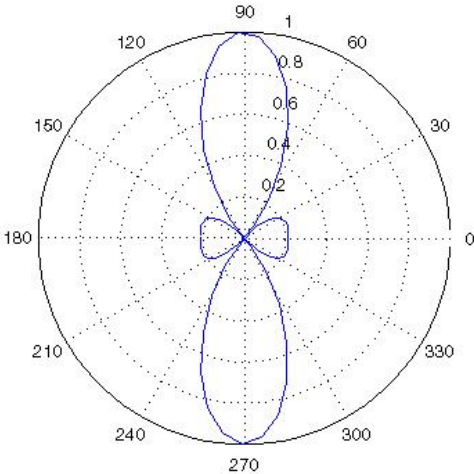
Figure 3.5: Relative strength at P for $A = 1.5$.
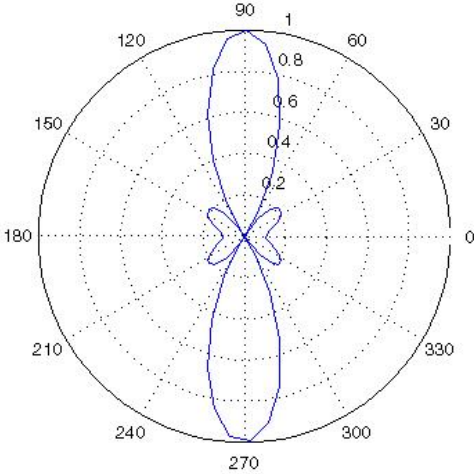
Figure 3.6: Relative strength at P for $A = 1.8$.
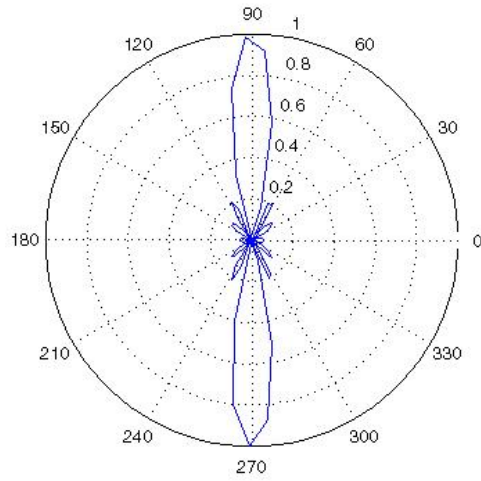
Figure 3.7: Relative strength at P for $A = 3.2$.
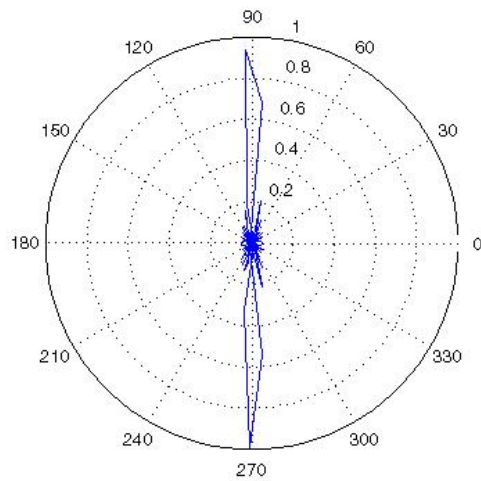
Figure 3.8: Relative strength at P for $A = 6.5$.

Part III

Signal Models

Chapter 4

Undetermined-Parameter Models

4.1 Chapter Summary

All of the techniques discussed in this book deal, in one way or another, with one fundamental problem: estimate the values of a function $f(x)$ from finitely many (usually noisy) measurements related to $f(x)$; here x can be a multi-dimensional vector, so that f can be a function of more than one variable. To keep the notation relatively simple here, we shall assume, throughout this chapter, that x is a real variable, but all of what we shall say applies to multi-variate functions as well.

4.2 Fundamental Calculations

In this section we present the two most basic calculational problems in signal processing. Both problems concern a real *trigonometric polynomial* $f(x)$, with

$$f(x) = \frac{1}{2}a_0 + \sum_{k=1}^{K} a_k \cos(kx) + b_k \sin(kx). \tag{4.1}$$

After we have discussed the complex exponential functions, we shall revisit the material in this section, using complex numbers. Then it will become clear why we call such functions trigonometric polynomials.

4.2.1   Evaluating a Trigonometric Polynomial

This function $f(x)$ is 2π-periodic, so we need to study it only over one period. For that reason, we shall restrict the variable x to the interval $[0, 2\pi]$. Now let $N = 2K + 1$, and

$$x_n = \frac{2\pi}{N}n,$$

for $n = 0, 1, ..., N - 1$. We define $f_n = f(x_n)$. The computational problem is to calculate the N real numbers f_n, knowing the N real numbers a_0 and a_k and b_k, for $k = 1, ..., K$.

This problem may seem trivial, and it is, in a sense. All we need to do is to write

$$f_n = \frac{1}{2}a_0 + \sum_{k=1}^{K} a_k \cos(\frac{2\pi}{N}nk) + b_k \sin(\frac{2\pi}{N}nk), \tag{4.2}$$

and compute the sum of the right side, for each $n = 0, 1, ..., N - 1$. The problem is that, in most practical applications, the N is very large, calculating each sum requires N multiplications, and there are N such sums to be evaluated. So this is an "N-squared problem" . As we shall see later, the fast Fourier transform (FFT) can be used to accelerate these calculations.

4.2.2   Determining the Coefficients

Now we reverse the problem. Suppose that we have determined the values f_n, say from measurements, and we want to find the coefficients a_0 and a_k and b_k, for $k = 1, ..., K$. Again we have

$$f_n = \frac{1}{2}a_0 + \sum_{k=1}^{K} a_k \cos(\frac{2\pi}{N}nk) + b_k \sin(\frac{2\pi}{N}nk), \tag{4.3}$$

only now it is the left side of each equation that we know. This problem is also trivial, in a sense; all we need to do is to solve this system of linear equations. Again, it is the size of N that is the problem, and again the FFT comes to the rescue.

In the next section we discuss two examples that lead to these calculational problems. Then we show how trigonometric identities can be used to obtain a type of orthogonality for finite sums of trig functions. This orthogonality will provide us with a quicker way to determine the coefficients. It will reduce the problem of solving the N by N system of linear equations to the simpler problem of evaluation discussed in the previous section. But we can simplify even further, as we shall see in our discussion of the FFT.

4.3   Two Examples

Signal processing begins with measurements. The next step is to use these measurements to perform various calculations. We consider two examples.

4.3.1   The Unknown Strength Problem

In our discussion of remote sensing we saw that, if each point x in the interval $[-L, L]$ is emitting a signal $f(x) \sin \omega t$, and $f(x)$ has the Fourier series expansion

$$f(x) = \frac{1}{2}a_0 + \sum_{k=1}^{\infty} a_k \cos(\frac{k\pi}{L}x) + b_k \sin(\frac{k\pi}{L}x), \qquad (4.4)$$

then, by measuring the propagating signals in the far-field, we can determine the Fourier coefficients a_k and b_k, for $k = 0, 1, 2, ..., K$, where K is the largest positive integer such that

$$K \le \frac{L\omega}{\pi c}.$$

Once we have these a_k and b_k, we can approximate $f(x)$ by calculating the finite sum

$$f_{DFT}(x) = \frac{1}{2}a_0 + \sum_{k=1}^{K} a_k \cos(\frac{k\pi}{L}x) + b_k \sin(\frac{k\pi}{L}x). \qquad (4.5)$$

To plot this approximation or to make use of it in some way, we need to evaluate $f_{DFT}(x)$ for some finite set of values of x.

   To evaluate this function at a single x requires $2K + 1$ multiplications. If K is large, and there are many x at which we wish to evaluate $f_{DFT}(x)$, then we must perform quite a few multiplications. The *fast Fourier transform* (FFT) algorithm, which we shall study later, is a fast method for obtaining these evaluations.

   Suppose, for example, that we choose to evaluate $f_{DFT}(x)$ at $N = 2K + 1$ values of x, equi-spaced within the interval $[-L, L]$; in other words, we evaluate $f_{DFT}(x)$ at the points

$$x_n = -L + \frac{2L}{N}n,$$

for $n = 0, 1, ..., N - 1$. Using trig identities, we can easily show that

$$f_{DFT}(x_n) = \frac{1}{2}a_0 + \sum_{k=1}^{K} a_k(-1)^k \cos(\frac{2\pi}{N}kn) + b_k(-1)^k \sin(\frac{2\pi}{N}kn). \quad (4.6)$$

4.3.2   Sampling in Time

Much of signal processing begins with taking samples, or evaluations, of a function of time. Let $f(t)$ be the function we are interested in, with the variable t denoting time. To learn about $f(t)$, we evaluate it at, say, the points $t = t_n$, for $n = 1, 2, ..., N$, so that our data are the N numbers $f(t_n)$.

Our ultimate objective may be to estimate a value of $f(t)$ that we haven't measured, perhaps to predict a future value of the function, or to fill in values of $f(t)$ for t between the t_n at which we have measurements.

It may be the case that the function $f(t)$ represents sound, someone singing or speaking, perhaps, and contains noise that we want to remove, if we can. In such cases, we think of $f(t)$ as $f(t) = s(t) + v(t)$, where $v(t)$ is the noise function, and $s(t)$ is the clear signal that we want. Then we may want to use all the values $f(t_n)$ to estimate $s(t)$ at some finite number of values of t, not necessarily the same t_n at which we have measured $f(t)$.

To estimate $f(t)$ from the sampled values, we often use signal models. These models are functions with finitely many unknown parameters, which are to be determined from the samples. For example, we may wish to think of the function $f(t)$ as made up of some finite number of sines and cosines; then

$$f(t) = \frac{1}{2}a_0 + \sum_{k=1}^{K} \Big(a_k \cos(\omega_k t) + b_k \sin(\omega_k t) \Big), \tag{4.7}$$

where the ω_k are chosen by us and, therefore, known, but the a_k and b_k are not known. Now the goal is to use the N data points $f(t_n)$ to determine the a_k and b_k. Once again, if N and K are large, this can be computationally costly. As with the previous problem, the FFT can help us here.

4.3.3   The Issue of Units

When we write $\cos \pi = -1$, it is with the understanding that π is a measure of angle, in radians; the function cos will always have an independent variable in units of radians. Therefore, when we write $\cos(x\omega)$, we understand the product $x\omega$ to be in units of radians. If x is measured in seconds, then ω is in units of radians per second; if x is in meters, then ω is in units of radians per meter. When x is in seconds, we sometimes use the variable $\frac{\omega}{2\pi}$; since 2π is then in units of radians per cycle, the variable $\frac{\omega}{2\pi}$ is in units of cycles per second, or Hertz. When we sample $f(x)$ at values of x spaced Δ apart, the Δ is in units of x-units per sample, and the reciprocal, $\frac{1}{\Delta}$, which is called the *sampling frequency*, is in units of samples per x-units. If x is in seconds, then Δ is in units of seconds per sample, and $\frac{1}{\Delta}$ is in units of samples per second.

4.4   Estimation and Models

Our measurements, call them d_m, for $m = 1, ..., M$, can be actual values of $f(x)$ measured at several different values of x, or the measurements can take the form of *linear functional* values:

$$d_m = \int f(x) g_m(x) dx,$$

for known functions $g_m(x)$. For example, we could have Fourier cosine transform values of $f(x)$,

$$d_m = \int_{-\infty}^{\infty} f(x) \cos(\omega_m x) dx,$$

or Fourier sine transform values of $f(x)$,

$$d_m = \int_{-\infty}^{\infty} f(x) \sin(\omega_m x) dx,$$

where the ω_m are known real constants, or Laplace transform values

$$d_m = \int_0^{\infty} f(x) e^{-s_m x} dx,$$

where the $s_m > 0$ are known constants. The point to keep in mind is that the number of measurements is finite, so, even in the absence of measurement error or noise, the data are not usually sufficient to single out precisely one function $f(x)$. For this reason, we think of the problem as *approximating* or *estimating* $f(x)$, rather than *finding* $f(x)$.

The process of approximating or estimating the function $f(x)$ often involves making simplifying assumptions about the algebraic form of $f(x)$. For example, we may assume that $f(x)$ is a polynomial, or a finite sum of trigonometric functions. In such cases, we are said to be *adopting a model* for $f(x)$. The models involve finitely many as yet unknown parameters, which we can determine from the data by solving systems of equations.

In the next section we discuss briefly the polynomial model, and then turn to a more detailed treatment of trigonometric models. In subsequent chapters we focus on the important topic of complex exponential-function models, which combine features of polynomial models and trigonometric models.

4.5   A Polynomial Model

A fundamental problem in signal processing is to extract information about a function $f(x)$ from finitely many values of that function. One way to solve

the problem is to model the function $f(x)$ as a member of a parametric family of functions. For example, suppose we have the measurements $f(x_n)$, for $n = 1, ..., N$, and we model $f(x)$ as a polynomial of degree $N - 1$, so that

$$f(x) = a_0 + a_1 x + a_2 x^2 + ... + a_{N-1} x^{N-1} = \sum_{k=0}^{N-1} a_k x^k,$$

for some coefficients a_k to be determined. Inserting the known values, we find that we must solve the system of N equations in N unknowns given by

$$f(x_n) = a_0 + a_1 x_n + a_2 x_n^2 + ... + a_{N-1} x_n^{N-1} = \sum_{k=0}^{N-1} a_k x_n^k,$$

for $n = 1, ..., N$. In theory, this is simple; all we need to do is to use MAT-LAB or some similar software that includes routines to solve such systems. In practice, the situation is usually more complicated, in that the system may be ill-conditioned and the solution highly sensitive to errors in the measurements $f(x_n)$; this will be the case if the x_n are not well separated. It is unwise, in such cases, to use as many parameters as we have data. For example, if we have reason to suspect that the function $f(x)$ is actually linear, we can do linear regression. When there are fewer parameters than measurements, we usually calculate a least-squares solution for the system of equations.

At this stage in our discussion, however, we shall ignore these practical problems and focus on the use of finite-parameter models.

4.6   Linear Trigonometric Models

Another popular finite-parameter model is to consider $f(x)$ as a finite sum of trigonometric functions.

Suppose that we have the values $f(x_n)$, for N values $x = x_n$, $n = 1, ..., N$, where, for convenience, we shall assume that $N = 2K + 1$ is odd. It is not uncommon to assume that $f(x)$ is a function of the form

$$f(x) = \frac{1}{2} a_0 + \sum_{k=1}^{K} \Big(a_k \cos(\omega_k x) + b_k \sin(\omega_k x) \Big), \tag{4.8}$$

where the ω_k are chosen by us and, therefore, known, but the a_k and b_k are not known. It is sometimes the case that the data values $f(x_n)$ are used to help us select the values of ω_k prior to using the model for $f(x)$ given by Equation (4.8); the problem of determining the ω_k from data will be discussed later, when we consider Prony's method.

Once again, we find the unknown a_k and b_k by fitting the model to the data. We insert the data $f(x_n)$ corresponding to the N points x_n, and we solve the system of N linear equations in N unknowns,

$$f(x_n) = \frac{1}{2}a_0 + \sum_{k=1}^{K} \Big(a_k \cos(\omega_k x_n) + b_k \sin(\omega_k x_n) \Big),$$

for $n = 0, ..., N - 1$, to find the a_k and b_k. When K is large, calculating the coefficients can be time-consuming. One particular choice for the x_n and ω_k reduces the computation time significantly.

4.6.1   Equi-Spaced Frequencies

It is often the case in signal processing that the variable x is time, in which case we usually replace the letter x with the letter t. The variables ω_k are then *frequencies*. When the variable x represents distance along its axis, the ω_k are called *spatial frequencies*. Here, for convenience, we shall refer to the ω_k as frequencies, without making any assumptions about the nature of the variable x.

Unless we have determined the frequencies ω_k from our data, or have prior knowledge of which frequencies ω_k are involved in the problem, it is convenient to select the ω_k equi-spaced within some interval. The simplest choice, from an algebraic stand-point, is $\omega_k = k$, with appropriately chosen units. Then our model becomes

$$f(x) = \frac{1}{2}a_0 + \sum_{k=1}^{K} \Big(a_k \cos(kx) + b_k \sin(kx) \Big). \tag{4.9}$$

The function $f(x)$ is then 2π-periodic, so we restrict the variable x to the interval $[0, 2\pi]$, which is one full period. The goal is still the same: calculate the coefficients from the values $f(x_n)$, $n = 0, 1, ..., N-1$, where $N = 2K+1$; this involves solving a system of N linear equations in N unknowns, which is computationally expensive when N is large. For particular choices of the x_n the computational cost can be considerably reduced.

4.6.2   Equi-Spaced Sampling

It is often the case that we can choose the x_n at which we evaluate the function $f(x)$. We suppose now that we have selected $x_n = n\Delta$, for $\Delta = \frac{2\pi}{N}$ and $n = 0, ..., N - 1$. In keeping with the common notation, we write $f_n = f(n\Delta)$ for $n = 0, ..., N - 1$. Then we have to solve the system

$$f_n = \frac{1}{2}a_0 + \sum_{k=1}^{K} \Big(a_k \cos(\frac{2\pi}{N}kn) + b_k \sin(\frac{2\pi}{N}kn) \Big), \tag{4.10}$$

for $n = 0, ..., N - 1$, to find the N coefficients a_0 and a_k and b_k, for $k = 1, ..., K$.

4.7 Recalling Fourier Series

4.7.1 Fourier Coefficients

In the study of Fourier series we encounter models having the form in Equation (4.9). The function $f(x)$ in that equation is 2π-periodic, and when we want to determine the coefficients, we integrate:

$$a_k = \frac{1}{\pi} \int_0^{2\pi} f(x) \cos(kx) dx, \tag{4.11}$$

and

$$b_k = \frac{1}{\pi} \int_0^{2\pi} f(x) \sin(kx) dx. \tag{4.12}$$

It is the mutual orthogonality of the functions $\cos(kx)$ and $\sin(kx)$ over the interval $[0, 2\pi]$ that enables us to write the values of the coefficients in such a simple way.

To determine the coefficients this way, we need to know the function $f(x)$ ahead of time, since we have to be able to calculate the integrals, or these integrals must be among the measurements we have taken. When all we know about $f(x)$ are its values at finitely many values of x, we cannot find the coefficients this way. As we shall see shortly, we can still exploit a type of orthogonality to obtain a relatively simple expression for the coefficients in terms of the sampled values of $f(x)$.

4.7.2 Riemann Sums

Suppose that we have obtained the values of the function $f(x)$ at the N points $\frac{2\pi n}{N}$, for $n = 0, 1, ..., N - 1$. We can get at least approximate values of the a_k and b_k by replacing the integrals in Equations (4.11) and (4.12) with Riemann sums. Then these integrals are replaced by the sums

$$\frac{1}{\pi} \int_0^{2\pi} f(x) \cos(kx) dx \approx \frac{2}{N} \sum_{n=0}^{N-1} f(\frac{2\pi n}{N}) \cos(\frac{2\pi}{N} nk), \tag{4.13}$$

and

$$\frac{1}{\pi} \int_0^{2\pi} f(x) \sin(kx) dx \approx \frac{2}{N} \sum_{n=0}^{N-1} f(\frac{2\pi n}{N}) \sin(\frac{2\pi}{N} nk). \tag{4.14}$$

What is remarkable here is that these sums give us the a_k and b_k exactly, not just approximately, when we select $N = 2K + 1$, so that the number of values of $f(x)$ is the same as the number of unknown coefficients we are attempting to find. This happens because there is a type of orthogonality for these finite sums of trigonometric functions that is analogous to the integral orthogonality of the trig functions. The details are in the next section.

4.8 Simplifying the Calculations

As we shall see in this section, choosing $N = 2K + 1$, $\omega_k = k$ and $\Delta = \frac{2\pi}{N}$ leads to a form of orthogonality that will allow us to calculate the parameters in a relatively simple manner. Because the function in Equation (4.9) is 2π-periodic, the measurements $f(n\Delta)$, $n = 0, 1, ..., N - 1$ will be repeated if we continue to sample $f(x)$ at points $n\Delta$, for $n > N - 1$.

4.8.1 The Main Theorem

As we remarked earlier, when we replace the integrals in Equations (4.11) and (4.12) with the particular Riemann sum approximations in Equations (4.13) and (4.14), we do not get approximate values of the a_k and b_k; we get the exact values.

We can view the Riemann sums another way. To calculate the Fourier coefficients in Equation (4.4), we multiply both sides of the equation by a sine or cosine function and integrate over x; orthogonality does the rest. Now we multiply each side of Equation (4.10) by a sine or cosine and sum over n; orthogonality does the rest once again.

For fixed $j = 1, ..., K$ consider the sums

$$\sum_{n=0}^{N-1} f_n \cos(\frac{2\pi}{N} jn)$$

and

$$\sum_{n=0}^{N-1} f_n \sin(\frac{2\pi}{N} jn).$$

Replacing f_n with the right side of Equation (4.10), we get

$$\sum_{n=0}^{N-1} f_n \cos(\frac{2\pi}{N} jn) = \frac{1}{2} a_0 \sum_{n=0}^{N-1} \cos(\frac{2\pi}{N} jn)$$

$$+ \sum_{k=1}^{K} \left(a_k \left(\sum_{n=0}^{N-1} \cos(\frac{2\pi}{N} kn) \cos(\frac{2\pi}{N} jn) \right) \right)$$

$$+b_k\Big(\sum_{n=0}^{N-1}\sin(\frac{2\pi}{N}kn)\cos(\frac{2\pi}{N}jn)\Big)\bigg), \tag{4.15}$$

and

$$\sum_{n=0}^{N-1}f_n\sin(\frac{2\pi}{N}jn) = \frac{1}{2}a_0\sum_{n=0}^{N-1}\sin(\frac{2\pi}{N}jn)$$

$$+\sum_{k=1}^{K}\bigg(a_k\Big(\sum_{n=0}^{N-1}\cos(\frac{2\pi}{N}kn)\sin(\frac{2\pi}{N}jn)\Big)$$

$$+b_k\Big(\sum_{n=0}^{N-1}\sin(\frac{2\pi}{N}kn)\sin(\frac{2\pi}{N}jn)\Big)\bigg). \tag{4.16}$$

Our main goal is the proof of the next theorem, which will follow immediately from Lemma 4.1.

Theorem 4.1 *The trigonometric coefficients can be found using the following formulas:*

$$\sum_{n=0}^{N-1}f_n = \frac{N}{2}a_0,$$

$$\sum_{n=0}^{N-1}f_n\cos(\frac{2\pi}{N}nj) = \frac{N}{2}a_j,$$

and

$$\sum_{n=0}^{N-1}f_n\sin(\frac{2\pi}{N}nj) = \frac{N}{2}b_j,$$

for $j = 1, ..., K$.

Lemma 4.1 *For $N = 2K + 1$ and $j, k = 0, 1, 2, ..., K$, we have*

$$\sum_{n=0}^{N-1}\sin(\frac{2\pi}{N}kn)\cos(\frac{2\pi}{N}jn) = 0,$$

$$\sum_{n=0}^{N-1}\cos(\frac{2\pi}{N}kn)\cos(\frac{2\pi}{N}jn) = \begin{cases} 0, & \text{if } j \neq k; \\ \frac{N}{2}, & \text{if } j = k \neq 0; \\ N, & \text{if } j = k = 0; \end{cases}$$

and

$$\sum_{n=0}^{N-1}\sin(\frac{2\pi}{N}kn)\sin(\frac{2\pi}{N}jn) = \begin{cases} 0, & \text{if } j \neq k, \text{ or } j = k = 0; \\ \frac{N}{2}, & \text{if } j = k \neq 0. \end{cases}$$

The proof of this lemma is contained in the following sequence of exercises.

4.8.2 The Proofs as Exercises

Exercise 4.1 *Using trigonometric identities, show that*

$$\cos(\frac{2\pi}{N}kn)\cos(\frac{2\pi}{N}jn) = \frac{1}{2}\Big(\cos(\frac{2\pi}{N}(k+j)n) + \cos(\frac{2\pi}{N}(k-j)n)\Big),$$

$$\sin(\frac{2\pi}{N}kn)\cos(\frac{2\pi}{N}jn) = \frac{1}{2}\Big(\sin(\frac{2\pi}{N}(k+j)n) + \sin(\frac{2\pi}{N}(k-j)n)\Big),$$

and

$$\sin(\frac{2\pi}{N}kn)\sin(\frac{2\pi}{N}jn) = -\frac{1}{2}\Big(\cos(\frac{2\pi}{N}(k+j)n) - \cos(\frac{2\pi}{N}(k-j)n)\Big).$$

Exercise 4.2 *Use trigonometric identities to show that*

$$\sin((n+\frac{1}{2})x) - \sin((n-\frac{1}{2})x) = 2\sin(\frac{x}{2})\cos(nx),$$

and

$$\cos((n+\frac{1}{2})x) - \cos((n-\frac{1}{2})x) = -2\sin(\frac{x}{2})\sin(nx).$$

Exercise 4.3 *Use the previous exercise to show that*

$$2\sin(\frac{x}{2})\sum_{n=0}^{N-1}\cos(nx) = \sin((N-\frac{1}{2})x) + \sin(\frac{x}{2}),$$

and

$$2\sin(\frac{x}{2})\sum_{n=0}^{N-1}\sin(nx) = \cos(\frac{x}{2}) - \cos((N-\frac{1}{2})x).$$

Hints: sum over $n = 0, 1, ..., N-1$ on both sides and note that

$$\sin(\frac{x}{2}) = -\sin(-\frac{x}{2}).$$

Exercise 4.4 *Use trigonometric identities to show that*

$$\sin((N-\frac{1}{2})x) + \sin(\frac{x}{2}) = 2\cos(\frac{N-1}{2}x)\sin(\frac{N}{2}x),$$

and

$$\cos\frac{x}{2} - \cos((N-\frac{1}{2})x) = 2\sin(\frac{N}{2}x)\sin(\frac{N-1}{2}x).$$

Hints: Use

$$N - \frac{1}{2} = \frac{N}{2} + \frac{N-1}{2},$$

and

$$\frac{1}{2} = \frac{N}{2} - \frac{N-1}{2}.$$

Exercise 4.5 *Use the previous exercises to show that*

$$\sin(\frac{x}{2}) \sum_{n=0}^{N-1} \cos(nx) = \sin(\frac{N}{2}x) \cos(\frac{N-1}{2}x),$$

and

$$\sin(\frac{x}{2}) \sum_{n=0}^{N-1} \sin(nx) = \sin(\frac{N}{2}x) \sin(\frac{N-1}{2}x).$$

Let m be any integer. Substituting $x = \frac{2\pi m}{N}$ in the equations in the previous exercise, we obtain

$$\sin(\frac{\pi}{N}m) \sum_{n=0}^{N-1} \cos(\frac{2\pi mn}{N}) = \sin(\pi m) \cos(\frac{N-1}{N}\pi m), \qquad (4.17)$$

and

$$\sin(\frac{\pi}{N}m) \sum_{n=0}^{N-1} \sin(\frac{2\pi mn}{N}) = \sin(\pi m) \sin(\frac{N-1}{N}\pi m). \qquad (4.18)$$

With $m = k + j$, we have

$$\sin(\frac{\pi}{N}(k+j)) \sum_{n=0}^{N-1} \cos(\frac{2\pi(k+j)n}{N}) = \sin(\pi(k+j)) \cos(\frac{N-1}{N}\pi(k+j)) \quad (4.19)$$

and

$$\sin(\frac{\pi}{N}(k+j)) \sum_{n=0}^{N-1} \sin(\frac{2\pi(k+j)n}{N}) = \sin(\pi(k+j)) \sin(\frac{N-1}{N}\pi(k+j)) \quad (4.20)$$

Similarly, with $m = k - j$, we obtain

$$\sin(\frac{\pi}{N}(k-j)) \sum_{n=0}^{N-1} \cos(\frac{2\pi(k-j)n}{N}) = \sin(\pi(k-j)) \cos(\frac{N-1}{N}\pi(k-j)) \quad (4.21)$$

and

$$\sin(\frac{\pi}{N}(k-j)) \sum_{n=0}^{N-1} \sin(\frac{2\pi(k-j)n}{N}) = \sin(\pi(k-j)) \sin(\frac{N-1}{N}\pi(k-j)) \quad (4.22)$$

Exercise 4.6 *Prove Lemma 4.1.*

4.8.3 More Computational Issues

In many applications of signal processing N, the number of measurements of the function $f(x)$, can be quite large. In the previous subsection, we found a relatively inexpensive way to find the undetermined parameters of the trigonometric model, but even this way poses computational problems when N is large. The computation of a single a_j or b_j requires N multiplications and we have to calculate $N-1$ of these parameters. Thus, the complexity of the problem is on the order of N squared. Fortunately, there is a fast algorithm, known as the *fast Fourier transform* (FFT), that enables us to perform these calculations in far fewer multiplications. We shall investigate the FFT in a later chapter, after we have discussed the complex exponential functions.

4.9 Approximation, Models, or Truth?

4.9.1 Approximating the Truth

In the unknown strength problem we are interested in the unknown function $f(x)$, with the Fourier series

$$f(x) = \frac{1}{2}a_0 + \sum_{k=1}^{\infty} a_k \cos(\frac{k\pi}{L}x) + b_k \sin(\frac{k\pi}{L}x). \qquad (4.23)$$

Because our far-field measurements only give us finitely many of its Fourier coefficients, we cannot obtain a perfect description of $f(x)$. Instead, we can try to approximate $f(x)$. One way to do this is to use the DFT:

$$f_{DFT}(x) = \frac{1}{2}a_0 + \sum_{k=1}^{K} a_k \cos(\frac{k\pi}{L}x) + b_k \sin(\frac{k\pi}{L}x). \qquad (4.24)$$

Once we have decided to use $f_{DFT}(x)$ as our approximation, we probably want to evaluate this approximation at some number of values of x, in order to plot $f_{DFT}(x)$, for example. This step is purely a calculation problem.

4.9.2 Modeling the Data

In the problem of sampling in time, we have some unknown function of time, $f(t)$, and we measure its values $f(t_n)$ at the N sampling points $t = t_n$, $n = 1, ..., N$. There are several different possible objectives that we may have at this point.

Extrapolation

We may want to estimate values of $f(t)$ at points t at which we do not have measurements; these other points may represent time in the future, for example, and we are trying to predict future values of $f(t)$. In such cases, it is common to adopt a model for $f(t)$, which is typically some function of t with finitely many as yet undetermined parameters, such as a polynomial or a sum of trig functions. We must select our model with care, particularly if the data is assumed to be noisy, as most data is. Even though we may have a large number of measurements, it may be a mistake to model $f(t)$ with as many parameters as we have data.

We do not really believe that $f(t)$ is a polynomial or a finite sum of trig functions. We may not even believe that the model is a good approximation of $f(t)$ for all values of t. We do believe, however, that adopting such a model will enable us to carry out our prediction task in a reasonably accurate way. The task may be something like predicting the temperature at noon tomorrow, on the basis of noon-time temperatures for the previous five days.

Filtering the Data

Suppose that the values $f(t_n)$ are sampled data from an old recording of a singer. We may want to clean up this digitized data, in order to be able to recapture the original sound. Now we may only desire to modify each of the values $f(t_n)$ in some way, to improve the quality. To perform this restoring task, we may model the data as samples of a finite sum of trig functions

$$f(t_n) = \frac{1}{2}a_0 + \sum_{k=1}^{K} \Big(a_k \cos(\omega_k t_n) + b_k \sin(\omega_k t_n) \Big), \tag{4.25}$$

where the frequencies ω_k are chosen by us. We then solve for the parameters a_k and b_k.

To clean up the sound, we may modify the values of the a_k and the b_k. For example, we may believe that certain of the frequencies come primarily from a noise component in the recording. To remove, or at least diminish, this component, we can reduce the associated a_k and b_k. We may feel that the original recording technology failed to capture some of the higher notes sung by the soprano. Then we can increase the values of the a_k and b_k associated with those frequencies that need to be restored. Obviously, restoring old recordings of opera singers is more involved than this, but you get the idea.

The point here is that we need not believe that the entire recording can be accurately described, or even approximated, by a finite sum of trig functions. The sum of trig functions in Equation (4.7) does give another

way to describe the measured data, and as such, another way to modify this data, namely by modifying the a_k and b_k. We do not need to believe that the entire opera can be accurately approximated by such a sum in order for this restoring procedure to be helpful.

Note that if our goal is to recapture a high note sung by the soprano, we do not really need to use samples of the function $f(t)$ that correspond to times when only the tenor was on stage singing. It would make more sense to process only those measurements taken right around the time the high note was sung by the soprano. This is *short-time* Fourier analysis, an issue that we deal with in the appendix on wavelets.

4.10   From Real to Complex

Throughout this chapter we have limited the discussion to real data and models involving only real coefficients and real-valued functions. Beginning with the next chapter, we shall turn to complex data and complex-valued models. Limiting the discussion to the real numbers comes at a price. Although complex variables may not be as familiar to the reader as real variables, there is some advantage in allowing the data and the models to be complex, as is the common practice in signal processing. The algebra is a bit simpler, in that we will no longer need to involve trigonometric identities at every turn, and the results that we shall obtain are, in some respects, better than those we obtained in this chapter.

Chapter 5

Complex Numbers

5.1 Chapter Summary

It is standard practice in signal processing to employ complex numbers whenever possible. One of the main reasons for doing this is that it enables us to represent the important sine and cosine functions in terms of complex exponential functions and to replace trigonometric identities with the somewhat simpler rules for the manipulation of exponents. In this chapter we review the basic algebra of complex numbers.

5.2 Definition and Basics

The complex numbers are the points in the x, y-plane: the complex number $z = (a, b)$ is identified with the point in the plane having $a = Re(z)$, the *real part* of z, for its x-coordinate and $b = Im(z)$, the *imaginary part* of z, for its y-coordinate. We call (a, b) the *rectangular form* of the complex number z. The *conjugate* of the complex number z is $\overline{z} = (a, -b)$. We can also represent z in its polar form: let the *magnitude* of z be $|z| = \sqrt{a^2 + b^2}$ and the *phase angle* of z, denoted $\theta(z)$, be the angle in $[0, 2\pi)$ with $\cos \theta(z) = a/|z|$. Then the *polar form* for z is

$$z = (|z| \cos \theta(z), |z| \sin \theta(z)).$$

Any complex number $z = (a, b)$ for which the imaginary part $Im(z) = b$ is zero is identified with (treated the same as) its real part $Re(z) = a$; that is, we identify a and $z = (a, 0)$. These real complex numbers lie along the x-axis in the plane, the so-called *real line*. If this were the whole story complex numbers would be unimportant; but they are not. It is the arithmetic associated with complex numbers that makes them important.

We add two complex numbers using their rectangular representations:

$$(a, b) + (c, d) = (a + c, b + d).$$

This is the same formula used to add two-dimensional vectors. We multiply complex numbers more easily when they are in their polar representations: the product of z and w has $|z||w|$ for its magnitude and $\theta(z) + \theta(w)$ modulo 2π for its phase angle. Notice that the complex number $z = (0, 1)$ has $\theta(z) = \pi/2$ and $|z| = 1$, so $z^2 = (-1, 0)$, which we identify with the real number -1. This tells us that within the realm of complex numbers the real number -1 has a square root, $i = (0, 1)$; note that $-i = (0, -1)$ is also a square root of -1.

To multiply $z = (a, b) = a + ib$ by $w = (c, d) = c + id$ in rectangular form, we simply multiply the binomials

$$(a + ib)(c + id) = ac + ibc + iad + i^2 bd$$

and recall that $i^2 = -1$ to get

$$zw = (ac - bd, bc + ad).$$

If (a, b) is real, that is, if $b = 0$, then $(a, b)(c, d) = (a, 0)(c, d) = (ac, ad)$, which we also write as $a(c, d)$. Therefore, we can rewrite the polar form for z as

$$z = |z|(\cos \theta(z), \sin \theta(z)) = |z|(\cos \theta(z) + i \sin \theta(z)).$$

We will have yet another way to write the polar form of z when we consider the complex exponential function.

Exercise 5.1 *Derive the formula for dividing one complex number in rectangular form by another (nonzero) one.*

Exercise 5.2 *Show that for any two complex numbers z and w we have*

$$|zw| \geq \frac{1}{2}(z\overline{w} + \overline{z}w). \tag{5.1}$$

Hint: *Write $|zw|$ as $|z\overline{w}|$ and $\overline{z}w$ as $\overline{z\overline{w}}$.*

Exercise 5.3 *Show that, for any constant a with $|a| \neq 1$, the function*

$$G(z) = \frac{z - \overline{a}}{1 - az}$$

has $|G(z)| = 1$ whenever $|z| = 1$.

5.3   Complex Numbers as Matrices

The rules for multiplying and dividing two complex numbers may seem a bit ad hoc; everything works out in the end, but there seems to be a lack of motivation for the definitions. In this section we take a different approach to complex numbers, thinking of them as special two-by-two matrices. From this perspective, multiplication and division of complex numbers become the usual matrix multiplication and multiplication by the inverse, respectively.

Let $\mathcal{K}$ be the set of all two-by-two real matrices having the form

$$Z = \begin{bmatrix} a & -b \\ b & a \end{bmatrix}, \tag{5.2}$$

where a and b are any real numbers. Let $\mathcal{R}$ be the subset of $\mathcal{K}$ consisting of those matrices for which $b = 0$. Clearly, if we make the natural association between the real numbers a and c and the matrices

$$A = \begin{bmatrix} a & 0 \\ 0 & a \end{bmatrix}$$

and

$$C = \begin{bmatrix} c & 0 \\ 0 & c \end{bmatrix},$$

respectively, then the product AC of the two matrices is in $\mathcal{R}$ and is naturally associated with the real number ac. In fact, the set $\mathcal{R}$, with the usual matrix operations, is *isomorphic* to the set of real numbers, which means that any differences between the two sets are merely superficial. In the exercises that follow, we shall study the isomorphism between the set $\mathcal{K}$ and the set of complex numbers.

Exercise 5.4   • **a.** *Show that multiplying a matrix Z by a matrix of the form*

$$D = \begin{bmatrix} d & 0 \\ 0 & d \end{bmatrix}$$

gives the matrix dZ.

• **b.** *Let $z = a + bi$ be the complex number naturally associated with the matrix Z, and $w = c + di$ the complex number associated with the matrix*

$$W = \begin{bmatrix} c & -d \\ d & c \end{bmatrix}.$$

Show that the matrix ZW is a member of $\mathcal{K}$ and is associated with the complex number zw.

Exercise 5.5 *The matrix naturally associated with the real number* 1 *is the identity matrix*

$$I = \begin{bmatrix} 1 & 0 \\ 0 & 1 \end{bmatrix},$$

since $a = 1$ *and* $b = 0$. *Show that the matrix naturally associated with the purely imaginary number* $i = 0 + 1i$, *the matrix*

$$E = \begin{bmatrix} 0 & -1 \\ 1 & 0 \end{bmatrix},$$

has the property that $E^2 = -I$, *so* E *is the square root of the matrix* $-I$, *just as* i *is the square root of* -1.

Exercise 5.6 *Relate the formula for the inverse of* Z *to the formula for dividing a non-zero complex number by* z. *Note that the non-zero* z *are naturally associated with the invertible matrices* Z *in* $\mathcal{K}$.

Exercise 5.7 *Show that multiplying a two-dimensional column vector* $(x, y)^T$ *by the matrix*

$$R_\theta = \begin{bmatrix} \cos\theta & -\sin\theta \\ \sin\theta & \cos\theta \end{bmatrix}$$

rotates the vector $(x, y)^T$ *counter-clockwise through an angle* θ, *so that multiplying a complex number* $z = a + bi$ *by the complex number* $\cos\theta + i\sin\theta$ *rotates* z *the same way.*

Chapter 6

Complex Exponential Functions

6.1 Chapter Summary

In signal processing, we are concerned with extracting information from measured data. Often, the data are values of some underlying function of one or several real variables. This function of interest may be the sum of several simpler component functions from parameterized families and the information we seek pertains to the number of these components and the values of their parameters. For example, the function may be the sum of trigonometric functions, each with an amplitude, a frequency and a phase. For reasons of notational and computational convenience, such trigonometric functions are often replaced by *complex exponential* functions, the main topic of this chapter.

6.2 The Complex Exponential Function

The most important function in signal processing is the complex-valued function of the real variable x defined by

$$h(x) = \cos(x) + i\sin(x). \tag{6.1}$$

For reasons that will become clear shortly, this function is called the *complex exponential function*. Notice that the magnitude of the complex number $h(x)$ is always equal to one, since $\cos^2(x) + \sin^2(x) = 1$ for all real x. Since the functions $\cos(x)$ and $\sin(x)$ are 2π-periodic, that is, $\cos(x+2\pi) = \cos(x)$ and $\sin(x+2\pi) = \sin(x)$ for all x, the complex exponential function $h(x)$ is also 2π-periodic.

6.2.1   Real Exponential Functions

In calculus we encounter functions of the form $g(x) = a^x$, where $a > 0$ is an arbitrary constant. These functions are the *exponential* functions, the most well-known of which is the function $g(x) = e^x$. Exponential functions are those with the property

$$g(u + v) = g(u)g(v) \tag{6.2}$$

for every u and v. Recall from calculus that for exponential functions $g(x) = a^x$ with $a > 0$ the derivative $g'(x)$ is

$$g'(x) = a^x \ln(a) = g(x)\ln(a). \tag{6.3}$$

Now we consider the function $h(x)$ in light of these ideas.

6.2.2   Why is $h(x)$ an Exponential Function?

We show now that the function $h(x)$ in Equation (6.1) has the property given in Equation (6.2), so we have a right to call it an exponential function; that is, $h(x) = c^x$ for some constant c. Since $h(x)$ has complex values, the constant c cannot be a real number, however.

Calculating $h(u)h(v)$, we find

$$h(u)h(v) = (\cos(u)\cos(v) - \sin(u)\sin(v)) + i(\cos(u)\sin(v) + \sin(u)\cos(v))$$

$$= \cos(u + v) + i\sin(u + v) = h(u + v).$$

So $h(x)$ is an exponential function; $h(x) = c^x$ for some complex constant c. Inserting $x = 1$, we find that c is

$$c = \cos(1) + i\sin(1).$$

Let's find another way to express c, using Equation (6.3). Since

$$h'(x) = -\sin(x) + i\cos(x) = i(\cos(x) + i\sin(x)) = ih(x),$$

we conjecture that $\ln(c) = i$; but what does this mean?

For $a > 0$ we know that $b = \ln(a)$ means that $a = e^b$. Therefore, we say that $\ln(c) = i$ means $c = e^i$; but what does it mean to take e to a complex power? To define e^i we turn to the Taylor series representation for the exponential function $g(x) = e^x$, defined for real x:

$$e^x = 1 + x + x^2/2! + x^3/3! + \dots.$$

Inserting i in place of x and using the fact that $i^2 = -1$, we find that

$$e^i = (1 - 1/2! + 1/4! - \dots) + i(1 - 1/3! + 1/5! - \dots);$$

note that the two series are the Taylor series for $\cos(1)$ and $\sin(1)$, respectively, so $e^i = \cos(1) + i\sin(1)$. Then the complex exponential function in Equation (6.1) is

$$h(x) = (e^i)^x = e^{ix}.$$

Inserting $x = \pi$, we get

$$h(\pi) = e^{i\pi} = \cos(\pi) + i\sin(\pi) = -1$$

or

$$e^{i\pi} + 1 = 0,$$

which is the remarkable relation discovered by Euler that combines the five most important constants in mathematics, e, π, i, 1, and 0, in a single equation.

Note that $e^{2\pi i} = e^{0i} = e^0 = 1$, so

$$e^{(2\pi + x)i} = e^{2\pi i}e^{ix} = e^{ix}$$

for all x.

6.2.3   What is e^z, for z complex?

We know from calculus what e^x means for real x, and now we also know what e^{ix} means. Using these we can define e^z for any complex number $z = a + ib$ by $e^z = e^{a+ib} = e^a e^{ib}$.

We know from calculus how to define $\ln(x)$ for $x > 0$, and we have just defined $\ln(c) = i$ to mean $c = e^i$. But we could also say that $\ln(c) = i(1 + 2\pi k)$ for any integer k; that is, the periodicity of the complex exponential function forces the function $\ln(x)$ to be multi-valued.

For any nonzero complex number $z = |z|e^{i\theta(z)}$, we have

$$\ln(z) = \ln(|z|) + \ln(e^{i\theta(z)}) = \ln(|z|) + i(\theta(z) + 2\pi k),$$

for any integer k. If $z = a > 0$ then $\theta(z) = 0$ and $\ln(z) = \ln(a) + i(k\pi)$ for any even integer k; in calculus class we just take the value associated with $k = 0$. If $z = a < 0$ then $\theta(z) = \pi$ and $\ln(z) = \ln(-a) + i(k\pi)$ for any odd integer k. So we can define the logarithm of a negative number; it just turns out not to be a real number. If $z = ib$ with $b > 0$, then $\theta(z) = \frac{\pi}{2}$ and $\ln(z) = \ln(b) + i(\frac{\pi}{2} + 2\pi k)$ for any integer k; if $z = ib$ with $b < 0$, then $\theta(z) = \frac{3\pi}{2}$ and $\ln(z) = \ln(-b) + i(\frac{3\pi}{2} + 2\pi k)$ for any integer k.

Adding $e^{-ix} = \cos(x) - i\sin(x)$ to e^{ix} given by Equation (6.1), we get

$$\cos(x) = \frac{1}{2}(e^{ix} + e^{-ix});$$

subtracting, we obtain

$$\sin(x) = \frac{1}{2i}(e^{ix} - e^{-ix}).$$

These formulas allow us to extend the definition of cos and sin to complex arguments z:

$$\cos(z) = \frac{1}{2}(e^{iz} + e^{-iz})$$

and

$$\sin(z) = \frac{1}{2i}(e^{iz} - e^{-iz}).$$

In signal processing the complex exponential function is often used to describe functions of time that exhibit periodic behavior:

$$h(\omega t + \theta) = e^{i(\omega t + \theta)} = \cos(\omega t + \theta) + i\sin(\omega t + \theta),$$

where the *frequency* ω and *phase angle* θ are real constants and t denotes time. We can alter the magnitude by multiplying $h(\omega t + \theta)$ by a positive constant $|A|$, called the *amplitude*, to get $|A|h(\omega t + \theta)$. More generally, we can combine the amplitude and the phase, writing

$$|A|h(\omega t + \theta) = |A|e^{i\theta}e^{i\omega t} = Ae^{i\omega t},$$

where A is the complex amplitude $A = |A|e^{i\theta}$. Many of the functions encountered in signal processing can be modeled as linear combinations of such complex exponential functions or *sinusoids*, as they are often called.

6.3   Complex Exponential Signal Models

In a previous chapter we considered signal models $f(x)$ that are sums of trigonometric functions;

$$f(x) = \frac{1}{2}a_0 + \sum_{k=1}^{L}\Big(a_k\cos(\omega_k x) + b_k\sin(\omega_k x)\Big), \tag{6.4}$$

where the ω_k are known, but the a_k and b_k are not. Now that we see how to convert sines and cosines to complex exponential functions, using

$$\cos(\omega_k x) = \frac{1}{2}\Big(\exp(i\omega_k x) + \exp(-i\omega_k x)\Big) \tag{6.5}$$

and

$$\sin(\omega_k x) = \frac{1}{2i}\Big(\exp(i\omega_k x) - \exp(-i\omega_k x)\Big), \tag{6.6}$$

we can write $f(x)$ as

$$f(x) = \sum_{m=-L}^{L} c_m \exp(i\omega_m x), \tag{6.7}$$

where $c_0 = \frac{1}{2}a_0$,

$$c_k = \frac{1}{2}(a_k - ib_k), \tag{6.8}$$

and

$$c_{-k} = \frac{1}{2}(a_k + ib_k), \tag{6.9}$$

for $k = 1, ..., L$. Note that if the original coefficients a_k and b_k are real numbers, then $c_{-m} = \overline{c_m}$.

6.4 Coherent and Incoherent Summation

We begin this section with an exercise.

Exercise 6.1 *On a blank sheet of paper, draw a horizontal and vertical axis. Starting at the origin, draw a vector with length one unit (a unit can be, say, one inch), in an arbitrary direction. Now, from the tip of the first vector, draw another vector of length one, again in an arbitrary direction. Repeat this process several times, using M vectors in all. Now measure the distance from the origin to the tip of the last vector drawn. Compare this length with the number M, which would be the distance from the origin to the tip of the last vector, if all the vectors had had the same direction.*

This exercise reveals the important difference between *coherent* and *incoherent summation*, or, if you will, between constructive and destructive interference. Each of the unit vectors drawn can be thought of as a complex number $e^{i\theta_m}$, where θ_m is its arbitrary angle. The distance from the origin to the tip of the last vector drawn is then

$$|e^{i\theta_1} + e^{i\theta_2} + ... + e^{i\theta_M}|. \tag{6.10}$$

If all the angles θ_m are equal, then this distance is M; in all other cases the distance is quite a bit less than M. The distinction between coherent and incoherent summation plays a central role in signal processing, as well as in quantum physics, as we discuss briefly in the next section.

6.5 Uses in Quantum Electrodynamics

In his experiments with light, Newton discovered the phenomenon of *partial reflection*. The proportion of the light incident on a glass surface that is reflected varies with the thickness of the glass, but the proportion oscillates between zero and about sixteen percent as the glass thickens. He tried to explain this puzzling behavior, but realized that he had not obtained a

satisfactory explanation. In his beautiful small book "QED: The Strange Theory of Light and Matter" [108], the physicist Richard Feynman illustrates how the quantum theory applied to light, *quantum electrodynamics* or *QED*, can be used to unravel many phenomena involving the interaction of light with matter, including the partial reflection observed by Newton, the *least time* principle, the array of colors we see on the surface of an oily mud puddle, and so on. He is addressing an audience of non-physicists, including even some non-scientists, and avoids mathematics as much as possible. The one mathematical notion that he uses repeatedly is the addition of two-dimensional vectors pointing in a variety of directions, that is, coherent and incoherent summation. The vector sum is the *probability amplitude* of the event being discussed, and the square of its length is the probability of the event.

6.6   Using Coherence and Incoherence

Suppose we are given as data the M complex numbers $d_m = e^{im\gamma}$, for $m = 1, ..., M$, and we are asked to find the real number γ. We can exploit the ideas of the previous section to get our answer.

First of all, from the data we have been given, we cannot distinguish γ from $\gamma + 2\pi$, since, for all integers m

$$e^{im(\gamma+2\pi)} = e^{im\gamma}e^{2m\pi i} = e^{im\gamma}(1) = e^{im\gamma}.$$

Therefore, we assume, from the beginning, that the γ we want to find lies in the interval $[-\pi, \pi)$. Note that we could have selected any interval of length 2π, not necessarily $[-\pi, \pi)$; if we have no prior knowledge of where γ is located, the intervals $[-\pi, \pi)$ or $[0, 2\pi)$ are the most obvious choices.

6.6.1   The Discrete Fourier Transform

Now we take any value ω in the interval $[-\pi, \pi)$, multiply each of the numbers d_m by $e^{-im\omega}$, and sum over m to get

$$DFT_{\mathbf{d}}(\omega) = \sum_{m=1}^{M} d_m e^{-im\omega}. \tag{6.11}$$

The sum we denote by $DFT_{\mathbf{d}}$ will be called the *discrete Fourier transform* (DFT) of the data (column) vector $\mathbf{d} = (d_1, ..., d_M)^T$. We define the column vector $\mathbf{e}_\omega$ to be

$$\mathbf{e}_\omega = (e^{i\omega}, e^{2i\omega}, ..., e^{iM\omega})^T, \tag{6.12}$$

which allows us to write $DFT_{\mathbf{d}} = \mathbf{e}_\omega^\dagger \mathbf{d}$, where the dagger denotes conjugate transformation of a matrix or vector.

Rewriting the exponential terms in the sum in Equation (6.11), we obtain

$$DFT_{\mathbf{d}}(\omega) = \sum_{m=1}^{M} d_m e^{-im\omega} = \sum_{m=1}^{M} e^{im(\gamma-\omega)}. \tag{6.13}$$

Performing this calculation for each ω in the interval $[-\pi, \pi)$, we obtain the function $DFT_{\mathbf{d}}(\omega)$. For each ω, the complex number $DFT_{\mathbf{d}}(\omega)$ is the sum of M complex numbers, each having length one, and angle $\theta_m = m(\gamma - \omega)$. So long as ω is not equal to γ, these θ_m are all different, and $DFT_{\mathbf{d}}(\omega)$ is an incoherent sum; consequently, $|DFT_{\mathbf{d}}(\omega)|$ will be smaller than M. However, when $\omega = \gamma$, each θ_m equals zero, and $DFT_{\mathbf{d}}(\omega) = |DFT_{\mathbf{d}}(\omega)| = M$; the reason for putting the minus sign in the exponent $e^{-im\omega}$ is so that we get the term $\gamma - \omega$, which is zero when $\gamma = \omega$. We find the true γ by computing the value $|DFT_{\mathbf{d}}(\omega)|$ for finitely many values of ω, plot the result and look for the highest value. Of course, it may well happen that the true value $\omega = \gamma$ is not exactly one of the points we choose to plot; it may happen that the true γ is half way between two of the plot's grid points, for example. Nevertheless, if we know in advance that there is only one true γ, this approach will give us a good idea of its value.

In many applications, the number M will be quite large, as will be the number of grid points we wish to use for the plot. This means that the number $DFT_{\mathbf{d}}(\omega)$ is a sum of a large number of terms, and that we must calculate this sum for many values of ω. Fortunately, there is a wonderful algorithm, called the *fast Fourier transform* (FFT), that we can use for this purpose.

6.7   Some Exercises on Coherent Summation

The exercises in this section are designed to make a bit more quantitative the ideas of the previous sections pertaining to coherent and incoherent summation. The formulas obtained in these exercises will be used repeatedly throughout the text.

Exercise 6.2 *Show that if* $\sin \frac{x}{2} \neq 0$ *then*

$$E_M(x) = \sum_{m=1}^{M} e^{imx} = e^{ix(\frac{M+1}{2})} \frac{\sin(Mx/2)}{\sin(x/2)}. \tag{6.14}$$

Hint: Note that $E_M(x)$ is the sum of terms in a geometric progression;

$$E_M(x) = e^{ix} + (e^{ix})^2 + (e^{ix})^3 + ... + (e^{ix})^M = e^{ix}(1 - e^{iMx})/(1 - e^{ix}).$$

Now use the fact that, for any t, we have

$$1 - e^{it} = e^{it/2}(e^{-it/2} - e^{it/2}) = e^{it/2}(-2i)\sin(t/2).$$

Exercise 6.3 *The* Dirichlet kernel *of size M is defined as*

$$D_M(x) = \sum_{m=-M}^{M} e^{imx}.$$

Use Equation (6.14) to obtain the closed-form expression

$$D_M(x) = \frac{\sin((M + \frac{1}{2})x)}{\sin(\frac{x}{2})};$$

note that $D_M(x)$ is real-valued.

Hint: Reduce the problem to that of Exercise 6.2 by factoring appropriately.

Exercise 6.4 *Use the result in Equation (6.14) to obtain the closed-form expressions*

$$\sum_{m=N}^{M} \cos mx = \cos\left(\frac{M+N}{2}x\right)\frac{\sin(\frac{M-N+1}{2}x)}{\sin\frac{x}{2}} \tag{6.15}$$

and

$$\sum_{m=N}^{M} \sin mx = \sin\left(\frac{M+N}{2}x\right)\frac{\sin(\frac{M-N+1}{2}x)}{\sin\frac{x}{2}}. \tag{6.16}$$

Hint: Recall that $\cos mx$ and $\sin mx$ are the real and imaginary parts of e^{imx}.

Exercise 6.5 *Obtain the formulas in the previous exercise using the trigonometric identity*

$$\sin\left((n + \frac{1}{2})x\right) - \sin\left((n - \frac{1}{2})x\right) = 2\sin\left(\frac{x}{2}\right)\cos(nx).$$

Exercise 6.6 *Graph the function $E_M(x)$ for various values of M.*

We note in passing that the function $E_M(x)$ equals M for $x = 0$ and equals zero for the first time at $x = 2\pi/M$. This means that the *main lobe* of $E_M(x)$, the inverted parabola-like portion of the graph centered at $x = 0$, crosses the x-axis at $x = 2\pi/M$ and $x = -2\pi/M$, so its height is M

and its width is $4\pi/M$. As M grows larger the main lobe of $E_M(x)$ gets higher and thinner.

In the exercise that follows we examine the resolving ability of the DFT. Suppose we have M equi-spaced samples of a function $f(x)$ having the form For $f(x)$ have the form

$$f(x) = e^{ix\gamma_1} + e^{ix\gamma_2},$$

where γ_1 and γ_2 are in the interval $(-\pi, \pi)$. If M is sufficiently large, the DFT should show two peaks, at roughly the values $\omega = \gamma_1$ and $\omega = \gamma_2$. As the distance $|\gamma_2 - \gamma_1|$ grows smaller, it will require a larger value of M for the DFT to show two peaks.

Exercise 6.7 *For this exercise, we take $\gamma_1 = -\alpha$ and $\gamma_2 = \alpha$, for some α in the interval $(0, \pi)$. Select a value of M that is greater than two and calculate the values $f(m)$ for $m = 1, ..., M$. Plot the graph of the function $|DFT_{\mathbf{d}}(\omega)|$ on $(-\pi, \pi)$. Repeat the exercise for various values of M and values of α closer to zero. Notice how $DFT_{\mathbf{d}}(0)$ behaves as α goes to zero. For each fixed value of M there will be a critical value of α such that, for any smaller values of α, $DFT_{\mathbf{d}}(0)$ will be larger than $DFT_{\mathbf{d}}(\alpha)$. This is loss of resolution.*

6.8 Complications

In the real world, of course, things are not so simple. In most applications, the data comes from measurements, and so contains errors, also called *noise*. The noise terms that appear in each d_m are usually viewed as random variables, and they may or may not be independent. If the noise terms are not independent, we say that we have *correlated noise*. If we know something about the statistics of the noises, we may wish to process the data using statistical estimation methods, such as the *best linear unbiased estimator* (BLUE).

6.8.1 Multiple Signal Components

It sometimes happens that there are two or more distinct values of ω that we seek. For example, suppose the data is

$$d_m = e^{im\alpha} + e^{im\beta},$$

for $m = 1, ..., M$, where α and β are two distinct numbers in the interval $[0, 2\pi)$, and we need to find both α and β. Now the function $DFT_{\mathbf{d}}(\omega)$ will be

$$DFT_{\mathbf{d}}(\omega) = \sum_{m=1}^{M} (e^{im\alpha} + e^{im\beta}) e^{-im\omega} = \sum_{m=1}^{M} e^{im\alpha} e^{-im\omega} + \sum_{m=1}^{M} e^{im\beta} e^{-im\omega},$$

so that

$$DFT_{\mathbf{d}}(\omega) = \sum_{m=1}^{M} e^{im(\alpha - \omega)} + \sum_{m=1}^{M} e^{im(\beta - \omega)}.$$

So the function $DFT_{\mathbf{d}}(\omega)$ is the sum of the $DFT_{\mathbf{d}}(\omega)$ that we would have obtained separately if we had had only α and only β.

6.8.2   Resolution

If the numbers α and β are well separated in the interval $[0, 2\pi)$ or M is very large, the plot of $|DFT\mathbf{d}(\omega)|$ will show two high values, one near $\omega = \alpha$ and one near $\omega = \beta$. However, if the M is smaller or the α and β are too close together, the plot of $|DFT\mathbf{d}(\omega)|$ may show only one broader high bump, centered between α and β; this is loss of resolution. How close is close will depend on the value of M and where loss of resolution occurs will depend on the M

6.8.3   Unequal Amplitudes and Complex Amplitudes

It is also often the case that two two signal components, the one from α and the one from β, are not equally strong. We could have

$$d_m = Ae^{im\alpha} + Be^{im\beta},$$

where $A > B > 0$. In fact, both A and B could be complex numbers, that is, $A = |A|e^{i\theta_1}$ and $B = |B|e^{i\theta_2}$, so that

$$d_m = |A|e^{im\alpha + \theta_1} + |B|e^{im\beta + \theta_2}.$$

In stochastic signal processing, the A and B are viewed as random variables; A and B may or may not be mutually independent.

6.8.4   Phase Errors

It sometimes happens that the hardware that provides the measured data is imperfect and instead of giving us the values $d_m = e^{im\alpha}$, we get $d_m = e^{im\alpha + \phi_m}$. Now each *phase error* ϕ_m depends on m, which makes matters worse than when we had θ_1 and θ_2 previously, neither depending on the index m.

6.9   Undetermined Exponential Models

In our previous discussion, we assumed that the frequencies were known and only the coefficients needed to be determined. The problem was then a linear one. It is sometimes the case that we also want to estimate the

frequencies from the data. This is computationally more difficult and is a nonlinear problem. Prony's method is one approach to this problem.

The date of publication of [190] is often taken by editors to be a typographical error and is replaced by 1995; or, since it is not written in English, perhaps 1895. But the 1795 date is the correct one. The mathematical problem Prony solved arises also in signal processing, and his method for solving it is still used today. Prony's method is also the inspiration for the eigenvector methods described in a later chapter.

6.9.1 Prony's Problem

Prony considers a function of the form

$$f(x) = \sum_{n=1}^{N} a_n e^{\gamma_n x}, \tag{6.17}$$

where we allow the a_n and the γ_n to be complex. If we take the $\gamma_n = i\omega_n$ to be imaginary, $f(x)$ becomes the sum of complex exponentials, which we discuss later; if we take γ_n to be real, then $f(x)$ is the sum of real exponentials, either increasing or decreasing. The problem is to determine from samples of $f(x)$ the number N, the γ_n, and the a_n.

6.9.2 Prony's Method

Suppose that we have data $f_m = f(m\Delta)$, for some $\Delta > 0$ and for $m = 1, ..., M$, where we assume that $M = 2N$. We seek a vector $\mathbf{c}$ with entries c_j, $j = 0, ..., N$ such that

$$c_0 f_{k+1} + c_1 f_{k+2} + c_2 f_{k+3} + ... + c_N f_{k+N+1} = 0, \tag{6.18}$$

for $k = 0, 1, ..., M - N - 1$. So, we want a complex vector $\mathbf{c}$ in C^{N+1} orthogonal to $M - N = N$ other vectors. In matrix-vector notation we are solving the linear system

$$
\begin{bmatrix}
f_1 & f_2 & \cdots & f_{N+1} \\
f_2 & f_3 & \cdots & f_{N+2} \\
. & & & \\
. & & & \\
. & & & \\
f_N & f_{N+1} & \cdots & f_M
\end{bmatrix}
\begin{bmatrix}
c_0 \\
c_1 \\
. \\
. \\
. \\
c_N
\end{bmatrix}
=
\begin{bmatrix}
0 \\
0 \\
. \\
. \\
. \\
0
\end{bmatrix},
$$

which we write as $F\mathbf{c} = \mathbf{0}$. Since $F^\dagger F\mathbf{c} = \mathbf{0}$ also, we see that $\mathbf{c}$ is an eigenvector associated with the eigenvalue zero of the hermitian nonnegative definite matrix $F^\dagger F$; here $F^\dagger$ denotes the conjugate transpose of the matrix F.

Fix a value of k and replace each of the f_{k+j} in Equation (6.18) with the value given by Equation (6.17) to get

$$0 = \sum_{n=0}^{N} a_n [\sum_{j=0}^{N} c_j e^{\gamma_n (k+j+1)\Delta}]$$

$$= \sum_{n=0}^{N} a_n e^{\gamma_n (k+1)\Delta} [\sum_{j=0}^{N} c_j (e^{\gamma_n \Delta})^j].$$

Since this is true for each of the N fixed values of k, we conclude that the inner sum is zero for each n; that is,

$$\sum_{j=0}^{N} c_j (e^{\gamma_n \Delta})^j = 0,$$

for each n. Therefore, the polynomial

$$C(z) = \sum_{j=0}^{N} c_j z^j$$

has for its roots the N values $z = e^{\gamma_n \Delta}$. Once we find the roots of this polynomial we have the values of $e^{\gamma_n \Delta}$. If the γ_n are real, they are uniquely determined from the values $e^{\gamma_n \Delta}$, whereas, for non-real γ_n, this is not the case, as we saw when we studied the complex exponential functions.

Then, we obtain the a_n by solving a linear system of equations. In practice we would not know N so would overestimate N somewhat in selecting M. As a result, some of the a_n would be zero.

If we believe that the number N is considerably smaller than M, we do not assume that $2N = M$. Instead, we select L somewhat larger than we believe N is and then solve the linear system

$$\begin{bmatrix} f_1 & f_2 & \cdots & f_{L+1} \\ f_2 & f_3 & \cdots & f_{L+2} \\ . & & & \\ . & & & \\ . & & & \\ . & & & \\ f_{M-L} & f_{M-L+1} & \cdots & f_M \end{bmatrix} \begin{bmatrix} c_0 \\ c_1 \\ . \\ . \\ . \\ . \\ c_L \end{bmatrix} = \begin{bmatrix} 0 \\ 0 \\ . \\ . \\ . \\ 0 \\ 0 \end{bmatrix}.$$

This system has $M - L$ equations and $L + 1$ unknowns, so is quite over-determined. We would then use the least-squares approach to obtain the vector $\mathbf{c}$. Again writing the system as $F\mathbf{c} = \mathbf{0}$, we note that the matrix $F^\dagger F$ is $L+1$ by $L+1$ and has $\lambda = 0$ for its lowest eigenvalue; therefore, it is

not invertible. When there is noise in the measurements, this matrix may become invertible, but will still have at least one very small eigenvalue.

Finding the vector **c** in either case can be tricky because we are looking for a nonzero solution of a homogeneous system of linear equations. For a discussion of the numerical issues involved in these calculations, the interested reader should consult the book by Therrien [214].

Chapter 7

Transmission and Remote Sensing- II

7.1 Chapter Summary

An important example of the use of the DFT is the design of directional transmitting or receiving arrays of antennas. In this chapter we revisit transmission and remote sensing, this time with emphasis on the roles played by complex exponential functions and the DFT.

7.2 Directional Transmission

Parabolic mirrors behind car headlamps reflect the light from the bulb, concentrating it directly ahead. Whispering at one focal point of an elliptical room can be heard clearly at the other focal point. When I call to someone across the street, I cup my hands in the form of a megaphone to concentrate the sound in that direction. In all these cases the transmitted signal has acquired *directionality*. In the case of the elliptical room, not only does the soft whispering reflect off the walls toward the opposite focal point, but the travel times are independent of where on the wall the reflections occur; otherwise, the differences in time would make the received sound unintelligible. Parabolic satellite dishes perform much the same function, concentrating incoming signals coherently. In this chapter we discuss the use of amplitude and phase modulation of transmitted signals to concentrate the signal power in certain directions. Following the lead of Richard Feynman in [109], we use radio broadcasting as a concrete example of the use of directional transmission.

Radio broadcasts are meant to be received and the amount of energy that reaches the receiver depends on the amount of energy put into the

transmission as well as on the distance from the transmitter to the receiver. If the transmitter broadcasts a spherical wave front, with equal power in all directions, the energy in the signal is the same over the spherical wave-fronts, so that the energy per unit area is proportional to the reciprocal of the surface area of the front. This means that, for omni-directional broadcasting, the energy per unit area, that is, the energy supplied to any receiver, falls off as the distance squared. The amplitude of the received signal is then proportional to the reciprocal of the distance.

Returning to the example we studied previously, suppose that you own a radio station in Los Angeles. Most of the population resides along the north-south coast, with fewer to the east, in the desert, and fewer still to the west, in the Pacific Ocean. You might well want to transmit the radio signal in a way that concentrates most of the power north and south. But how can you do this? The answer is to broadcast directionally. By shaping the wavefront to have most of its surface area north and south you will enable to have the broadcast heard by more people without increasing the total energy in the transmission. To achieve this shaping you can use an array of multiple antennas.

7.3   Multiple-Antenna Arrays

7.3.1   The Array of Equi-Spaced Antennas

We place $2N + 1$ transmitting antennas a distance $\Delta > 0$ apart along an east-west axis, as shown in Figure 7.1. For convenience, let the locations of the antennas be $n\Delta$, $n = -N, ..., N$. To begin with, let us suppose that we have a fixed frequency ω and each of the transmitting antennas sends out the same signal $f_n(t) = \frac{1}{\sqrt{2N+1}} \cos(\omega t)$. With this normalization the total energy is independent of N. Let (x, y) be an arbitrary location on the ground, and let $\mathbf{s}$ be the vector from the origin to the point (x, y). Let θ be the angle measured clockwise from the positive horizontal axis to the vector $\mathbf{s}$. Let D be the distance from (x, y) to the origin. Then, if (x, y) is sufficiently distant from the antennas, the distance from $n\Delta$ on the horizontal axis to (x, y) is approximately $D - n\Delta \cos(\theta)$. The signals arriving at (x, y) from the various antennas will have traveled for different times and so will be out of phase with one another to a degree that depends on the location of (x, y).

7.3.2   The Far-Field Strength Pattern

Since we are concerned only with wavefront shape, we omit for now the distance-dependence in the amplitude of the received signal. The signal

received at (x, y) is proportional to

$$f(\mathbf{s}, t) = \frac{1}{\sqrt{2N + 1}} \sum_{n=-N}^{N} \cos(\omega(t - t_n)),$$

where

$$t_n = \frac{1}{c}(D - n\Delta \cos(\theta))$$

and c is the speed of propagation of the signal. Writing

$$\cos(\omega(t - t_n)) = \cos(\omega(t - \frac{D}{c}) + n\gamma \cos(\theta))$$

for $\gamma = \frac{\omega \Delta}{c}$, we have

$$\cos(\omega(t - t_n)) = \cos(\omega(t - \frac{D}{c})) \cos(n\gamma \cos(\theta)) - \sin(\omega(t - \frac{D}{c})) \sin(n\gamma \cos(\theta)).$$

Using Equations (6.15) and (6.16), we find that the signal received at (x, y) is

$$f(\mathbf{s}, t) = \frac{1}{\sqrt{2N + 1}} A(\theta) \cos(\omega(t - \frac{D}{c})) \tag{7.1}$$

for

$$A(\theta) = \frac{\sin((N + \frac{1}{2})\gamma \cos(\theta))}{\sin(\frac{1}{2}\gamma \cos(\theta))};$$

when the denominator equals zero the signal equals $\sqrt{2N + 1} \cos(\omega(t - \frac{D}{c}))$.

7.3.3 Can the Strength be Zero?

We see from Equation (7.1) that the maximum power is in the north-south direction. What about the east-west direction? In order to have negligible signal power wasted in the east-west direction, we want the numerator, but not the denominator, in Equation (7.1) to be zero when $\theta = 0$. This means that $\Delta = m\lambda/(2N + 1)$, where $\lambda = 2\pi c/\omega$ is the wavelength and m is some positive integer less than $2N + 1$. Recall that the wavelength for broadcast radio is tens to hundreds of meters.

Exercise 7.1 *Graph the function $A(\theta)$ in polar coordinates for various choices of N and Δ.*

Figures at the end of this chapter show that transmission pattern $A(\theta)$ for various choices of m and N. In Figure 7.2 $N = 5$ for each plot and the m changes, illustrating the effect of changing the spacing of the array elements. The plots in Figure 7.3 differ from those in Figure 7.2 only in that $N = 21$ now. In Figure 7.4 we allow the m to be less than one, showing the loss of the nulls in the east and west directions.

7.3.4   Diffraction Gratings

I have just placed on the table next to me a CD, with the shinier side up. Beyond it is a lamp. The CD acts as a mirror, and I see in the CD the reflection of the lamp. Every point of the lamp seems to be copied in a particular point on the surface of the CD, as if the ambient light that illuminates a particular point of the lamp travels only to a single point on the CD and then is reflected on into my eye. Each point of the lamp has its own special point on the CD. We know from basic optics that that point is such that the angle of incidence equals the angle of reflection, and the path (apparently) taken by the light beam is the shortest path the light can take to get from the lamp to the CD and then on to my eye. But how does the light know where to go?

In fact, what happens is that light beams take many paths from each particular point on the lamp to the CD and on to my eye. The reason I see only the one path is that all the other paths require different travel times, and so light beams on different paths arrive at my eye out of phase with one another. Only those paths very close to the one I see have travel times sufficiently similar to avoid this destructive interference. Speaking a bit more mathematically, if we define the function that associates with each path the time to travel along that path, then, at the shortest path, the *first derivative* of this function, in the sense of the calculus of variations, is zero. Therefore deviations from the shortest path correspond only to second-order changes in travel time, not first-order ones, which reduces the destructive interference.

But, as I look at the CD on the table, I see more than the reflection of the lamp. I see streaks of color also. There is a window off to the side and the sun is shining into the room through this window. When I place my hand between the CD and the window, some of the colored streaks disappear, and other colored streaks seem to appear. I am not seeing a direct reflection of the sun; it is off to the side. What is happening is that the grooves on the surface of the CD are each reflecting sunlight and acting as little transmitters. Each color in the spectrum corresponds to a particular frequency ω of light and at just the proper angle the spacing between the grooves on the CD leads to coherent transmission of the reflected light in the direction of my eye. The combination of frequency and spacing between the grooves determines what color I see and at what angle. When I reach over and tilt the CD off the table, the colors of the streaks change, because I have changed the spacing of the little transmitters, relative to my eye. An arrangement like this is called a *diffraction grating* and has many uses in physics. For a wonderful, and largely math-free, introduction to these ideas, see the book by Feynman [108].

7.4 Phase and Amplitude Modulation

In the previous section the signal broadcast from each of the antennas was the same. Now we look at what directionality can be obtained by using different amplitudes and phases at each of the antennas. Let the signal broadcast from the antenna at $n\Delta$ be

$$f_n(t) = |A_n|\cos(\omega t - \phi_n) = |A_n|\cos(\omega(t - \tau_n)),$$

for some amplitude $|A_n| > 0$ and phase $\phi_n = \omega\tau_n$. Now the signal received at $\mathbf{s}$ is proportional to

$$f(\mathbf{s}, t) = \sum_{n=-N}^{N} |A_n|\cos(\omega(t - t_n - \tau_n)). \qquad (7.2)$$

If we wish, we can repeat the calculations done earlier to see what the effect of the amplitude and phase changes is. Using complex notation simplifies things somewhat.

Let us consider a complex signal; suppose that the signal transmitted from the antenna at $n\Delta$ is $g_n(t) = |A_n|e^{i\omega(t-\tau_n)}$. Then, the signal received at location $\mathbf{s}$ is proportional to

$$g(\mathbf{s}, t) = \sum_{n=-N}^{N} |A_n|e^{i\omega(t - t_n - \tau_n)}.$$

Then we have

$$g(\mathbf{s}, t) = B(\theta)e^{i\omega(t - \frac{D}{c})}$$

for $A_n = |A_n|e^{-i\phi_n}$, $x = \frac{\omega\Delta}{c}\cos(\theta)$, and

$$B(\theta) = \sum_{n=-N}^{N} A_n e^{inx}.$$

Note that the complex amplitude function $B(\theta)$ depends on our choices of N and Δ and takes the form of a finite Fourier series or DFT. We can design $B(\theta)$ to approximate the desired directionality by choosing the appropriate complex coefficients A_n and selecting the amplitudes $|A_n|$ and phases ϕ_n accordingly. We can generalize further by allowing the antennas to be spaced irregularly along the east-west axis, or even distributed irregularly over a two-dimensional area on the ground.

7.5 Steering the Array

In our previous discussion, we selected $A_n = 1$ and $\phi_n = 0$ for all n and saw that the maximum transmitted power was along the north-to-south

axis. Suppose that we want to design a transmitting array that maximally concentrates signal power in another direction. Theoretically, we could physically rotate or steer the array until it ran along a different axis, and then proceed as before, with $A_n = 1$ and $\phi_n = 0$. This is not practical, in most cases. There is an alternative, fortunately. We can "steer" the array mathematically.

If $A_n = 1$, and

$$\phi_n = -\frac{n\Delta\omega}{c}\cos\alpha,$$

for some angle α, then, for $x = \frac{\omega\Delta}{c}\cos(\theta)$, we have

$$B(\theta) = \sum_{n=-N}^{N} e^{inx}e^{i\phi_n} = \sum_{n=-N}^{N} e^{in\frac{\omega\Delta}{c}(\cos\theta-\cos\alpha)}.$$

The maximum absolute value of $B(\theta)$ occurs when $\cos\theta = \cos\alpha$, or when $\theta = \alpha$ or $\theta = -\alpha$. Now the greatest power is concentrated in these directions. The point here is that we have altered the directionality of the transmission, not by physically moving the array of antennas, but by changing the phases of the transmitted signals. This approach is sometimes called *phase steering*. The same basic idea applies when we are receiving signals, rather than sending them. In radar and sonar, the array of sensors is steered mathematically, by modifying the phases of the measured data, to focus the sensitivity of the detecting array in a particular direction.

7.6   Maximal Concentration in a Sector

In this section we take $\Delta = \frac{\pi c}{\omega}$, so that $\frac{\omega\Delta}{c} = \pi$. Suppose that we want to concentrate the transmitted power in the directions θ corresponding to $x = \frac{\omega\Delta}{c}\cos(\theta)$ in the sub-interval $[a, b]$ of the interval $[-\frac{\omega\Delta}{c}, \frac{\omega\Delta}{c}]$. Let $\mathbf{u} = (A_{-N}, ..., A_N)^T$ be the vector of coefficients for the function

$$B(x) = \sum_{n=-N}^{N} A_n e^{-inx}.$$

We want $|B(x)|$ to be concentrated in the interval $a \leq x \leq b$.

Exercise 7.2 *Show that*

$$\frac{1}{2\pi}\int_{-\frac{\omega\Delta}{c}}^{\frac{\omega\Delta}{c}} |B(x)|^2 dx = \mathbf{u}^\dagger \mathbf{u},$$

and

$$\frac{1}{2\pi}\int_{a}^{b} |B(x)|^2 dx = \mathbf{u}^\dagger Q\mathbf{u},$$

where Q is the matrix with entries

$$Q_{mn} = \frac{1}{2\pi} \int_a^b \exp(i(m-n)x)\,dx.$$

Maximizing the concentration of power within the interval $[a, b]$ is then equivalent to finding the vector $\mathbf{u}$ that maximizes the ratio $\mathbf{u}^\dagger Q \mathbf{u} / \mathbf{u}^\dagger \mathbf{u}$. The matrix Q is positive-definite, all its eigenvalues are positive, and the optimal $\mathbf{u}$ is the eigenvector of Q associated with the largest eigenvalue. This largest eigenvalue is the desired ratio and is always less than one. As N increases this ratio approaches one, for any fixed sub-interval $[a, b]$.

7.7 Higher Dimensional Arrays

Up to now, we have considered sensors placed within a one-dimensional interval $[-L, L]$ and signals propagating within a plane containing $[-L, L]$. In such an arrangement there is a bit of ambiguity; we cannot tell if a signal is coming from the angle θ or the angle $\theta + \pi$. When propagating signals can come to the array from any direction in three-dimensional space, there is greater ambiguity. To resolve the ambiguities, we can employ two- and three-dimensional arrays of sensors. To analyze the higher-dimensional cases, it is helpful to use the wave equation.

7.7.1 The Wave Equation

In many areas of remote sensing, what we measure are the fluctuations in time of an electromagnetic or acoustic field. Such fields are described mathematically as solutions of certain partial differential equations, such as the *wave equation*. A function $u(x, y, z, t)$ is said to satisfy the *three-dimensional wave equation* if

$$u_{tt} = c^2(u_{xx} + u_{yy} + u_{zz}) = c^2 \nabla^2 u, \tag{7.3}$$

where u_{tt} denotes the second partial derivative of u with respect to the time variable t twice and $c > 0$ is the (constant) speed of propagation. More complicated versions of the wave equation permit the speed of propagation c to vary with the spatial variables x, y, z, but we shall not consider that here.

We use the method of *separation of variables* at this point, to get some idea about the nature of solutions of the wave equation. Assume, for the moment, that the solution $u(t, x, y, z)$ has the simple form

$$u(t, x, y, z) = f(t)g(x, y, z). \tag{7.4}$$

Inserting this separated form into the wave equation, we get

$$f''(t)g(x, y, z) = c^2 f(t)\nabla^2 g(x, y, z) \tag{7.5}$$

or

$$f''(t)/f(t) = c^2 \nabla^2 g(x, y, z)/g(x, y, z). \tag{7.6}$$

The function on the left is independent of the spatial variables, while the one on the right is independent of the time variable; consequently, they must both equal the same constant, which we denote $-\omega^2$. From this we have two separate equations,

$$f''(t) + \omega^2 f(t) = 0, \tag{7.7}$$

and

$$\nabla^2 g(x, y, z) + \frac{\omega^2}{c^2} g(x, y, z) = 0. \tag{7.8}$$

Equation (7.8) is the *Helmholtz equation*.

Equation (7.7) has for its solutions the functions $f(t) = \cos(\omega t)$ and $\sin(\omega t)$. Functions $u(t, x, y, z) = f(t)g(x, y, z)$ with such time dependence are called *time-harmonic* solutions.

7.7.2   Planewave Solutions

Suppose that, beginning at time $t = 0$, there is a localized disturbance. As time passes, that disturbance spreads out spherically. When the radius of the sphere is very large, the surface of the sphere appears planar, to an observer on that surface, who is said then to be in the *far field*. This motivates the study of solutions of the wave equation that are constant on planes; the so-called *planewave solutions*.

Let $\mathbf{s} = (x, y, z)$ and $u(\mathbf{s}, t) = u(x, y, z, t) = e^{i\omega t} e^{i\mathbf{k} \cdot \mathbf{s}}$. Then we can show that u satisfies the wave equation $u_{tt} = c^2 \nabla^2 u$ for any real vector $\mathbf{k}$, so long as $||\mathbf{k}||^2 = \omega^2/c^2$. This solution is a planewave associated with frequency ω and *wavevector* $\mathbf{k}$; at any fixed time the function $u(\mathbf{s}, t)$ is constant on any plane in three-dimensional space having $\mathbf{k}$ as a normal vector.

In radar and sonar, the field $u(\mathbf{s}, t)$ being sampled is usually viewed as a discrete or continuous superposition of planewave solutions with various amplitudes, frequencies, and wavevectors. We sample the field at various spatial locations $\mathbf{s}$, for various times t. Here we simplify the situation a bit by assuming that all the planewave solutions are associated with the same frequency, ω. If not, we can perform an FFT on the functions of time received at each sensor location $\mathbf{s}$ and keep only the value associated with the desired frequency ω.

7.7.3 Superposition and the Fourier Transform

It is notationally convenient now to use the complex exponential functions

$$e^{i\omega t} = \cos(\omega t) + i\sin(\omega t)$$

instead of $\cos(\omega t)$ and $\sin(\omega t)$.

In the continuous superposition model, the field is

$$u(\mathbf{s}, t) = e^{i\omega t} \int F(\mathbf{k}) e^{i\mathbf{k}\cdot\mathbf{s}} d\mathbf{k}. \tag{7.9}$$

Our measurements at the sensor locations $\mathbf{s}$ give us the values

$$f(\mathbf{s}) = \int F(\mathbf{k}) e^{i\mathbf{k}\cdot\mathbf{s}} d\mathbf{k}. \tag{7.10}$$

The data are then Fourier transform values of the complex function $F(\mathbf{k})$; $F(\mathbf{k})$ is defined for all three-dimensional real vectors $\mathbf{k}$, but is zero, in theory, at least, for those $\mathbf{k}$ whose squared length $||\mathbf{k}||^2$ is not equal to ω^2/c^2. Our goal is then to estimate $F(\mathbf{k})$ from measured values of its Fourier transform. Since each $\mathbf{k}$ is a normal vector for its planewave field component, determining the value of $F(\mathbf{k})$ will tell us the strength of the planewave component coming from the direction $\mathbf{k}$.

7.7.4 The Spherical Model

We can imagine that the sources of the planewave fields are the points P that lie on the surface of a large sphere centered at the origin. For each P, the ray from the origin to P is parallel to some wavevector $\mathbf{k}$. The function $F(\mathbf{k})$ can then be viewed as a function $F(P)$ of the points P. Our measurements will be taken at points $\mathbf{s}$ inside this sphere. The radius of the sphere is assumed to be orders of magnitude larger than the distance between sensors. The situation is that of astronomical observation of the heavens using ground-based antennas. The sources of the optical or electromagnetic signals reaching the antennas are viewed as lying on a large sphere surrounding the earth. Distance to the sources is not considered now, and all we are interested in are the amplitudes $F(\mathbf{k})$ of the fields associated with each direction $\mathbf{k}$.

7.7.5 The Two-Dimensional Array

In some applications the sensor locations are essentially arbitrary, while in others their locations are carefully chosen. Sometimes, the sensors are collinear, as in sonar towed arrays. Figure 14.1 illustrates a line array.

Suppose now that the sensors are in locations $\mathbf{s} = (x, y, 0)$, for various x and y; then we have a *planar array* of sensors. Then the dot product $\mathbf{s} \cdot \mathbf{k}$ that occurs in Equation (7.10) is

$$\mathbf{s} \cdot \mathbf{k} = xk_1 + yk_2; \tag{7.11}$$

we cannot *see* the third component, k_3. However, since we know the size of the vector $\mathbf{k}$, we can determine $|k_3|$. The only ambiguity that remains is that we cannot distinguish sources on the upper hemisphere from those on the lower one. In most cases, such as astronomy, it is obvious in which hemisphere the sources lie, so the ambiguity is resolved.

The function $F(\mathbf{k})$ can then be viewed as $F(k_1, k_2)$, a function of the two variables k_1 and k_2. Our measurements give us values of $f(x, y)$, the two-dimensional Fourier transform of $F(k_1, k_2)$. Because of the limitation $||\mathbf{k}|| = \frac{\omega}{c}$, the function $F(k_1, k_2)$ has bounded support. Consequently, its Fourier transform cannot have bounded support. As a result, we can never have all the values of $f(x, y)$, and so cannot hope to reconstruct $F(k_1, k_2)$ exactly, even for noise-free data.

7.7.6   The One-Dimensional Array

If the sensors are located at points $\mathbf{s}$ having the form $\mathbf{s} = (x, 0, 0)$, then we have a *line array* of sensors, as we discussed previously. The dot product in Equation (7.10) becomes

$$\mathbf{s} \cdot \mathbf{k} = xk_1. \tag{7.12}$$

Now the ambiguity is greater than in the planar array case. Once we have k_1, we know that

$$k_2^2 + k_3^2 = \left(\frac{\omega}{c}\right)^2 - k_1^2, \tag{7.13}$$

which describes points P lying on a circle on the surface of the distant sphere, with the vector $(k_1, 0, 0)$ pointing at the center of the circle. It is said then that we have a *cone of ambiguity*. One way to resolve the situation is to assume $k_3 = 0$; then $|k_2|$ can be determined and we have remaining only the ambiguity involving the sign of k_2. Once again, in many applications, this remaining ambiguity can be resolved by other means.

Once we have resolved any ambiguity, we can view the function $F(\mathbf{k})$ as $F(k_1)$, a function of the single variable k_1. Our measurements give us values of $f(x)$, the Fourier transform of $F(k_1)$. As in the two-dimensional case, the restriction on the size of the vectors $\mathbf{k}$ means that the function $F(k_1)$ has bounded support. Consequently, its Fourier transform, $f(x)$, cannot have bounded support. Therefore, we shall never have all of $f(x)$, and so cannot hope to reconstruct $F(k_1)$ exactly, even for noise-free data.

7.7.7   Limited Aperture

In both the one- and two-dimensional problems, the sensors will be placed within some bounded region, such as $|x| \leq A$, $|y| \leq B$ for the two-dimensional problem, or $|x| \leq L$ for the one-dimensional case. The size of these bounded regions, in units of wavelength, are the *apertures* of the arrays. The larger these apertures are, the better the resolution of the reconstructions. In digital array processing there are only finitely many sensors, which then places added limitations on our ability to reconstruction the field amplitude function $F(\mathbf{k})$.

7.7.8   Other Limitations on Resolution

In imaging regions of the earth from satellites in orbit there is a trade-off between resolution and the time available to image a given site. Satellites in *geostationary orbit*, such as weather and TV satellites, remain stationary, relative to a fixed position on the earth's surface, but to do so must orbit $22,000$ miles above the earth. If we tried to image the earth from that height, a telescope like the Hubble Space Telescope would have a resolution of about 21 feet, due to the unavoidable blurring caused by the optics of the lens itself. The Hubble orbits 353 miles above the earth, but because it looks out into space, not down to earth, it only needs to be high enough to avoid atmospheric distortions. Spy satellites operate in *low Earth orbit* (LEO), about 200 miles above the earth, and achieve a resolution of about 2 or 3 inches, at the cost of spending only about 1 or 2 minutes over their target. The satellites used in the GPS system maintain a *medium Earth orbit* (MEO) at a height of about $12,000$ miles, high enough to be seen over the horizon most of the time, but no so high as to require great power to send their signals.

In the February 2003 issue of *Harper's Magazine* there is an article on "scientific apocalypse", dealing with the search for near-earth asteroids. These objects are initially detected by passive optical observation, as small dots of reflected sunlight; once detected, they are then imaged by active radar to determine their size, shape, rotation and such. Some Russian astronomers are concerned about the near-earth asteroid Apophis 2004 MN4, which, they say, will pass within $30,000$ km of earth in 2029, and come even closer in 2036. This is closer to earth than the satellites in geostationary orbit. As they say, "Stay tuned for further developments."

7.8   An Example: The Solar-Emission Problem

In [23] Bracewell discusses the *solar-emission* problem. In 1942, it was observed that radio-wave emissions in the one-meter wavelength range were arriving from the sun. Were they coming from the entire disk of the sun or were the sources more localized, in sunspots, for example? The problem then was to view each location on the sun's surface as a potential source of these radio waves and to determine the intensity of emission corresponding to each location.

For electromagnetic waves the propagation speed is the speed of light in a vacuum, which we shall take here to be $c = 3 \times 10^8$ meters per second. The wavelength λ for gamma rays is around one Angstrom, that is, 10^{-10} meters, which is about the diameter of an atom; for x-rays it is about one millimicron, or 10^{-9} meters. The visible spectrum has wavelengths that are a little less than one micron, that is, 10^{-6} meters, while infrared radiation (IR), predominantly associated with heat, has a wavelength somewhat longer. Infrared radiation with a wavelength around 6 or 7 microns can be used to detect water vapor; we use near IR, with a wavelength near that of visible light, to change the channels on our TV sets. Shortwave radio has a wavelength around one millimeter. Microwaves have wavelengths between one centimeter and one meter; those used in radar imaging have a wavelength about one inch and can penetrate clouds and thin layers of leaves. Broadcast radio has a λ running from about 10 meters to 1000 meters. The so-called long radio waves can have wavelengths several thousand meters long, necessitating clever methods of large-antenna design for radio astronomy.

The sun has an angular diameter of 30 min. of arc, or one-half of a degree, when viewed from earth, but the needed resolution was more like 3 min. of arc. Such resolution requires a radio telescope 1000 wavelengths across, which means a diameter of 1km at a wavelength of 1 meter; in 1942 the largest military radar antennas were less than 5 meters across. A solution was found, using the method of reconstructing an object from line-integral data, a technique that surfaced again in tomography.

7.9   Another Example: Scattering in Crystallography

In [150] Körner reveals how surprised he was when he heard that large amounts of computer time are spent by crystallographers computing Fourier transforms numerically. He goes on to describe this application.

The structure to be analyzed consists of some finite number of particles

that will retransmit (scatter) in all directions any electromagnetic radiation that hits them. A beam of monochromatic light with unit strength and frequency ω is sent into the structure and the resulting scattered beams are measured at some number of observation points.

We say that the scattering particles are located in space at the points $\mathbf{r}_m$, $m = 1, ..., M$, and that the incoming light arrives as a planewave with wavevector $\mathbf{k}_0$. Then the planewave field generated by the incoming light is

$$g(\mathbf{s}, t) = e^{i\omega t} e^{i\mathbf{k}_0 \cdot \mathbf{s}}.$$

What is received at each $\mathbf{r}_m$ is then

$$g(\mathbf{r}_m, t) = e^{i\omega t} e^{i\mathbf{k}_0 \cdot \mathbf{r}_m}.$$

We observe the scattered signals at $\mathbf{s}$, where the retransmitted signal coming from $\mathbf{r}_m$ is

$$f(\mathbf{s}, t) = e^{i\omega t} e^{i\mathbf{k}_0 \cdot \mathbf{r}_m} e^{i\|\mathbf{s} - \mathbf{r}_m\|}.$$

When $\mathbf{s}$ is sufficiently remote from the scattering particles, the retransmitted signal from $\mathbf{r}_m$ arrives at $\mathbf{s}$ as a planewave with wavevector

$$\mathbf{k}_m = \frac{\omega}{c}(\mathbf{s} - \mathbf{r}_m)/\|\mathbf{s} - \mathbf{r}_m\|.$$

Therefore, at $\mathbf{s}$ we receive

$$u(\mathbf{s}, t) = e^{i\omega t} \sum_{m=1}^{M} e^{i\mathbf{k}_m \cdot \mathbf{s}}.$$

The objective is to determine the $\mathbf{k}_m$, which will then tell us the locations $\mathbf{r}_m$ of the scattering particles. To do this, we imagine an infinity of possible locations $\mathbf{r}$ for the particles and define $a(\mathbf{r}) = 1$ if $\mathbf{r} = \mathbf{r}_m$ for some m, and $a(\mathbf{r}) = 0$ otherwise. More precisely, we define $a(\mathbf{r})$ as a sum of unit-strength Dirac delta functions supported at the $\mathbf{r}_m$, a topic we shall deal with later. At each $\mathbf{r}$ we obtain (in theory) a value of the function $A(\mathbf{k})$, the Fourier transform of the function $a(\mathbf{r})$.

In practice, the crystallographers cannot measure the complex numbers $A(\mathbf{k})$, but only the magnitudes $|A(\mathbf{k})|$; the phase angle of $A(\mathbf{k})$ is lost. This presents the crystallographers with the *phase problem*, in which we must estimate a function from values of the magnitude of its Fourier transform.

In 1985, Hauptman and Karle won the Nobel Prize in Chemistry for developing a new method for finding $a(\mathbf{s})$ from measurements. Their technique is highly mathematical. It is comforting to know that, although there is no Nobel Prize in Mathematics, it is still possible to win the prize for doing mathematics.
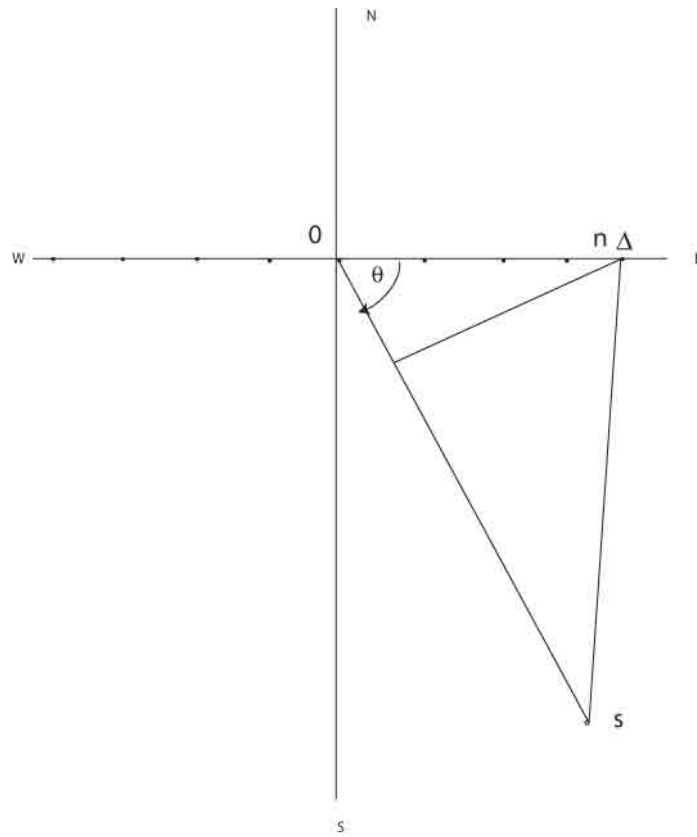
Figure 7.1: Antenna array and far-field receiver.
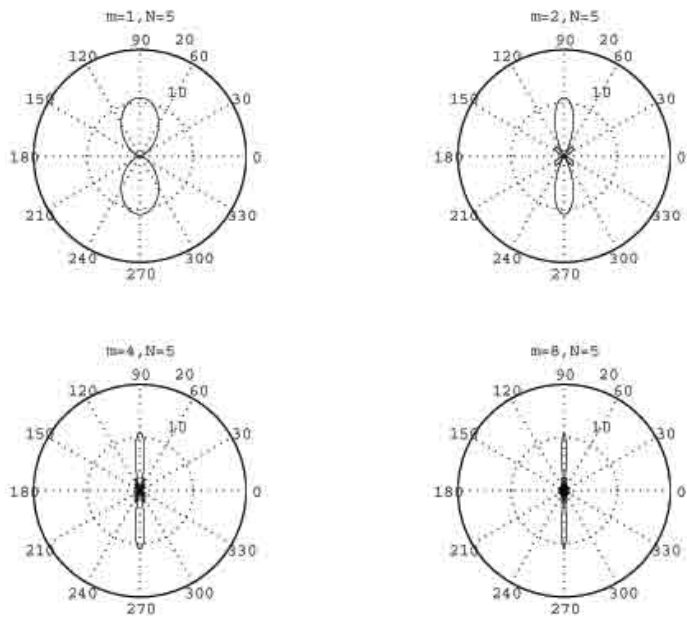
Figure 7.2: Transmission Pattern $A(\theta)$: $m = 1, 2, 4, 8$ and $N = 5$.
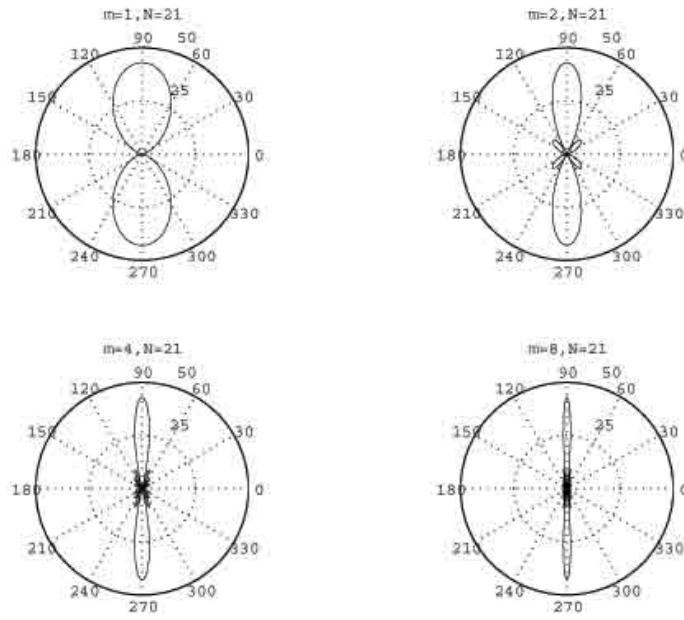
Figure 7.3: Transmission Pattern $A(\theta)$: $m = 1, 2, 4, 8$ and $N = 21$.
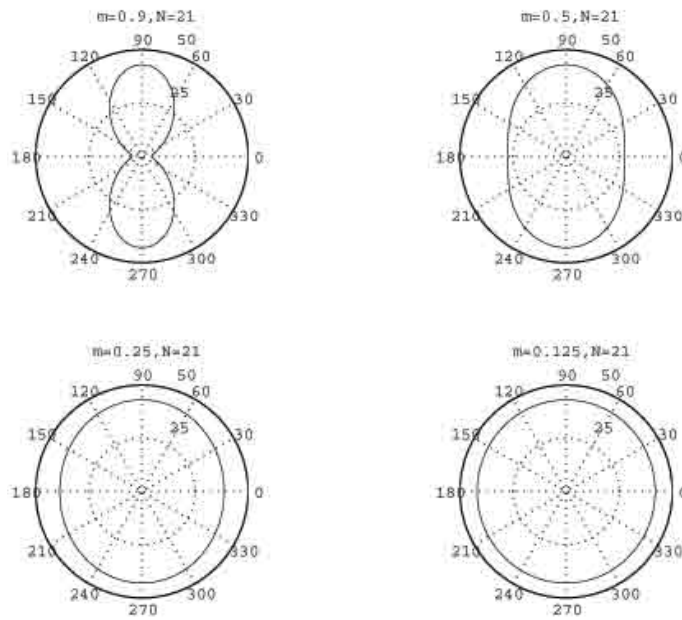
Figure 7.4: Transmission Pattern $A(\theta)$: $m = 0.9, 0.5, 0.25, 0.125$ and $N = 21$.

Part IV

Fourier Methods

Chapter 8

Fourier Analysis

8.1 Chapter Summary

The Fourier transform and Fourier series play major roles in signal and image processing. They are useful in understanding the workings of a broad class of linear systems. In transmission tomography, magnetic-resonance imaging, radar, sonar and array processing in general, what we are able to measure is related by the Fourier transform to what we are interested in.

8.2 The Fourier Transform

Let $f(x)$ be a complex-valued function of the real variable x. The *Fourier transform* (FT) of $f(x)$, also called the *Fourier integral*, is the function $F(\omega)$ defined for all real ω by

$$F(\omega) = \int_{-\infty}^{\infty} f(x)e^{ix\omega}. \tag{8.1}$$

If we know $F(\omega)$, we can recapture $f(x)$ using the formula for the *Inverse Fourier Transform* (IFT)

$$f(x) = \frac{1}{2\pi} \int_{-\infty}^{\infty} F(\omega)e^{-ix\omega} d\omega. \tag{8.2}$$

The Fourier transform is related to Fourier series, a topic that may be more familiar.

In particular applications the variables x and ω will take on actual physical meaning. If x is time, in which case we usually replace x with t, the variable ω becomes frequency. If x is spatial, that is, position along the x-axis, then ω is spatial frequency. Spatial frequencies become more

important when we consider functions of more than one variable, as in image processing. In our theoretical discussions of Fourier transformation, however, the variables x and ω have no physical significance.

There is one situation, which we encounter in the next section, in which the use of the variable ω may cause some confusion and the reader is cautioned to be careful. In the unknown strength problem, we have both a temporal frequency and a spatial frequency, so we need two different variables. We are interested in what is received at various locations in the far-field when a single-frequency signal is broadcast from the various points of the interval $[-L, L]$. By convention, we denote by ω the fixed frequency of signal that is broadcast. The strength of the signal broadcast at x is $f(x)$, and its Fourier transform, which we shall denote by $F(\gamma)$, will then be evaluated at points on a circle in the far-field. The variable γ will be proportional to the cosine of the angle determined by the far-field point and the x-axis. We use γ, and not ω, in this case, because ω is already being used to denote the temporal frequency of the broadcast signal. In the later sections and in the chapters that follow,we shall return to the original choice of the variables.

As an example of Fourier transformation, consider the function $F(\omega) = \chi_\Omega(\omega)$ that is one for $|\omega| \leq \Omega$, and zero otherwise. Inserting this function into Equation (8.2), we get

$$f(x) = \frac{1}{2\pi} \int_{-\Omega}^{\Omega} e^{-ix\omega} d\omega = \frac{1}{2\pi} \int_{-\Omega}^{\Omega} \cos(x\omega) d\omega,$$

since the sine function is odd and its integral is therefore zero. We can see easily that

$$f(0) = \frac{\Omega}{\pi}.$$

For $x \neq 0$, we perform the integration, and obtain

$$f(x) = \frac{1}{2\pi} \frac{1}{x} \Big(\sin(\Omega x) - \sin(-\Omega x) \Big) = \frac{\sin(\Omega x)}{\pi x}. \tag{8.3}$$

8.3   The Unknown Strength Problem Again

To help us appreciate the role of the Fourier transform in remote sensing, we revisit the unknown strength problem discussed earlier.

In our previous discussion, we assumed that each point x in the interval $[-L, L]$ was sending the signal $f(x) \sin \omega t$, where the value of $f(x)$ was the strength of the signal sent from x. Because we had not yet introduced complex exponential functions, it was necessary to rely on sines and cosines throughout. As you may recall, this required the use of trigonometric identities and led to somewhat involved calculations. In addition, to obtain

the Fourier coefficients, it was necessary to combine the readings at two different locations 180 degrees apart. Now we want to make use of complex exponential functions to simplify the calculations.

Note that in the discussion of the transmission problems the variable ω is the frequency of the signal transmitted, not the argument of the Fourier transform, as it is elsewhere in this chapter.

Because $\sin \omega t$ can be written as

$$\sin \omega t = \frac{1}{2i}\left(e^{i\omega t} - e^{-i\omega t}\right),$$

we shall consider the purely theoretical problem of finding what each point P in the far-field would receive if each point x is sending only the signal $f(x)e^{i\omega t}$, where

$$f(x) = |f(x)|e^{i\phi(x)},$$

with $|f(x)| \geq 0$ the strength of the signal, and $\phi(x)$ its *phase*. We shall return to the original problem at the end.

The same far-field assumption we used previously tells us that the point P receives from x a delayed version of what x sent; the point P receives

$$f(x)\exp(i\omega(t - \frac{1}{c}(D - x\cos\theta))) = f(x)\exp(i\frac{\omega\cos\theta}{c}x)\exp(i\omega t)\exp(-i\frac{\omega D}{c}).$$

What P receives from all the points x in $[-L, L]$ is then

$$\exp(i\omega t)\exp(-i\frac{\omega D}{c})\int_{-L}^{L} f(x)\exp(i\frac{\omega\cos\theta}{c}x)dx.$$

Ignoring the first two factors, which do not depend on what is coming from the points x, we see that what P receives is $F(\frac{\omega\cos\theta}{c})$, which we can write as $F(\gamma)$, where $\gamma = \frac{\omega\cos\theta}{c}$.

So, by measuring what each point P in the far-field receives, we obtain values of $F(\gamma)$, the Fourier transform of the function $f(x)$, for any value of the variable γ in the interval $[-\frac{\omega}{c}, \frac{\omega}{c}]$.

To get back to the original problem, in which the point x sends $f(x)\sin\omega t$, we simply repeat the derivation in the previous paragraphs, but imagine that the point x now sends the signal $f(x)e^{-i\omega t}$. Then P receives

$$\exp(-i\omega t)\exp(i\frac{\omega D}{c})\int_{-L}^{L} f(x)\exp(-i\frac{\omega\cos\theta}{c}x)dx.$$

Combining what P receives in the two cases, we get back what we found in our earlier discussion.

The point here is that we can simplify our calculations by using complex exponential signals and complex exponential functions in the definition of the Fourier transform, without losing anything. While it is true that

what is actually sent and received involves only real-valued functions, not complex-valued ones, we can always return to the real case by expressing the complex exponential functions in terms of sines and cosines. We are simply replacing the more complicated calculations of trigonometric identities with the simpler algebra of exponential functions. This is standard practice throughout signal processing.

8.4   Two-Dimensional Fourier Transforms

More generally, we consider a function $f(x, y)$ of two real variables. Its Fourier transformation is

$$F(\alpha, \beta) = \int \int f(x, y) e^{i(x\alpha + y\beta)} dx dy. \tag{8.4}$$

For example, suppose that $f(x, y) = 1$ for $\sqrt{x^2 + y^2} \leq R$, and zero, otherwise. Then we have

$$F(\alpha, \beta) = \int_{-\pi}^{\pi} \int_0^R e^{-i(\alpha r \cos\theta + \beta r \sin\theta)} r \, dr \, d\theta. \tag{8.5}$$

In polar coordinates, with $\alpha = \rho \cos\phi$ and $\beta = \rho \sin\phi$, we have

$$F(\rho, \phi) = \int_0^R \int_{-\pi}^{\pi} e^{ir\rho \cos(\theta - \phi)} d\theta \, r \, dr. \tag{8.6}$$

The inner integral is well known;

$$\int_{-\pi}^{\pi} e^{ir\rho \cos(\theta - \phi)} d\theta = 2\pi J_0(r\rho), \tag{8.7}$$

where J_0 and J_n denote the 0th order and nth order Bessel functions, respectively. Using the following identity

$$\int_0^z t^n J_{n-1}(t) dt = z^n J_n(z), \tag{8.8}$$

we have

$$F(\rho, \phi) = \frac{2\pi R}{\rho} J_1(\rho R). \tag{8.9}$$

Notice that, since $f(x, z)$ is a radial function, that is, dependent only on the distance from $(0, 0)$ to (x, y), its Fourier transform is also radial.

The first positive zero of $J_1(t)$ is around $t = 4$, so when we measure F at various locations and find $F(\rho, \phi) = 0$ for a particular (ρ, ϕ), we can estimate $R \approx 4/\rho$. So, even when a distant spherical object, like a star, is too far away to be imaged well, we can sometimes estimate its size by finding where the intensity of the received signal is zero [150].

8.4.1 Two-Dimensional Fourier Inversion

Just as in the one-dimensional case, the Fourier transformation that produced $F(\alpha, \beta)$ can be inverted to recover the original $f(x, y)$. The Fourier Inversion Formula in this case is

$$f(x, y) = \frac{1}{4\pi^2} \int \int F(\alpha, \beta) e^{-i(\alpha x + \beta y)} d\alpha d\beta. \qquad (8.10)$$

It is important to note that this procedure can be viewed as two one-dimensional Fourier inversions: first, we invert $F(\alpha, \beta)$, as a function of, say, β only, to get the function of α and y

$$g(\alpha, y) = \frac{1}{2\pi} \int F(\alpha, \beta) e^{-i\beta y} d\beta; \qquad (8.11)$$

second, we invert $g(\alpha, y)$, as a function of α, to get

$$f(x, y) = \frac{1}{2\pi} \int g(\alpha, y) e^{-i\alpha x} d\alpha. \qquad (8.12)$$

If we write the functions $f(x, y)$ and $F(\alpha, \beta)$ in polar coordinates, we obtain alternative ways to implement the two-dimensional Fourier inversion. We shall consider these other ways when we discuss the tomography problem of reconstructing a function $f(x, y)$ from line-integral data.

8.5 Fourier Series and Fourier Transforms

When the function $F(\omega)$ is zero outside of some finite interval, there is a useful relationship between the Fourier coefficients of $F(\omega)$ and its inverse Fourier transform, $f(x)$.

8.5.1 Support-Limited $F(\omega)$

Suppose now that $F(\omega)$ is zero, except for ω in the interval $[-\Omega, \Omega]$. We then say that $F(\omega)$ is *support-limited* to the band $[-\Omega, \Omega]$. Then $F(\omega)$ has a *Fourier series* expansion

$$F(\omega) = \sum_{n=-\infty}^{+\infty} a_n e^{i\frac{\pi}{\Omega} n \omega}, \qquad (8.13)$$

where the Fourier coefficients a_n are given by

$$a_n = \frac{1}{2\Omega} \int_{-\Omega}^{\Omega} F(\omega) e^{-i\frac{\pi}{\Omega} n \omega} d\omega. \qquad (8.14)$$

Comparing Equations (8.2) and (8.14), we see that $a_n = \frac{\pi}{\Omega} f(n \frac{\pi}{\Omega})$. With $\Delta = \frac{\pi}{\Omega}$, we can write

$$F(\omega) = \Delta \sum_{n=-\infty}^{+\infty} f(n\Delta) e^{i\omega n \Delta}. \tag{8.15}$$

8.5.2   Shannon's Sampling Theorem

This tells us that if $F(\omega)$ is zero outside the interval $[-\Omega, \Omega]$, then $F(\omega)$ can be completely determined by the values of its inverse Fourier transform $f(x)$ at the infinite discrete set of points $x = n\frac{\pi}{\Omega}$. Once we have determined $F(\omega)$ from these *discrete samples*, as they are called, we can also determine all of the function $f(x)$, by applying the inversion formula in Equation (8.2). Inserting $F(\omega)$ as given in Equation (8.15) into the integral in Equation (8.2), and using Equation (8.3), we get

$$f(x) = \sum_{n=-\infty}^{+\infty} f(n\Delta) \frac{\sin(\Omega(n\Delta - x))}{\Omega(n\Delta - x)}. \tag{8.16}$$

This result is known as *Shannon's Sampling Theorem*.

8.5.3   Sampling Terminology

In electrical engineering it is common to consider frequency in units of cycles per second, or Hertz, and to denote frequency by the variable f, not to be confused with the function $f(x)$, where $2\pi f = \omega$. When we say that ω lies in the interval $[-\Omega, \Omega]$, we are also saying that f lies in the interval $[-\frac{\Omega}{2\pi}, \frac{\Omega}{2\pi}]$. Then

$$\Delta = \frac{\pi}{\Omega} = \frac{1}{2f_{\max}},$$

where $f_{\max}$ is the largest value of f involved. For this reason, we sometimes speak of the *sampling rate* as

$$\frac{1}{\Delta} = 2f_{\max},$$

and say that the appropriate sampling rate is twice the highest frequency involved.

It is important to remember that this rule of thumb that the appropriate sampling rate is twice the highest frequency, measured in Hertz, has meaning only in the context of Shannon's Sampling Theorem, which deals with infinite sequences of data.

8.5.4 What Shannon Does Not Say

It is important to remember that Shannon's Sampling Theorem tells us that the *doubly infinite* sequence of values $\{f(n\Delta)\}_{n=-\infty}^{\infty}$ is sufficient to recover exactly the function $F(\omega)$ and, thereby, the function $f(x)$. Therefore, sampling at the rate of twice the highest frequency (in Hertz) is sufficient only when we have the complete doubly infinite sequence of samples. Of course, in practice, we never have an infinite number of values of anything, so the rule of thumb expressed by Shannon's Sampling Theorem is not valid. Since we know that we will end up with only finitely many samples, each additional data value is additional information. There is no reason to stick to the sampling rate of twice the highest frequency.

Exercise 8.1 *Let $\Delta = \pi$, $f_m = f(m)$, and $g_m = g(m)$. Use the orthogonality of the functions $e^{im\omega}$ on $[-\pi, \pi]$ to establish Parseval's equation:*

$$\langle f, g \rangle = \sum_{m=-\infty}^{\infty} f_m \overline{g_m} = \int_{-\pi}^{\pi} F(\omega)\overline{G(\omega)}d\omega/2\pi,$$

from which it follows that

$$\langle f, f \rangle = \int_{-\infty}^{\infty} |F(\omega)|^2 d\omega/2\pi.$$

Exercise 8.2 *Let $f(x)$ be defined for all real x and let $F(\omega)$ be its FT. Let*

$$g(x) = \sum_{k=-\infty}^{\infty} f(x + 2\pi k),$$

assuming the sum exists. Show that g is a 2π -periodic function. Compute its Fourier series and use it to derive the Poisson summation formula:

$$\sum_{k=-\infty}^{\infty} f(2\pi k) = \frac{1}{2\pi} \sum_{n=-\infty}^{\infty} F(n).$$

8.5.5 Sampling from a Limited Interval

It is often the case that we have the opportunity to extract as many values of $f(x)$ as we desire, provided we take x within some fixed interval. If $x = t$ is time, for example, the signal $f(t)$ may die out rapidly, so that we can take measurements of $f(t)$ only for t in an interval $[0, T]$, say. Do we limit ourselves to a sampling rate of twice the highest frequency, if by doing that we obtain only a small number of values of $f(t)$? No! We should *over-sample*, and take data at a faster rate, to get more values of $f(t)$. How we then process this over-sampled data becomes an important issue, and noise

is ultimately the limiting factor in how much information we can extract from over-sampled data.

In the next section we take a closer look at the problems presented by the finiteness of the data.

8.6   The Problem of Finite Data

In practice, of course, we never have infinite sequences; we have finitely many data points. In a number of important applications, such as sonar, radar, and medical tomography, the object of interest will be represented by the function $F(\omega)$, or a multi-dimensional version, and the data will be finitely many values of $f(x)$. Our goal is then to estimate $F(\omega)$ from the data.

Suppose, for example, that $F(\omega) = 0$, for $|\omega| > \Omega$, $\Delta = \frac{\pi}{\Omega}$, and we have the values $f(n\Delta)$, for $n = 0, 1, ..., N-1$. Motivated by Equation (8.15), we may take as an estimate of the function $F(\omega)$ the *discrete Fourier transform* (DFT) of the data from the function $f(x)$, which is the finite sum

$$DFT(\omega) = \Delta \sum_{n=0}^{N-1} f(n\Delta)e^{in\Delta\omega}, \tag{8.17}$$

defined for $|\omega| \leq \Omega$. It is good to note that the DFT is *consistent with the data*, meaning that, if we insert $DFT(\omega)$ into the integral in Equation (8.2) and set $x = n\Delta$, for any $n = 0, 1, ..., N-1$ the result is exactly the data value $f(n\Delta)$.

8.7   Best Approximation

The basic problem here is to estimate $F(\omega)$ from finitely many values of $f(x)$, under the assumption that $F(\omega) = 0$ for $|\omega| > \Omega$, for some $\Omega > 0$. Since we do not have all of $f(x)$, the best we can hope to do is to approximate $F(\omega)$ in some sense. To help us understand how best approximation works, we consider the *orthogonality principle*.

8.7.1   The Orthogonality Principle

Imagine that you are standing and looking down at the floor. The point B on the floor that is closest to the tip of your nose, which we label F, is the unique point on the floor such that the vector from B to any other point A on the floor is perpendicular to the vector from B to F; that is, $FB \cdot AB = 0$. This is a simple illustration of the *orthogonality principle*.

When two vectors are perpendicular to one another, their dot product is zero. This idea can be extended to functions. We say that two functions

$F(\omega)$ and $G(\omega)$ defined on the interval $[-\Omega, \Omega]$ are *orthogonal* if

$$\int_{-\Omega}^{\Omega} F(\omega)\overline{G(\omega)}d\omega = 0. \tag{8.18}$$

Suppose that $G_n(\omega)$, $n = 0, ..., N - 1$, are known functions, and

$$A(\omega) = \sum_{n=0}^{N-1} a_n G_n(\omega),$$

for any coefficients a_n. We want to minimize the approximation error

$$\int_{-\Omega}^{\Omega} |F(\omega) - A(\omega)|^2 d\omega, \tag{8.19}$$

over all coefficients a_n. Suppose that the best choices are $a_n = b_n$. The orthogonality principle tells us that the best approximation

$$B(\omega) = \sum_{n=0}^{N-1} b_n G_n(\omega)$$

is such that the function $F(\omega) - B(\omega)$ is orthogonal to $A(\omega) - B(\omega)$ for every choice of the a_n.

Suppose that we fix m and select $a_n = b_n$, for $n \neq m$, and $a_m = b_m + 1$. Then we have

$$\int_{-\Omega}^{\Omega} (F(\omega) - B(\omega))\overline{G_m(\omega)}d\omega = 0. \tag{8.20}$$

We can use Equation (8.20) to help us find the best b_n.

From Equation (8.20) we have

$$\int_{-\Omega}^{\Omega} F(\omega)\overline{G_m(\omega)}d\omega = \sum_{n=0}^{N-1} b_n \int_{-\Omega}^{\Omega} G_n(\omega)\overline{G_m(\omega)}d\omega.$$

Since we know the $G_n(\omega)$, we know the integrals

$$\int_{-\Omega}^{\Omega} G_n(\omega)\overline{G_m(\omega)}d\omega.$$

If we can learn the values

$$\int_{-\Omega}^{\Omega} F(\omega)\overline{G_m(\omega)}d\omega$$

from measurements, then we simply solve a system of linear equations to find the b_n.

8.7.2   An Example

Suppose that we have measured the values $f(x_n)$, for $n = 0, ..., N - 1$, where the x_n are arbitrary real numbers. Then, from these measurements, we can find the best approximation of $F(\omega)$ of the form

$$A(\omega) = \sum_{n=0}^{N-1} a_n G_n(\omega),$$

if we select $G_n(\omega) = e^{i\omega x_n}$.

8.7.3   The DFT as Best Approximation

Suppose now that our data values are $f(\Delta n)$, for $n = 0, 1, ..., N - 1$, where we have chosen $\Delta = \frac{\pi}{\Omega}$. We can view the DFT as a best approximation of the function $F(\omega)$ over the interval $[-\Omega, \Omega]$, in the following sense. Consider all functions of the form

$$A(\omega) = \sum_{n=0}^{N-1} a_n e^{in\Delta\omega}, \tag{8.21}$$

where the best coefficients $a_n = b_n$ are to be determined. Now select those b_n for which the approximation error

$$\int_{-\Omega}^{\Omega} |F(\omega) - A(\omega)|^2 d\omega \tag{8.22}$$

is minimized. Then it is easily shown that these optimal b_n are precisely

$$b_n = \Delta f(n\Delta),$$

for $n = 0, 1, ..., N - 1$.

Exercise 8.3 *Show that $b_n = \Delta f(n\Delta)$, for $n = 0, 1, ..., N - 1$, are the optimal coefficients.*

The DFT estimate is reasonably accurate when N is large, but when N is not large there are usually better ways to estimate $F(\omega)$, as we shall see.

8.7.4   The Modified DFT (MDFT)

We suppose, as in the previous subsection, that $F(\omega) = 0$, for $|\omega| > \Omega$, and that our data values are $f(n\Delta)$, for $n = 0, 1, ..., N - 1$. It is often convenient to use a sampling interval Δ that is smaller than $\frac{\pi}{\Omega}$ in order to

obtain more data values. Therefore, we assume now that $\Delta < \frac{\pi}{\Omega}$. Once again, we seek the function of the form

$$A(\omega) = \sum_{n=0}^{N-1} a_n e^{in\Delta\omega}, \tag{8.23}$$

defined for $|\omega| \leq \Omega$, for which the error measurement

$$\int_{-\Omega}^{\Omega} |F(\omega) - A(\omega)|^2 d\omega$$

is minimized.

In the previous example, for which $\Delta = \frac{\pi}{\Omega}$, we have

$$\int_{-\Omega}^{\Omega} e^{i(n-m)\Delta\omega} d\omega = 0,$$

for $m \neq n$. As the reader will discover in doing Exercise 8.3, this greatly simplifies the system of linear equations that we need to solve to get the optimal b_n. Now, because $\Delta \neq \frac{\pi}{\Omega}$, we have

$$\int_{-\Omega}^{\Omega} e^{i(n-m)\Delta\omega} d\omega = \frac{\sin((n-m)\Delta\Omega)}{\pi(n-m)\Delta},$$

which is not zero when $n \neq m$. This means that we have to solve a more complicated system of linear equations in order to find the b_n. It is important to note that the optimal b_n are not equal to $\Delta f(n\Delta)$ now, so the DFT is not the optimal approximation. The best approximation in this case we call the *modified* DFT (MDFT).

8.7.5 The PDFT

In the previous subsection, the functions $A(\omega)$ were defined for $|\omega| \leq \Omega$. Therefore, we could have written them as

$$A(\omega) = \chi_\Omega(\omega) \sum_{n=0}^{N-1} a_n e^{in\Delta\omega},$$

where $\chi_\Omega(\omega)$ is the function that is one for $|\omega| \leq \Omega$ and zero otherwise. The factor $\chi_\Omega(\omega)$ serves to incorporate into our approximating function our prior knowledge that $F(\omega) = 0$ outside the interval $[-\Omega, \Omega]$. What can we do if we have additional prior knowledge about the broad features of $F(\omega)$ that we wish to include?

Suppose that $P(\omega) \geq 0$ is a prior estimate of $|F(\omega)|$. Now we approximate $F(\omega)$ with functions of the form

$$C(\omega) = P(\omega) \sum_{n=0}^{N-1} c_n e^{in\Delta\omega}. \tag{8.24}$$

As we shall see later in the text, the best choice of the c_n are the ones that satisfy the equations

$$f(m\Delta) = \sum_{n=0}^{N-1} c_n p((n-m)\Delta), \tag{8.25}$$

for $m = 0, 1, ..., N - 1$, where

$$p(x) = \frac{1}{2\pi} \int_{-\Omega}^{\Omega} P(\omega) e^{-ix\omega} d\omega$$

is the inverse Fourier transform of the function $P(\omega)$. This best approximation we call the PDFT.

8.8   The Vector DFT

We turn now to the *vector DFT*, which may appear, initially, to be unrelated to the Fourier transform and Fourier series.

Let $\mathbf{f} = (f_0, f_1, ..., f_{N-1})^T$ be a column vector with complex entries; here the superscript T denotes transposition. For $k = 0, 1, ..., N - 1$, define the complex number F_k by

$$F_k = \sum_{n=0}^{N-1} f_n e^{i\frac{2\pi}{N}kn}, \tag{8.26}$$

and let $\mathbf{F} = (F_0, F_1, ..., F_{N-1})^T$. We shall call the vector $\mathbf{F}$ the *vector DFT* (vDFT) of the vector $\mathbf{f}$. For the moment we attach no specific significance to the entries of $\mathbf{f}$ or $\mathbf{F}$.

Exercise 8.4 *Let G be the N by N matrix with entries*

$$G_{jm} = e^{i\frac{2\pi}{N}(j-1)(m-1)}.$$

Show that

$$\mathbf{F} = G\mathbf{f}.$$

Exercise 8.5 *Show that the inverse of G is $\frac{1}{N}G^\dagger$, where the superscript $\dagger$ denotes conjugate transposition. Therefore,*

$$\mathbf{f} = \frac{1}{N}G^\dagger \mathbf{F}.$$

Exercise 8.6 *Suppose that the function $f(x)$ of interest is known to have the form*

$$f(x) = \sum_{k=0}^{N-1} a_k e^{i\frac{2\pi}{N}kx},$$

for some coefficients a_k, and suppose also that we have sampled $f(x)$ to obtain the values $f(n)$, for $n = 0, 1, ..., N-1$. Use the results of the previous exercises to show that $a_k = \frac{1}{N}F_{N-k}$, for $k = 0, 1, ..., N-1$. If, once we have found the a_k, we insert these values into the sum above and set $x = n$, for each $n = 0, 1, ..., N-1$, do we get back the original values $f(n)$? Compare these results with those obtained previously for the function given by the trigonometric polynomial in Equation (4.9).

Later, we shall study the *fast Fourier transform* (FFT) algorithm, which provides an efficient way to calculate **F** from **f**. Now, we relate the vector DFT to the DFT.

8.9 Using the Vector DFT

Suppose now that the function we want to estimate is $F(\omega)$ and that $F(\omega) = 0$ for $|\omega| > \Omega$. We take $\Delta = \frac{\pi}{\Omega}$ and sample the function $f(x)$ to get our data $f(n\Delta)$, for $n = 0, 1, ..., N - 1$. Note that we could have used any N sample points with spacing Δ and our choice here is simply for notational convenience.

Let us take N equi-spaced values of ω in the interval $[-\Omega, \Omega)$, with $\omega_0 = -\Omega$, $\omega_1 = -\Omega + \frac{2\Omega}{N}$, and so on, that is, with

$$\omega_k = -\Omega + \frac{2\Omega}{N}k,$$

for $k = 0, 1, ..., N - 1$. Now we evaluate the function

$$DFT(\omega) = \Delta \sum_{n=0}^{N-1} f(n\Delta)e^{in\Delta\omega}$$

at the points $\omega = \omega_k$. We get

$$DFT(\omega_k) = \Delta \sum_{n=0}^{N-1} f(n\Delta)e^{in\Delta(-\Omega+\frac{2\Omega}{N}k)},$$

or

$$DFT(\omega_k) = \Delta \sum_{n=0}^{N-1} f(n\Delta)e^{-in\pi}e^{i\frac{2\pi}{N}kn}.$$

If we let $f_n = \Delta f(n\Delta)e^{-in\pi}$ in the definition of the vector DFT, we find that

$$DFT(\omega_k) = F_k = \sum_{n=0}^{N-1} f_n e^{i\frac{2\pi}{N}kn},$$

for $k = 0, 1, ..., N-1$.

What we have just seen is that the vector DFT, applied to the f_n obtained from the sampled data $f(n\Delta)$, has for its entries the values of the $DFT(\omega)$ at the N points ω_k. So, when the vector DFT is used on data consisting of sampled values of the function $f(x)$, what we get are not values of $F(\omega)$ itself, but rather values of the DFT estimate of $F(\omega)$. How useful or accurate the vector DFT is in such cases depends entirely on how useful or accurate the DFT is as an estimator of the true $F(\omega)$ in each case.

There is one case, which we shall discuss in the next section, in which the vector DFT gives us more than merely an approximation. This case, although highly unrealistic, is frequently employed to motivate the use of the vector DFT.

8.10   A Special Case of the Vector DFT

For concreteness, in this section we shall replace the variable x with the time variable t and speak of the variable ω as *frequency*.

Suppose that we have sampled the function $f(t)$ at the times $t = n\Delta$, and that $F(\omega) = 0$ for $|\omega| > \Omega = \frac{\pi}{\Delta}$. In addition, we assume that $f(t)$ has the special form

$$f(t) = \sum_{k=0}^{N-1} c_k e^{-i(-\Omega + \frac{2\Omega}{N}k)t}, \tag{8.27}$$

for some coefficients c_k. Inserting $t = n\Delta$, we get

$$f(n\Delta) = \sum_{k=0}^{N-1} c_k e^{-i(-\Omega + \frac{2\Omega}{N}k)n\Delta} = \sum_{k=0}^{N-1} c_k e^{in\pi} e^{-i\frac{2\pi}{N}kn}.$$

Therefore, we can write

$$f(n\Delta)e^{-in\pi} = \sum_{k=0}^{N-1} c_k e^{-i\frac{2\pi}{N}kn}.$$

It follows that

$$c_k = \frac{1}{N}F_k,$$

for

$$f_n = f(n\Delta)e^{-in\pi}.$$

So, in this special case, the vector DFT formed by using f_n provides us with exact values of c_k, and so allows us to recapture $f(t)$ completely. However, this special case is not at all realistic and gives a misleading impression of what the vector DFT is doing.

First of all, the complex exponential functions $e^{-i(-\Omega + \frac{2\Omega}{N}k)t}$ are periodic, with period $N\Delta$. This means that, if we were to observe more values of the function $f(t)$, at the spacing Δ, we would see merely an endless string of the N values already observed. How convenient that we stopped our measurements of $f(t)$ precisely when taking more of them would have been unnecessary anyway. Besides, how would we ever know that a real-world function of time was actually periodic? Second, the number of periodic components in $f(t)$ happens to be N, precisely the number of data values we have taken. Third, the frequency of each component is an integer multiple of the fundamental frequency $\frac{2\Omega}{N}$, which just happens to involve N, the number of data points. It should be obvious by now that this special case serves no practical purpose and only misleads us into thinking that the vector DFT is doing more than it really is. In general, the vector DFT is simply giving us N values of the DFT estimate of the true function $F(\omega)$.

8.11 Plotting the DFT

Once we have decided to use the DFT as an estimate of the function $F(\omega)$, we may wish to plot it. Then we need to evaluate the DFT at some finite number of ω points. There is no particular reason why we must let the number of grid points be N; we can take any number.

As we noted previously, the FFT is a fast algorithm for calculating the vector DFT of any vector $\mathbf{f}$. When we have as our data $f(n\Delta)$, for $n = 0, 1, ..., N-1$, we can use the FFT to evaluate the DFT of the data at N equi-spaced values of ω. The FFT is most efficient when the number of entries in $\mathbf{f}$ is a power of two. Therefore, it is common to augment the data by including some number of zero values, to make a vector with the number of its entries a power of two. For example, suppose we have six data points, $f(0), f(\Delta), ..., f(5\Delta)$. We form the vector

$$\mathbf{f} = (\Delta f(0), \Delta f(\Delta), \Delta f(2\Delta), ..., \Delta f(5\Delta), 0, 0)^T,$$

which has eight entries. The vector DFT has for its entries eight equi-spaced values of the DFT estimator in the interval $[-\Omega, \Omega)$.

Appending zero values to make the vector $\mathbf{f}$ longer is called *zero-padding*. We can also use it to obtain the values of the DFT on a grid with any number of points. Suppose, for example, that we have 400 samples of $f(t)$,

that is, $f(n\Delta)$, for $n = 0, 1, ..., 399$. If we want to evaluate the DFT at, say, 512 grid points, for the purpose of graphing, we make the first 400 entries of **f** the data, and make the remaining 112 entries all zero. The DFT, as a function of ω, is unchanged by this zero-padding, but the vector DFT now produces 512 evaluations.

In a later chapter we consider how we can use prior knowledge to improve the DFT estimate.

8.12   The Vector DFT in Two Dimensions

We consider now a complex-valued function $f(x, y)$ of two real variables, with Fourier transformation

$$F(\alpha, \beta) = \int \int f(x, y) e^{i(x\alpha + y\beta)} dx dy. \tag{8.28}$$

Suppose that $F(\alpha, \beta) = 0$, except for α and β in the interval $[0, 2\pi]$; this means that the function $F(\alpha, \beta)$ represents a two-dimensional object with bounded support, such as a picture. Then $F(\alpha, \beta)$ has a Fourier series expansion

$$F(\alpha, \beta) = \sum_{m=-\infty}^{\infty} \sum_{n=-\infty}^{\infty} f(m, n) e^{im\alpha} e^{in\beta} \tag{8.29}$$

for $0 \leq \alpha \leq 2\pi$ and $0 \leq \beta \leq 2\pi$.

In image processing, $F(\alpha, \beta)$ is our two-dimensional analogue image, where α and β are continuous variables. The first step in digital image processing is to digitize the image, which means forming a two-dimensional array of numbers $F_{j,k}$, for $j, k = 0, 1, ..., N - 1$. For concreteness, we let the $F_{j,k}$ be the values $F(\frac{2\pi}{N}j, \frac{2\pi}{N}k)$.

From Equation (8.29) we can write

$$F_{j,k} = F(\frac{2\pi}{N}j, \frac{2\pi}{N}k) = \sum_{m=-\infty}^{\infty} \sum_{n=-\infty}^{\infty} f(m, n) e^{i\frac{2\pi}{N}jm} e^{i\frac{2\pi}{N}kn}, \tag{8.30}$$

for $j, k = 0, 1, ..., N - 1$.

We can also find coefficients $f_{m,n}$, for $m, n = 0, 1, ..., N - 1$, such that

$$F_{j,k} = F(\frac{2\pi}{N}j, \frac{2\pi}{N}k) = \sum_{m=0}^{N-1} \sum_{n=0}^{N-1} f_{m,n} e^{i\frac{2\pi}{N}jm} e^{i\frac{2\pi}{N}kn}, \tag{8.31}$$

for $j, k = 0, 1, ..., N - 1$. These $f_{m,n}$ are only approximations of the values $f(m, n)$, as we shall see.

Just as in the one-dimensional case, we can make use of orthogonality to find the coefficients $f_{m,n}$. We have

$$f_{m,n} = \frac{1}{N^2} \sum_{j=0}^{N-1} \sum_{k=0}^{N-1} F(\frac{2\pi}{N}jm, \frac{2\pi}{N}kn)e^{-i\frac{2\pi}{N}jm}e^{-i\frac{2\pi}{N}kn}, \qquad (8.32)$$

for $m, n = 0, 1, ..., N-1$. Now we show how the $f_{m,n}$ can be thought of as approximations of the $f(m,n)$.

We know from the Fourier Inversion Formula in two dimensions, Equation (8.10), that

$$f(m,n) = \frac{1}{4\pi^2} \int_0^{2\pi} \int_0^{2\pi} F(\alpha, \beta)e^{-i(\alpha m + \beta n)} d\alpha d\beta. \qquad (8.33)$$

When we replace the right side of Equation (8.33) with a Riemann sum, we get

$$f(m,n) \approx \frac{1}{N^2} \sum_{j=0}^{N-1} \sum_{k=0}^{N-1} F(\frac{2\pi}{N}jm, \frac{2\pi}{N}kn)e^{-i\frac{2\pi}{N}jm}e^{-i\frac{2\pi}{N}kn}; \qquad (8.34)$$

the right side is precisely $f_{m,n}$, according to Equation (8.32).

Notice that we can compute the $f_{m,n}$ from the $F_{j,k}$ using one-dimensional vDFTs. For each fixed j we compute the one-dimensional vDFT

$$G_{j,n} = \frac{1}{N} \sum_{k=0}^{N-1} F_{j,k}e^{-i\frac{2\pi}{N}kn},$$

for $n = 0, 1, ..., N-1$. Then for each fixed n we compute the one-dimensional vDFT

$$f_{m,n} = \sum_{j=0}^{N-1} G_{j,n}e^{-i\frac{2\pi}{N}jm},$$

for $m = 0, 1, ..., N-1$. From this, we see that estimating $f(x, y)$ by calculating the two-dimensional vDFT of the values from $F(\alpha, \beta)$ requires us to obtain $2N$ one-dimensional vector DFTs.

Calculating the $f_{m,n}$ from the pixel values $F_{j,k}$ is the main operation in digital image processing. The $f_{m,n}$ approximate the spatial frequencies in the image and modifications to the image, such as smoothing or edge enhancement, can be made by modifying the values $f_{m,n}$. Improving the resolution of the image can be done by extrapolating the $f_{m,n}$, that is, by approximating values of $f(x, y)$ other than $x = m$ and $y = n$. Once we have modified the $f_{m,n}$, we return to the new values of $F_{j,k}$, so calculating $F_{j,k}$ from the $f_{m,n}$ is also an important step in image processing.

In some areas of medical imaging, such as transmission tomography and magnetic-resonance imaging, the scanners provide the $f_{m,n}$. Then the desired digitized image of the patient is the array $F_{j,k}$. In such cases, the f_{mn} are considered to be approximate values of $f(m,n)$. For more on the role of the two-dimensional Fourier transform in medical imaging, see the appendices on transmission tomography.

Even if we managed to have the true values, that is, even if $f_{m,n} = f(m,n)$, the values $F_{j,k}$ are not the true values $F(\frac{2\pi}{N}m, \frac{2\pi}{N}n)$. The number $F_{j,k}$ is a value of the DFT approximation of $F(\alpha, \beta)$. This DFT approximation is the function given by

$$DFT(\alpha, \beta) = \sum_{m=0}^{N-1} \sum_{n=0}^{N-1} f_{m,n} e^{i\alpha m} e^{i\beta n}. \tag{8.35}$$

The number $F_{j,k}$ is the value of this approximation at the point $\alpha = \frac{2\pi}{N}j$ and $\beta = \frac{2\pi}{N}k$. In other words,

$$F_{j,k} = DFT(\frac{2\pi}{N}j, \frac{2\pi}{N}k),$$

for $j, k = 0, 1, ..., N-1$. How good this discrete image is as an approximation of the true $F(\alpha, \beta)$ depends primarily on two things: first, how accurate an approximation of the numbers $f(m,n)$ the numbers $f_{m,n}$ are; and second, how good an approximation of the function $F(\alpha, \beta)$ the function $DFT(\alpha, \beta)$ is.

We can easily see now how important the fast Fourier transform algorithm is. Without the fast Fourier transform to accelerate the calculations, obtaining a two-dimensional vDFT would be prohibitively expensive.

Exercise 8.7 *Show that if $f(x, y)$ is radial then its FT F is also radial. Find the FT of the radial function $f(x, y) = \frac{1}{\sqrt{x^2+y^2}}$.*

Chapter 9

Properties of the Fourier Transform

9.1 Chapter Summary

In this chapter we review the basic properties of the Fourier transform.

9.2 Fourier-Transform Pairs

Let $f(x)$ be defined for the real variable x in $(-\infty, \infty)$. The *Fourier transform* (FT) of $f(x)$ is the function of the real variable ω given by

$$F(\omega) = \int_{-\infty}^{\infty} f(x)e^{i\omega x}dx. \tag{9.1}$$

Precisely how we interpret the infinite integrals that arise in the discussion of the Fourier transform will depend on the properties of the function $f(x)$. A detailed treatment of this issue, which is beyond the scope of this book, can be found in almost any text on the Fourier transform (see, for example, [116]).

If we have $F(\omega)$ for all real ω, then we can recover the function $f(x)$ using the *Fourier Inversion Formula*:

$$f(x) = \frac{1}{2\pi} \int_{-\infty}^{\infty} F(\omega)e^{-i\omega x}d\omega. \tag{9.2}$$

The functions $f(x)$ and $F(\omega)$ are called a *Fourier-transform pair*, and $f(x)$ is sometimes called the *inverse Fourier transform* (IFT) of $F(\omega)$.

Note that the definitions of the FT and IFT just given may differ slightly from the ones found elsewhere; our definitions are those of Bochner and

Chandrasekharan [20] and Twomey [218]. The differences are minor and involve only the placement of the quantity 2π and of the minus sign in the exponent. One sometimes sees the Fourier transform of the function f denoted $\hat{f}$; here we shall reserve the symbol $\hat{f}$ for estimates of the function f.

Once again, the proper interpretation of Equation (9.2) will depend on the properties of the functions involved. It may happen that one or both of these integrals will fail to be defined in the usual way and will be interpreted as the principal value of the integral [116].

9.2.1 Decomposing $f(x)$

One way to view Equation (9.2) is that it shows us the function $f(x)$ as a superposition of complex exponential functions $e^{-i\omega x}$, where ω runs over the entire real line. The use of the minus sign here is simply for notational convenience later. For each fixed value of ω, the complex number $F(\omega) = |F(\omega)|e^{i\theta(\omega)}$ tells us that the amount of $e^{i\omega x}$ in $f(x)$ is $|F(\omega)|$, and that $e^{i\omega x}$ involves a phase shift by $\theta(\omega)$.

9.3 Basic Properties of the Fourier Transform

In this section we present the basic properties of the Fourier transform. Proofs of these assertions are left as exercises.

Exercise 9.1 *Let $F(\omega)$ be the FT of the function $f(x)$. Use the definitions of the FT and IFT given in Equations (9.1) and (9.2) to establish the following basic properties of the Fourier transform operation:*

- **Symmetry:** The FT of the function $F(x)$ is $2\pi f(-\omega)$. For example, the FT of the function $f(x) = \frac{\sin(\Omega x)}{\pi x}$ is $\chi_\Omega(\omega)$, so the FT of $g(x) = \chi_\Omega(x)$ is $G(\omega) = 2\pi\frac{\sin(\Omega\omega)}{\pi\omega}$.

- **Conjugation:** The FT of $\overline{f(x)}$ is $\overline{F(-\omega)}$.

- **Scaling:** The FT of $f(ax)$ is $\frac{1}{|a|}F(\frac{\omega}{a})$ for any nonzero constant a.

- **Shifting:** The FT of $f(x - a)$ is $e^{ia\omega}F(\omega)$.

- **Modulation:** The FT of $f(x)\cos(\omega_0 x)$ is $\frac{1}{2}[F(\omega + \omega_0) + F(\omega - \omega_0)]$.

- **Differentiation:** The FT of the nth derivative, $f^{(n)}(x)$ is $(-i\omega)^n F(\omega)$. The IFT of $F^{(n)}(\omega)$ is $(ix)^n f(x)$.

- **Convolution in** x**:** Let $f, F,\ g, G$ and h, H be FT pairs, with

$$h(x) = \int f(y)g(x-y)dy,$$

so that $h(x) = (f * g)(x)$ is the convolution of $f(x)$ and $g(x)$. Then $H(\omega) = F(\omega)G(\omega)$. For example, if we take $g(x) = \overline{f(-x)}$, then

$$h(x) = \int f(x+y)\overline{f(y)}dy = \int f(y)\overline{f(y-x)}dy = r_f(x)$$

is the *autocorrelation function* associated with $f(x)$ and

$$H(\omega) = |F(\omega)|^2 = R_f(\omega) \geq 0$$

is the *power spectrum* of $f(x)$.

- **Convolution in** ω**:** Let $f, F,\ g, G$ and h, H be FT pairs, with $h(x) = f(x)g(x)$. Then $H(\omega) = \frac{1}{2\pi}(F * G)(\omega)$.

9.4 Some Fourier-Transform Pairs

In this section we present several Fourier-transform pairs.

Exercise 9.2 *Show that the Fourier transform of $f(x) = e^{-\alpha^2 x^2}$ is $F(\omega) = \frac{\sqrt{\pi}}{\alpha}e^{-(\frac{\omega}{2\alpha})^2}$.*

Hint: Calculate the derivative $F'(\omega)$ by differentiating under the integral sign in the definition of F and integrating by parts. Then solve the resulting differential equation. Alternatively, perform the integration by completing the square.

Let $u(x)$ be the *Heaviside function* that is $+1$ if $x \geq 0$ and 0 otherwise. Let $\chi_A(x)$ be the *characteristic function* of the interval $[-A, A]$ that is $+1$ for x in $[-A, A]$ and 0 otherwise. Let $\text{sgn}(x)$ be the *sign function* that is $+1$ if $x > 0$, -1 if $x < 0$ and zero for $x = 0$.

Exercise 9.3 *Show that the FT of the function $f(x) = u(x)e^{-ax}$ is $F(\omega) = \frac{1}{a-i\omega}$, for every positive constant a, where $u(x)$ is the Heaviside function.*

Exercise 9.4 *Show that the FT of $f(x) = \chi_A(x)$ is $F(\omega) = 2\frac{\sin(A\omega)}{\omega}$.*

Exercise 9.5 *Show that the IFT of the function $F(\omega) = 2i/\omega$ is $f(x) = \text{sgn}(x)$.*

Hints: Write the formula for the inverse Fourier transform of $F(\omega)$ as

$$f(x) = \frac{1}{2\pi} \int_{-\infty}^{+\infty} \frac{2i}{\omega} \cos \omega x \, d\omega - \frac{i}{2\pi} \int_{-\infty}^{+\infty} \frac{2i}{\omega} \sin \omega x \, d\omega,$$

which reduces to

$$f(x) = \frac{1}{\pi} \int_{-\infty}^{+\infty} \frac{1}{\omega} \sin \omega x \, d\omega,$$

since the integrand of the first integral is odd. For $x > 0$ consider the Fourier transform of the function $\chi_x(t)$. For $x < 0$ perform the change of variables $u = -x$.

Generally, the functions $f(x)$ and $F(\omega)$ are complex-valued, so that we may speak about their real and imaginary parts. The next exercise explores the connections that hold among these real-valued functions.

Exercise 9.6 *Let $f(x)$ be arbitrary and $F(\omega)$ its Fourier transform. Let $F(\omega) = R(\omega) + iX(\omega)$, where R and X are real-valued functions, and similarly, let $f(x) = f_1(x) + if_2(x)$, where f_1 and f_2 are real-valued. Find relationships between the pairs R,X and f_1,f_2.*

Definition 9.1 *We define the* even part *of $f(x)$ to be the function*

$$f_e(x) = \frac{f(x) + f(-x)}{2},$$

and the odd part *of $f(x)$ to be*

$$f_o(x) = \frac{f(x) - f(-x)}{2};$$

define F_e and F_o similarly for F the FT of f.

Exercise 9.7 *Show that $F(\omega)$ is real-valued and even if and only if $f(x)$ is real-valued and even.*

Exercise 9.8 *Let $F(\omega) = R(\omega) + iX(\omega)$ be the decomposition of F into its real and imaginary parts. We say that f is a causal function if $f(x) = 0$ for all $x < 0$. Show that, if f is causal, then R and X are related; specifically, show that X is the Hilbert transform of R, that is,*

$$X(\omega) = \frac{1}{\pi} \int_{-\infty}^{\infty} \frac{R(\alpha)}{\omega - \alpha} d\alpha.$$

Hint: If $f(x) = 0$ for $x < 0$ then $f(x)\mathrm{sgn}(x) = f(x)$. Apply the convolution theorem, then compare real and imaginary parts.

9.5 Dirac Deltas

We saw earlier that the $F(\omega) = \chi_\Omega(\omega)$ has for its inverse Fourier transform the function $f(x) = \frac{\sin \Omega x}{\pi x}$; note that $f(0) = \frac{\Omega}{\pi}$ and $f(x) = 0$ for the first time when $\Omega x = \pi$ or $x = \frac{\pi}{\Omega}$. For any Ω-band-limited function $g(x)$ we have $G(\omega) = G(\omega)\chi_\Omega(\omega)$, so that, for any x_0, we have

$$g(x_0) = \int_{-\infty}^{\infty} g(x) \frac{\sin \Omega(x - x_0)}{\pi(x - x_0)} dx.$$

We describe this by saying that the function $f(x) = \frac{\sin \Omega x}{\pi x}$ has the *sifting property* for all Ω-band-limited functions $g(x)$.

As Ω grows larger, $f(0)$ approaches $+\infty$, while $f(x)$ goes to zero for $x \neq 0$. The limit is therefore not a function; it is a *generalized function* called *the Dirac delta function at zero*, denoted $\delta(x)$. For this reason the function $f(x) = \frac{\sin \Omega x}{\pi x}$ is called an *approximate delta function*. The FT of $\delta(x)$ is the function $F(\omega) = 1$ for all ω. The Dirac delta function $\delta(x)$ enjoys the *sifting property* for all $g(x)$; that is,

$$g(x_0) = \int_{-\infty}^{\infty} g(x) \delta(x - x_0) dx.$$

It follows from the sifting and shifting properties that the FT of $\delta(x - x_0)$ is the function $e^{ix_0\omega}$.

The formula for the inverse FT now says

$$\delta(x) = \frac{1}{2\pi} \int_{-\infty}^{\infty} e^{-ix\omega} d\omega. \tag{9.3}$$

If we try to make sense of this integral according to the rules of calculus we get stuck quickly. The problem is that the integral formula doesn't mean quite what it does ordinarily and the $\delta(x)$ is not really a function, but an operator on functions; it is sometimes called a *distribution*. The Dirac deltas are mathematical fictions, not in the bad sense of being lies or fakes, but in the sense of being made up for some purpose. They provide helpful descriptions of impulsive forces, probability densities in which a discrete point has nonzero probability, or, in array processing, objects far enough away to be viewed as occupying a discrete point in space.

We shall treat the relationship expressed by Equation (9.3) as a formal statement, rather than attempt to explain the use of the integral in what is surely an unconventional manner.

If we move the discussion into the ω domain and define the Dirac delta function $\delta(\omega)$ to be the FT of the function that has the value $\frac{1}{2\pi}$ for all x, then the FT of the complex exponential function $\frac{1}{2\pi}e^{-i\omega_0 x}$ is $\delta(\omega - \omega_0)$, visualized as a "spike" at ω_0, that is, a generalized function that has the value $+\infty$ at $\omega = \omega_0$ and zero elsewhere. This is a useful result, in that it provides the motivation for considering the Fourier transform of a signal $s(t)$ containing hidden periodicities. If $s(t)$ is a sum of complex exponentials with frequencies $-\omega_n$, then its Fourier transform will consist of Dirac delta functions $\delta(\omega - \omega_n)$. If we then estimate the Fourier transform of $s(t)$ from sampled data, we are looking for the peaks in the Fourier transform that approximate the infinitely high spikes of these delta functions.

Exercise 9.9 *Use the fact that* $\text{sgn}(x) = 2u(x) - 1$ *and Exercise 9.5 to show that* $f(x) = u(x)$ *has the FT* $F(\omega) = i/\omega + \pi\delta(\omega)$.

Exercise 9.10 *Let* f, F *be a FT pair. Let* $g(x) = \int_{-\infty}^{x} f(y)dy$. *Show that the FT of* $g(x)$ *is* $G(\omega) = \pi F(0)\delta(\omega) + \frac{iF(\omega)}{\omega}$.

Hint: For $u(x)$ the Heaviside function we have

$$\int_{-\infty}^{x} f(y)dy = \int_{-\infty}^{\infty} f(y)u(x - y)dy.$$

9.6   More Properties of the Fourier Transform

We can use properties of the Dirac delta functions to extend the Parseval Equation in Fourier series to Fourier transforms, where it is usually called the *Parseval-Plancherel* Equation.

Exercise 9.11 *Let* $f(x), F(\omega)$ *and* $g(x), G(\omega)$ *be Fourier transform pairs. Use Equation (9.3) to establish the Parseval-Plancherel equation*

$$\langle f, g \rangle = \int f(x)\overline{g(x)}dx = \frac{1}{2\pi}\int F(\omega)\overline{G(\omega)}d\omega,$$

from which it follows that

$$||f||^2 = \langle f, f \rangle = \int |f(x)|^2 dx = \frac{1}{2\pi}\int |F(\omega)|^2 d\omega.$$

Exercise 9.12 *The one-sided Laplace transform (LT) of f is $\mathcal{F}$ given by*

$$\mathcal{F}(z) = \int_0^\infty f(x)e^{-zx}dx.$$

Compute $\mathcal{F}(z)$ for $f(x) = u(x)$, the Heaviside function. Compare $\mathcal{F}(-i\omega)$ with the FT of u.

9.7 Convolution Filters

Let $h(x)$ and $H(\omega)$ be a Fourier-transform pair. We have mentioned several times the basic problem of estimating the function $H(\omega)$ from finitely many values of $h(x)$; for convenience now we use the symbols h and H, rather than f and F, as we did previously. Sometimes it is $H(\omega)$ that we really want. Other times it is the unmeasured values of $h(x)$ that we want, and we try to estimate them by first estimating $H(\omega)$. Sometimes, neither of these functions is our main interest; it may be the case that what we want is another function, $f(x)$, and $h(x)$ is a distorted version of $f(x)$. For example, suppose that x is time and $f(x)$ represents what a speaker says into a telephone. The phone line distorts the signal somewhat, often diminishing the higher frequencies. What the person at the other end hears is not $f(x)$, but a related signal function, $h(x)$. For another example, suppose that $f(x, y)$ is a two-dimensional picture viewed by someone with poor eyesight. What that person sees is not $f(x, y)$ but a related function, $h(x, y)$, that is a distorted version of the true $f(x, y)$. In both examples, our goal is to recover the original undistorted signal or image. To do this, it helps to model the distortion. Convolution filters are commonly used for this purpose.

9.7.1 Blurring and Convolution Filtering

We suppose that what we measure are not values of $f(x)$, but values of $h(x)$, where the Fourier transform of $h(x)$ is

$$H(\omega) = F(\omega)G(\omega).$$

The function $G(\omega)$ describes the effects of the system, the telephone line in our first example, or the weak eyes in the second example, or the refraction of light as it passes through the atmosphere, in optical imaging. If we can use our measurements of $h(x)$ to estimate $H(\omega)$ and if we have some knowledge of the system distortion function, that is, some knowledge of $G(\omega)$ itself, then there is a chance that we can estimate $F(\omega)$, and thereby estimate $f(x)$.

If we apply the Fourier Inversion Formula to $H(\omega) = F(\omega)G(\omega)$, we get

$$h(x) = \frac{1}{2\pi} \int F(\omega)G(\omega)e^{-i\omega x}dx. \tag{9.4}$$

The function $h(x)$ that results is $h(x) = (f * g)(x)$, the *convolution* of the functions $f(x)$ and $g(x)$, with the latter given by

$$g(x) = \frac{1}{2\pi} \int G(\omega)e^{-i\omega x}dx. \tag{9.5}$$

Note that, if $f(x) = \delta(x)$, then $h(x) = g(x)$. In the image processing example, this says that if the true picture f is a single bright spot, the blurred image h is g itself. For that reason, the function g is called the *point-spread function* of the distorting system.

Convolution filtering refers to the process of converting any given function, say $f(x)$, into a different function, say $h(x)$, by convolving $f(x)$ with a fixed function $g(x)$. Since this process can be achieved by multiplying $F(\omega)$ by $G(\omega)$ and then inverse Fourier transforming, such convolution filters are studied in terms of the properties of the function $G(\omega)$, known in this context as the *system transfer function*, or the *optical transfer function* (OTF); when ω is a frequency, rather than a spatial frequency, $G(\omega)$ is called the *frequency-response function* of the filter. The magnitude of $G(\omega)$, $|G(\omega)|$, is called the *modulation transfer function* (MTF). The study of convolution filters is a major part of signal processing. Such filters provide both reasonable models for the degradation signals undergo, and useful tools for reconstruction. For an important example of the use of filtering, see Appendix: Reverberation and Echo-Cancellation.

Let us rewrite Equation (9.4), replacing $F(\omega)$ with its definition, as given by Equation (9.1). Then we have

$$h(x) = \int (\frac{1}{2\pi} \int f(t)e^{i\omega t}dt)G(\omega)e^{-i\omega x}d\omega. \tag{9.6}$$

Interchanging the order of integration, we get

$$h(x) = \int f(t)(\frac{1}{2\pi} \int G(\omega)e^{i\omega(t-x)}d\omega)dt. \tag{9.7}$$

The inner integral is $g(x - t)$, so we have

$$h(x) = \int f(t)g(x - t)dt; \tag{9.8}$$

this is the definition of the convolution of the functions f and g.

9.7.2 Low-Pass Filtering

If we know the nature of the blurring, then we know $G(\omega)$, at least to some degree of precision. We can try to remove the blurring by taking measurements of $h(x)$, then estimating $H(\omega) = F(\omega)G(\omega)$, then dividing these numbers by the value of $G(\omega)$, and then inverse Fourier transforming. The problem is that our measurements are always noisy, and typical functions $G(\omega)$ have many zeros and small values, making division by $G(\omega)$ dangerous, except where the values of $G(\omega)$ are not too small. These values of ω tend to be the smaller ones, centered around zero, so that we end up with estimates of $F(\omega)$ itself only for the smaller values of ω. The result is a *low-pass filtering* of the object $f(x)$.

To investigate such low-pass filtering, we suppose that $G(\omega) = 1$, for $|\omega| \leq \Omega$, and is zero, otherwise. Then the filter is called the ideal Ω-low-pass filter. In the far-field propagation model, the variable x is spatial, and the variable ω is spatial frequency, related to how the function $f(x)$ changes spatially, as we move x. Rapid changes in $f(x)$ are associated with values of $F(\omega)$ for large ω. For the case in which the variable x is time, the variable ω becomes frequency, and the effect of the low-pass filter on $f(x)$ is to remove its higher-frequency components.

One effect of low-pass filtering in image processing is to smooth out the more rapidly changing features of an image. This can be useful if these features are simply unwanted oscillations, but if they are important detail, such as edges, the smoothing presents a problem. Restoring such wanted detail is often viewed as removing the unwanted effects of the low-pass filtering; in other words, we try to recapture the missing high-spatial-frequency values that have been zeroed out. Such an approach to image restoration is called *frequency-domain extrapolation* . How can we hope to recover these missing spatial frequencies, when they could have been anything? To have some chance of estimating these missing values we need to have some prior information about the image being reconstructed.

9.8 Functions in the Schwartz Class

As we noted previously, the integrals in Equations (9.1) and (9.2) may have to be interpreted carefully if they are to be applied to fairly general classes of functions $f(x)$ and $F(\omega)$. In this section we describe a class of functions for which these integrals can be defined. This section may be skipped with no great loss.

If both $f(x)$ and $F(\omega)$ are measurable and absolutely integrable then both functions are continuous. To illustrate some of the issues involved, we consider the functions in the Schwartz class [116]

9.8.1   The Schwartz Class

A function $f(x)$ is said to be in the *Schwartz class*, or to be a *Schwartz function*, if $f(x)$ is infinitely differentiable and

$$|x|^m f^{(n)}(x) \to 0 \tag{9.9}$$

as x goes to $-\infty$ and $+\infty$. Here $f^{(n)}(x)$ denotes the nth derivative of $f(x)$. An example of a Schwartz function is $f(x) = e^{-x^2}$, with Fourier transform $F(\omega) = \sqrt{\pi}e^{-\omega^2/4}$. The following proposition tells us that Schwartz functions are absolutely integrable on the real line, and so the Fourier transform is well defined.

Proposition 9.1 *If $f(x)$ is a Schwartz function, then*

$$\int_{-\infty}^{\infty} |f(x)|dx < +\infty.$$

Proof: There is a constant $M > 0$ such that $|x|^2|f(x)| \leq 1$, for $|x| \geq M$. Then

$$\int_{-\infty}^{\infty} |f(x)|dx \leq \int_{-M}^{M} |f(x)|dx + \int_{|x|\geq M} |x|^{-2}dx < +\infty.$$

∎

If $f(x)$ is a Schwartz function, then so is its Fourier transform. To prove the Fourier Inversion Formula it is sufficient to show that

$$f(0) = \int_{-\infty}^{\infty} F(\omega)d\omega/2\pi. \tag{9.10}$$

Write

$$f(x) = f(0)e^{-x^2} + (f(x) - f(0)e^{-x^2}) = f(0)e^{-x^2} + g(x). \tag{9.11}$$

Then $g(0) = 0$, so $g(x) = xh(x)$, where $h(x) = g(x)/x$ is also a Schwartz function. Then the Fourier transform of $g(x)$ is the derivative of the Fourier transform of $h(x)$; that is,

$$G(\omega) = H'(\omega). \tag{9.12}$$

The function $H(\omega)$ is a Schwartz function, so it goes to zero at the infinities. Computing the Fourier transform of both sides of Equation (9.11), we obtain

$$F(\omega) = f(0)\sqrt{\pi}e^{-\omega^2/4} + H'(\omega). \tag{9.13}$$

Therefore,

$$\int_{-\infty}^{\infty} F(\omega)d\omega = 2\pi f(0) + H(+\infty) - H(-\infty) = 2\pi f(0). \qquad (9.14)$$

To prove the Fourier Inversion Formula, we let $K(\omega) = F(\omega)e^{-ix_0\omega}$, for fixed x_0. Then the inverse Fourier transform of $K(\omega)$ is $k(x) = f(x + x_0)$, and therefore

$$\int_{-\infty}^{\infty} K(\omega)d\omega = 2\pi k(0) = 2\pi f(x_0). \qquad (9.15)$$

In the next subsection we consider a discontinuous $f(x)$.

9.8.2 A Discontinuous Function

Consider the function $f(x) = \frac{1}{2A}$, for $|x| \le A$, and $f(x) = 0$, otherwise. The Fourier transform of this $f(x)$ is

$$F(\omega) = \frac{\sin(A\omega)}{A\omega}, \qquad (9.16)$$

for all real $\omega \ne 0$, and $F(0) = 1$. Note that $F(\omega)$ is nonzero throughout the real line, except for isolated zeros, but that it goes to zero as we go to the infinities. This is typical behavior. Notice also that the smaller the A, the slower $F(\omega)$ dies out; the first zeros of $F(\omega)$ are at $|\omega| = \frac{\pi}{A}$, so the main lobe widens as A goes to zero. The function $f(x)$ is not continuous, so its Fourier transform cannot be absolutely integrable. In this case, the Fourier Inversion Formula must be interpreted as involving convergence in the L^2 norm.

Chapter 10

The Fourier Transform and Convolution Filtering

10.1   Chapter Summary

A major application of the Fourier transform is in the study of systems. We may think of a system as a device that accepts functions as input and produces functions as output. For example, the *differentiation system* accepts a differentiable function $f(x)$ as input and produces its derivative function $f'(x)$ as output. If the input is the function $f(x) = 5f_1(x) + 3f_2(x)$, then the output is $5f'_1(x) + 3f'_2(x)$; the differentiation system is *linear*. We shall describe systems algebraically by $h = Tf$, where f is any input function, h is the resulting output function from the system, and T denotes the operator induced by the system itself. For the differentiation system we would write the differentiation operator as $Tf = f'$.

10.2   Linear Filters

The system operator T is *linear* if

$$T(af_1 + bf_2) = aT(f_1) + bT(f_2),$$

for any scalars a and b and functions f_1 and f_2. We shall be interested only in linear systems.

10.3   Shift-Invariant Filters

We denote by S_a the system that shifts an input function by a; that is, if $f(x)$ is the input to system S_a, then $f(x-a)$ is the output. A system

operator T is said to be *shift-invariant* if

$$T(S_a(f)) = S_a(T(f)),$$

which means that, if input $f(x)$ leads to output $h(x)$, then input $f(x - a)$ leads to output $h(x - a)$; shifting the input just shifts the output. When the variable x is time, we speak of *time-invariant* systems. When T is a shift-invariant linear system operator we say that T is a SILO.

10.4   Some Properties of a SILO

We show first that $(Tf)' = Tf'$. Suppose that $h(x) = (Tf)(x)$. For any Δx we can write

$$f(x + \Delta x) = (S_{-\Delta x} f)(x)$$

and

$$(TS_{-\Delta x} f)(x) = (S_{-\Delta x} Tf)(x) = (S_{-\Delta x} h)(x) = h(x + \Delta x).$$

When the input to the system is

$$\frac{1}{\Delta x}\Big(f(x + \Delta x) - f(x)\Big),$$

the output is

$$\frac{1}{\Delta x}\Big(h(x + \Delta x) - h(x)\Big).$$

Now we take limits, as $\Delta x \to 0$, so that, assuming continuity, we can conclude that $Tf' = h'$. We apply this now to the case in which $f(x) = e^{-ix\omega}$ for some real constant ω.

Since $f'(x) = -i\omega f(x)$ and $f(x) = \frac{i}{\omega} f'(x)$ in this case, we have

$$h(x) = (Tf)(x) = \frac{i}{\omega}(Tf')(x) = \frac{i}{\omega} h'(x),$$

so that

$$h'(x) = -i\omega h(x).$$

Solving this differential equation, we obtain

$$h(x) = ce^{-ix\omega},$$

for some constant c. Note that since the c may vary when we vary the selected ω, we must write $c = c(\omega)$. The main point here is that, when T is a SILO and the input function is a complex exponential with frequency ω, then the output is again a complex exponential with the same frequency ω, multiplied by a complex number $c(\omega)$. This multiplication by $c(\omega)$ only modifies the amplitude and phase of the exponential function; it does not alter its frequency. So SILOs do not change the input frequencies, but only modify their strengths and phases.

Exercise 10.1 *Let T be a SILO. Show that T is a convolution operator by showing that, for each input function f, the output function $h = Tf$ is the convolution of f with g, where $g(x)$ is the inverse FT of the function $c(\omega)$ obtained above. Hint: write the input function $f(x)$ as*

$$f(x) = \frac{1}{2\pi} \int_{-\infty}^{\infty} F(\omega)e^{-ix\omega}d\omega,$$

and assume that

$$(Tf)(x) = \frac{1}{2\pi} \int_{-\infty}^{\infty} F(\omega)(Te^{-ix\omega})d\omega.$$

Now that we know that a SILO is a convolution filter, the obvious question to ask is What is $g(x)$? This is the *system identification* problem. One way to solve this problem is to consider what the output is when the input is the Heaviside function $u(x)$. In that case, we have

$$h(x) = \int_{-\infty}^{\infty} u(y)g(x-y)dy = \int_{0}^{\infty} g(x-y)dy = \int_{-\infty}^{x} g(t)dt.$$

Therefore, $h'(x) = g(x)$.

10.5   The Dirac Delta

The *Dirac delta*, denoted $\delta(x)$, is not truly a function. Its job is best described by its *sifting property*: for any fixed value of x,

$$f(x) = \int f(y)\delta(x-y)dy.$$

In order for the Dirac delta to perform the sifting operator on any $f(x)$ it would have to be zero, except at $x = 0$, where it would have to be infinitely large. It is possible to give a rigorous treatment of the Dirac delta, using *generalized functions*, but that is beyond the scope of this course. The Dirac delta is useful in our discussion of filters, which is why it is used.

10.6   The Impulse Response Function

We can solve the system identification problem by seeing what the output is when the input is the Dirac delta; as we shall see, the output is $g(x)$; that is, $T\delta = g$. Since the SILO T is a convolution operator, we know that

$$h(x) = \int_{-\infty}^{\infty} \delta(y)g(x-y)dy = g(x).$$

For this reason, the function $g(x)$ is called the *impulse-response function* of the system.

10.7   Using the Impulse-Response Function

Suppose now that we take as our input the function $f(x)$, but write it as

$$f(x) = \int f(y)\delta(x - y)dy.$$

Then, since T is linear, and the integral is more or less a big sum, we have

$$T(f)(x) = \int f(y)T(\delta(x - y))dy = \int f(y)g(x - y)dy.$$

The function on the right side of this equation is the *convolution* of the functions f and g, written $f * g$. This shows, as we have seen, that T does its job by convolving any input function f with its impulse-response function g, to get the output function $h = Tf = f * g$. It is useful to remember that order does not matter in convolution:

$$\int f(y)g(x - y)dy = \int g(y)f(x - y)dy.$$

10.8   The Filter Transfer Function

Now let us take as input the complex exponential $f(x) = e^{-ix\omega}$, where ω is fixed. Then the output is

$$h(x) = T(f)(x) = \int e^{-iy\omega}g(x - y)dy = \int g(y)e^{-i(x-y)\omega}dy = e^{-ix\omega}G(\omega),$$

where $G(\omega)$ is the Fourier transform of the impulse-response function $g(x)$; note that $G(\omega) = c(\omega)$ from Exercise 10.1. This tells us that when the input to T is a complex exponential function with "frequency" ω, the output is the same complex exponential function, the "frequency" is unchanged, but multiplied by a complex number $G(\omega)$. This multiplication by $G(\omega)$ can change both the amplitude and phase of the complex exponential, but the "frequency" ω does not change. In filtering, this function $G(\omega)$ is called the *transfer function* of the filter, or sometimes the *frequency-response function*.

10.9   The Multiplication Theorem for Convolution

Now let's take as input a function $f(x)$, but now write it using Equation (8.2),

$$f(x) = \frac{1}{2\pi}\int F(\omega)e^{-ix\omega}d\omega.$$

Then, taking the operator inside the integral, we find that the output is

$$h(x) = T(f)(x) = \frac{1}{2\pi} \int F(\omega)T(e^{-ix\omega})d\omega = \frac{1}{2\pi} \int e^{-ix\omega}F(\omega)G(\omega)d\omega.$$

But, from Equation (8.2), we know that

$$h(x) = \frac{1}{2\pi} \int e^{-ix\omega}H(\omega)d\omega.$$

This tells us that the Fourier transform $H(\omega)$ of the function $h = f * g$ is the simply product of $F(\omega)$ and $G(\omega)$; this is the most important property of convolution.

10.10 Summing Up

It is helpful to take stock of what we have just discovered:

- 1. if $h = T(f)$ then $h' = T(f')$;

- 2. $T(e^{-i\omega x}) = G(\omega)e^{-i\omega x}$;

- 3. writing

$$f(x) = \frac{1}{2\pi} \int F(\omega)e^{-i\omega x}d\omega,$$

  we obtain

$$h(x) = (Tf)(x) = \frac{1}{2\pi} \int F(\omega)T(e^{-i\omega x})d\omega,$$

  so that

$$h(x) = \frac{1}{2\pi} \int F(\omega)G(\omega)e^{-i\omega x}d\omega;$$

- 4. since we also have

$$h(x) = \frac{1}{2\pi} \int H(\omega)e^{-i\omega x}d\omega,$$

  we can conclude that $H(\omega) = F(\omega)G(\omega)$;

- 5. if we define $g(x)$ to be $(T\delta)(x)$, then

$$g(x - y) = (T\delta)(x - y).$$

  Writing

$$f(x) = \int f(y)\delta(x - y)dy,$$

we get

$$h(x) = (Tf)(x) = \int f(y)(T\delta)(x-y)dy = \int f(y)g(x-y)dy,$$

so that h is the convolution of f and g;

- 6. $g(x)$ is the inverse Fourier transform of $G(\omega)$.

10.11   A Project

Previously, we allowed the operator T to move inside the integral. We know, however, that this is not always permissible. The differentiation operator $T = D$, with $D(f) = f'$, cannot always be moved inside the integral; as we learn in advanced calculus, we cannot always differentiate under the integral sign. This raises the interesting issue of how to represent the differentiation operator as a shift-invariant linear filter. In particular, what is the impulse-response function? The exercise is to investigate this issue. Pay some attention to the problem of differentiating the delta function, to the Green's Function method for representing the inversion of linear differential operators, and to generalized functions or distributions.

10.12   Band-Limiting

Suppose that $G(\omega) = \chi_\Omega(\omega)$. Then if $F(\omega)$ is the Fourier transform of the input function, the Fourier transform of the output function $h(t)$ will be

$$H(\omega) = \begin{cases} F(\omega), \text{if } |\omega| \leq \Omega\,; \\ 0, \text{if } |\omega| > \Omega\,. \end{cases}$$

The effect of the filter is to leave values $F(\omega)$ unchanged, if $|\omega| \leq \Omega$, and to replace $F(\omega)$ with zero, if $|\omega| > \Omega$. This is called *band-limiting*. Since the inverse Fourier transform of $G(\omega)$ is

$$g(t) = \frac{\sin(\Omega t)}{\pi t},$$

the band-limiting system can be described using convolution:

$$h(t) = \int f(s)\frac{\sin(\Omega(t-s))}{\pi(t-s)}ds.$$

Chapter 11

Infinite Sequences and Discrete Filters

11.1   Chapter Summary

Many textbooks on signal processing present filters in the context of infinite sequences. Although infinite sequences are no more realistic than functions $f(t)$ defined for all times t, they do simplify somewhat the discussion of filtering, particularly when it comes to the impulse response and to random signals. Systems that have as input and output infinite sequences are called *discrete* systems.

11.2   Shifting

We denote by $f = \{f_n\}_{n=-\infty}^{\infty}$ an infinite sequence. For a fixed integer k, the system that accepts f as input and produces as output the shifted sequence $h = \{h_n = f_{n-k}\}$ is denoted S_k; therefore, we write $h = S_k f$.

11.3   Shift-Invariant Discrete Linear Systems

A discrete system T is *linear* if

$$T(af^1 + bf^2) = aT(f^1) + bT(f^2),$$

for any infinite sequences f^1 and f^2 and scalars a and b. As previously, a system T is *shift-invariant* if $TS_k = S_kT$. This means that if input f has output h, then input $S_k f$ has output $S_k h$; shifting the input by k just shifts the output by k.

11.4 The Delta Sequence

The *delta sequence* $\delta = \{\delta_n\}$ has $\delta_0 = 1$ and $\delta_n = 0$, for n not equal to zero. Then $S_k(\delta)$ is the sequence $S_k(\delta) = \{\delta_{n-k}\}$. For any sequence f we have

$$f_n = \sum_{m=-\infty}^{\infty} f_m \delta_{n-m} = \sum_{m=-\infty}^{\infty} \delta_m f_{n-m}. \qquad (11.1)$$

This means that we can write the sequence f as an infinite sum of the sequences $S_m \delta$:

$$f = \sum_{m=-\infty}^{\infty} f_m S_m(\delta). \qquad (11.2)$$

As in the continuous case, we use the delta sequence to understand better how a shift-invariant discrete linear system T works.

11.5 The Discrete Impulse Response

We let δ be the input to the shift-invariant discrete linear system T, and denote the output sequence by $g = T(\delta)$. Now, for any input sequence f with $h = T(f)$, we write f using Equation (11.2), so that

$$h = T(f) = T\left(\sum_{m=-\infty}^{\infty} f_m S_m \delta \right) = \sum_{m=-\infty}^{\infty} f_m T S_m(\delta)$$

$$= \sum_{m=-\infty}^{\infty} f_m S_m T(\delta) = \sum_{m=-\infty}^{\infty} f_m S_m(g).$$

Therefore, we have

$$h_n = \sum_{m=-\infty}^{\infty} f_m g_{n-m}, \qquad (11.3)$$

for each n. Equation (11.3) is the definition of *discrete convolution* or the *convolution of sequences*. This tells us that the output sequence $h = T(f)$ is the convolution of the input sequence f with the impulse-response sequence g; that is, $h = T(f) = f * g$.

11.6 The Discrete Transfer Function

Associated with each ω in the interval $[0, 2\pi)$ we have the sequence $e_\omega = \{e^{-in\omega}\}_{n=-\infty}^{\infty}$; the minus sign in the exponent is just for notational convenience later. What happens when we let $f = e_\omega$ be the input to the system

T? The output sequence h will be the convolution of the sequence e_ω with the sequence g; that is,

$$h_n = \sum_{m=-\infty}^{\infty} e^{-im\omega} g_{n-m} = \sum_{m=-\infty}^{\infty} g_m e^{-i(n-m)\omega} = e^{-in\omega} \sum_{m=-\infty}^{\infty} g_m e^{im\omega}.$$

Defining

$$G(\omega) = \sum_{m=-\infty}^{\infty} g_m e^{im\omega} \tag{11.4}$$

for $0 \le \omega < 2\pi$, we can write

$$h_n = e^{-in\omega} G(\omega),$$

or

$$h = T(e_\omega) = G(\omega) e_\omega.$$

This tells us that when e_ω is the input, the output is a multiple of the input; the "frequency" ω has not changed, but the multiplication by $G(\omega)$ can alter the amplitude and phase of the complex-exponential sequence.

Notice that Equation (11.4) is the definition of the Fourier series associated with the sequence g viewed as a sequence of Fourier coefficients. It follows that, once we have the function $G(\omega)$, we can recapture the original g_n from the formula for Fourier coefficients:

$$g_n = \frac{1}{2\pi} \int_0^{2\pi} G(\omega) e^{-in\omega} d\omega. \tag{11.5}$$

11.7 Using Fourier Series

For any sequence $f = \{f_n\}$, we can define the function

$$F(\omega) = \sum_{n=-\infty}^{\infty} f_n e^{in\omega}, \tag{11.6}$$

for ω in the interval $[0, 2\pi)$. Then each f_n is a Fourier coefficient of $F(\omega)$ and we have

$$f_n = \frac{1}{2\pi} \int_0^{2\pi} F(\omega) e^{-in\omega} d\omega. \tag{11.7}$$

It follows that we can write

$$f = \frac{1}{2\pi} \int_0^{2\pi} F(\omega) e_\omega d\omega. \tag{11.8}$$

We interpret this as saying that the sequence f is a superposition of the individual sequences e_ω, with coefficients $F(\omega)$.

11.8 The Multiplication Theorem for Convolution

Now consider f as the input to the system T, with $h = T(f)$ as output. Using Equation (11.8), we can write

$$h = T(f) = T\left(\frac{1}{2\pi} \int_0^{2\pi} F(\omega)e_\omega d\omega\right)$$

$$= \frac{1}{2\pi} \int_0^{2\pi} F(\omega)T(e_\omega)d\omega = \frac{1}{2\pi} \int_0^{2\pi} F(\omega)G(\omega)e_\omega d\omega.$$

But, applying Equation (11.8) to h, we have

$$h = \frac{1}{2\pi} \int_0^{2\pi} H(\omega)e_\omega d\omega.$$

It follows that $H(\omega) = F(\omega)G(\omega)$, which is analogous to what we found in the case of continuous systems. This tells us that the system T works by multiplying the function $F(\omega)$ associated with the input by the transfer function $G(\omega)$, to get the function $H(\omega)$ associated with the output $h = T(f)$. In the next section we give an example.

11.9 The Three-Point Moving Average

We consider now the linear, shift-invariant system T that performs the *three-point moving average* operation on any input sequence. Let f be any input sequence. Then the output sequence is h with

$$h_n = \frac{1}{3}(f_{n-1} + f_n + f_{n+1}).$$

The impulse-response sequence is g with $g_{-1} = g_0 = g_1 = \frac{1}{3}$, and $g_n = 0$, otherwise.

To illustrate, for the input sequence with $f_n = 1$ for all n, the output is $h_n = 1$ for all n. For the input sequence

$$f = \{..., 3, 0, 0, 3, 0, 0, ...\},$$

the output h is again the sequence $h_n = 1$ for all n. If our input is the difference of the previous two input sequences, that is, the input is $\{..., 2, -1, -1, 2, -1, -1, ...\}$, then the output is the sequence with all entries equal to zero.

The transfer function $G(\omega)$ is

$$G(\omega) = \frac{1}{3}(e^{i\omega} + 1 + e^{-i\omega}) = \frac{1}{3}(1 + 2\cos\omega).$$

The function $G(\omega)$ has a zero when $\cos\omega = -\frac{1}{2}$, or when $\omega = \frac{2\pi}{3}$ or $\omega = \frac{4\pi}{3}$. Notice that the sequence given by

$$f_n = \left(e^{i\frac{2\pi}{3}n} + e^{-i\frac{2\pi}{3}n}\right) = 2\cos\frac{2\pi}{3}n$$

is the sequence $\{...,2,-1,-1,2,-1,-1,...\}$, which, as we have just seen, has as its output the zero sequence. We can say that the reason the output is zero is that the transfer function has a zero at $\omega = \frac{2\pi}{3}$ and at $\omega = \frac{4\pi}{3} = \frac{-2\pi}{3}$. Those complex-exponential components of the input sequence that correspond to values of ω where $G(\omega) = 0$ will be removed in the output. This is a useful role that filtering can play; we can *null out* undesired complex-exponential components of an input signal by designing $G(\omega)$ to have a root at those values of ω.

11.10 Autocorrelation

If we take the input to our convolution filter to be the sequence f related to the impulse-response sequence by

$$f_n = \overline{g}_{-n},$$

then the output sequence is h with entries

$$h_n = \sum_{k=-\infty}^{+\infty} g_k\overline{g_{k-n}}$$

and $H(\omega) = |G(\omega)|^2$. The sequence h is called the *autocorrelation sequence* for g and $|G(\omega)|^2$ is the *power spectrum* of g.

Autocorrelation sequences have special properties not shared with ordinary sequences, as the exercise below shows. The Cauchy inequality is valid for infinite sequences: with the length of g defined by

$$\|g\| = \left(\sum_{n=-\infty}^{+\infty} |g_n|^2\right)^{1/2}$$

and the inner product of any sequences f and g given by

$$\langle f, g\rangle = \sum_{n=-\infty}^{+\infty} f_n\overline{g_n},$$

we have

$$|\langle f, g\rangle| \le \|f\|\,\|g\|,$$

with equality if and only if g is a constant multiple of f.

Exercise 11.1 *Let h be the autocorrelation sequence for g. Show that $h_{-n} = \overline{h_n}$ and $h_0 \ge |h_n|$ for all n.*

11.11   Stable Systems

An infinite sequence $f = \{f_n\}$ is called *bounded* if there is a constant $A > 0$ such that $|f_n| \leq A$, for all n. The shift-invariant linear system with impulse-response sequence $g = T(\delta)$ is said to be *stable* [179] if the output sequence $h = \{h_n\}$ is bounded whenever the input sequence $f = \{f_n\}$ is. In Exercise 11.2 below we ask the reader to prove that, in order for the system to be stable, it is both necessary and sufficient that

$$\sum_{n=-\infty}^{\infty} |g_n| < +\infty.$$

Given a doubly infinite sequence, $g = \{g_n\}_{n=-\infty}^{+\infty}$, we associate with g its *z-transform*, the function of the complex variable z given by

$$G(z) = \sum_{n=-\infty}^{+\infty} g_n z^{-n}.$$

Doubly infinite series of this form are called *Laurent series* and occur in the representation of functions analytic in an annulus. Note that if we take $z = e^{-i\omega}$ then $G(z)$ becomes $G(\omega)$ as defined by Equation (11.4). The z-transform is a somewhat more flexible tool in that we are not restricted to those sequences g for which the z-transform is defined for $z = e^{-i\omega}$.

Exercise 11.2 *Show that the shift-invariant linear system with impulse-response sequence g is stable if and only if*

$$\sum_{n=-\infty}^{+\infty} |g_n| < +\infty.$$

Hint: If, on the contrary,

$$\sum_{n=-\infty}^{+\infty} |g_n| = +\infty,$$

consider as input the bounded sequence f with

$$f_n = \overline{g_{-n}}/|g_n|$$

and show that $h_0 = +\infty$.

Exercise 11.3 *Consider the linear system determined by the sequence $g_0 = 2$, $g_n = (\frac{1}{2})^{|n|}$, for $n \neq 0$. Show that this system is stable. Calculate the z-transform of $\{g_n\}$ and determine its region of convergence.*

11.12 Causal Filters

The shift-invariant linear system with impulse-response sequence g is said to be a *causal system* if the sequence $\{g_n\}$ is itself *causal*; that is, $g_n = 0$ for $n < 0$.

Exercise 11.4 *Show that the function $G(z) = (z - z_0)^{-1}$ is the z-transform of a causal sequence g, where z_0 is a fixed complex number. What is the region of convergence? Show that the resulting linear system is stable if and only if $|z_0| < 1$.*

Chapter 12

Convolution and the Vector DFT

12.1 Chapter Summary

Convolution is an important concept in signal processing and occurs in several distinct contexts. In previous chapters, we considered the convolution of functions of a continuous variable and of infinite sequences. The reader may also recall an earlier encounter with convolution in a course on differential equations. In this chapter we shall discuss *non-periodic convolution* and *periodic convolution* of vectors.

The simplest example of convolution is the non-periodic convolution of finite vectors, which is what we do to the coefficients when we multiply two polynomials together.

12.2 Non-periodic Convolution

Recall the algebra problem of multiplying one polynomial by another. Suppose

$$A(x) = a_0 + a_1 x + \ldots + a_M x^M$$

and

$$B(x) = b_0 + b_1 x + \ldots + b_N x^N.$$

Let $C(x) = A(x)B(x)$. With

$$C(x) = c_0 + c_1 x + \ldots + c_{M+N} x^{M+N},$$

each of the coefficients c_j, $j = 0, \ldots, M+N$, can be expressed in terms of the a_m and b_n (an easy exercise!). The vector $c = (c_0, \ldots, c_{M+N})$ is called the

non-periodic convolution of the vectors $a = (a_0, ..., a_M)$ and $b = (b_0, ..., b_N)$. Non-periodic convolution can be viewed as a particular case of periodic convolution, as we shall see.

12.3   The DFT as a Polynomial

Given the complex numbers $f_0, f_1, ..., f_{N-1}$, we form the vector $\mathbf{f} = (f_0, f_1, ..., f_{N-1})^T$. The DFT of the vector $\mathbf{f}$ is the function

$$DFT_{\mathbf{f}}(\omega) = \sum_{n=0}^{N-1} f_n e^{in\omega},$$

defined for ω in the interval $[0, 2\pi)$. Because $e^{in\omega} = (e^{i\omega})^n$, we can write the DFT as a polynomial

$$DFT_{\mathbf{f}}(\omega) = \sum_{n=0}^{N-1} f_n (e^{i\omega})^n.$$

If we have a second vector, say $\mathbf{d} = (d_0, d_1, ..., d_{N-1})^T$, then we define $DFT_{\mathbf{d}}(\omega)$ similarly. When we multiply $DFT_{\mathbf{f}}(\omega)$ by $DFT_{\mathbf{d}}(\omega)$, we are multiplying two polynomials together, so the result is a sum of powers of the form

$$c_0 + c_1 e^{i\omega} + c_2 (e^{i\omega})^2 + ... + c_{2N-2}(e^{i\omega})^{2N-2}, \tag{12.1}$$

for

$$c_j = f_0 d_j + f_1 d_{j-1} + ... + f_j d_0.$$

This is *non-periodic convolution* again. In the next section, we consider what happens when, instead of using arbitrary values of ω, we consider only the N special values $\omega_k = \frac{2\pi}{N}k$, $k = 0, 1, ..., N - 1$. Because of the periodicity of the complex exponential function, we have

$$(e^{i\omega_k})^{N+j} = (e^{i\omega_k})^j,$$

for each k. As a result, all the powers higher than $N - 1$ that showed up in the previous multiplication in Equation (12.1) now become equal to lower powers, and the product now only has N terms, instead of the $2N - 1$ terms we got previously. When we calculate the coefficients of these powers, we find that we get more than we got when we did the non-periodic convolution. Now what we get is called *periodic convolution*.

12.4 The Vector DFT and Periodic Convolution

As we just discussed, non-periodic convolution is another way of looking at the multiplication of two polynomials. This relationship between convolution on the one hand and multiplication on the other is a fundamental aspect of convolution. Whenever we have a convolution we should ask what related mathematical objects are being multiplied. We ask this question now with regard to periodic convolution; the answer turns out to be the *vector discrete Fourier transform* (vDFT).

12.4.1 The Vector DFT

Let $\mathbf{f} = (f_0, f_1, ..., f_{N-1})^T$ be a column vector whose entries are N arbitrary complex numbers. For $k = 0, 1, ..., N-1$, we let

$$F_k = \sum_{n=0}^{N-1} f_n e^{2\pi i k n/N} = DFT_{\mathbf{f}}(\omega_k). \tag{12.2}$$

Then we let $\mathbf{F} = (F_0, F_1, ..., F_{N-1})^T$ be the column vector with the N complex entries F_k. The vector $\mathbf{F}$ is called the *vector discrete Fourier transform* of the vector $\mathbf{f}$, and we denote it by $\mathbf{F} = vDFT_{\mathbf{f}}$.

The entries of the vector $\mathbf{F} = vDFT_{\mathbf{f}}$ are N equi-spaced values of the function $DFT_{\mathbf{f}}(\omega)$. If the Fourier transform $F(\omega)$ is zero for ω outside the interval $[0, 2\pi]$, and $f_n = f(n)$, for $n = 0, 1, ..., N-1$, then the entries of the vector $\mathbf{F}$ are N estimated values of $F(\omega)$.

Exercise 12.1 *Let f_n be real, for each n. Show that $F_{N-k} = \overline{F_k}$, for each k.*

As we can see from Equation (12.2), there are N multiplications involved in the calculation of each F_k, and there are N values of k, so it would seem that, in order to calculate the vector DFT of $\mathbf{f}$, we need N^2 multiplications. In many applications, N is quite large and calculating the vector $\mathbf{F}$ using the definition would be unrealistically time-consuming. The *fast Fourier transform* algorithm (FFT), to be discussed later, gives a quick way to calculate the vector $\mathbf{F}$ from the vector $\mathbf{f}$. The FFT, usually credited to Cooley and Tukey, was discovered in the mid-1960's and revolutionized signal and image processing.

12.4.2 Periodic Convolution

Given the N by 1 vectors $\mathbf{f}$ and $\mathbf{d}$ with complex entries f_n and d_n, respectively, we define a third N by 1 vector $\mathbf{f} * \mathbf{d}$, the *periodic convolution* of $\mathbf{f}$

and $\mathbf{d}$, to have the entries

$$(\mathbf{f} * \mathbf{d})_n = f_0 d_n + f_1 d_{n-1} + ... + f_n d_0 + f_{n+1} d_{N-1} + ... + f_{N-1} d_{n+1} \quad (12.3)$$

for $n = 0, 1, ..., N - 1$.

Notice that the term on the right side of Equation (12.3) is the sum of all products of entries, one from $\mathbf{f}$ and one from $\mathbf{d}$, where the sum of their respective indices is either n or $n + N$. Periodic convolution is illustrated in Figure 12.1. The first exercise relates the periodic convolution to the vector DFT.

In the exercises that follow we investigate properties of the vector DFT and relate it to periodic convolution. It is not an exaggeration to say that these two exercises are the most important ones in signal processing. The first exercise establishes for finite vectors and periodic convolution a version of the multiplication theorems we saw earlier for continuous and discrete convolution.

Exercise 12.2 *Let* $\mathbf{F} = vDFT_{\mathbf{f}}$ *and* $\mathbf{D} = vDFT_{\mathbf{d}}$. *Define a third vector* $\mathbf{E}$ *having for its kth entry* $E_k = F_k D_k$, *for* $k = 0, ..., N - 1$. *Show that* $\mathbf{E}$ *is the vDFT of the vector* $\mathbf{f} * \mathbf{d}$.

The vector $vDFT_{\mathbf{f}}$ can be obtained from the vector $\mathbf{f}$ by means of matrix multiplication by a certain matrix G, called the *DFT matrix*. The matrix G has an inverse that is easily computed and can be used to go from $\mathbf{F} = vDFT_{\mathbf{f}}$ back to the original $\mathbf{f}$. The details are in Exercise 12.3.

Exercise 12.3 *Let* G *be the* N *by* N *matrix whose entries are* $G_{jk} = e^{i(j-1)(k-1)2\pi/N}$. *The matrix* G *is sometimes called the DFT matrix. Show that the inverse of* G *is* $G^{-1} = \frac{1}{N}G^{\dagger}$, *where* $G^{\dagger}$ *is the conjugate transpose of the matrix* G. *Then* $\mathbf{f} * \mathbf{d} = G^{-1}\mathbf{E} = \frac{1}{N}G^{\dagger}\mathbf{E}$.

12.5   The vDFT of Sampled Data

For a doubly infinite sequence $\{f_n| - \infty < n < \infty\}$, the function of $F(\gamma)$ given by the infinite series

$$F(\gamma) = \sum_{n=-\infty}^{\infty} f_n e^{in\gamma} \quad (12.4)$$

is sometimes called the *discrete-time Fourier transform* (DTFT) of the sequence, and the f_n are called its *Fourier coefficients*. The function $F(\gamma)$ is 2π-periodic, so we restrict our attention to the interval $0 \le \gamma \le 2\pi$. If

we start with a function $F(\gamma)$, for $0 \leq \gamma \leq 2\pi$, we can find the Fourier coefficients by

$$f_n = \frac{1}{2\pi} \int_0^{2\pi} F(\gamma) e^{-i\gamma n} d\gamma. \tag{12.5}$$

12.5.1 Superposition of Sinusoids

This equation suggests a model for a function of a continuous variable x:

$$f(x) = \frac{1}{2\pi} \int_0^{2\pi} F(\gamma) e^{-i\gamma x} d\gamma. \tag{12.6}$$

The values f_n then can be viewed as $f_n = f(n)$, that is, the f_n are sampled values of the function $f(x)$, sampled at the points $x = n$. The function $F(\gamma)$ is now said to be the *spectrum* of the function $f(x)$. The function $f(x)$ is then viewed as a superposition of infinitely many simple functions, namely the complex exponentials or *sinusoidal functions* $e^{-i\gamma x}$, for values of γ that lie in the interval $[0, 2\pi]$. The relative contribution of each $e^{-i\gamma x}$ to $f(x)$ is given by the complex number $\frac{1}{2\pi} F(\gamma)$.

12.5.2 Rescaling

In the model just discussed, we sampled the function $f(x)$ at the points $x = n$. In applications, the variable x can have many meanings. In particular, x is often time, denoted by the variable t. Then the variable γ will be related to frequency. Depending on the application, the frequencies involved in the function $f(t)$ may be quite large numbers, or quite small ones; there is no reason to assume that they will all be in the interval $[0, 2\pi]$. For this reason, we have to modify our formulas.

Suppose that the function $g(t)$ is known to involve only frequencies in the interval $[0, \frac{2\pi}{\Delta}]$. Define $f(x) = g(x\Delta)$, so that

$$g(t) = f(t/\Delta) = \frac{1}{2\pi} \int_0^{2\pi} F(\gamma) e^{-i\gamma t/\Delta} d\gamma. \tag{12.7}$$

Introducing the variable $\omega = \gamma/\Delta$, and writing $G(\omega) = \Delta F(\omega\Delta)$, we get

$$g(t) = \frac{1}{2\pi} \int_0^{\frac{2\pi}{\Delta}} G(\omega) e^{-i\omega t} d\omega. \tag{12.8}$$

Now the typical problem is to estimate $G(\omega)$ from measurements of $g(t)$. Note that, using Equation (12.4), the function $G(\omega)$ can be written as follows:

$$G(\omega) = \Delta F(\omega\Delta) = \Delta \sum_{n=-\infty}^{\infty} f_n e^{in\omega\Delta},$$

so that

$$G(\omega) = \Delta \sum_{n=-\infty}^{\infty} g(n\Delta)e^{i(n\Delta)\omega}. \tag{12.9}$$

Note that this is the same result as in Equation (8.15) and shows that the functions $G(\omega)$ and $g(t)$ can be completely recovered from the *infinite* sequence of samples $\{g(n\Delta)\}$, whenever $G(\omega)$ is zero outside an interval of total length $\frac{2\pi}{\Delta}$.

12.5.3   The Aliasing Problem

In the previous subsection, we assumed that we knew that the only frequencies involved in $g(t)$ were in the interval $[0, \frac{2\pi}{\Delta}]$, and that Δ was our sampling spacing. Notice that, given our data $g(n\Delta)$, it is impossible for us to distinguish a frequency ω from $\omega + \frac{2\pi k}{\Delta}$, for any integer k: for any integers k and n we have

$$e^{i(\omega + \frac{2\pi k}{\Delta})n\Delta} = e^{i\omega n\Delta}e^{2\pi ikn}.$$

12.5.4   The Discrete Fourier Transform

In practice, we will have only finitely measurements $g(n\Delta)$; even these will typically be noisy, but we shall overlook this for now. Suppose our data is $g(n\Delta)$, for $n = 0, 1, ..., N-1$. For notational simplicity, we let $f_n = g(n\Delta)$. It seems reasonable, in this case, to base our estimate $\hat{G}(\omega)$ of $G(\omega)$ on Equation (12.9) and write

$$\hat{G}(\omega) = \Delta \sum_{n=0}^{N-1} g(n\Delta)e^{i(n\Delta)\omega}. \tag{12.10}$$

We shall call $\hat{G}(\omega)$ the DFT estimate of the function $G(\omega)$ and write

$$DFT(\omega) = \hat{G}(\omega);$$

it will be clear from the context that the DFT uses samples of $g(t)$ and estimates $G(\omega)$.

12.5.5   Calculating Values of the DFT

Suppose that we want to evaluate this estimate of $G(\omega)$ at the $N-1$ points $\omega_k = \frac{2\pi k}{N\Delta}$, for $k = 0, 1, ..., N-1$. Then we have

$$\hat{G}(\omega_k) = \Delta \sum_{n=0}^{N-1} g(n\Delta)e^{i(n\Delta)\frac{2\pi k}{N\Delta}} = \sum_{n=0}^{N-1} \Delta g(n\Delta)e^{2\pi ikn/N}. \tag{12.11}$$

Notice that this is the vector DFT entry F_k for the choices $f_n = \Delta g(n\Delta)$.

To summarize, given the samples $g(n\Delta)$, for $n = 0, 1, ..., N-1$, we can get the N values $\hat{G}(\frac{2\pi k}{N\Delta})$ by taking the vector DFT of the vector $\mathbf{f} = (\Delta g(0), \Delta g(\Delta), ..., \Delta g((N-1)\Delta))^T$. We would normally use the FFT algorithm to perform these calculations.

12.5.6   Zero-Padding

Suppose we simply want to graph the DFT estimate $DFT(\omega) = \hat{G}(\omega)$ on some uniform grid in the interval $[0, \frac{2\pi}{\Delta}]$, but want to use more than N points in the grid. The FFT algorithm always gives us back a vector with the same number of entries as the one we begin with, so if we want to get, say, $M > N$ points in the grid, we need to give the FFT algorithm a vector with M entries. We do this by *zero-padding*, that is, by taking as our input to the FFT algorithm the M by 1 column vector

$$\mathbf{f} = (\Delta g(0), \Delta g(\Delta), ..., \Delta g((N-1)\Delta), 0, 0, ..., 0)^T.$$

The resulting vector DFT $\mathbf{F}$ then has the entries

$$F_k = \Delta \sum_{n=0}^{N-1} g(n\Delta)e^{2\pi ikn/M},$$

for $k = 0, 1, ..., M-1$; therefore, we have $F_k = \hat{G}(2\pi k/M)$.

12.5.7   What the vDFT Achieves

It is important to note that the values F_k we calculate by applying the FFT algorithm to the sampled data $g(n\Delta)$ are not values of the function $G(\omega)$, but of the estimate, $\hat{G}(\omega)$. Zero-padding allows us to use the FFT to see more of the values of $\hat{G}(\omega)$. It does not improve resolution, but simply shows us what is already present in the function $\hat{G}(\omega)$, which we may not have seen without the zero-padding. The FFT algorithm is most efficient when N is a power of two, so it is common practice to zero-pad $\mathbf{f}$ using as M the smallest power of two not less than N.

12.5.8   Terminology

In the signal processing literature no special name is given to what we call here $DFT(\omega)$, and the vector DFT of the data vector is called the DFT of the data. This is unfortunate, because the function of the continuous variable given in Equation (12.10) is the more fundamental entity, the vector DFT being merely the evaluation of that function at N equi-spaced points. If we should wish to evaluate the $DFT(\omega)$ at $M > N$ equi-spaced

points, say, for example, for the purpose of graphing the function, we would *zero-pad* the data vector, as we just discussed. The resulting vector DFT is not the same vector as the one obtained prior to zero-padding; it is not even the same size. But both of these vectors have, as their entries, values of the same function, $DFT(\omega)$.

12.6   Understanding the Vector DFT

Let $g(t)$ be the signal we are interested in. We sample the signal at the points $t = n\Delta$, for $n = 0, 1, ..., N - 1$, to get our data values, which we label $f_n = g(n\Delta)$. To illustrate the significance of the vector DFT, we consider the simplest case, in which the signal $g(t)$ we are sampling is a single sinusoid.

Suppose that $g(t)$ is a complex exponential function with frequency the negative of $\omega_m = 2\pi m/N\Delta$; the reason for the negative is a technical one that we can safely ignore at this stage. Then

$$g(t) = e^{-i(2\pi m/N\Delta)t}, \tag{12.12}$$

for some non-negative integer $0 \le m \le N - 1$. Our data is then

$$f_n = \Delta g(n\Delta) = \Delta e^{-i(2\pi m/N\Delta)n\Delta} = \Delta e^{-2\pi imn/N}.$$

Now we calculate the components F_k of the vector DFT. We have

$$F_k = \sum_{n=0}^{N-1} f_n e^{2\pi ikn/N} = \Delta \sum_{n=0}^{N-1} e^{2\pi i(k-m)/N}.$$

If $k = m$, then $F_m = N\Delta$, while, according to Exercise 6.14, $F_k = 0$, for k not equal to m. Let's try this on a more complicated signal.

Suppose now that our signal has the form

$$f(t) = \sum_{m=0}^{N-1} A_m e^{-2\pi imt/N\Delta}. \tag{12.13}$$

The data vector is now

$$f_n = \Delta \sum_{m=0}^{N-1} A_m e^{-2\pi imn/N}.$$

The entry F_m of the vector DFT is now the sum of the values it would have if the signal had consisted only of the single sinusoid $e^{-i(2\pi m/N\Delta)t}$. As we just saw, all but one of these values would be zero, and so $F_m = N\Delta A_m$, and this holds for each $m = 0, 1, ..., N - 1$.

Summarizing, when the signal $f(t)$ is a sum of N sinusoids, with the frequencies $\omega_k = 2\pi k/N\Delta$, for $k = 0, 1, ..., N-1$, and we sample at $t = n\Delta$, for $n = 0, 1, ..., N-1$, the entries F_k of the vector DFT are precisely $N\Delta$ times the corresponding amplitudes A_k. For this particular situation, calculating the vector DFT gives us the amplitudes of the different sinusoidal components of $f(t)$. We must remember, however, that this applies only to the case in which $f(t)$ has the form in Equation (12.13). In general, the entries of the vector DFT are to be understood as approximations, in the sense discussed above.

As mentioned previously, non-periodic convolution is really a special case of periodic convolution. Extend the $M+1$ by 1 vector a to an $M+N+1$ by 1 vector by appending N zero entries; similarly, extend the vector b to an $M + N + 1$ by 1 vector by appending zeros. The vector c is now the periodic convolution of these extended vectors. Therefore, since we have an efficient algorithm for performing periodic convolution, namely the Fast Fourier Transform algorithm (FFT), we have a fast way to do the periodic (and thereby non-periodic) convolution and polynomial multiplication.
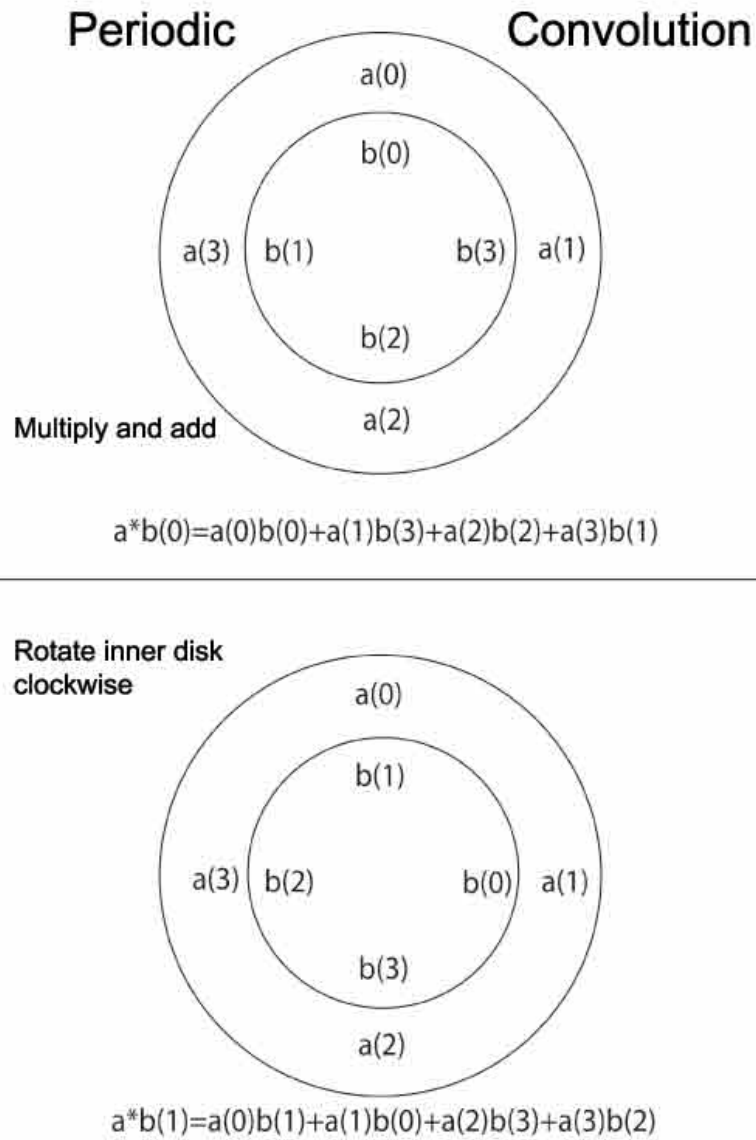
Figure 12.1: Periodic convolution of vectors $a = (a(0), a(1), a(2), a(3))$ and $b = (b(0), b(1), b(2), b(3))$.

Chapter 13

The Fast Fourier Transform (FFT)

13.1 Chapter Summary

A fundamental problem in signal processing is to estimate finitely many values of the function $F(\omega)$ from finitely many values of its (inverse) Fourier transform, $f(t)$. As we have seen, the DFT arises in several ways in that estimation effort. The *fast Fourier transform* (FFT), discovered in 1965 by Cooley and Tukey, is an important and efficient algorithm for calculating the vector DFT [86]. John Tukey has been quoted as saying that his main contribution to this discovery was the firm and often voiced belief that such an algorithm must exist.

13.2 Evaluating a Polynomial

To illustrate the main idea underlying the FFT, consider the problem of evaluating a real polynomial $P(x)$ at a point, say $x = c$. Let the polynomial be

$$P(x) = a_0 + a_1 x + a_2 x^2 + \dots + a_{2K} x^{2K},$$

where a_{2K} might be zero. Performing the evaluation efficiently by Horner's method,

$$P(c) = (((a_{2K} c + a_{2K-1})c + a_{2K-2})c + a_{2K-3})c + \dots,$$

requires $2K$ multiplications, so the complexity is on the order of the degree of the polynomial being evaluated. But suppose we also want $P(-c)$. We can write

$$P(x) = (a_0 + a_2 x^2 + \dots + a_{2K} x^{2K}) + x(a_1 + a_3 x^2 + \dots + a_{2K-1} x^{2K-2})$$

or

$$P(x) = Q(x^2) + xR(x^2).$$

Therefore, we have $P(c) = Q(c^2) + cR(c^2)$ and $P(-c) = Q(c^2) - cR(c^2)$. If we evaluate $P(c)$ by evaluating $Q(c^2)$ and $R(c^2)$ separately, one more multiplication gives us $P(-c)$ as well. The FFT is based on repeated use of this idea, which turns out to be more powerful when we are using complex exponentials, because of their periodicity.

13.3   The DFT and Vector DFT

Suppose that the data are the samples are $\{f(n\Delta), n = 1, ..., N\}$, where $\Delta > 0$ is the sampling increment or sampling spacing.

   The DFT estimate of $F(\omega)$ is the function $F_{DFT}(\omega)$, defined for ω in $[-\pi/\Delta, \pi/\Delta]$, and given by

$$F_{DFT}(\omega) = \Delta \sum_{n=1}^{N} f(n\Delta)e^{in\Delta\omega}.$$

The DFT estimate $F_{DFT}(\omega)$ is data consistent; its inverse Fourier-transform value at $t = n\Delta$ is $f(n\Delta)$ for $n = 1, ..., N$. The DFT is sometimes used in a slightly more general context in which the coefficients are not necessarily viewed as samples of a function $f(t)$.

   Given the complex N-dimensional column vector $\mathbf{f} = (f_0, f_1, ..., f_{N-1})^T$, define the DFT of vector $\mathbf{f}$ to be the function $DFT_{\mathbf{f}}(\omega)$, defined for ω in $[0, 2\pi)$, given by

$$DFT_{\mathbf{f}}(\omega) = \sum_{n=0}^{N-1} f_n e^{in\omega}.$$

Let $\mathbf{F}$ be the complex N-dimensional vector $\mathbf{F} = (F_0, F_1, ..., F_{N-1})^T$, where $F_k = DFT_{\mathbf{f}}(2\pi k/N), k = 0, 1, ..., N-1$. So the vector $\mathbf{F}$ consists of N values of the function $DFT_{\mathbf{f}}$, taken at N equispaced points $2\pi/N$ apart in $[0, 2\pi)$.

   From the formula for $DFT_{\mathbf{f}}$ we have, for $k = 0, 1, ..., N - 1$,

$$F_k = F(2\pi k/N) = \sum_{n=0}^{N-1} f_n e^{2\pi i n k/N}. \tag{13.1}$$

To calculate a single F_k requires N multiplications; it would seem that to calculate all N of them would require N^2 multiplications. However, using the FFT algorithm, we can calculate vector $\mathbf{F}$ in approximately $N \log_2(N)$ multiplications.

13.4 Exploiting Redundancy

Suppose that $N = 2M$ is even. We can rewrite Equation (13.1) as follows:

$$F_k = \sum_{m=0}^{M-1} f_{2m}e^{2\pi i(2m)k/N} + \sum_{m=0}^{M-1} f_{2m+1}e^{2\pi i(2m+1)k/N},$$

or, equivalently,

$$F_k = \sum_{m=0}^{M-1} f_{2m}e^{2\pi imk/M} + e^{2\pi ik/N}\sum_{m=0}^{M-1} f_{2m+1}e^{2\pi imk/M}. \qquad (13.2)$$

Note that if $0 \le k \le M - 1$ then

$$F_{k+M} = \sum_{m=0}^{M-1} f_{2m}e^{2\pi imk/M} - e^{2\pi ik/N}\sum_{m=0}^{M-1} f_{2m+1}e^{2\pi imk/M}, \qquad (13.3)$$

so there is no additional computational cost in calculating the second half of the entries of **F**, once we have calculated the first half. The FFT is the algorithm that results when we take full advantage of the savings obtainable by splitting a DFT calculating into two similar calculations of half the size.

We assume now that $N = 2^L$. Notice that if we use Equations (13.2) and (13.3) to calculate vector **F**, the problem reduces to the calculation of two similar DFT evaluations, both involving half as many entries, followed by one multiplication for each of the k between 0 and $M - 1$. We can split these in half as well. The FFT algorithm involves repeated splitting of the calculations of DFTs at each step into two similar DFTs, but with half the number of entries, followed by as many multiplications as there are entries in either one of these smaller DFTs. We use recursion to calculate the cost $C(N)$ of computing **F** using this FFT method. From Equation (13.2) we see that $C(N) = 2C(N/2) + (N/2)$. Applying the same reasoning to get $C(N/2) = 2C(N/4) + (N/4)$, we obtain

$$C(N) = 2C(N/2) + (N/2) = 4C(N/4) + 2(N/2) = ...$$

$$= 2^L C(N/2^L) + L(N/2) = N + L(N/2).$$

Therefore, the cost required to calculate **F** is approximately $N\log_2 N$.

From our earlier discussion of discrete linear filters and convolution, we see that the FFT can be used to calculate the periodic convolution (or even the nonperiodic convolution) of finite length vectors.

Finally, let's return to the original context of estimating the Fourier transform $F(\omega)$ of function $f(t)$ from finitely many samples of $f(t)$. If we have N equispaced samples, we can use them to form the vector **f** and

perform the FFT algorithm to get vector $\mathbf{F}$ consisting of N values of the DFT estimate of $F(\omega)$. It may happen that we wish to calculate more than N values of the DFT estimate, perhaps to produce a smooth looking graph. We can still use the FFT, but we must trick it into thinking we have more data that the N samples we really have. We do this by *zero-padding*. Instead of creating the N-dimensional vector $\mathbf{f}$, we make a longer vector by appending, say, J zeros to the data, to make a vector that has dimension $N + J$. The DFT estimate is still the same function of ω, since we have only included new zero coefficients as fake data; but, the FFT thinks we have $N + J$ data values, so it returns $N + J$ values of the DFT, at $N + J$ equispaced values of ω in $[0, 2\pi)$.

13.5   The Two-Dimensional Case

Suppose now that we have the data $\{f(m\Delta_x, n\Delta_y)\}$, for $m = 1, ..., M$ and $n = 1, ..., N$, where $\Delta_x > 0$ and $\Delta_y > 0$ are the sample spacings in the x and y directions, respectively. The DFT of this data is the function $F_{DFT}(\alpha, \beta)$ defined by

$$F_{DFT}(\alpha, \beta) = \Delta_x \Delta_y \sum_{m=1}^{M} \sum_{n=1}^{N} f(m\Delta_x, n\Delta_y) e^{i(\alpha m\Delta_x + \beta n\Delta_y)},$$

for $|\alpha| \leq \pi/\Delta_x$ and $|\beta| \leq \pi/\Delta_y$. The two-dimensional FFT produces MN values of $F_{DFT}(\alpha, \beta)$ on a rectangular grid of M equi-spaced values of α and N equi-spaced values of β. This calculation proceeds as follows. First, for each fixed value of n, a FFT of the M data points $\{f(m\Delta_x, n\Delta_y)\}, m = 1, ..., M$ is calculated, producing a function, say $G(\alpha_m, n\Delta_y)$, of M equi-spaced values of α and the N equispaced values $n\Delta_y$. Then, for each of the M equi-spaced values of α, the FFT is applied to the N values $G(\alpha_m, n\Delta_y), n = 1, ..., N$, to produce the final result.

Chapter 14

Plane-wave Propagation

14.1   Chapter Summary

In this chapter we demonstrate how the Fourier transform arises naturally as we study the signals received in the far-field from an array of transmitters or reflectors. We restrict our attention to single-frequency, or narrow-band, signals. We begin with a simple illustration of some of the issues we deal with in greater detail later in this chapter.

14.2   The Bobbing Boats

Imagine a large swimming pool in which there are several toy boats arrayed in a straight line. Although we use Figure 14.1 for a slightly different purpose elsewhere, for now we can imagine that the black dots in that figure represent our toy boats. Far across the pool, someone is slapping the water repeatedly, generating waves that proceed outward, in essentially concentric circles, across the pool. By the time the waves reach the boats, the circular shape has flattened out so that the wavefronts are essentially straight lines. The straight lines in Figure 14.1 at the end of this chapter can represent these wavefronts.

   As the wavefronts reach the boats, the boats bob up and down. If the lines of the wavefronts were oriented parallel to the line of the boats, then the boats would bob up and down in unison. When the wavefronts come in at some angle, as shown in the figure, the boats will bob up and down *out of sync* with one another, generally. By measuring the time it takes for the peak to travel from one boat to the next, we can estimate the angle of arrival of the wavefronts.

This leads to two questions:

- 1. Is it possible to get the boats to bob up and down in unison, even though the wavefronts arrive at an angle, as shown in the figure?

- 2. Is it possible for wavefronts corresponding to two different angles of arrival to affect the boats in the same way, so that we cannot tell which of the two angles is the real one?

We need a bit of mathematical notation. We let the distance from each boat to the ones on both sides be a constant distance Δ. We assume that the water is slapped f times per second, so f is the *frequency*, in units of cycles per second. As the wavefronts move out across the pool, the distance from one peak to the next is called the *wavelength*, denoted λ. The product λf is the *speed of propagation* c; so $\lambda f = c$. As the frequency changes, so does the wavelength, while the speed of propagation, which depends solely on the depth of the pool, remains constant. The angle θ measures the tilt between the line of the wavefronts and the line of the boats, so that $\theta = 0$ indicates that these wavefront lines are parallel to the line of the boats, while $\theta = \frac{\pi}{2}$ indicates that the wavefront lines are perpendicular to the line of the boats.

Exercise 14.1 *Let the angle θ be arbitrary, but fixed, and let Δ be fixed. Can we select the frequency f in such a way that we can make all the boats bob up and down in unison?*

Exercise 14.2 *Suppose now that the frequency f is fixed, but we are free to alter the spacing Δ. Can we choose Δ so that we can always determine the true angle of arrival?*

14.3   Transmission and Remote-Sensing

For pedagogical reasons, we shall discuss separately what we shall call the transmission and the remote-sensing problems, although the two problems are opposite sides of the same coin, in a sense. In the one-dimensional transmission problem, it is convenient to imagine the transmitters located at points $(x, 0)$ within a bounded interval $[-A, A]$ of the x-axis, and the measurements taken at points P lying on a circle of radius D, centered at the origin. The radius D is large, with respect to A. It may well be the case that no actual sensing is to be performed, but rather, we are simply interested in what the received signal pattern is at points P distant from the transmitters. Such would be the case, for example, if we were analyzing or constructing a transmission pattern of radio broadcasts. In the remote-sensing problem, in contrast, we imagine, in the one-dimensional

case, that our sensors occupy a bounded interval of the x-axis, and the transmitters or reflectors are points of a circle whose radius is large, with respect to the size of the bounded interval. The actual size of the radius does not matter and we are interested in determining the amplitudes of the transmitted or reflected signals, as a function of angle only. Such is the case in astronomy, farfield sonar or radar, and the like. Both the transmission and remote-sensing problems illustrate the important role played by the Fourier transform.

14.4 The Transmission Problem

We identify two distinct transmission problems: the direct problem and the inverse problem. In the direct transmission problem, we wish to determine the farfield pattern, given the complex amplitudes of the transmitted signals. In the inverse transmission problem, the array of transmitters or reflectors is the object of interest; we are given, or we measure, the farfield pattern and wish to determine the amplitudes. For simplicity, we consider only single-frequency signals.

We suppose that each point x in the interval $[-A, A]$ transmits the signal $f(x)e^{i\omega t}$, where $f(x)$ is the complex amplitude of the signal and $\omega > 0$ is the common fixed frequency of the signals. Let $D > 0$ be large, with respect to A, and consider the signal received at each point P given in polar coordinates by $P = (D, \theta)$. The distance from $(x, 0)$ to P is approximately $D - x \cos \theta$, so that, at time t, the point P receives from $(x, 0)$ the signal $f(x)e^{i\omega(t - (D - x \cos \theta)/c)}$, where c is the propagation speed. Therefore, the combined signal received at P is

$$B(P, t) = e^{i\omega t} e^{-i\omega D/c} \int_{-A}^{A} f(x) e^{ix \frac{\omega \cos \theta}{c}} dx. \qquad (14.1)$$

The integral term, which gives the farfield pattern of the transmission, is

$$F(\frac{\omega \cos \theta}{c}) = \int_{-A}^{A} f(x) e^{ix \frac{\omega \cos \theta}{c}} dx, \qquad (14.2)$$

where $F(\gamma)$ is the Fourier transform of $f(x)$, given by

$$F(\gamma) = \int_{-A}^{A} f(x) e^{ix\gamma} dx. \qquad (14.3)$$

How $F(\frac{\omega \cos \theta}{c})$ behaves, as a function of θ, as we change A and ω, is discussed in some detail in the chapter on direct transmission.

Consider, for example, the function $f(x) = 1$, for $|x| \leq A$, and $f(x) = 0$, otherwise. The Fourier transform of $f(x)$ is

$$F(\gamma) = 2A\text{sinc}(A\gamma), \qquad (14.4)$$

where $\text{sinc}(t)$ is defined to be

$$\text{sinc}(t) = \frac{\sin(t)}{t}, \tag{14.5}$$

for $t \neq 0$, and $\text{sinc}(0) = 1$. Then $F(\frac{\omega \cos \theta}{c}) = 2A$ when $\cos \theta = 0$, so when $\theta = \frac{\pi}{2}$ and $\theta = \frac{3\pi}{2}$. We will have $F(\frac{\omega \cos \theta}{c}) = 0$ when $A\frac{\omega \cos \theta}{c} = \pi$, or $\cos \theta = \frac{\pi c}{A\omega}$. Therefore, the transmission pattern has no nulls if $\frac{\pi c}{A\omega} > 1$. In order for the transmission pattern to have nulls, we need $A > \frac{\lambda}{2}$, where $\lambda = \frac{2\pi c}{\omega}$ is the wavelength. This rather counterintuitive fact, namely that we need more signals transmitted in order to receive less at certain locations, illustrates the phenomenon of destructive interference.

14.5   Reciprocity

For certain remote-sensing applications, such as sonar and radar array processing and astronomy, it is convenient to switch the roles of sender and receiver. Imagine that superimposed planewave fields are sensed at points within some bounded region of the interior of the sphere, having been transmitted or reflected from the points P on the surface of a sphere whose radius D is large with respect to the bounded region. The *reciprocity principle* tells us that the same mathematical relation holds between points P and $(x, 0)$, regardless of which is the sender and which the receiver. Consequently, the data obtained at the points $(x, 0)$ are then values of the inverse Fourier transform of the function describing the amplitude of the signal sent from each point P.

14.6   Remote Sensing

A basic problem in remote sensing is to determine the nature of a distant object by measuring signals transmitted by or reflected from that object. If the object of interest is sufficiently remote, that is, is in the *farfield*, the data we obtain by sampling the propagating spatio-temporal field is related, approximately, to what we want by *Fourier transformation*. The problem is then to estimate a function from finitely many (usually noisy) values of its *Fourier transform*. The application we consider here is a common one of remote-sensing of transmitted or reflected waves propagating from distant sources. Examples include optical imaging of planets and asteroids using reflected sunlight, radio-astronomy imaging of distant sources of radio waves, active and passive sonar, and radar imaging.

14.7 The Wave Equation

In many areas of remote sensing, what we measure are the fluctuations in time of an electromagnetic or acoustic field. Such fields are described mathematically as solutions of certain partial differential equations, such as the *wave equation*. A function $u(x, y, z, t)$ is said to satisfy the *three-dimensional wave equation* if

$$u_{tt} = c^2(u_{xx} + u_{yy} + u_{zz}) = c^2 \nabla^2 u, \tag{14.6}$$

where u_{tt} denotes the second partial derivative of u with respect to the time variable t twice and $c > 0$ is the (constant) speed of propagation. More complicated versions of the wave equation permit the speed of propagation c to vary with the spatial variables x, y, z, but we shall not consider that here.

We use the method of *separation of variables* at this point, to get some idea about the nature of solutions of the wave equation. Assume, for the moment, that the solution $u(t, x, y, z)$ has the simple form

$$u(t, x, y, z) = g(t)f(x, y, z). \tag{14.7}$$

Inserting this separated form into the wave equation, we get

$$g''(t)f(x, y, z) = c^2 g(t)\nabla^2 f(x, y, z) \tag{14.8}$$

or

$$g''(t)/g(t) = c^2 \nabla^2 f(x, y, z)/f(x, y, z). \tag{14.9}$$

The function on the left is independent of the spatial variables, while the one on the right is independent of the time variable; consequently, they must both equal the same constant, which we denote $-\omega^2$. From this we have two separate equations,

$$g''(t) + \omega^2 g(t) = 0, \tag{14.10}$$

and

$$\nabla^2 f(x, y, z) + \frac{\omega^2}{c^2} f(x, y, z) = 0. \tag{14.11}$$

Equation (14.11) is the *Helmholtz equation*.

Equation (14.10) has for its solutions the functions $g(t) = \cos(\omega t)$ and $\sin(\omega t)$, or, in complex form, the complex exponential functions $g(t) = e^{i\omega t}$ and $g(t) = e^{-i\omega t}$. Functions $u(t, x, y, z) = g(t)f(x, y, z)$ with such time dependence are called *time-harmonic* solutions.

14.8   Planewave Solutions

Suppose that, beginning at time $t = 0$, there is a localized disturbance. As time passes, that disturbance spreads out spherically. When the radius of the sphere is very large, the surface of the sphere appears planar, to an observer on that surface, who is said then to be in the *far field*. This motivates the study of solutions of the wave equation that are constant on planes; the so-called *planewave solutions*.

Let $\mathbf{s} = (x, y, z)$ and $u(\mathbf{s}, t) = u(x, y, z, t) = e^{i\omega t}e^{i\mathbf{k}\cdot\mathbf{s}}$. Then we can show that u satisfies the wave equation $u_{tt} = c^2\nabla^2 u$ for any real vector $\mathbf{k}$, so long as $||\mathbf{k}||^2 = \omega^2/c^2$. This solution is a planewave associated with frequency ω and *wavevector* $\mathbf{k}$; at any fixed time the function $u(\mathbf{s}, t)$ is constant on any plane in three-dimensional space having $\mathbf{k}$ as a normal vector.

In radar and sonar, the field $u(\mathbf{s}, t)$ being sampled is usually viewed as a discrete or continuous superposition of planewave solutions with various amplitudes, frequencies, and wavevectors. We sample the field at various spatial locations $\mathbf{s}$, for various times t. Here we simplify the situation a bit by assuming that all the planewave solutions are associated with the same frequency, ω. If not, we can perform an FFT on the functions of time received at each sensor location $\mathbf{s}$ and keep only the value associated with the desired frequency ω.

14.9   Superposition and the Fourier Transform

In the continuous superposition model, the field is

$$u(\mathbf{s}, t) = e^{i\omega t}\int F(\mathbf{k})e^{i\mathbf{k}\cdot\mathbf{s}}d\mathbf{k}. \tag{14.12}$$

Our measurements at the sensor locations $\mathbf{s}$ give us the values

$$f(\mathbf{s}) = \int F(\mathbf{k})e^{i\mathbf{k}\cdot\mathbf{s}}d\mathbf{k}. \tag{14.13}$$

The data are then Fourier transform values of the complex function $F(\mathbf{k})$; $F(\mathbf{k})$ is defined for all three-dimensional real vectors $\mathbf{k}$, but is zero, in theory, at least, for those $\mathbf{k}$ whose squared length $||\mathbf{k}||^2$ is not equal to ω^2/c^2. Our goal is then to estimate $F(\mathbf{k})$ from measured values of its Fourier transform. Since each $\mathbf{k}$ is a normal vector for its planewave field component, determining the value of $F(\mathbf{k})$ will tell us the strength of the planewave component coming from the direction $\mathbf{k}$.

14.9.1   The Spherical Model

We can imagine that the sources of the planewave fields are the points P that lie on the surface of a large sphere centered at the origin. For each

P, the ray from the origin to P is parallel to some wavevector $\mathbf{k}$. The function $F(\mathbf{k})$ can then be viewed as a function $F(P)$ of the points P. Our measurements will be taken at points $\mathbf{s}$ inside this sphere. The radius of the sphere is assumed to be orders of magnitude larger than the distance between sensors. The situation is that of astronomical observation of the heavens using ground-based antennas. The sources of the optical or electromagnetic signals reaching the antennas are viewed as lying on a large sphere surrounding the earth. Distance to the sources is not considered now, and all we are interested in are the amplitudes $F(\mathbf{k})$ of the fields associated with each direction $\mathbf{k}$.

14.10 Sensor Arrays

In some applications the sensor locations are essentially arbitrary, while in others their locations are carefully chosen. Sometimes, the sensors are collinear, as in sonar towed arrays. Figure 14.1 illustrates a line array.

14.10.1 The Two-Dimensional Array

Suppose now that the sensors are in locations $\mathbf{s} = (x, y, 0)$, for various x and y; then we have a *planar array* of sensors. Then the dot product $\mathbf{s} \cdot \mathbf{k}$ that occurs in Equation (14.13) is

$$\mathbf{s} \cdot \mathbf{k} = xk_1 + yk_2; \tag{14.14}$$

we cannot *see* the third component, k_3. However, since we know the size of the vector $\mathbf{k}$, we can determine $|k_3|$. The only ambiguity that remains is that we cannot distinguish sources on the upper hemisphere from those on the lower one. In most cases, such as astronomy, it is obvious in which hemisphere the sources lie, so the ambiguity is resolved.

The function $F(\mathbf{k})$ can then be viewed as $F(k_1, k_2)$, a function of the two variables k_1 and k_2. Our measurements give us values of $f(x, y)$, the two-dimensional Fourier transform of $F(k_1, k_2)$. Because of the limitation $||\mathbf{k}|| = \frac{\omega}{c}$, the function $F(k_1, k_2)$ has bounded support. Consequently, its Fourier transform cannot have bounded support. As a result, we can never have all the values of $f(x, y)$, and so cannot hope to reconstruct $F(k_1, k_2)$ exactly, even for noise-free data.

14.10.2 The One-Dimensional Array

If the sensors are located at points $\mathbf{s}$ having the form $\mathbf{s} = (x, 0, 0)$, then we have a *line array* of sensors. The dot product in Equation (14.13) becomes

$$\mathbf{s} \cdot \mathbf{k} = xk_1. \tag{14.15}$$

Now the ambiguity is greater than in the planar array case. Once we have k_1, we know that

$$k_2^2 + k_3^2 = (\frac{\omega}{c})^2 - k_1^2, \qquad (14.16)$$

which describes points P lying on a circle on the surface of the distant sphere, with the vector $(k_1, 0, 0)$ pointing at the center of the circle. It is said then that we have a *cone of ambiguity*. One way to resolve the situation is to assume $k_3 = 0$; then $|k_2|$ can be determined and we have remaining only the ambiguity involving the sign of k_2. Once again, in many applications, this remaining ambiguity can be resolved by other means.

Once we have resolved any ambiguity, we can view the function $F(\mathbf{k})$ as $F(k_1)$, a function of the single variable k_1. Our measurements give us values of $f(x)$, the Fourier transform of $F(k_1)$. As in the two-dimensional case, the restriction on the size of the vectors $\mathbf{k}$ means that the function $F(k_1)$ has bounded support. Consequently, its Fourier transform, $f(x)$, cannot have bounded support. Therefore, we shall never have all of $f(x)$, and so cannot hope to reconstruct $F(k_1)$ exactly, even for noise-free data.

14.10.3   Limited Aperture

In both the one- and two-dimensional problems, the sensors will be placed within some bounded region, such as $|x| \leq A$, $|y| \leq B$ for the two-dimensional problem, or $|x| \leq A$ for the one-dimensional case. These bounded regions are the *apertures* of the arrays. The larger these apertures are, in units of the wavelength, the better the resolution of the reconstructions.

In digital array processing there are only finitely many sensors, which then places added limitations on our ability to reconstruction the field amplitude function $F(\mathbf{k})$.

14.11   The Remote-Sensing Problem

We shall begin our discussion of the remote-sensing problem by considering an extended object transmitting or reflecting a single-frequency, or *narrowband*, signal. The narrowband, extended-object case is a good place to begin, since a point object is simply a limiting case of an extended object, and broadband received signals can always be filtered to reduce their frequency band.

14.11.1   The Solar-Emission Problem

In [23] Bracewell discusses the *solar-emission* problem. In 1942, it was observed that radio-wave emissions in the one-meter wavelength range were

arriving from the sun. Were they coming from the entire disk of the sun or were the sources more localized, in sunspots, for example? The problem then was to view each location on the sun's surface as a potential source of these radio waves and to determine the intensity of emission corresponding to each location.

For electromagnetic waves the propagation speed is the speed of light in a vacuum, which we shall take here to be $c = 3 \times 10^8$ meters per second. The wavelength λ for gamma rays is around one Angstrom, which is 10^{-10} meters; for x-rays it is about one millimicron, or 10^{-9} meters. The visible spectrum has wavelengths that are a little less than one micron, that is, 10^{-6} meters. Shortwave radio has a wavelength around one millimeter; microwaves have wavelengths between one centimeter and one meter. Broadcast radio has a λ running from about 10 meters to 1000 meters, while the so-called long radio waves can have wavelengths several thousand meters long.

The sun has an angular diameter of 30 min. of arc, or one-half of a degree, when viewed from earth, but the needed resolution was more like 3 min. of arc. As we shall see shortly, such resolution requires a radio telescope 1000 wavelengths across, which means a diameter of 1km at a wavelength of 1 meter; in 1942 the largest military radar antennas were less than 5 meters across. A solution was found, using the method of reconstructing an object from line-integral data, a technique that surfaced again in tomography. The problem here is inherently two-dimensional, but, for simplicity, we shall begin with the one-dimensional case.

14.12 Sampling

In the one-dimensional case, the signal received at the point $(x, 0, 0)$ is essentially the inverse Fourier transform $f(x)$ of the function $F(k_1)$; for notational simplicity, we write $k = k_1$. The $F(k)$ supported on a bounded interval $|k| \leq \frac{\omega}{c}$, so $f(x)$ cannot have bounded support. As we noted earlier, to determine $F(k)$ exactly, we would need measurements of $f(x)$ on an unbounded set. But, which unbounded set?

Because the function $F(k)$ is zero outside the interval $[-\frac{\omega}{c}, \frac{\omega}{c}]$, the function $f(x)$ is *band-limited*. The *Nyquist spacing* in the variable x is therefore

$$\Delta_x = \frac{\pi c}{\omega}. \tag{14.17}$$

The wavelength λ associated with the frequency ω is defined to be

$$\lambda = \frac{2\pi c}{\omega}, \tag{14.18}$$

so that

$$\Delta_x = \frac{\lambda}{2}. \tag{14.19}$$

The significance of the Nyquist spacing comes from *Shannon's Sampling Theorem*, which says that if we have the values $f(m\Delta_x)$, for all integers m, then we have enough information to recover $F(k)$ exactly. In practice, of course, this is never the case.

14.13   The Limited-Aperture Problem

In the remote-sensing problem, our measurements at points $(x, 0, 0)$ in the farfield give us the values $f(x)$. Suppose now that we are able to take measurements only for limited values of x, say for $|x| \leq A$; then $2A$ is the *aperture* of our antenna or array of sensors. We describe this by saying that we have available measurements of $f(x)h(x)$, where $h(x) = \chi_A(x) = 1$, for $|x| \leq A$, and zero otherwise. So, in addition to describing blurring and low-pass filtering, the convolution-filter model can also be used to model the limited-aperture problem. As in the low-pass case, the limited-aperture problem can be attacked using extrapolation, but with the same sort of risks described for the low-pass case. A much different approach is to increase the aperture by physically moving the array of sensors, as in *synthetic aperture radar* (SAR).

Returning to the farfield remote-sensing model, if we have Fourier transform data only for $|x| \leq A$, then we have $f(x)$ for $|x| \leq A$. Using $h(x) = \chi_A(x)$ to describe the limited aperture of the system, the point-spread function is $H(\gamma) = 2A\mathrm{sinc}(\gamma A)$, the Fourier transform of $h(x)$. The first zeros of the numerator occur at $|\gamma| = \frac{\pi}{A}$, so the main lobe of the point-spread function has width $\frac{2\pi}{A}$. For this reason, the resolution of such a limited-aperture imaging system is said to be on the order of $\frac{1}{A}$. Since $|k| \leq \frac{\omega}{c}$, we can write $k = \frac{\omega}{c}\sin\theta$, where θ denotes the angle between the positive y-axis and the vector $\mathbf{k} = (k_1, k_2, 0)$; that is, θ points in the direction of the point P associated with the wavevector $\mathbf{k}$. The resolution, as measured by the width of the main lobe of the point-spread function $H(\gamma)$, in units of k, is $\frac{2\pi}{A}$, but, the angular resolution will depend also on the frequency ω. Since $k = \frac{2\pi}{\lambda}\sin\theta$, a distance of one unit in k may correspond to a large change in θ when ω is large, but only to a relatively small change in θ when ω is small. For this reason, the aperture of the array is usually measured in units of the wavelength; an aperture of $A = 5$ meters may be acceptable if the frequency is high, so that the wavelength is small, but not if the radiation is in the one-meter-wavelength range.

14.14   Resolution

If $F(k) = \delta(k)$ and $h(x) = \chi_A(x)$ describes the aperture-limitation of the imaging system, then the point-spread function is $H(\gamma) = 2A\mathrm{sinc}(\gamma A)$. The maximum of $H(\gamma)$ still occurs at $\gamma = 0$, but the main lobe of $H(\gamma)$

extends from $-\frac{\pi}{A}$ to $\frac{\pi}{A}$; the point source has been spread out. If the point-source object shifts, so that $F(k) = \delta(k-a)$, then the reconstructed image of the object is $H(k-a)$, so the peak is still in the proper place. If we know *a priori* that the object is a single point source, but we do not know its location, the spreading of the point poses no problem; we simply look for the maximum in the reconstructed image. Problems arise when the object contains several point sources, or when we do not know *a priori* what we are looking at, or when the object contains no point sources, but is just a continuous distribution.

Suppose that $F(k) = \delta(k-a) + \delta(k-b)$; that is, the object consists of two point sources. Then Fourier transformation of the aperture-limited data leads to the reconstructed image

$$R(k) = 2A\Big(\mathrm{sinc}(A(k-a)) + \mathrm{sinc}(A(k-b))\Big). \qquad (14.20)$$

If $|b-a|$ is large enough, $R(k)$ will have two distinct maxima, at approximately $k = a$ and $k = b$, respectively. For this to happen, we need π/A, half the width of the main lobe of the function $\mathrm{sinc}(Ak)$, to be less than $|b-a|$. In other words, to resolve the two point sources a distance $|b-a|$ apart, we need $A \geq \pi/|b-a|$. However, if $|b-a|$ is too small, the distinct maxima merge into one, at $k = \frac{a+b}{2}$ and resolution will be lost. How small is too small will depend on both A and ω.

Suppose now that $F(k) = \delta(k-a)$, but we do not know *a priori* that the object is a single point source. We calculate

$$R(k) = H(k-a) = 2A\mathrm{sinc}(A(k-a)) \qquad (14.21)$$

and use this function as our reconstructed image of the object, for all k. What we see when we look at $R(k)$ for some $k = b \neq a$ is $R(b)$, which is the same thing we see when the point source is at $k = b$ and we look at $k = a$. Point-spreading is, therefore, more than a cosmetic problem. When the object is a point source at $k = a$, but we do not know *a priori* that it is a point source, the spreading of the point causes us to believe that the object function $F(k)$ is nonzero at values of k other than $k = a$. When we look at, say, $k = b$, we see a nonzero value that is caused by the presence of the point source at $k = a$.

Suppose now that the object function $F(k)$ contains no point sources, but is simply an ordinary function of k. If the aperture A is very small, then the function $H(k)$ is nearly constant over the entire extent of the object. The convolution of $F(k)$ and $H(k)$ is essentially the integral of $F(k)$, so the reconstructed object is $R(k) = \int F(k)dk$, for all k.

Let's see what this means for the solar-emission problem discussed earlier.

14.14.1   The Solar-Emission Problem Revisited

The wavelength of the radiation is $\lambda = 1$ meter. Therefore, $\frac{\omega}{c} = 2\pi$, and k in the interval $[-2\pi, 2\pi]$ corresponds to the angle θ in $[0, \pi]$. The sun has an angular diameter of 30 minutes of arc, which is about 10^{-2} radians. Therefore, the sun subtends the angles θ in $[\frac{\pi}{2} - (0.5)\cdot 10^{-2}, \frac{\pi}{2} + (0.5)\cdot 10^{-2}]$, which corresponds roughly to the variable k in the interval $[-3 \cdot 10^{-2}, 3 \cdot 10^{-2}]$. Resolution of 3 minutes of arc means resolution in the variable k of $3 \cdot 10^{-3}$. If the aperture is $2A$, then to achieve this resolution, we need

$$\frac{\pi}{A} \leq 3 \cdot 10^{-3}, \tag{14.22}$$

or

$$A \geq \frac{\pi}{3} \cdot 10^3 \tag{14.23}$$

meters, or A not less than about 1000 meters.

The radio-wave signals emitted by the sun are focused, using a parabolic radio-telescope. The telescope is pointed at the center of the sun. Because the sun is a great distance from the earth and the subtended arc is small (30 min.), the signals from each point on the sun's surface arrive at the parabola nearly head-on, that is, parallel to the line from the vertex to the focal point, and are reflected to the receiver located at the focal point of the parabola. The effect of the parabolic antenna is not to discriminate against signals coming from other directions, since there are none, but to effect a summation of the signals received at points $(x, 0, 0)$, for $|x| \leq A$, where $2A$ is the diameter of the parabola. When the aperture is large, the function $h(x)$ is nearly one for all x and the signal received at the focal point is essentially

$$\int f(x)dx = F(0); \tag{14.24}$$

we are now able to distinguish between $F(0)$ and other values $F(k)$. When the aperture is small, $h(x)$ is essentially $\delta(x)$ and the signal received at the focal point is essentially

$$\int f(x)\delta(x)dx = f(0) = \int F(k)dk; \tag{14.25}$$

now all we get is the contribution from all the k, superimposed, and all resolution is lost.

Since the solar emission problem is clearly two-dimensional, and we need 3 min. resolution in both dimensions, it would seem that we would need a circular antenna with a diameter of about one kilometer, or a rectangular antenna roughly one kilometer on a side. Eventually, this problem was solved by converting it into essentially a tomography problem and applying the same techniques that are today used in CAT scan imaging.

14.15 Discrete Data

A familiar topic in signal processing is the passage from functions of continuous variables to discrete sequences. This transition is achieved by *sampling*, that is, extracting values of the continuous-variable function at discrete points in its domain. Our example of farfield propagation can be used to explore some of the issues involved in sampling.

Imagine an infinite *uniform line array* of sensors formed by placing receivers at the points $(n\Delta, 0, 0)$, for some $\Delta > 0$ and all integers n. Then our data are the values $f(n\Delta)$. Because we defined $k = \frac{\omega}{c}\cos\theta$, it is clear that the function $F(k)$ is zero for k outside the interval $[-\frac{\omega}{c}, \frac{\omega}{c}]$.

Our discrete array of sensors cannot distinguish between the signal arriving from θ and a signal with the same amplitude, coming from an angle α with

$$\frac{\omega}{c}\cos\alpha = \frac{\omega}{c}\cos\theta + \frac{2\pi}{\Delta}m, \tag{14.26}$$

where m is an integer. To resolve this ambiguity, we select $\Delta > 0$ so that

$$-\frac{\omega}{c} + \frac{2\pi}{\Delta} \geq \frac{\omega}{c}, \tag{14.27}$$

or

$$\Delta \leq \frac{\pi c}{\omega} = \frac{\lambda}{2}. \tag{14.28}$$

The sensor spacing $\Delta_s = \frac{\lambda}{2}$ is the *Nyquist spacing*.

In the sunspot example, the object function $F(k)$ is zero for k outside of an interval much smaller than $[-\frac{\omega}{c}, \frac{\omega}{c}]$. Knowing that $F(k) = 0$ for $|k| > K$, for some $0 < K < \frac{\omega}{c}$, we can accept ambiguities that confuse θ with another angle that lies outside the angular diameter of the object. Consequently, we can redefine the Nyquist spacing to be

$$\Delta_s = \frac{\pi}{K}. \tag{14.29}$$

This tells us that when we are imaging a distant object with a small angular diameter, the Nyquist spacing is greater than $\frac{\lambda}{2}$. If our sensor spacing has been chosen to be $\frac{\lambda}{2}$, then we have *oversampled*. In the oversampled case, band-limited extrapolation methods can be used to improve resolution.

14.15.1 Reconstruction from Samples

From the data gathered at our infinite array we have extracted the Fourier transform values $f(n\Delta)$, for all integers n. The obvious question is whether or not the data is sufficient to reconstruct $F(k)$. We know that, to avoid

ambiguity, we must have $\Delta \leq \frac{\pi c}{\omega}$. The good news is that, provided this condition holds, $F(k)$ is uniquely determined by this data and formulas exist for reconstructing $F(k)$ from the data; this is the content of the *Shannon's Sampling Theorem*. Of course, this is only of theoretical interest, since we never have infinite data. Nevertheless, a considerable amount of traditional signal-processing exposition makes use of this infinite-sequence model. The real problem, of course, is that our data is always finite.

14.16   The Finite-Data Problem

Suppose that we build a *uniform line array* of sensors by placing receivers at the points $(n\Delta, 0, 0)$, for some $\Delta > 0$ and $n = -N, ..., N$. Then our data are the values $f(n\Delta)$, for $n = -N, ..., N$. Suppose, as previously, that the object of interest, the function $F(k)$, is nonzero only for values of k in the interval $[-K, K]$, for some $0 < K < \frac{\omega}{c}$. Once again, we must have $\Delta \leq \frac{\pi c}{\omega}$ to avoid ambiguity; but this is not enough, now. The finite Fourier data is no longer sufficient to determine a unique $F(k)$. The best we can hope to do is to estimate the true $F(k)$, using both our measured Fourier data and whatever prior knowledge we may have about the function $F(k)$, such as where it is nonzero, if it consists of Dirac delta point sources, or if it is nonnegative. The data is also noisy, and that must be accounted for in the reconstruction process.

In certain applications, such as sonar array processing, the sensors are not necessarily arrayed at equal intervals along a line, or even at the grid points of a rectangle, but in an essentially arbitrary pattern in two, or even three, dimensions. In such cases, we have values of the Fourier transform of the object function, but at essentially arbitrary values of the variable. How best to reconstruct the object function in such cases is not obvious.

14.17   Functions of Several Variables

Fourier transformation applies, as well, to functions of several variables. As in the one-dimensional case, we can motivate the multi-dimensional Fourier transform using the farfield propagation model. As we noted earlier, the solar emission problem is inherently a two-dimensional problem.

14.17.1   Two-Dimensional Farfield Object

Assume that our sensors are located at points $\mathbf{s} = (x, y, 0)$ in the x,y-plane. As discussed previously, we assume that the function $F(\mathbf{k})$ can be viewed as a function $F(k_1, k_2)$. Since, in most applications, the distant object has a small angular diameter when viewed from a great distance - the sun's is

only 30 minutes of arc - the function $F(k_1, k_2)$ will be supported on a small subset of vectors (k_1, k_2).

14.17.2 Limited Apertures in Two Dimensions

Suppose we have the values of the Fourier transform, $f(x, y)$, for $|x| \leq A$ and $|y| \leq A$. We describe this limited-data problem using the function $h(x, y)$ that is one for $|x| \leq A$, and $|y| \leq A$, and zero, otherwise. Then the point-spread function is the Fourier transform of this $h(x, y)$, given by

$$H(\alpha, \beta) = 4AB\text{sinc}(A\alpha)\text{sinc}(B\beta). \tag{14.30}$$

The resolution in the horizontal (x) direction is on the order of $\frac{1}{A}$, and $\frac{1}{B}$ in the vertical, where, as in the one-dimensional case, aperture is best measured in units of wavelength.

Suppose our aperture is circular, with radius A. Then we have Fourier transform values $f(x, y)$ for $\sqrt{x^2 + y^2} \leq A$. Let $h(x, y)$ equal one, for $\sqrt{x^2 + y^2} \leq A$, and zero, otherwise. Then the point-spread function of this limited-aperture system is the Fourier transform of $h(x, y)$, given by $H(\alpha, \beta) = \frac{2\pi A}{r} J_1(rA)$, with $r = \sqrt{\alpha^2 + \beta^2}$. The resolution of this system is roughly the distance from the origin to the first null of the function $J_1(rA)$, which means that $rA = 4$, roughly.

For the solar emission problem, this says that we would need a circular aperture with radius approximately one kilometer to achieve 3 minutes of arc resolution. But this holds only if the antenna is stationary; a moving antenna is different! The solar emission problem was solved by using a rectangular antenna with a large A, but a small B, and exploiting the rotation of the earth. The resolution is then good in the horizontal, but bad in the vertical, so that the imaging system discriminates well between two distinct vertical lines, but cannot resolve sources within the same vertical line. Because B is small, what we end up with is essentially the integral of the function $f(x, z)$ along each vertical line. By tilting the antenna, and waiting for the earth to rotate enough, we can get these integrals along any set of parallel lines. The problem then is to reconstruct $F(k_1, k_2)$ from such line integrals. This is also the main problem in tomography.

14.18 Broadband Signals

We have spent considerable time discussing the case of a distant point source or an extended object transmitting or reflecting a single-frequency signal. If the signal consists of many frequencies, the so-called broadband case, we can still analyze the received signals at the sensors in terms of time delays, but we cannot easily convert the delays to phase differences, and thereby make good use of the Fourier transform. One approach is

to filter each received signal, to remove components at all but a single frequency, and then to proceed as previously discussed. In this way we can process one frequency at a time. The object now is described in terms of a function of both $\mathbf{k}$ and ω, with $F(\mathbf{k}, \omega)$ the complex amplitude associated with the wave vector $\mathbf{k}$ and the frequency ω. In the case of radar, the function $F(\mathbf{k}, \omega)$ tells us how the material at P reflects the radio waves at the various frequencies ω, and thereby gives information about the nature of the material making up the object near the point P.

There are times, of course, when we do not want to decompose a broad-band signal into single-frequency components. A satellite reflecting a TV signal is a broadband point source. All we are interested in is receiving the broadband signal clearly, free of any other interfering sources. The direction of the satellite is known and the antenna is turned to face the satellite. Each location on the parabolic dish reflects the same signal. Because of its parabolic shape, the signals reflected off the dish and picked up at the focal point have exactly the same travel time from the satellite, so they combine coherently, to give us the desired TV signal.
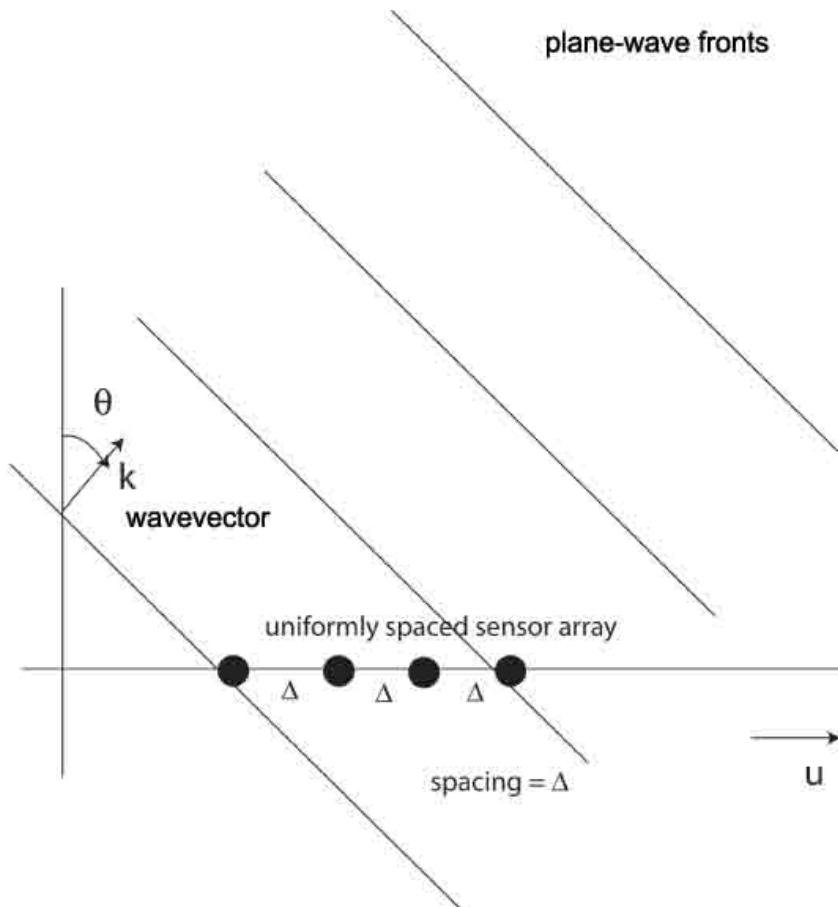
Figure 14.1: A uniform line array sensing a planewave field.

Part V

Nonlinear Models

Chapter 15

Random Sequences

15.1 Chapter Summary

When we sample a function $f(x)$ we usually make some error, and the data we get is not precisely $f(n\Delta)$, but contains *additive noise*, that is, our data value is really $f(n\Delta) +$ noise. Noise is best viewed as random, so it becomes necessary to treat *random sequences* $f = \{f_n\}$ in which each f_n is a random variable. The random variables f_n and f_m may or may not be statistically independent.

15.2 What is a Random Variable?

The simplest answer to the question What is a random variable? is A random variable is a mathematical model. Imagine that we repeatedly drop a baseball from eye-level to the floor. Each time, the baseball behaves the same. If we were asked to describe this behavior with a mathematical model, we probably would choose to use a differential equation as our model. Ignoring everything except the force of gravity, we would write

$$h''(t) = -32$$

as the equation describing the downward acceleration due to gravity. Integrating, we have

$$h'(t) = -32t + h'(0)$$

as the velocity of the baseball at time $t \geq 0$, and integrating once more,

$$h(t) = -16t^2 + h'(0)t + h(0)$$

as the equation of position of the baseball at time $t \geq 0$, up to the moment when it hits the floor. Knowing $h(0)$, the distance from eye-level to the

175

floor, and knowing that, since we dropped the ball, $h'(0) = 0$, we can determine how long it will take the baseball to hit the floor, and the speed with which it will hit. This analysis will apply every time we drop the baseball. There will, of course, be slight differences from one drop to the next, depending, perhaps, on how the ball was held, but these will be so small as to be insignificant.

Now imagine that, instead of a baseball, we drop a feather. A few repetitions are all that is necessary to convince us that the model used for the baseball no longer suffices. The factors such as air resistance, air currents and how the object was held that we safely ignored with regard to the baseball, now become important. The feather does not always land in the same place, it doesn't always take the same amount of time to reach the floor, and doesn't always land with the same velocity. It doesn't even fall in straight vertical line. How can we possibly model such behavior? Must we try to describe accurately the air resistance encountered by the feather? The answer is that we use random variables as our model.

While we cannot say precisely where the feather will land, and, of course, we must be careful to specify how we are to determine "the place", we can learn, from a number of trials, where it tends to land, and we can postulate the probability that it will land within any given region of the floor. In this way, the place where the feather will land becomes a random variable with associated probability density function. Similarly, we can postulate the probability that the time for the fall will lie within any interval of elapsed time, making the elapsed time a random variable. Finally, we can postulate the probability that its velocity vector upon hitting the ground will lie within any given set of three-dimensional vectors, making the velocity a random vector. On the basis of these probabilistic models we can proceed to predict the outcome of the next drop.

It is important to remember that the random variable is the model that we set up prior to the dropping of the feather, not the outcome of any particular drop.

15.3   The Coin-Flip Random Sequence

The simplest example of a random sequence is the *coin-flip* sequence, which we denote by $c = \{c_n\}_{n=-\infty}^{\infty}$. We imagine that, at each "time" n, a coin is flipped, and $c_n = 1$ if the coin shows heads, and $c_n = -1$ if the coin shows tails. When we speak of this coin-flip sequence, we refer to this random model, not to any specific sequence of ones and minus ones; the random coin-flip sequence is not, therefore, a particular sequence, just as a random variable is not actually a specific number. Any particular sequence of ones and minus ones can be thought of as having resulted from such an infinite number of flips of the coin, and is called a *realization* of the random coin-flip

sequence.

It will be convenient to allow for the coin to be *biased*, that is, for the probabilities of heads and tails to be unequal. We denote by p the probability that heads occurs and $1-p$ the probability of tails; the coin is called *unbiased* or *fair* if $p = 1/2$. To find the *expected value* of c_n, written $E(c_n)$, we multiply each possible value of c_n by its probability and sum; that is,

$$E(c_n) = (+1)p + (-1)(1-p) = 2p - 1.$$

If the coin is fair then $E(c_n) = 0$. The variance of the random variable c_n, measuring its tendency to deviate from its expected value, is $var(c_n) = E([c_n - E(c_n)]^2)$. We have

$$var(c_n) = [+1 - (2p-1)]^2 p + [-1 - (2p-1)]^2 (1-p) = 4p - 4p^2.$$

If the coin is fair then $var(c_n) = 1$. It is important to note that we do not change the coin at any time during the generation of a realization of the random sequence c; in particular, the p does not depend on n. Also, we assume that the random variables c_n are statistically independent.

15.4 Correlation

Let u and v be (possibly complex-valued) random variables with expected values $E(u)$ and $E(v)$, respectively. The covariance between u and v is defined to be

$$cov(u,v) = E\Big((u - E(u))\overline{(v - E(v))}\Big),$$

and the cross-correlation between u and v is

$$corr(u,v) = E(u\overline{v}).$$

It is easily shown that $cov(u,v) = corr(u,v) - E(u)\overline{E(v)}$. When $u = v$ we get $cov(u,u) = var(u)$ and $corr(u,u) = E(|u|^2)$. If $E(u) = E(v) = 0$ then $cov(u,v) = corr(u,v)$. In statistics the "correlation coefficient" is the quantity $cov(u,v)$ divided by the standard deviations of u and v.

When u and v are independent, we have

$$E(u\overline{v}) = E(u)E(\overline{v}),$$

and

$$E\Big((u - E(u))\overline{(v - E(v))}\Big) = E(u - E(u))E(\overline{(v - E(v))}) = 0.$$

To illustrate, let $u = c_n$ and $v = c_{n-m}$. Then, if the coin is fair, $E(c_n) = E(c_{n-m}) = 0$ and

$$cov(c_n, c_{n-m}) = corr(c_n, c_{n-m}) = E(c_n \overline{c_{n-m}}).$$

Because the c_n are independent, $E(c_n\overline{c_{n-m}}) = 0$ for m not equal to 0, and $E(|c_n|^2) = var(c_n) = 1$. Therefore

$$cov(c_n, c_{n-m}) = corr(c_n, c_{n-m}) = 0, \text{for } m \neq 0,$$

and

$$cov(c_n, c_n) = corr(c_n, c_n) = 1.$$

In the next section we shall use the random coin-flip sequence to generate a wide class of random sequences, obtained by viewing $c = \{c_n\}$ as the input into a shift-invariant discrete linear filter.

15.5   Filtering Random Sequences

Suppose, once again, that T is a shift-invariant discrete linear filter with impulse-response sequence g. Now let us take as input, not a particular sequence, but the random coin-flip sequence c, with $p = 0.5$. The output will therefore not be a particular sequence either, but will be another random sequence, say d. Then, for each n the random variable d_n is

$$d_n = \sum_{m=-\infty}^{\infty} c_m g_{n-m} = \sum_{m=-\infty}^{\infty} g_m c_{n-m}. \tag{15.1}$$

We compute the correlation $corr(d_n, d_{n-m}) = E(d_n\overline{d_{n-m}})$. Using the convolution formula Equation (15.1), we find that

$$corr(d_n, d_{n-m}) = \sum_{k=-\infty}^{\infty} \sum_{j=-\infty}^{\infty} g_k\overline{g_j}corr(c_{n-k}, c_{n-m-j}).$$

Since

$$corr(c_{n-k}, c_{n-m-j}) = 0, \text{for } k \neq m + j,$$

we have

$$corr(d_n, d_{n-m}) = \sum_{k=-\infty}^{\infty} g_k\overline{g_{k-m}}. \tag{15.2}$$

The expression of the right side of Equation (15.2) is the definition of the *autocorrelation* of the non-random sequence g, denoted $\rho_g = \{\rho_g(m)\}$; that is,

$$\rho_g(m) = \sum_{k=-\infty}^{\infty} g_k\overline{g_{k-m}}. \tag{15.3}$$

It is important to note that the expected value of d_n is

$$E(d_n) = \sum_{k=-\infty}^{\infty} g_k E(c_{n-k}) = 0$$

and the correlation $corr(d_n, d_{n-m})$ depends only on m; neither quantity depends on n and the sequence d is therefore called *weak-sense stationary*. Let's consider an example.

15.6   An Example

Take $g_0 = g_1 = 0.5$ and $g_k = 0$ otherwise. Then the system is the two-point moving-average, with

$$d_n = 0.5c_n + 0.5c_{n-1}.$$

In the case of the random-coin-flip sequence c each c_n is unrelated to all other c_m; the coin flips are independent. This is no longer the case for the d_n; one effect of the filter g is to introduce correlation into the output. To illustrate, since d_0 and d_1 both depend, to some degree, on the value c_0, they are related. Using Equation (15.3) we have

$$corr(d_n, d_n) = \rho_g(0) = g_0 g_0 + g_1 g_1 = 0.25 + 0.25 = 0.5,$$

$$corr(d_n, d_{n+1}) = \rho_g(-1) = g_0 g_1 = 0.25,$$
$$corr(d_n, d_{n-1}) = \rho_g(+1) = g_1 g_0 = 0.25,$$

and

$$corr(d_n, d_{n-m}) = \rho_g(m) = 0, \text{otherwise}.$$

So we see that d_n and d_{n-m} are related, for $m = -1, 0, +1$, but not otherwise.

15.7   Correlation Functions and Power Spectra

As we have seen, any non-random sequence $g = \{g_n\}$ has its autocorrelation function defined, for each integer m, by

$$\rho_g(m) = \sum_{k=-\infty}^{\infty} g_k \overline{g_{k-m}}.$$

For a random sequence d_n that is wide-sense stationary, its correlation function is defined to be

$$\rho_d(m) = E(d_n \overline{d_{n-m}}).$$

The *power spectrum* of g is defined for ω in $[-\pi, \pi]$ by

$$R_g(\omega) = \sum_{m=-\infty}^{\infty} \rho_g(m) e^{im\omega}.$$

It is easy to see that

$$R_g(\omega) = |G(\omega)|^2,$$

where

$$G(\omega) = \sum_{n=-\infty}^{\infty} g_n e^{in\omega},$$

so that $R_g(\omega) \geq 0$. The power spectrum of the random sequence $d = \{d_n\}$ is defined as

$$R_d(\omega) = \sum_{m=-\infty}^{\infty} \rho_d(m) e^{im\omega}.$$

Although it is not immediately obvious, we also have $R_d(\omega) \geq 0$. One way to see this is to consider

$$D(\omega) = \sum_{n=-\infty}^{\infty} d_n e^{in\omega}$$

and to calculate

$$E(|D(\omega)|^2) = \sum_{m=-\infty}^{\infty} E(d_n \overline{d_{n-m}}) e^{im\omega} = R_d(\omega).$$

Given any power spectrum $R_d(\omega) \geq 0$ we can construct $G(\omega)$ by selecting an arbitrary phase angle θ and letting

$$G(\omega) = \sqrt{R_d(\omega)} e^{i\theta}.$$

We then obtain the non-random sequence g associated with $G(\omega)$ using

$$g_n = \frac{1}{2\pi} \int_{-\pi}^{\pi} G(\omega) e^{-in\omega} d\omega.$$

It follows that $\rho_g(m) = \rho_d(m)$ for each m and $R_g(\omega) = R_d(\omega)$ for each ω.

What we have discovered is that, when the input to the system is the random-coin-flip sequence c, the output sequence d has a correlation function $\rho_d(m)$ that is equal to the autocorrelation of the sequence g. As we just saw, for any weak-sense stationary random sequence d with expected value $E(d_n)$ constant and correlation function $corr(d_n, d_{n-m})$ independent of n, there is a shift-invariant discrete linear system T with impulse-response sequence g, such that $\rho_g(m) = \rho_d(m)$ for each m. Therefore, any weak-sense stationary random sequence d can be viewed as the output of a shift-invariant discrete linear system, when the input is the random-coin-flip sequence $c = \{c_n\}$.

15.8 The Dirac Delta in Frequency Space

Consider the "function" defined by the infinite sum

$$\delta(\omega) = \frac{1}{2\pi} \sum_{n=-\infty}^{\infty} e^{in\omega} = \frac{1}{2\pi} \sum_{n=-\infty}^{\infty} e^{-in\omega}. \qquad (15.4)$$

This is a Fourier series in which all the Fourier coefficients are one. The series doesn't converge in the usual sense, but still has some uses. In particular, look what happens when we take

$$F(\omega) = \sum_{n=-\infty}^{\infty} f(n)e^{-in\omega},$$

for $\pi \leq \omega \leq \pi$, and calculate

$$\int_{-\pi}^{\pi} F(\omega)\delta(\omega)d\omega = \sum_{n=-\infty}^{\infty} \frac{1}{2\pi} \int_{-\pi}^{\pi} F(\omega)e^{-in\omega}d\omega.$$

We have

$$\int_{-\pi}^{\pi} F(\omega)\delta(\omega)d\omega = \frac{1}{2\pi} \sum_{n=-\infty}^{\infty} f(n) = F(0),$$

where the $f(n)$ are the Fourier coefficients of $F(\omega)$. This means that $\delta(\omega)$ has the *sifting property*, just like we saw with the Dirac delta $\delta(x)$; that is why we call it $\delta(\omega)$. When we shift $\delta(\omega)$ to get $\delta(\omega - \alpha)$, we find that

$$\int_{-\pi}^{\pi} F(\omega)\delta(\omega - \alpha)d\omega = F(\alpha).$$

The "function" $\delta(\omega)$ is the Dirac delta for ω space.

15.9 Random Sinusoidal Sequences

Consider $A = |A|e^{i\theta}$, with amplitude $|A|$ a positive-valued random variable and phase angle θ a random variable taking values in the interval $[-\pi, \pi]$; then A is a complex-valued random variable. For a fixed frequency ω_0 we define a random sinusoidal sequence $s = \{s_n\}$ by $s_n = Ae^{-in\omega_0}$. We assume that θ has the uniform distribution over $[-\pi, \pi]$ so that the expected value of s_n is zero. The correlation function for s is

$$\rho_s(m) = E(s_n\overline{s_{n-m}}) = E(|A|^2)e^{-im\omega_0}$$

and the power spectrum of s is

$$R_s(\omega) = E(|A|^2) \sum_{m=-\infty}^{\infty} e^{-im(\omega_0-\omega)},$$

so that, by Equation (15.4), we have

$$R_s(\omega) = 2\pi E(|A|^2)\delta(\omega - \omega_0).$$

We generalize this example to the case of multiple independent sinusoids. Suppose that, for $j = 1, ..., J$, we have fixed frequencies ω_j and independent complex-valued random variables A_j. We let our random sequence be defined by

$$s_n = \sum_{j=1}^{J} A_j e^{-in\omega_j}.$$

Then the correlation function for s is

$$\rho_s(m) = \sum_{j=1}^{J} E(|A_j|^2)e^{-im\omega_j}$$

and the power spectrum for s is

$$R_s(\omega) = 2\pi \sum_{j=1}^{J} E(|A_j|^2)\delta(\omega - \omega_j).$$

This is the commonly used model of independent sinusoids. The problem of *power spectrum estimation* is to determine the values J, the frequencies ω_j and the variances $E(|A_j|^2)$ from finitely many samples from one or more realizations of the random sequence s.

15.10   Random Noise Sequences

Let $q = \{q_n\}$ be an arbitrary weak-sense stationary discrete random sequence, with correlation function $\rho_q(m)$ and power spectrum $R_q(\omega)$. We say that q is *white noise* if $\rho_q(m) = 0$ for m not equal to zero, or, equivalently, if the power spectrum $R_q(\omega)$ is constant over the interval $[-\pi, \pi]$. The *independent sinusoids in additive white noise* model is a random sequence of the form

$$x_n = \sum_{j=1}^{J} A_j e^{-in\omega_j} + q_n.$$

The *signal power* is defined to be $\rho_s(0)$, which is the sum of the $E(|A_j|^2)$, while the noise power is $\rho_q(0)$. The *signal-to-noise ratio* (SNR) is the ratio of signal power to noise power.

15.11 Increasing the SNR

It is often the case that the SNR is quite low and it is desirable to process the data from x to enhance this ratio. The data we have is typically finitely many values of one realization of x. We say we have f_n for $n = 1, 2, ..., N$; we don't say we have x_n because x_n is the random variable, not one value of the random variable. One way to process the data is to estimate $\rho_x(m)$ for some small number of integers m around zero, using, for example, the *lag products* estimate

$$\hat{\rho}_x(m) = \frac{1}{N-m} \sum_{n=1}^{N-m} f_n \overline{f_{n-m}},$$

for $m = 0, 1, ..., M < N$ and $\hat{\rho}_x(-m) = \overline{\hat{\rho}_x(m)}$. Because $\rho_q(m) = 0$ for m not equal to zero, we will have $\hat{\rho}_x(m)$ approximating $\rho_s(m)$ for nonzero values of m, thereby reducing the effect of the noise. Therefore, our estimates of $\rho_s(m)$ are relatively noise-free for $m \neq 0$.

15.12 Colored Noise

The additive noise is said to be *correlated* or *non-white* if it is not the case that $\rho_x(m) = 0$ for all nonzero m. In this case the noise power spectrum is not constant, and so may be concentrated in certain regions of the interval $[-\pi, \pi]$.

The next few sections deal with applications of random sequences.

15.13 Spread-Spectrum Communication

In this section we return to the random-coin-flip model, this time allowing the coin to be biased, that is, p need not be 0.5. Let $s = \{s_n\}$ be a random sequence, such as $s_n = Ae^{in\omega_0}$, with $E(s_n) = \mu$ and correlation function $\rho_s(m)$. Define a second random sequence x by

$$x_n = s_n c_n.$$

The random sequence x is generated from the random signal s by randomly changing its signs. We can show that

$$E(x_n) = \mu(2p - 1)$$

and, for m not equal to zero,

$$\rho_x(m) = \rho_s(m)(2p - 1)^2,$$

with

$$\rho_x(0) = \rho_s(0) + 4p(1 - p)\mu^2.$$

Therefore, if $p = 1$ or $p = 0$ we get $\rho_x(m) = \rho_s(m)$ for all m, but for $p = 0.5$ we get $\rho_x(m) = 0$ for m not equal to zero. If the coin is unbiased, then the random sign changes convert the original signal s into white noise. Generally, we have

$$R_x(\omega) = (2p - 1)^2 R_s(\omega) + (1 - (2p - 1)^2)(\mu^2 + \rho_s(0)),$$

which says that the power spectrum of x is a combination of the signal power spectrum and a white-noise power spectrum, approaching the white-noise power spectrum as p approaches 0.5. If the original signal power spectrum is concentrated within a small interval, then the effect of the random sign changes is to spread that spectrum. Once we know what the particular realization of the random sequence c is that has been used, we can recapture the original signal from $s_n = x_n c_n$. The use of such a spread spectrum permits the sending of multiple narrow-band signals, without confusion, as well as protecting against any narrow-band additive interference.

15.14   Stochastic Difference Equations

The ordinary first-order differential equation $y'(t) + ay(t) = f(t)$, with initial condition $y(0) = 0$, has for its solution $y(t) = e^{-at} \int_0^t e^{as} f(s) ds$. One way to look at such differential equations is to consider $f(t)$ to be the input to a system having $y(t)$ as its output. The system determines which terms will occur on the left side of the differential equation. In many applications the input $f(t)$ is viewed as random noise and the output is then a continuous-time random process. Here we want to consider the discrete analog of such differential equations.

We replace the first derivative with the first difference, $y_{n+1} - y_n$ and we replace the input with the random-coin-flip sequence $c = \{c_n\}$, to obtain the random difference equation

$$y_{n+1} - y_n + ay_n = c_n. \tag{15.5}$$

With $b = 1 - a$ and $0 < b < 1$ we have

$$y_{n+1} - by_n = c_n. \tag{15.6}$$

The solution is $y = \{y_n\}$ given by

$$y_n = b^{n-1} \sum_{k=-\infty}^{n-1} b^{-k} c_k. \tag{15.7}$$

Comparing this with the solution of the differential equation, we see that the term b^{n-1} plays the role of $e^{-at} = (e^{-a})^t$, so that $b = 1 - a$ is substituting for e^{-a}. The infinite sum replaces the infinite integral, with $b^{-k}c_k$ replacing the integrand $e^{as}f(s)$.

The solution sequence y given by Equation (15.7) is a weak-sense stationary random sequence and its correlation function is

$$\rho_y(m) = b^m/(1 - b^2).$$

Since

$$b^{n-1}\sum_{k=-\infty}^{n-1} b^{-k} = \frac{1}{1 - b},$$

the random sequence $(1 - b)y_n = ay_n$ is an infinite *moving-average* random sequence formed from the random sequence c.

We can derive the solution in Equation (15.7) using *z-transforms*. We write

$$Y(z) = \sum_{n=-\infty}^{\infty} y_n z^{-n},$$

and

$$C(z) = \sum_{n=-\infty}^{\infty} c_n z^{-n}.$$

From Equation (15.6) we have

$$zY(z) - bY(z) = C(z),$$

or

$$Y(z) = C(z)(z - b)^{-1}.$$

Expanding in a geometric series, we get

$$Y(z) = C(z)z^{-1}\Big(1 + bz^{-1} + b^2 z^{-2} + ...\Big),$$

from which the solution given in Equation (15.7) follows immediately.

15.15 Random Vectors and Correlation Matrices

In estimation and detection theory, the task is to distinguish *signal vectors* from *noise vectors*. In order to perform such a task, we need to know how signal vectors differ from noise vectors. Most frequently, what we have is statistical information. The signal vectors of interest, which we denote by $\mathbf{s} = (s_1, ..., s_N)^T$, typically exhibit some patterns of behavior among their

entries. For example, a constant signal, such as $\mathbf{s} = (1, 1, ..., 1)^T$, has all its entries identical. A sinusoidal signal, such as $\mathbf{s} = (1, -1, 1, -1, ..., 1, -1)^T$, exhibits a periodicity in its entries. If the signal is a vectorization of a two-dimensional image, then the patterns will be more difficult to describe, but will be there, nevertheless. In contrast, a typical noise vector, denoted $\mathbf{q} = (q_1, ..., q_N)^T$, may have entries that are statistically unrelated to each other, as in white noise. Of course, what is signal and what is noise depends on the context; unwanted interference in radio may be viewed as noise, even though it may be a weather report or a song.

To deal with these notions mathematically, we adopt statistical models. The entries of $\mathbf{s}$ and $\mathbf{q}$ are taken to be random variables, so that $\mathbf{s}$ and $\mathbf{q}$ are random vectors. Often we assume that the mean values, $E(\mathbf{s})$ and $E(\mathbf{q})$, are both equal to the zero vector. Then patterns that may exist among the entries of these vectors are described in terms of *correlations*. The *noise covariance matrix*, which we denote by Q, has for its entries $Q_{mn} = E\left((q_m - E(q_m))\overline{(q_n - E(q_n))}\right)$, for $m, n = 1, ..., N$. The signal covariance matrix is defined similarly. If $E(q_n) = 0$ and $E(|q_n|^2) = 1$ for each n, then Q is the *noise correlation matrix*. Such matrices Q are Hermitian and non-negative definite, that is, $\mathbf{x}^\dagger Q \mathbf{x}$ is non-negative, for every vector $\mathbf{x}$. If Q is a positive multiple of the identity matrix, then the noise vector $\mathbf{q}$ is said to be a *white noise* random vector.

Chapter 16

Classical and Modern Methods

16.1 Chapter Summary

It is common to speak of classical, as opposed to modern, signal processing methods. In this chapter we describe briefly the distinction.

16.2 The Classical Methods

In [66] Candy locates the beginning of the classical period of spectral estimation in Schuster's use of Fourier techniques in 1898 to analyze sun-spot data [198]. The role of Fourier techniques grew with the discovery, by Wiener in the USA and Khintchine in the USSR, of the relation between the power spectrum and the autocorrelation function. Much of Wiener's important work on control and communication remained classified and became known only with the publication of his classic text *Time Series* in 1949 [225]. The book by Blackman and Tukey, *Measurement of Power Spectra* [17], provides perhaps the best description of the classical methods. With the discovery of the FFT by Cooley and Tukey in 1965, all the pieces were in place for the rapid development of this DFT-based approach to spectral estimation.

16.3 Modern Signal Processing and Entropy

Until about the middle of the 1970s most signal processing depended almost exclusively on the DFT, as implemented using the FFT. Algorithms such as the Gerchberg-Papoulis bandlimited extrapolation method were performed

187

as iterative operations on finite vectors, using the FFT at every step. Linear filters and related windowing methods involving the FFT were also used to enhance the resolution of the reconstructed objects. The proper design of these filters was an area of interest to quite a number of researchers, John Tukey among them. Then, around the end of that decade, interest in entropy maximization began to grow, as researchers began to wonder if high-resolution methods developed for seismic oil exploration could be applied successfully in other areas.

John Burg had developed his *maximum entropy method* (MEM) while working in the oil industry in the 1960s. He then went to Stanford as a mature graduate student and received his doctorate in 1975 for a thesis based largely on his earlier work on MEM [32]. This thesis and a handful of earlier presentations at meetings [30, 31] fueled the interest in entropy.

It was not only the effectiveness of Burg's techniques that attracted the attention of members of the signal-processing community. The classical methods seemed to some to be *ad hoc*, and they sought a more intellectually satisfying basis for spectral estimation. Classical methods start with the time series data, say x_n, for $n = 1, ..., N$. In the direct approach, slightly simplified, the data is *windowed*; that is, x_n is replaced with $x_n w_n$ for some choice of constants w_n. Then, the vDFT is computed, using the FFT, and the squared magnitudes of the entries of the vDFT provide the desired estimate of the power spectrum. In the more indirect approach, autocorrelation values $r_x(m)$ are first estimated, for $m = 0, 1, ..., M$, where M is some fraction of the data length N. Then, these estimates of $r_x(m)$ are windowed and the vDFT calculated, again using the FFT.

What some people objected to was the use of these windows. After all, the measured data was x_n, not $x_n w_n$, so why corrupt the data at the first step? The classical methods produced answers that depended to some extent on which window function one used; there had to be a better way. Entropy maximization was the answer to their prayers.

In 1981 the first of several international workshops on entropy maximization was held at the University of Wyoming, bring together most of the people working in this area. The books [205] and [206] contain the papers presented at those workshops. As one can see from reading those papers, the general theme is that a new day has dawned.

16.4   Related Methods

It was soon recognized that maximum entropy methods were closely related to model-based techniques that had been part of statistical time series for decades. This realization led to a broader use of *autoregressive* (AR) and *autoregressive, moving average* (ARMA) models for spectral estimation [189], as well as of eigenvector methods, such as Pisarenko's method [186].

What Candy describes as the modern approach to spectral estimation is one based on explicit parametric models, in contrast to the classical non-parametric approach. The book edited by Don Childers [76] is a collection of journal articles that captures the state-of-the-art at the end of the 1970s.

In a sense the transition from the classical ways to the modern methods solved little; the choice of models is as *ad hoc* as the choice of windows was before. On the other hand, we do have a wider collection of techniques from which to choose and we can examine these techniques to see when they perform well and when they do not. We do not expect one approach to work in all cases. High-speed computation permits the use of more complicated parametric models tailored to the physics of a given situation.

Our estimates will, eventually, be used for some purpose. In medical imaging a doctor is going to make a diagnosis based in part on what the image reveals. How good the image needs to be depends on the purpose for which it is made. Judging the quality of a reconstructed image based on somewhat subjective criteria, such as how useful it is to a doctor, is a problem that is not yet solved. Human-observer studies are one way to obtain this nonmathematical evaluation of reconstruction and estimation methods. The next step beyond that is to develop computer software that judges the images or spectra as a human would.

Chapter 17

Entropy Maximization

17.1 Chapter Summary

The problem of estimating the nonnegative function $R(\omega)$, for $|\omega| \leq \pi$, from the finitely many Fourier-transform values

$$r(n) = \int_{-\pi}^{\pi} R(\omega) \exp(-in\omega) d\omega / 2\pi, \; n = -N, ..., N$$

is an *under-determined problem*, meaning that the data alone is insufficient to determine a unique answer. In such situations we must select one solution out of the infinitely many that are mathematically possible. The obvious questions we need to answer are: What criteria do we use in this selection? How do we find algorithms that meet our chosen criteria? In this chapter we look at some of the answers people have offered and at one particular algorithm, Burg's *maximum entropy method* (MEM) [30, 31].

17.2 Estimating Non-Negative Functions

The values $r(n)$ are autocorrelation function values associated with a random process having $R(\omega)$ for its power spectrum. In many applications, such as seismic remote sensing, these autocorrelation values are estimates obtained from relatively few samples of the underlying random process, so that N is not large. The DFT estimate,

$$R_{DFT}(\omega) = \sum_{n=-N}^{N} r(n) \exp(in\omega),$$

is real-valued and consistent with the data, but is not necessarily nonnegative. For small values of N, the DFT may not be sufficiently resolving

191

to be useful. This suggests that one criterion we can use to perform our selection process is to require that the method provide better resolution than the DFT for relatively small values of N, when reconstructing power spectra that consist mainly of delta functions.

17.3   Philosophical Issues

Generally speaking, we would expect to do a better job of estimating a function from data pertaining to that function if we also possess additional prior information about the function to be estimated and are able to employ estimation techniques that make use of that additional information. There is the danger, however, that we may end up with an answer that is influenced more by our prior guesses than by the actual measured data. Striking a balance between including prior knowledge and letting the data speak for itself is a noble goal; how to achieve that is the question. At this stage, we begin to suspect that the problem is as much philosophical as it is mathematical.

We are essentially looking for principles of induction that enable us to extrapolate from what we have measured to what we have not. Unwilling to turn the problem over entirely to the philosophers, a number of mathematicians and physicists have sought mathematical solutions to this inference problem, framed in terms of what the *most likely* answer is, or which answer involves the smallest amount of additional prior information [90]. This is not, of course, a new issue; it has been argued for centuries with regard to the use of what we now call Bayesian statistics; *objective* Bayesians allow the use of prior information, but only if it is the right prior information. The interested reader should consult the books [205] and [206], containing papers by Ed Jaynes, Roy Frieden, and others originally presented at workshops on this topic held in the early 1980s.

The maximum entropy method is a general approach to such problems that includes Burg's algorithm as a particular case. It is argued that by maximizing entropy we are, in some sense, being maximally noncommittal about what we do not know and thereby introducing a minimum of prior knowledge (some would say prior guesswork) into the solution. In the case of Burg's MEM, a somewhat more mathematical argument is available.

Let $\{x_n\}_{n=-\infty}^{\infty}$ be a stationary random process with autocorrelation sequence $r(m)$ and power spectrum $R(\omega)$, $|\omega| \leq \pi$. The prediction problem is the following: suppose we have measured the values of the process prior to time n and we want to predict the value of the process at time n. On average, how much error do we expect to make in predicting x_n from knowledge of the infinite past? The answer, according to Szegö's theorem

[135], is

$$\exp[\int_{-\pi}^{\pi} \log R(\omega)d\omega];$$

the integral

$$\int_{-\pi}^{\pi} \log R(\omega)d\omega$$

is the *Burg entropy* of the random process [189]. Processes that are very predictable have low entropy, while those that are quite unpredictable, or, like white noise, completely unpredictable, have high entropy; to make entropies comparable, we assume a fixed value of $r(0)$. Given the data $r(n)$, $|n| \leq N$, Burg's method selects that power spectrum consistent with these autocorrelation values that corresponds to the most unpredictable random process.

Other similar procedures are also based on selection through optimization. We have seen the minimum norm approach to finding a solution to an underdetermined system of linear equations, and the minimum expected squared error approach in statistical filtering, and later we shall see the maximum likelihood method used in detection. We must keep in mind that, however comforting it may be to know that we are on solid philosophical ground (if such exists) in choosing our selection criteria, if the method does not work well, we must use something else. As we shall see, the MEM, like every other reasonable method, works well sometimes and not so well other times. There is certainly philosophical precedent for considering the consequences of our choices, as Blaise Pascal's famous wager about the existence of God nicely illustrates. As an attentive reader of the books [205] and [206] will surely note, there is a certain theological tone to some of the arguments offered in support of entropy maximization. One group of authors (reference omitted) went so far as to declare that entropy maximization was what one did if one cared what happened to one's data.

The objective of Burg's MEM for estimating a power spectrum is to seek better resolution by combining nonnegativity and data-consistency in a single closed-form estimate. The MEM is remarkable in that it is the only closed-form (that is, noniterative) estimation method that is guaranteed to produce an estimate that is both nonnegative and consistent with the autocorrelation samples. Later we shall consider a more general method, the inverse PDFT (IPDFT), that is both data-consistent and positive in most cases.

17.4 The Autocorrelation Sequence $\{r(n)\}$

We begin our discussion with important properties of the sequence $\{r(n)\}$. Because $R(\omega) \geq 0$, the values $r(n)$ are often called *autocorrelation values*.

Since $R(\omega) \geq 0$, it follows immediately that $r(0) \geq 0$. In addition, $r(0) \geq |r(n)|$ for all n:

$$|r(n)| = |\int_{-\pi}^{\pi} R(\omega) \exp(-in\omega) d\omega / 2\pi|$$

$$\leq \int_{-\pi}^{\pi} R(\omega) |\exp(-in\omega)| d\omega / 2\pi = r(0).$$

In fact, if $r(0) = |r(n)| > 0$ for some $n > 0$, then R is a sum of at most $n + 1$ delta functions with nonnegative amplitudes. To see this, suppose that $r(n) = |r(n)| \exp(i\theta) = r(0) \exp(i\theta)$. Then,

$$\int_{-\pi}^{\pi} R(\omega) |1 - \exp(i(\theta + n\omega))|^2 d\omega / 2\pi$$

$$= \int_{-\pi}^{\pi} R(\omega)(1 - \exp(i(\theta + n\omega)))(1 - \exp(-i(\theta + n\omega))) d\omega / 2\pi$$

$$= \int_{-\pi}^{\pi} R(\omega)[2 - \exp(i(\theta + n\omega)) - \exp(-i(\theta + n\omega))] d\omega / 2\pi$$

$$= 2r(0) - \exp(i\theta)\overline{r(n)} - \exp(-i\theta)r(n) = 2r(0) - r(0) - r(0) = 0.$$

Therefore, $R(\omega) > 0$ only at the values of ω where $|1 - \exp(i(\theta + n\omega))|^2 = 0$; that is, only at $\omega = n^{-1}(2\pi k - \theta)$ for some integer k. Since $|\omega| \leq \pi$, there are only finitely many such k.

This result is important in any discussion of resolution limits. It is natural to feel that if we have only the Fourier coefficients $r(n)$ for $|n| \leq N$ then we have only the low frequency information about the function $R(\omega)$. How is it possible to achieve higher resolution? Notice, however, that in the case just considered, the infinite sequence of Fourier coefficients is periodic. Of course, we do not know this *a priori*, necessarily. The fact that $|r(N)| = r(0)$ does not, *by itself*, tell us that $R(\omega)$ consists solely of delta functions and that the sequence of Fourier coefficients is periodic. But, under the added assumption that $R(\omega) \geq 0$, it does! When we put in this prior information about $R(\omega)$ we find that the data now tells us more than it did before. This is a good example of the point made in the Introduction; to get information out we need to put information in.

In discussing the Burg MEM estimate, we shall need to refer to the concept of *minimum-phase* vectors. We consider that briefly now.

17.5   Minimum-Phase Vectors

We say that the finite column vector with complex entries $(a_0, a_1, ..., a_N)^T$ is a *minimum-phase* vector if the complex polynomial

$$A(z) = a_0 + a_1 z + ... + a_N z^N$$

has the property that $A(z) = 0$ implies that $|z| > 1$; that is, all roots of $A(z)$ are outside the unit circle. Consequently, the function $B(z)$ given by $B(z) = 1/A(z)$ is analytic in a disk centered at the origin and including the unit circle. Therefore, we can write

$$B(z) = b_0 + b_1 z + b_2 z^2 + ...,$$

and taking $z = \exp(i\omega)$, we get

$$B(\exp(i\omega)) = b_0 + b_1 \exp(i\omega) + b_2 \exp(2i\omega) + ... \ .$$

The point here is that $B(\exp(i\omega))$ is a one-sided trigonometric series, with only terms corresponding to $\exp(in\omega)$ for nonnegative n.

17.6 Burg's MEM

The approach is to estimate $R(\omega)$ by the function $S(\omega) > 0$ that maximizes the so-called Burg entropy, $\int_{-\pi}^{\pi} \log S(\omega) d\omega$, subject to the data constraints.

The Euler-Lagrange equation from the calculus of variations allows us to conclude that $S(\omega)$ has the form

$$S(\omega) = 1/H(\omega)$$

for

$$H(\omega) = \sum_{n=-N}^{N} h_n e^{in\omega} > 0.$$

From the Fejér-Riesz Theorem 31.1 we know that $H(\omega) = |A(e^{i\omega})|^2$ for minimum phase $A(z)$. As we now show, the coefficients a_n satisfy a system of linear equations formed using the data $r(n)$.

Given the data $r(n), |n| \leq N$, we form the *autocorrelation matrix* R with entries $R_{mn} = r(m - n)$, for $-N \leq m, n \leq N$. Let δ be the column vector $\delta = (1, 0, ..., 0)^T$. Let $a = (a_0, a_1, ..., a_N)^T$ be the solution of the system $Ra = \delta$. Then, Burg's MEM estimate is the function $S(\omega) = R_{MEM}(\omega)$ given by

$$R_{MEM}(\omega) = a_0/|A(\exp(i\omega))|^2, |\omega| \leq \pi.$$

Once we show that $a_0 \geq 0$, it will be obvious that $R_{MEM}(\omega) \geq 0$. We also must show that R_{MEM} is data-consistent; that is,

$$r(n) = \int_{-\pi}^{\pi} R_{MEM}(\omega) \exp(-in\omega) d\omega / 2\pi =, \ n = -N, ..., N.$$

Let us write $R_{MEM}(\omega)$ as a Fourier series; that is,

$$R_{MEM}(\omega) = \sum_{n=-\infty}^{+\infty} q(n) \exp(in\omega), \ |\omega| \leq \pi.$$

From the form of $R_{MEM}(\omega)$, we have

$$R_{MEM}(\omega)\overline{A(\exp(i\omega))} = a_0 B(\exp(i\omega)). \qquad (17.1)$$

Suppose, as we shall see shortly, that $A(z)$ has all its roots outside the unit circle, so $B(\exp(i\omega))$ is a one-sided trigonometric series, with only terms corresponding to $\exp(in\omega)$ for nonnegative n. Then, multiplying on the left side of Equation (17.1), and equating coefficients corresponding to $n = 0, -1, -2, ...$, we find that, provided $q(n) = r(n)$, for $|n| \leq N$, we must have $Ra = \delta$. Notice that these are precisely the same equations we solve in calculating the coefficients of an AR process. For that reason the MEM is sometimes called an autoregressive method for spectral estimation.

17.6.1   The Minimum-Phase Property

We now show that if $Ra = \delta$ then $A(z)$ has all its roots outside the unit circle. Let $r\exp(i\theta)$ be a root of $A(z)$. Then, write

$$A(z) = (z - r\exp(i\theta))C(z),$$

where

$$C(z) = c_0 + c_1 z + c_2 z^2 + ... + c_{N-1}z^{N-1}.$$

The vector $a = (a_0, a_1, ..., a_N)^T$ can be written as $a = -r\exp(i\theta)c + d$, where $c = (c_0, c_1, ..., c_{N-1}, 0)^T$ and $d = (0, c_0, c_1, ..., c_{N-1})^T$. So, $\delta = Ra = -r\exp(i\theta)Rc + Rd$ and

$$0 = d^\dagger\delta = -r\exp(i\theta)d^\dagger Rc + d^\dagger Rd,$$

so that

$$r\exp(i\theta)d^\dagger Rc = d^\dagger Rd.$$

From the Cauchy inequality we know that

$$|d^\dagger Rc|^2 \leq (d^\dagger Rd)(c^\dagger Rc) = (d^\dagger Rd)^2, \qquad (17.2)$$

where the last equality comes from the special form of the matrix R and the similarity between c and d.

   With

$$D(\omega) = c_0 e^{i\omega} + c_1 e^{2i\omega}... + c_{N-1}e^{iN\omega}$$

and

$$C(\omega) = c_0 + c_1 e^{i\omega} + ... + c_{N-1}e^{i(N-1)\omega},$$

we can easily show that

$$d^\dagger Rd = c^\dagger Rc = \frac{1}{2\pi}\int_{-\pi}^{\pi} R(\omega)|D(\omega)|^2 d\omega$$

and

$$d^\dagger Rc = \frac{1}{2\pi} \int_{-\pi}^{\pi} R(\omega)\overline{D(\omega)}C(\omega)d\omega.$$

If there is equality in the Cauchy Inequality (17.2), then $r = 1$ and we would have

$$\exp(i\theta)\frac{1}{2\pi} \int_{-\pi}^{\pi} R(\omega)\overline{D(\omega)}C(\omega)d\omega = \frac{1}{2\pi} \int_{-\pi}^{\pi} R(\omega)|D(\omega)|^2 d\omega.$$

From the Cauchy Inequality for integrals, we can conclude that

$$\exp(i\theta)\overline{D(\omega)}C(\omega) = |D(\omega)|^2$$

for all ω for which $R(\omega) > 0$. But,

$$\exp(i\omega)C(\omega) = D(\omega).$$

Therefore, we cannot have $r = 1$ unless $R(\omega)$ consists of a single delta function; that is, $R(\omega) = \delta(\omega - \theta)$. In all other cases we have

$$|d^\dagger Rc|^2 < |r|^2|d^\dagger Rc|^2,$$

from which we conclude that $|r| > 1$.

17.6.2   Solving $Ra = \delta$ Using Levinson's Algorithm

Because the matrix R is Toeplitz, that is, constant on diagonals, and positive definite, there is a fast algorithm for solving $Ra = \delta$ for a. Instead of a single R, we let R_M be the matrix defined for $M = 0, 1, ..., N$ by

$$R_M = \begin{bmatrix} r(0) & r(-1) & ... & r(-M) \\ r(1) & r(0) & ... & r(-M+1) \\ . & & & \\ . & & & \\ . & & & \\ r(M) & r(M-1) & ... & r(0) \end{bmatrix}$$

so that $R = R_N$. We also let δ^M be the $(M+1)$-dimensional column vector $\delta^M = (1, 0, ..., 0)^T$. We want to find the column vector $a^M = (a_0^M, a_1^M, ..., a_M^M)^T$ that satisfies the equation $R_M a^M = \delta^M$. The point of Levinson's algorithm is to calculate a^{M+1} quickly from a^M.

For fixed M find constants α and β so that

$$\delta^M = R_M \left\{ \alpha \begin{bmatrix} a_0^{M-1} \\ a_1^{M-1} \\ . \\ . \\ . \\ a_{M-1}^{M-1} \\ 0 \end{bmatrix} + \beta \begin{bmatrix} 0 \\ \overline{a}_{M-1}^{M-1} \\ \overline{a}_{M-2}^{M-1} \\ . \\ . \\ . \\ \overline{a}_0^{M-1} \end{bmatrix} \right\}$$

$$= \left\{ \alpha \begin{bmatrix} 1 \\ 0 \\ . \\ . \\ . \\ 0 \\ \gamma^M \end{bmatrix} + \beta \begin{bmatrix} \overline{\gamma}^M \\ 0 \\ . \\ . \\ . \\ 0 \\ 1 \end{bmatrix} \right\},$$

where

$$\gamma^M = r(M)a_0^{M-1} + r(M-1)a_1^{M-1} + ... + r(1)a_{M-1}^{M-1}.$$

We then have

$$\alpha + \beta\overline{\gamma^M} = 1, \ \alpha\gamma^M + \beta = 0$$

or

$$\beta = -\alpha\gamma^M, \ \alpha - \alpha|\gamma^M|^2 = 1,$$

so

$$\alpha = 1/(1 - |\gamma^M|^2), \ \beta = -\gamma^M/(1 - |\gamma^M|^2).$$

Therefore, the algorithm begins with $M = 0$, $R_0 = [r(0)], a_0^0 = r(0)^{-1}$. At each step calculate the γ^M, solve for α and β and form the next a^M.

The MEM resolves better than the DFT when the true power spectrum being reconstructed is a sum of delta functions plus a flat background. When the background itself is not flat, performance of the MEM degrades rapidly; the MEM tends to interpret any nonflat background in terms of additional delta functions. In the next chapter we consider an extension of the MEM, called the indirect PDFT (IPDFT), that corrects this flaw.

Why Burg's MEM and the IPDFT are able to resolve closely spaced sinusoidal components better than the DFT is best answered by studying the eigenvalues and eigenvectors of the matrix R; we turn to this topic in a later chapter.

17.7   A Sufficient Condition for Positive-definiteness

If the function

$$R(\omega) = \sum_{n=-\infty}^{\infty} r(n)e^{in\omega}$$

is nonnegative on the interval $[-\pi, \pi]$, then the matrices R_M are nonnegative-definite for every M. Theorems by Herglotz and by Bochner go in the reverse direction [4]. Katznelson [148] gives the following result.

Theorem 17.1 *Let $\{f(n)\}_{n=-\infty}^{\infty}$ be a sequence of nonnegative real numbers converging to zero, with $f(-n) = f(n)$ for each n. If, for each $n > 0$, we have*

$$(f(n-1) - f(n)) - (f(n) - f(n+1)) > 0,$$

then there is a nonnegative function $R(\omega)$ on the interval $[-\pi, \pi]$ with $f(n) = r(n)$ for each n.

The following figures illustrate the behavior of the MEM. In Figures 17.1, 17.2, and 17.3, the true object has two delta functions at 0.95π and 1.05π. The data is $f(n)$ for $|n| \leq 10$. The DFT cannot resolve the two spikes. The SNR is high in Figure 17.1, and the MEM easily resolves them. In Figure 17.2 the SNR is much lower and MEM no longer resolves the spikes.

Exercise 17.1 *In Figure 17.3 the SNR is much higher than in Figure 17.1. Explain why the graph looks as it does.*

In Figure 17.4 the true object is a box supported between 0.75π and 1.25π. Here $N = 10$, again. The MEM does a poor job reconstructing the box. This weakness in MEM will become a problem in the last two figures, in which the true object consists of the box with the two spikes added. In Figure 17.5 we have $N = 10$, while, in Figure 17.6, $N = 25$.
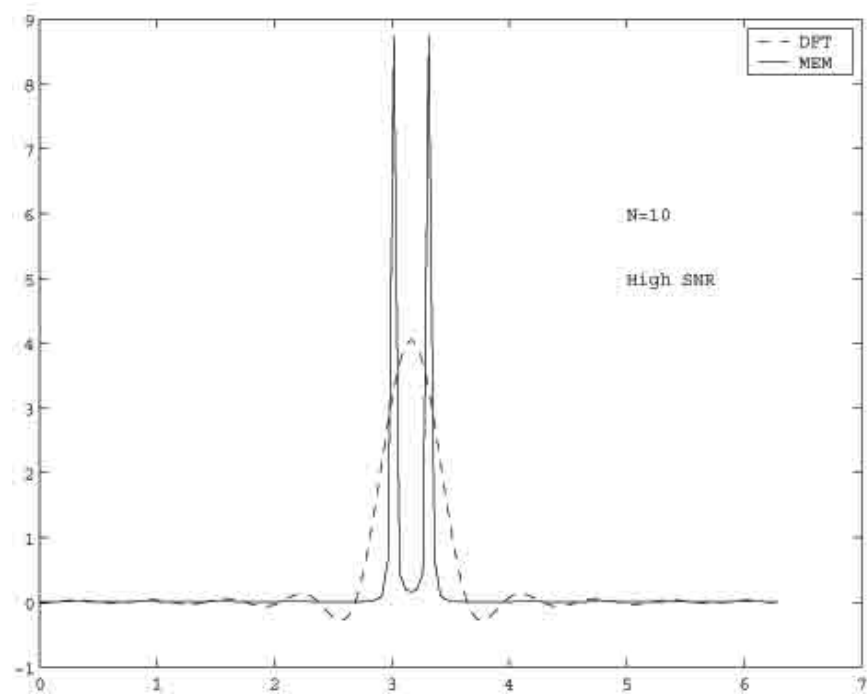
Figure 17.1: The DFT and MEM, $N = 10$, high SNR.
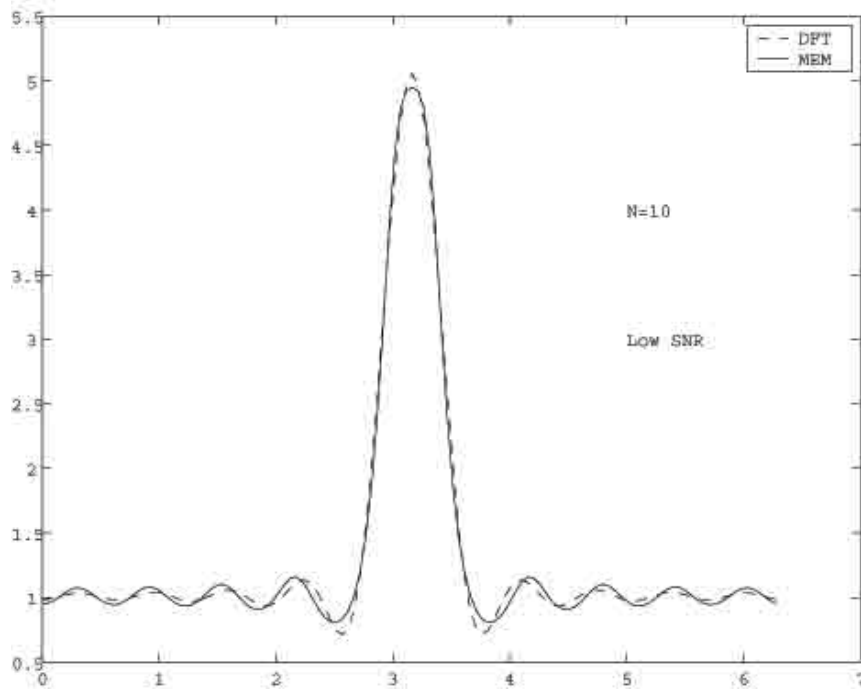
Figure 17.2: The DFT and MEM, $N = 10$, low SNR.
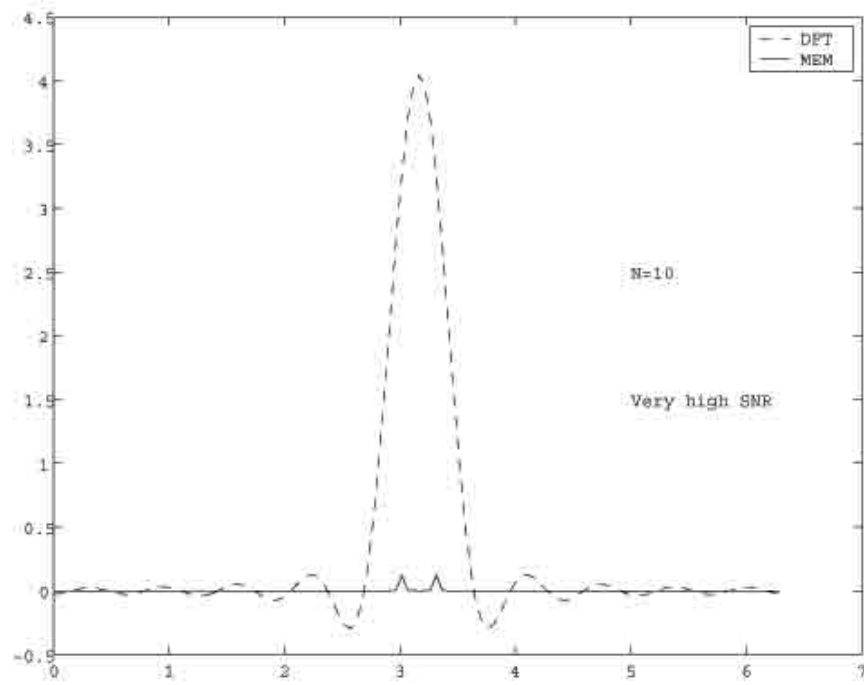
Figure 17.3: The DFT and MEM, $N = 10$, very high SNR. What happened?
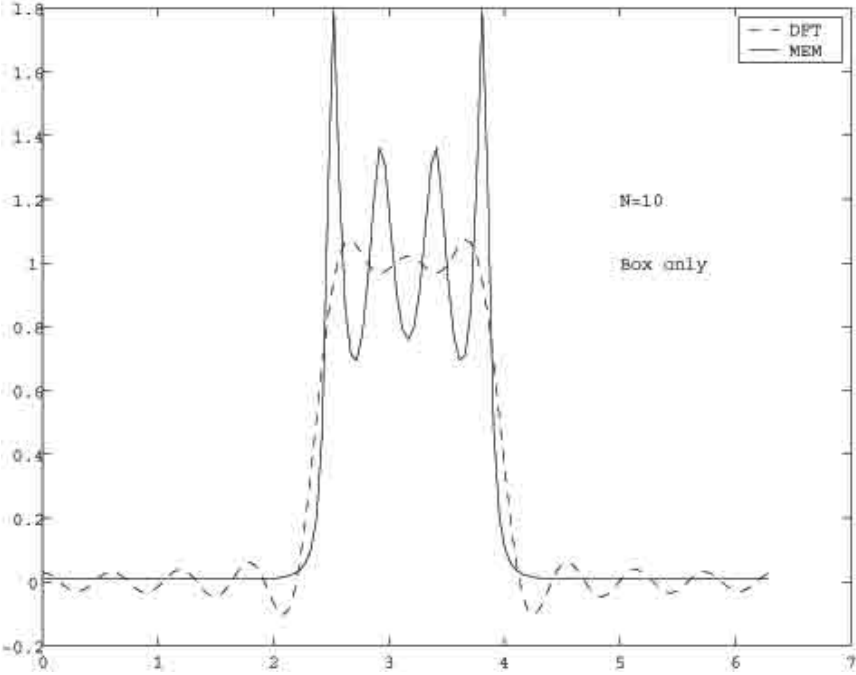
Figure 17.4: MEM and DFT for a box object; $N = 10$.
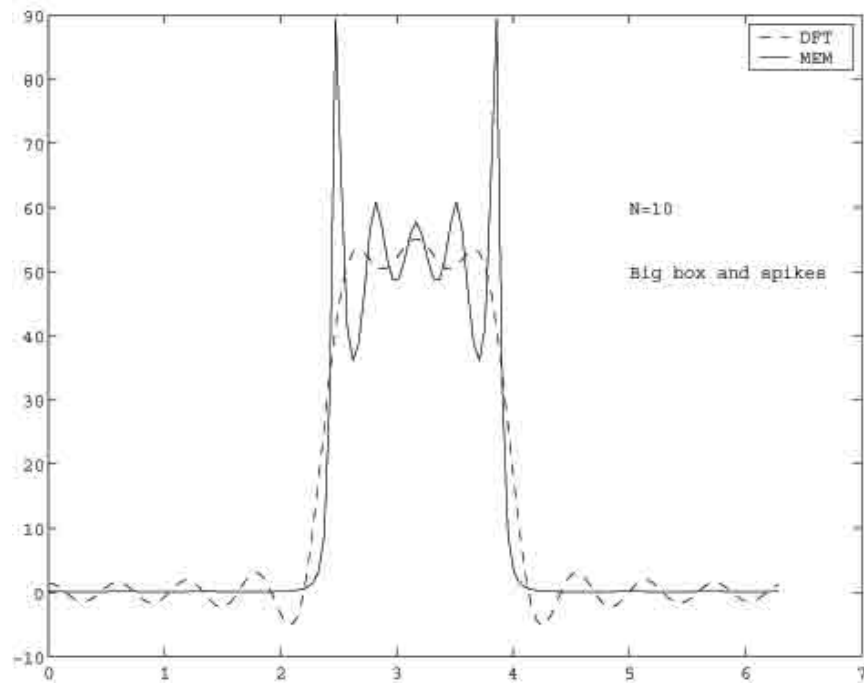
Figure 17.5: The DFT and MEM: two spikes on a large box; $N = 10$.
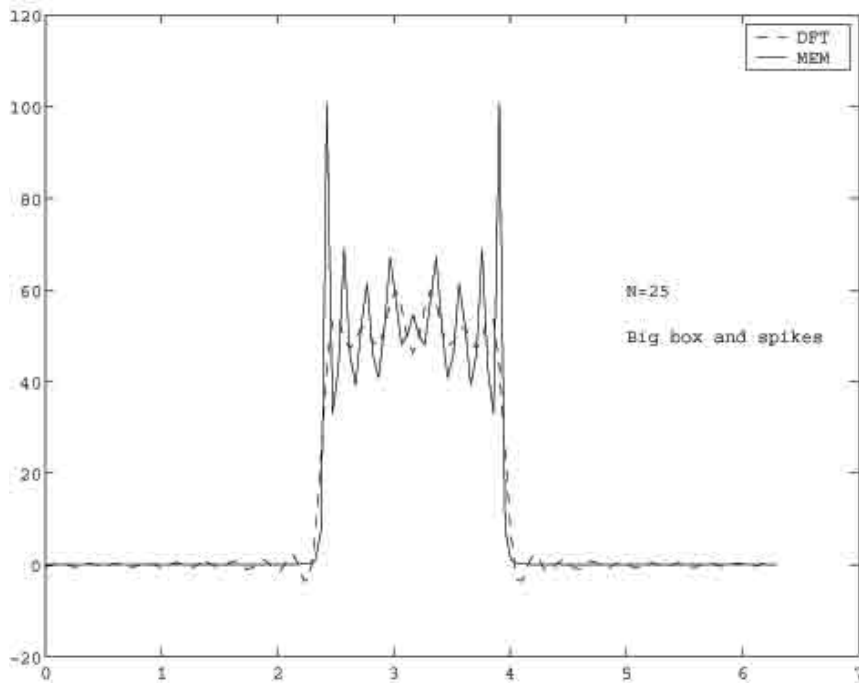
Figure 17.6: The DFT and MEM: two spikes on a large box; $N = 25$.

Chapter 18

Eigenvector Methods in Estimation

18.1 Chapter Summary

Prony's method showed that information about the signal can sometimes be obtained from the roots of certain polynomials formed from the data. Eigenvectors methods are similar, as we shall see.

18.2 Some Eigenvector Methods

Eigenvector methods assume the data are correlation values and involve polynomials formed from the eigenvectors of the correlation matrix. Schmidt's *multiple signal classification* (MUSIC) algorithm is one such method [196]. A related technique used in direction-of-arrival array processing is the *estimation of signal parameters by rotational invariance techniques* (ESPRIT) of Paulraj, Roy, and Kailath [183].

18.3 The Sinusoids-in-Noise Model

We suppose now that the function $f(t)$ being measured is signal plus noise, with the form

$$f(t) = \sum_{j=1}^{J} |A_j| e^{i\theta_j} e^{-i\omega_j t} + n(t) = s(t) + n(t),$$

where the phases θ_j are random variables, independent and uniformly distributed in the interval $[0, 2\pi)$, and $n(t)$ denotes the random complex stationary noise component. Assume that $E(n(t)) = 0$ for all t and that

the noise is independent of the signal components. We want to estimate J, the number of sinusoidal components, their magnitudes $|A_j|$ and their frequencies ω_j.

18.4 Autocorrelation

The autocorrelation function associated with $s(t)$ is

$$r_s(\tau) = \sum_{j=1}^{J} |A_j|^2 e^{-i\omega_j \tau},$$

and the signal power spectrum is the Fourier transform of $r_s(\tau)$,

$$R_s(\omega) = \sum_{j=1}^{J} |A_j|^2 \delta(\omega - \omega_j).$$

The noise autocorrelation is denoted $r_n(\tau)$ and the noise power spectrum is denoted $R_n(\omega)$. For the remainder of this section we shall assume that the noise is *white noise*; that is, $R_n(\omega)$ is constant and $r_n(\tau) = 0$ for $\tau \neq 0$.

We collect samples of the function $f(t)$ and use them to estimate some of the values of $r_s(\tau)$. From these values of $r_s(\tau)$, we estimate $R_s(\omega)$, primarily looking for the locations ω_j at which there are delta functions.

We assume that the samples of $f(t)$ have been taken over an interval of time sufficiently long to take advantage of the independent nature of the phase angles θ_j and the noise. This means that when we estimate the $r_s(\tau)$ from products of the form $f(t+\tau)\overline{f(t)}$, the cross terms between one signal component and another, as well as between a signal component and the noise, are nearly zero, due to destructive interference coming from the random phases.

Suppose now that we have the values $r_f(m)$ for $m = -(M-1), ..., M-1$, where $M > J$, $r_f(m) = r_s(m)$ for $m \neq 0$, and $r_f(0) = r_s(0) + \sigma^2$, for σ^2 the variance (or *power*) of the noise. We form the M by M autocorrelation matrix R with entries $R_{m,k} = r_f(m - k)$.

Exercise 18.1 *Show that the matrix R has the following form:*

$$R = \sum_{j=1}^{J} |A_j|^2 \mathbf{e}_j \mathbf{e}_j^\dagger + \sigma^2 I,$$

where $\mathbf{e}_j$ is the column vector with entries $e^{-i\omega_j n}$, for $n = 0, 1, ..., M - 1$.

Let $\mathbf{u}$ be an eigenvector of R with $\|u\| = 1$ and associated eigenvalue λ. Then we have

$$\lambda = \mathbf{u}^\dagger R \mathbf{u} = \sum_{j=1}^{J} |A_j|^2 |\mathbf{e}_j^\dagger \mathbf{u}|^2 + \sigma^2 \geq \sigma^2.$$

Therefore, the smallest eigenvalue of R is σ^2

Because $M > J$, there must be non-zero M-dimensional vectors $\mathbf{v}$ that are orthogonal to all of the $\mathbf{e}_j$; in fact, we can say that there are $M - J$ linearly independent such $\mathbf{v}$. For each such vector $\mathbf{v}$ we have

$$R\mathbf{v} = \sum_{j=1}^{J} |A_j|^2 \mathbf{e}_j^\dagger \mathbf{v} \mathbf{e}_j + \sigma^2 \mathbf{v} = \sigma^2 \mathbf{v};$$

consequently, $\mathbf{v}$ is an eigenvector of R with associated eigenvalue σ^2.

Let $\lambda_1 \geq \lambda_2 \geq ... \geq \lambda_M > 0$ be the eigenvalues of R and let $\mathbf{u}^m$ be a norm-one eigenvector associated with λ_m. It follows from the previous paragraph that $\lambda_m = \sigma^2$, for $m = J + 1, ..., M$, while $\lambda_m > \sigma^2$ for $m = 1, ..., J$. This leads to the MUSIC method for determining the ω_j.

18.5 Determining the Frequencies

By calculating the eigenvalues of R and noting how many of them are greater than the smallest one, we find J. Now we seek the ω_j.

For each ω, we let $\mathbf{e}_\omega$ have the entries $e^{-i\omega n}$, for $n = 0, 1, ..., M - 1$ and form the function

$$T(\omega) = \sum_{m=J+1}^{M} |\mathbf{e}_\omega^\dagger \mathbf{u}^m|^2.$$

This function $T(\omega)$ will have zeros at precisely the values $\omega = \omega_j$, for $j = 1, ..., J$. Once we have determined J and the ω_j, we estimate the magnitudes $|A_j|$ using Fourier transform estimation techniques already discussed. This is basically Schmidt's MUSIC method.

We have made several assumptions here that may not hold in practice and we must modify this eigenvector approach somewhat. First, the time over which we are able to measure the function $f(t)$ may not be long enough to give good estimates of the $r_f(\tau)$. In that case we may work directly with the samples of $f(t)$. Second, the smallest eigenvalues will not be exactly equal to σ^2 and some will be larger than others. If the ω_j are not well separated, or if some of the $|A_j|$ are quite small, it may be hard to tell what the value of J is. Third, we often have measurements of $f(t)$ that have errors other than those due to background noise; inexpensive sensors can introduce their own random phases that can complicate the estimation

process. Finally, the noise may not be white, so that the estimated $r_f(\tau)$ will not equal $r_s(\tau)$ for $\tau \neq 0$, as before. If we know the noise power spectrum or have a decent idea what it is, we can perform a pre-whitening to R, which will then return us to the case considered above, although this can be a tricky procedure.

18.6   The Case of Non-White Noise

When the noise power spectrum has a component that is not white the eigenvalues and eigenvectors of R behave somewhat differently from the white-noise case. The eigenvectors tend to separate into three groups. Those in the first group correspond to the smallest eigenvalues and are approximately orthogonal to both the signal components and the nonwhite noise component. Those in the second group, whose eigenvalues are somewhat larger than those in the previous group, tend to be orthogonal to the signal components but to have a sizable projection onto the nonwhite-noise component. Those in the third group, with the largest eigenvalues, have sizable projection onto both the signal and nonwhite noise components. Since the DFT estimate uses R, as opposed to R^{-1}, the DFT spectrum is determined largely by the eigenvectors in the third group. The MEM estimator, which uses R^{-1}, makes most use of the eigenvectors in the first group, but in the formation of the denominator. In the presence of a nonwhite-noise component, the orthogonality of those eigenvectors to both the signals and the nonwhite noise shows up as peaks throughout the region of interest, masking or distorting the signal peaks we wish to see.

There is a second problem exacerbated by the nonwhite component-sensitivity of nonlinear and eigenvector methods to phase errors. We have assumed up to now that the data we have obtained is accurate, but there isn't enough of it. In some cases the machinery used to obtain the measured data may not be of the highest quality; certain applications of SONAR make use of relatively inexpensive hydrophones that will sink into the ocean after they have been used briefly. In such cases the complex numbers $r(n)$ will be distorted. Errors in the measurement of their phases are particularly damaging. The following figures illustrate these issues.

18.7   Sensitivity

In the following figures the true power spectrum is the box and spikes object used earlier in our discussion of the MEM and IPDFT. It consists of two delta functions at $\omega = 0.95\pi$ and 1.05π, along with a box extending from 0.75π to 1.25π. There is also a small white-noise component that is flat across $[0, 2\pi]$, contributing only to the $r(0)$ value. The data, in the

absence of phase errors, is $r(n)$, $|n| \leq N = 25$. Three different amounts of phase perturbation are introduced in the other cases.

Figure 18.1 shows the function $T(\omega)$ for the two eigenvectors in the second group; here, $J = 18$ and $M = 21$. The approximate zeros at 0.95π and 1.05π are clearly seen in the error-free case and remain fairly stable as the phase errors are introduced. Figure 18.2 uses the eigenvectors in the first group, with $J = 0$ and $M = 18$. The approximate nulls at 0.95π and 1.05π are hard to distinguish even in the error-free case and get progressively worse as phase errors are introduced. Stable nonlinear methods, such as the IPDFT, rely most on the eigenvectors in the second group.
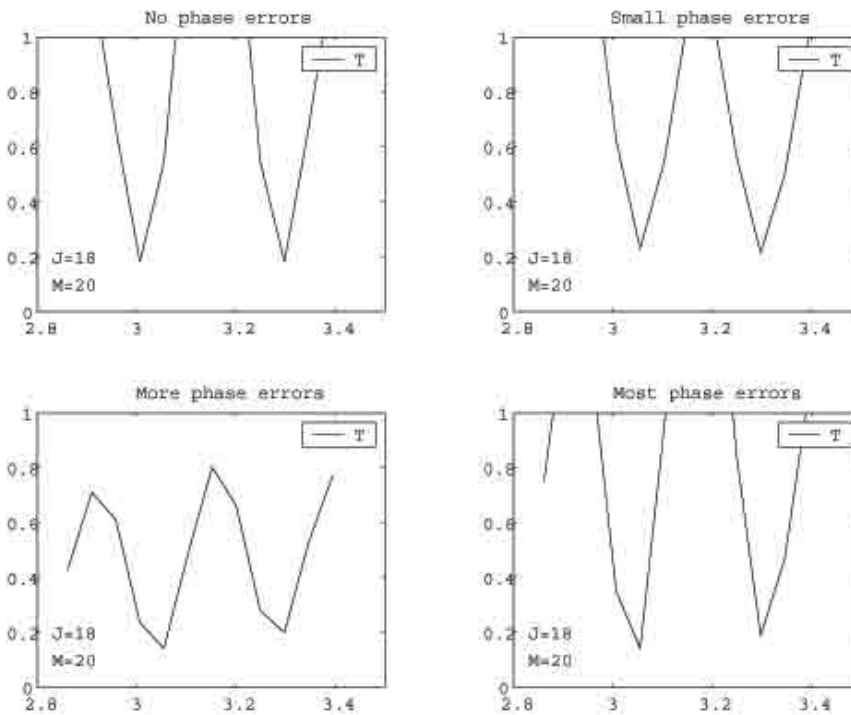
Figure 18.1: $T(\omega)$ for $J = 18$, $M = 21$, varying degrees of phase errors.
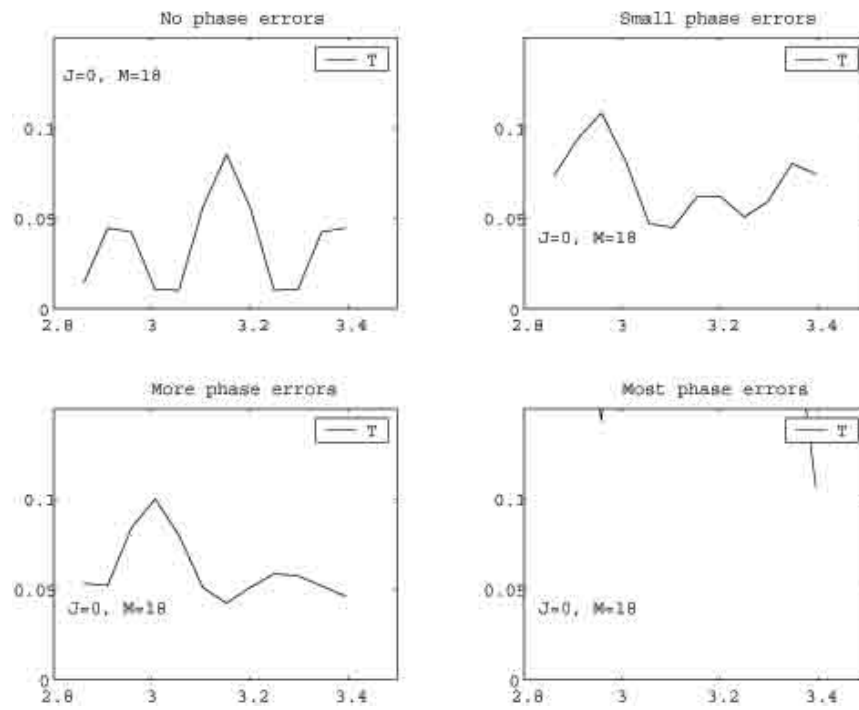
Figure 18.2: $T(\omega)$ for $J = 0$, $M = 18$, varying degrees of phase errors.

Chapter 19

The IPDFT

19.1 Chapter Summary

Experience with Burg's MEM shows that it is capable of resolving closely spaced delta functions better than the DFT, provided that the background is flat. When the background is not flat, MEM tends to interpret the non-flat background as additional delta functions to be resolved. In this chapter we consider an extension of MEM based on the PDFT that can resolve in the presence of non-flat background. This method is called the *indirect PDFT* (IPDFT) [56].

19.2 The Need for Prior Information in Non-Linear Estimation

As we saw previously, the PDFT is a linear method for incorporating prior knowledge into the estimation of the Fourier transform. Burg's MEM is a nonlinear method for estimating a non-negative Fourier transform.

The IPDFT applies to the reconstruction of one-dimensional power spectra, but the main idea can be used to generate high-resolution methods for multi-dimensional spectra as well. The IPDFT method is suggested by considering the MEM equations $R\mathbf{a} = \delta$ as a particular case of the equations that arise in Wiener filter approximation. As in the previous chapter, we assume that we have the autocorrelation values $r(n)$ for $|n| \leq N$, from which we wish to estimate the power spectrum

$$R(\omega) = \sum_{n=-\infty}^{+\infty} r(n)e^{in\omega}, \ |\omega| \leq \pi.$$

213

19.3   What Wiener Filtering Suggests

In the appendix on Wiener filter approximation, we show that the best
finite length filter approximation of the Wiener filter is obtained by mini-
mizing the integral in Equation (30.4)

$$\int_{-\pi}^{\pi} |H(\omega) - \sum_{k=-K}^{L} f_k e^{ik\omega}|^2 (R_s(\omega) + R_u(\omega))d\omega.$$

The optimal coefficients then must satisfy Equation (30.5):

$$r_s(m) = \sum_{k=-K}^{L} f_k(r_s(m-k) + r_u(m-k)), \qquad (19.1)$$

for $-K \leq m \leq L$.

Consider the case in which the power spectrum we wish to estimate
consists of a signal component that is the sum of delta functions and a noise
component that is white noise. If we construct a finite-length Wiener filter
that filters out the signal component and leaves only the noise, then that
filter should be able to zero out the delta function components. By finding
the locations of those zeros, we can find the supports of the delta functions.
So the approach is to reverse the roles of signal and noise, viewing the
signal as the component called u and the noise as the component called s
in the discussion of the Wiener filter. The autocorrelation function $r_s(n)$
corresponds to the white noise now and so $r_s(n) = 0$ for $n \neq 0$. The terms
$r_s(n) + r_u(n)$ are the data values $r(n)$, for $|n| \leq N$. Taking $K = 0$ and
$L = N$ in Equation (19.1), we obtain

$$\sum_{k=0}^{N} f_k r(m-k) = 0,$$

for $m = 1, 2, ..., N$ and

$$\sum_{k=0}^{N} f_k r(0-k) = r(0),$$

which is precisely that same system $R\mathbf{a} = \delta$ that occurs in MEM.

This approach reveals that the vector $\mathbf{a} = (a_0, ..., a_N)^T$ we find in MEM
can be viewed an a finite-length approximation of the Wiener filter designed
to remove the delta-function component and to leave the remaining flat
white-noise component untouched. The polynomial

$$A(\omega) = \sum_{n=0}^{N} a_n e^{in\omega}$$

will then have zeros near the supports of the delta functions. What happens to MEM when the background is not flat is that the filter tries to eliminate any component that is not white noise and so places the zeros of $A(\omega)$ in the wrong places.

19.4   Using a Prior Estimate

Suppose we take $P(\omega) \geq 0$ to be our estimate of the background component of $R(\omega)$; that is, we believe that $R(\omega)$ equals a multiple of $P(\omega)$ plus a sum of delta functions. We now ask for the finite length approximation of the Wiener filter that removes the delta functions and leaves any background component that looks like $P(\omega)$ untouched. We then take $r_s(n) = p(n)$, where

$$P(\omega) = \sum_{n=-\infty}^{+\infty} p(n)e^{in\omega}, \ |\omega| \leq \pi.$$

The desired filter is $\mathbf{f} = (f_0, ..., f_N)^T$ satisfying the equations

$$p(m) = \sum_{k=0}^{N} f_k r(m - k). \tag{19.2}$$

Once we have found $\mathbf{f}$ we form the polynomial

$$F(\omega) = \sum_{k=0}^{N} f_k e^{ik\omega}, \ |\omega| \leq \pi.$$

The zeros of $F(\omega)$ should then be near the supports of the delta function components of the power spectrum $R(\omega)$, provided that our original estimate of the background is not too inaccurate.

In the PDFT it is important to select the prior estimate $P(\omega)$ nonzero wherever the function being reconstructed is nonzero; for the IPDFT the situation is different. Comparing Equation (19.2) with Equation (28.5), we see that in the IPDFT the true $R(\omega)$ is playing the role previously given to $P(\omega)$, while $P(\omega)$ is in the role previously played by the function we wished to estimate, which, in the IPDFT, is $R(\omega)$. It is important, therefore, that $R(\omega)$ not be zero where $P(\omega) \neq 0$; that is, we should choose the $P(\omega) = 0$ wherever $R(\omega) = 0$. Of course, we usually do not know the support of $R(\omega)$ *a priori*. The point is simply that it is better to make $P(\omega) = 0$ than to make it nonzero, if we have any doubt as to the value of $R(\omega)$.

19.5   Properties of the IPDFT

In our discussion of the MEM, we obtained an estimate for the function $R(\omega)$, not simply a way of locating the delta-function components. As

we shall show, the IPDFT can also be used to estimate $R(\omega)$. Although the resulting estimate is not guaranteed to be either nonnegative nor data consistent, it usually is both of these.

For any function $G(\omega)$ on $[-\pi, \pi]$ with Fourier series

$$G(\omega) = \sum_{n=-\infty}^{\infty} g(n)e^{in\omega},$$

the *additive causal part* of the function $G(\omega)$ is

$$G_+(\omega) = \sum_{n=0}^{\infty} g(n)e^{in\omega}.$$

Any function such as G_+ that has Fourier coefficients that are zero for negative indices is called a *causal function*. The Equation (19.2) then says that the two causal functions P_+ and $(FR)_+$ have Fourier coefficients that agree for $m = 0, 1, ..., N$.

Because $F(\omega)$ is a finite causal trigonometric polynomial, we can write

$$(FR)_+(\omega) = R_+(\omega)F(\omega) + J(\omega),$$

where

$$J(\omega) = \sum_{m=0}^{N-1} [\sum_{k=1}^{N-m} r(-k)f(m+k)]e^{im\omega}.$$

Treating P_+ as approximately equal to $(FR)_+ = R_+F + J$, we obtain as an estimate of R_+ the function $Q = (P_+ - J)/F$. In order for this estimate of R_+ to be causal, it is sufficient that the function $1/F$ be causal. This means that the trigonometric polynomial $F(\omega)$ must be minimum phase; that is, all its roots lie outside the unit circle. In the chapter on MEM, we saw that this is always the case for MEM. It is not always the case for the IPDFT, but it is usually the case in practice; in fact, it was difficult (but possible) to construct a counterexample. We then construct our IPDFT estimate of $R(\omega)$, which is

$$R_{IPDFT}(\omega) = 2\text{Re}(Q(\omega)) - r(0).$$

The IPDFT estimate is real-valued and, when $1/F$ is causal, guaranteed to be data consistent. Although this estimate is not guaranteed to be nonnegative, it usually is.

We showed in the chapter on entropy maximization that the vector $\mathbf{a}$ that solves $R\mathbf{a} = \delta$ corresponds to a polynomial $A(z)$ having all its roots on or outside the unit circle; that is, it is minimum phase. The IPDFT involves the solution of the system $R\mathbf{f} = \mathbf{p}$, where $\mathbf{p} = (p(0), ..., p(N))^T$ is the vector of initial Fourier coefficients of another power spectrum, $P(\omega) \geq 0$

on $[-\pi, \pi]$. When $P(\omega)$ is constant, we get $\mathbf{p} = \delta$. For the IPDFT to be data-consistent, it is sufficient that the polynomial $F(z) = f_0 + ... + f_N z^N$ be minimum phase. Although this need not be the case, it is usually observed in practice.

Exercise 19.1 *Find conditions on the power spectra $R(\omega)$ and $P(\omega)$ that cause $F(z)$ to be minimum phase.*

Warning: This is probably not an easy exercise.

19.6   Illustrations

The following figures illustrate the IPDFT. The prior function in each case is the box object supported on the central fourth of the interval $[0, 2\pi]$. The value $r(0)$ has been increased slightly to regularize the matrix inversion. Figure 19.1 shows the behavior of the IPDFT when the object is only the box. Contrast this with the behavior of MEM in this case, as seen in Figure 17.4. Figures 19.2 and 19.3 show the abilty of the IPDFT to resolve the two spikes at 0.95π and 1.05π against the box background. Again, contrast this with the MEM reconstructions in Figures 17.5 and 17.6. To show that the IPDFT is actually indicating the presence of the spikes and not just rolling across the top of the box, we reconstruct two unequal spikes in Figure 19.4. Figure 19.5 shows how the IPDFT behaves when we increase the number of data points; now, $N = 25$ and the SNR is very low.
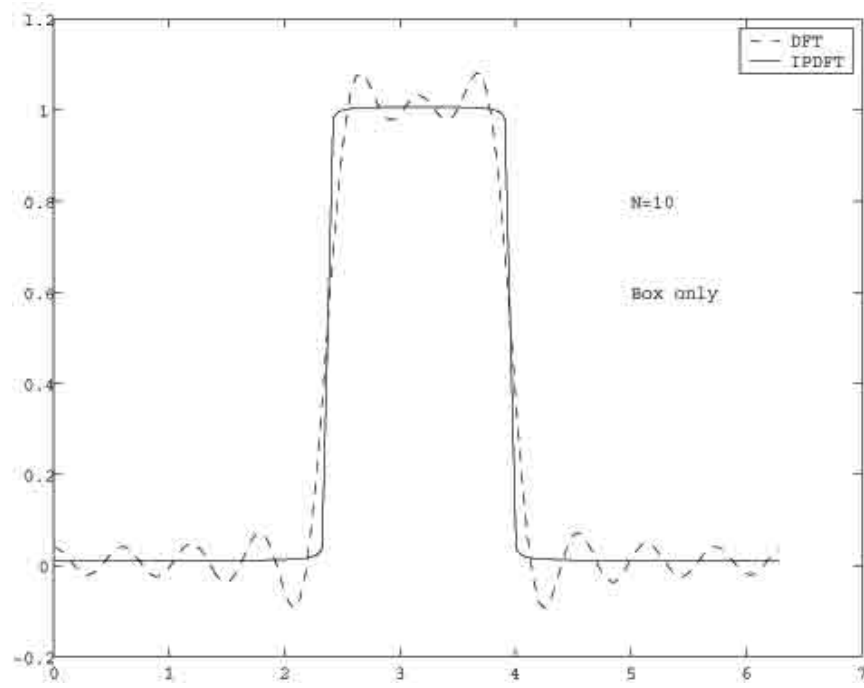
Figure 19.1: The DFT and IPDFT: box only, $N = 1$.
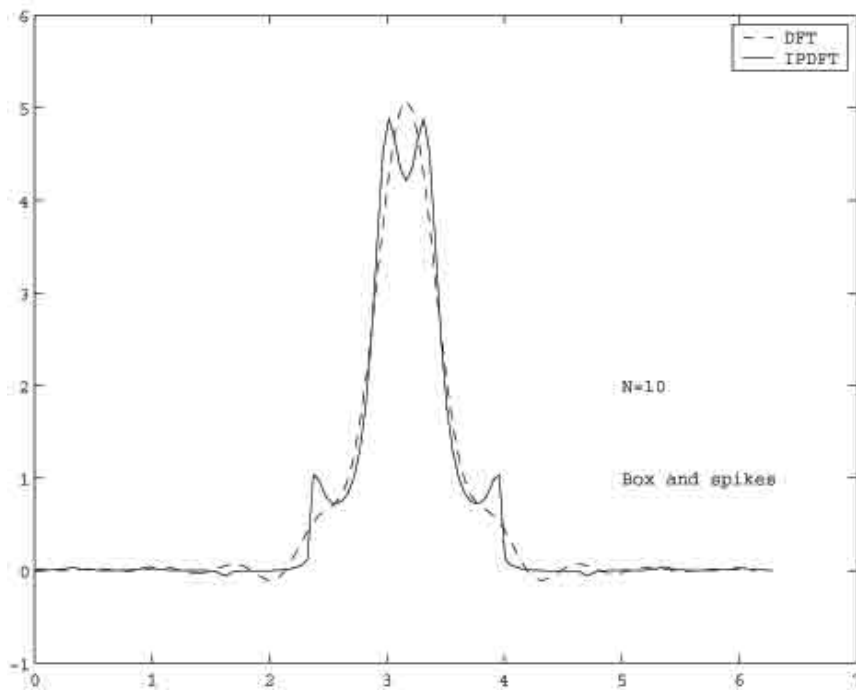
Figure 19.2: The DFT and IPDFT, box and two spikes, $N = 10$, high SNR.
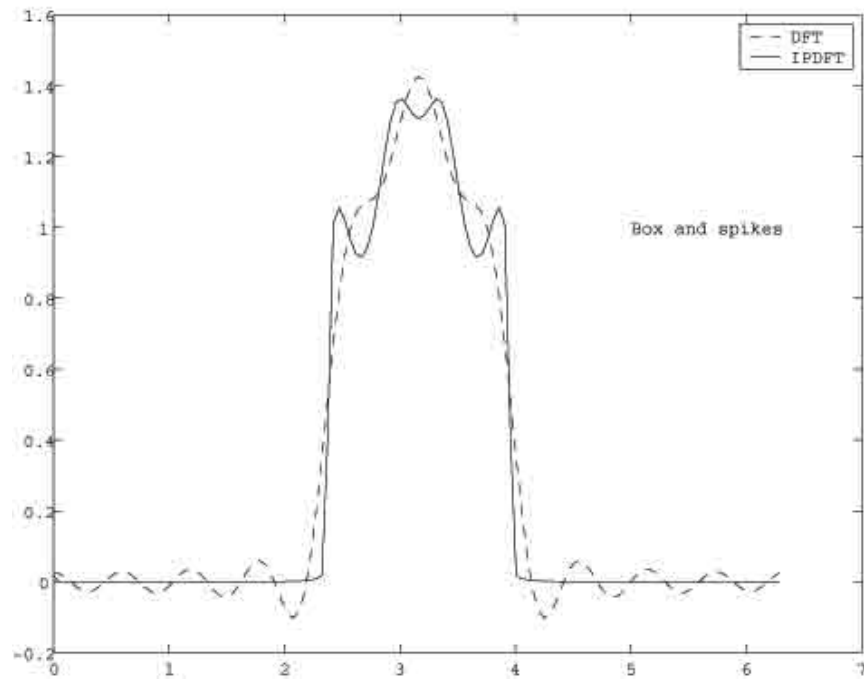
Figure 19.3: The DFT and IPDFT, box and two spikes, $N = 10$, moderate SNR.
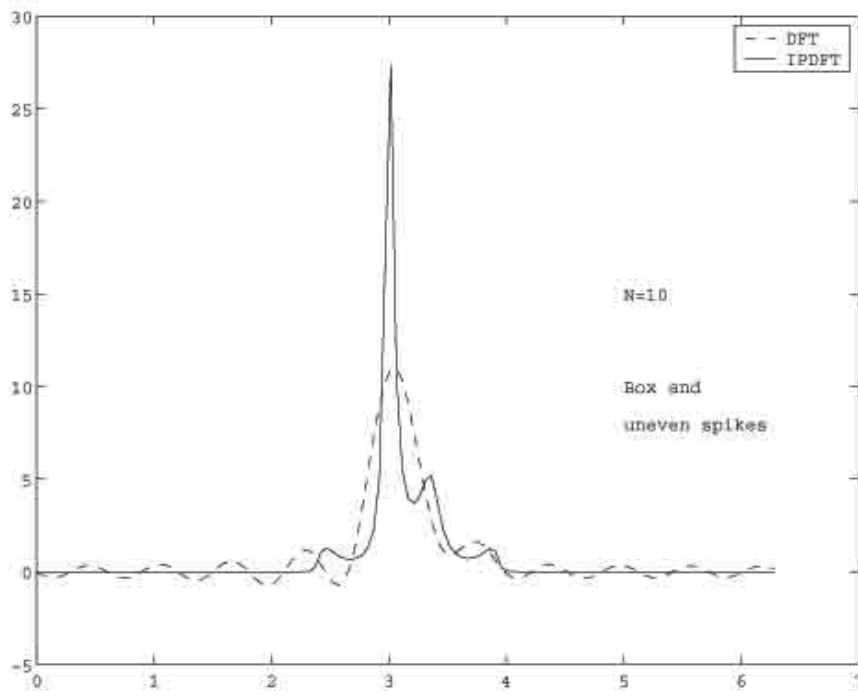
Figure 19.4: The DFT and IPDFT, box and unequal spikes, $N = 10$, high SNR.
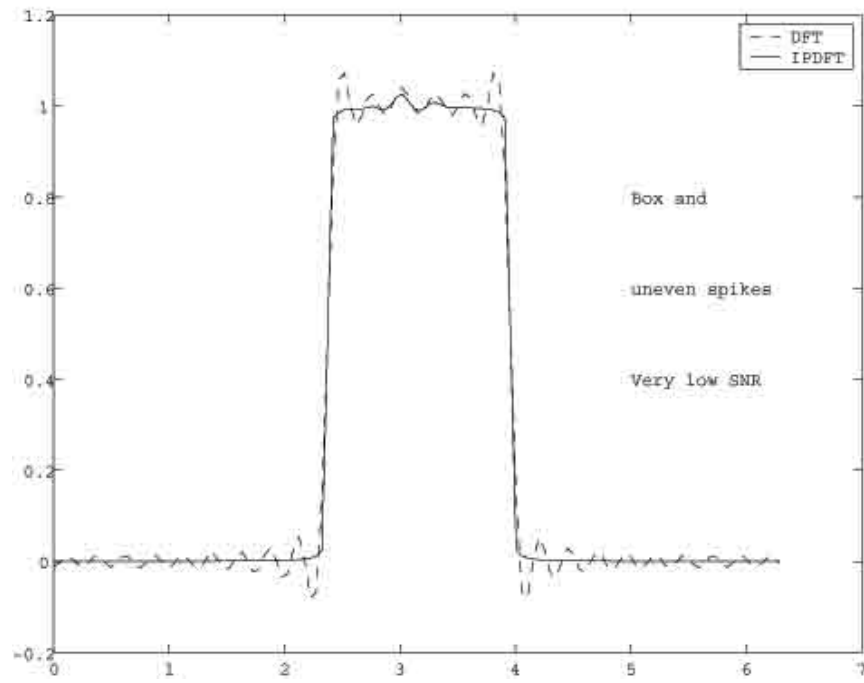
Figure 19.5: The DFT and IPDFT, box and unequal spikes, $N = 25$, very low SNR.

Part VI

Wavelets

Chapter 20

Analysis and Synthesis

20.1   Chapter Summary

Analysis and synthesis in signal processing refers to the effort to study complicated functions in terms of simpler ones. The basic building blocks are orthogonal bases and frames.

20.2   The Basic Idea

An important theme that runs through most of mathematics, from the geometry of the early Greeks to modern signal processing, is *analysis and synthesis*, or, less formally, *breaking up and putting back together*. The Greeks estimated the area of a circle by breaking it up into sectors that approximated triangles. The Riemann approach to integration involves breaking up the area under a curve into pieces that approximate rectangles or other simple shapes. Viewed differently, the Riemann approach is first to approximate the function to be integrated by a step function and then to integrate the step function.

Along with geometry, Euclid includes a good deal of number theory, in which we find analysis and synthesis. His theorem that every positive integer is divisible by a prime is analysis; division does the breaking up and the simple pieces are the primes. The fundamental theorem of arithmetic, which asserts that every positive integer can be written in an essentially unique way as the product of powers of primes, is synthesis, with the putting back together done by multiplication.

20.3   Polynomial Approximation

The individual power functions, x^n, are not particularly interesting by themselves, but when finitely many of them are scaled and added to form a polynomial, interesting functions can result, as the famous approximation theorem of Weierstrass confirms [150]:

Theorem 20.1 *If $f : [a, b] \to R$ is continuous and $\epsilon > 0$ is given, we can find a polynomial P such that $|f(x) - P(x)| \leq \epsilon$ for every x in $[a, b]$.*

The idea of building complicated functions from powers is carried a step further with the use of infinite series, such as Taylor series. The sine function, for example, can be represented for all real x by the infinite power series

$$\sin x = x - \frac{1}{3!}x^3 + \frac{1}{5!}x^5 - \frac{1}{7!}x^7 + \dots.$$

The most interesting thing to note about this is that the sine function has properties that none of the individual power functions possess; for example, it is bounded and periodic. So we see that an infinite sum of simple functions can be qualitatively different from the components in the sum. If we take the sum of only finitely many terms in the Taylor series for the sine function we get a polynomial, which cannot provide a good approximation of the sine function for all x; that is, the finite sum does not approximate the sine function uniformly over the real line. The approximation is better for x near zero and poorer as we move away from zero. However, for any selected x and for any $\epsilon > 0$, there is a positive integer N, depending on the x and on the ϵ, with the sum of the first n terms of the series within ϵ of $\sin x$ for $n \geq N$; that is, the series converges pointwise to $\sin x$ for each real x. In Fourier analysis the trigonometric functions themselves are viewed as the simple functions, and we try to build more complicated functions as (possibly infinite) sums of trig functions. In wavelet analysis we have more freedom to design the simple functions to fit the problem at hand.

20.4   Signal Analysis

When we speak of *signal analysis*, we often mean that we believe the signal to be a superposition of simpler signals of a known type and we wish to know which of these simpler signals are involved and to what extent. For example, received sonar or radar data may be the superposition of individual components corresponding to spatially localized targets of interest. As we shall see in our discussion of the ambiguity function and of wavelets, we want to tailor the family of simpler signals to fit the physical problem being considered.

Sometimes it is not the individual components that are significant by themselves, but groupings of these components. For example, if our received signal is believed to consist of a lower frequency signal of interest plus a noise component employing both low and high frequencies, we can remove some of the noise by performing a low-pass filtering. This amounts to analyzing the received signal to determine what its low-pass and high-pass components are. We formulate this operation mathematically using the Fourier transform, which decomposes the received signal $f(t)$ into complex exponential function components corresponding to different frequencies.

More generally, we may analyze a signal $f(t)$ by calculating certain inner products $\langle f, g_n \rangle$, $n = 1, ..., N$. We may wish to encode the signal using these N numbers, or to make a decision about the signal, such as recognizing a voice. If the signal is a two-dimensional image, say a fingerprint, we may want to construct a data-base of these N-dimensional vectors, for identification. In such a case we are not necessarily claiming that the signal $f(t)$ is a superposition of the $g_n(t)$ in any sense, nor do we necessarily expect to reconstruct $f(t)$ at some later date from the stored inner products. For example, one might identify a piece of music using only the upward or downward progression of the first few notes.

There are many cases, on the other hand, in which we do wish to reconstruct the signal $f(t)$ from measurements or stored compressed versions. In such cases we need to consider this when we design the measuring or compression procedures. For example, we may have values of the signal or its Fourier transform at some finite number of points and want to recapture $f(t)$ itself. Even in those cases mentioned previously in which reconstruction is not desired, such as the fingerprint case, we do wish to be reasonably sure that similar vectors of inner products correspond to similar signals and distinct vectors of inner products correspond to distinct signals, within the obvious limitations imposed by the finiteness of the stored inner products. The twin processes of analysis and synthesis are dealt with mathematically using the notions of *frames* and *bases.*

20.5 Practical Considerations in Signal Analysis

Perhaps the most basic problem in signal analysis is determining which sinusoidal components make up a given signal. Let the analog signal $f(t)$ be given for all real t by

$$f(t) = \sum_{j=1}^{J} A_j e^{i \omega_j t}, \tag{20.1}$$

where the A_j are complex amplitudes and the ω_j are real numbers. If we view the variable t as time, then the ω_j are frequencies. In theory, we can determine J, the ω_j, and the A_j simply by calculating the Fourier transform $F(\omega)$ of $f(t)$. The function $F(\omega)$ will have Dirac delta components at $\omega = \omega_j$ for each j, and will be zero elsewhere. Obviously, this is not a practical solution to the problem. The first step in developing a practical approach is to pass from analog signals, which are functions of the continuous variable t, to digital signals or sequences, which are functions of the integers.

In theoretical discussions of digital signal processing, analog signals are converted to discrete signals or sequences by sampling. We begin by choosing a positive sampling spacing $\Delta > 0$ and define the nth entry of the sequence $x = \{x(n)\}$ by

$$x(n) = f(n\Delta), \tag{20.2}$$

for all integers n.

Notice that, since

$$e^{i\omega_j n\Delta} = e^{i(\omega_j + \frac{2\pi}{\Delta})n\Delta}$$

for all n, we cannot distinguish frequency ω_j from $\omega_j + \frac{2\pi}{\Delta}$. We try to select Δ small enough so that each of the ω_j we seek lies in the interval $(-\frac{\pi}{\Delta}, \frac{\pi}{\Delta})$. If we fail to make Δ small enough we *under-sample*, with the result that some of the ω_j will be mistaken for lower frequencies; this is *aliasing*. Our goal now is to process the sequence x to determine J, the ω_j, and the A_j. We do this with matched filtering.

Every linear shift-invariant system operates through convolution; associated with the system is a sequence h, such that, when x is the input sequence, the output sequence is y, with

$$y(n) = \sum_{k=-\infty}^{\infty} h(k)x(n-k), \tag{20.3}$$

for each integer n. In theoretical *matched filtering* we design a whole family of such systems or filters, one for each frequency ω in the interval $(-\frac{\pi}{\Delta}, \frac{\pi}{\Delta})$. We then use our sequence x as input to each of these filters and use the outputs of each to solve our signal-analysis problem.

For each ω in the interval $(-\frac{\pi}{\Delta}, \frac{\pi}{\Delta})$ and each positive integer K, we consider the shift-invariant linear filter with $h = e_{K,\omega}$, where

$$e_\omega(k) = \frac{1}{2K+1}e^{i\omega k\Delta}, \tag{20.4}$$

for $|k| \leq K$ and $e_{K,\omega}(k) = 0$ otherwise. Using x as input to this system, we find that the output value $y(0)$ is

$$y(0) = \sum_{j=1}^{J} A_j\left[\frac{1}{2K+1} \sum_{k=-K}^{K} e^{i(\omega-\omega_j)k\Delta}\right]. \tag{20.5}$$

Recall the following identity for the Dirichlet kernel:

$$\sum_{k=-K}^{K} e^{ik\omega} = \frac{\sin((K+\frac{1}{2})\omega)}{\sin(\frac{\omega}{2})}, \tag{20.6}$$

for $\sin(\frac{\omega}{2}) \neq 0$. As $K \to +\infty$, the inner sum in equation (20.5) goes to zero for every ω except $\omega = \omega_j$. Therefore the limit, as $K \to +\infty$, of $y(0)$ is zero, if ω is not equal to any of the ω_j, and equals A_j, if $\omega = \omega_j$. Therefore, in theory, at least, we can successfully decompose the digital signal into its constituent parts and distinguish one frequency component from another, no matter how close together the two frequencies may be.

It is important to note that, to achieve the perfect analysis described above, we require noise-free values $x(n)$ and we need to take K to infinity; in practice, of course, neither of these conditions is realistic. We consider next the practical matter of having only finitely many values of $x(n)$; we leave the noisy case for another chapter.

20.5.1 The Finite Data Problem

In reality we have only finitely many values of $x(n)$, say for $n = -N, ..., N$. In matched filtering we can only take $K \leq N$. For the choice of $K = N$, we get

$$y(0) = \sum_{j=1}^{J} A_j \left[\frac{1}{2N+1} \sum_{k=-N}^{N} e^{i(\omega-\omega_j)k\Delta} \right], \tag{20.7}$$

for each fixed ω different from the ω_j, and $y(0) = A_j$ for $\omega = \omega_j$. We can then write

$$y(0) = \sum_{j=1}^{J} A_j \left[\frac{1}{2N+1} \frac{\sin((\omega-\omega_j)(N+\frac{1}{2})\Delta)}{\sin((\omega-\omega_j)(\frac{\Delta}{2}))} \right], \tag{20.8}$$

for ω not equal to ω_j. The problem we face for finite data is that the $y(0)$ is not necessarily zero when ω is not one of the ω_j.

In our earlier discussion of signal analysis it was shown that, if we are willing to make a simplifying assumption, we can continue as in the infinite-data case. The simplifying assumption is that the ω_j we seek are J of the $2N+1$ frequencies equally spaced in the interval $(-\frac{\pi}{\Delta}, \frac{\pi}{\Delta})$, beginning with $\alpha_1 = -\frac{\pi}{\Delta} + \frac{2\pi}{(2N+1)\Delta}$ and ending with $\alpha_{2N+1} = \frac{\pi}{\Delta}$. Therefore,

$$\alpha_m = -\frac{\pi}{\Delta} + \frac{2\pi m}{(2N+1)\Delta},$$

for $m = 1, ..., 2N+1$.

Having made this simplifying assumption, we then design the matched filters corresponding to the frequencies α_n, for $n = 1, ..., 2N + 1$. Because

$$\sum_{k=-N}^{N} e^{i(\alpha_m - \alpha_n)k\Delta} = \sum_{k=-N}^{N} e^{2\pi i \frac{m-n}{2N+1} k}$$

$$= \frac{\sin(2\pi \frac{m-n}{2N+1}(N + \frac{1}{2}))}{\sin(\pi \frac{m-n}{2N+1})}, \tag{20.9}$$

it follows that

$$\sum_{k=-N}^{N} e^{i(\alpha_m - \alpha_n)k\Delta} = 0,$$

for $m \neq n$ and it is equal to $2N + 1$ when $m = n$. We conclude that, provided the frequencies we seek are among the α_m, we can determine J and the ω_j. Once we have these pieces of information, we find the A_j simply by solving a system of linear equations.

20.6   Frames

Although in practice we deal with finitely many measurements or inner product values, it is convenient, in theoretical discussions, to imagine that the signal $f(t)$ has been associated with an infinite sequence of inner products $\{\langle f, g_n \rangle, n = 1, 2, ...\}$. It is also convenient to assume that $||f||^2 = \int_{-\infty}^{\infty} |f(t)|^2 dt < +\infty$; that is, we assume that f is in the Hilbert space $H = L^2$. The sequence $\{g_n | n = 1, 2, ...\}$ in any Hilbert space H is called a *frame* for H if there are positive constants $A \leq B$ such that, for all f in H,

$$A||f||^2 \leq \sum_{n=1}^{\infty} |\langle f, g_n \rangle|^2 \leq B||f||^2. \tag{20.10}$$

The inequalities in (20.10) define the *frame property*. A frame is said to be *tight* if $A = B$.

To motivate this definition, suppose that $f = g - h$. If g and h are nearly equal, then f is near zero, so that $||f||^2$ is near zero. Consequently, the numbers $|\langle f, g_n \rangle|^2$ are all small, meaning that $\langle g, g_n \rangle$ is nearly equal to $\langle h, g_n \rangle$ for each n. Conversely, if $\langle g, g_n \rangle$ is nearly equal to $\langle h, g_n \rangle$ for each n, then the numbers $|\langle f, g_n \rangle|^2$ are all small. Therefore, $||f||^2$ is small, from which we conclude that g is close to h. The *analysis* operator is the one that takes us from f to the sequence $\{\langle f, g_n \rangle\}$, while the *synthesis* operator takes us from the sequence $\{\langle f, g_n \rangle\}$ to f. This discussion of frames and related notions is based on the treatment in Christensen's book [77].

In the case of finite dimensional space, any finite set $\{g_n, \; n = 1, ..., N\}$ is a frame for the space H of all f that are linear combinations of the g_n.

Exercise 20.1 *An interesting example of a frame in $H = R^2$ is the so-called Mercedes frame: let $g_1 = (0, 1)$, $g_2 = (-\sqrt{3}/2, -1/2)$ and $g_3 = (\sqrt{3}/2, -1/2)$. Show that for this frame $A = B = 3/2$, so the Mercedes frame is tight.*

The frame property in (20.10) provides a necessary condition for stable application of the decomposition and reconstruction operators. But it does more than that; it actually provides a reconstruction algorithm. The *frame operator S* is given by

$$Sf = \sum_{n=1}^{\infty} \langle f, g_n \rangle \, g_n.$$

The frame property implies that the frame operator is invertible. The *dual frame* is the sequence $\{S^{-1} g_n, \; n = 1, 2, ...\}$.

Exercise 20.2 *Use the definitions of the frame operator S and the dual frame to obtain the following reconstruction formulas:*

$$f = \sum_{n=1}^{\infty} \langle f, g_n \rangle \, S^{-1} g_n;$$

and

$$f = \sum_{n=1}^{\infty} \langle f, S^{-1} g_n \rangle \, g_n.$$

If the frame is tight, then the dual frame is $\{\frac{1}{A} g_n, \; n = 1, 2, ...\}$; if the frame is not tight, inversion of the frame operator is done only approximately.

20.7   Bases, Riesz Bases and Orthonormal Bases

The sequence $\{g_n, \; n = 1, 2, ...\}$ in H is a *basis* for H if, for every f in H, there is a unique sequence $\{c_n, \; n = 1, 2, ...\}$ with

$$f = \sum_{n=1}^{\infty} c_n g_n.$$

A basis is called a *Riesz basis* if it is also a frame for H. It can be shown that a frame is a Riesz basis if the removal of any one element causes the

loss of the frame property; since the second inequality in Inequality (20.10) is not lost, it follows that it is the first inequality that can now be violated for some f. A basis is an *orthonormal basis* for H if $||g_n|| = 1$ for all n and $\langle g_n, g_m \rangle = 0$ for distinct m and n.

We know that the complex exponentials

$$\{e_n(t) = \frac{1}{\sqrt{2\pi}} e^{int}, \ -\infty < n < \infty\}$$

form an orthonormal basis for the Hilbert space $L^2(-\pi, \pi)$ consisting of all f supported on $(-\pi, \pi)$ with $\int_{-\pi}^{\pi} |f(t)|^2 dt < +\infty$. Every such f can be written as

$$f(t) = \frac{1}{\sqrt{2\pi}} \sum_{n=-\infty}^{+\infty} a_n e^{int},$$

for

$$a_n = \langle f, e_n \rangle = \frac{1}{\sqrt{2\pi}} \int_{-\pi}^{\pi} f(t) e^{-int} dt.$$

Consequently, this is true for every f in $L^2(-\pi/2, \pi/2)$, although the set of functions $\{g_n\}$ formed by restricting the $\{e_n\}$ to the interval $(-\pi/2, \pi/2)$ is no longer a basis for $H = L^2(-\pi/2, \pi/2)$. It is still a tight frame with $A = 1$, but is no longer normalized, since the norm of g_n in $L^2(-\pi/2, \pi/2)$ is $1/\sqrt{2}$. An orthonormal basis can be characterized as any sequence with $||g_n|| = 1$ for all n that is a tight frame with $A = 1$. The sequence $\{\sqrt{2}g_{2k}, \ k = -\infty, ..., \infty\}$ is an orthonormal basis for $L^2(-\pi/2, \pi/2)$, as is the sequence $\{\sqrt{2}g_{2k+1}, \ k = -\infty, ..., \infty\}$. The sequence $\{\langle f, g_n \rangle, n = -\infty, ..., \infty\}$ is redundant; the half corresponding either to the odd n or to the even n suffices to recover f. Because of this redundancy we can tolerate more inaccuracy in measuring these values; indeed, this is one of the main attractions of frames in signal processing.

Chapter 21

Ambiguity Functions

21.1 Chapter Summary

We turn now to signal-processing problems arising in *radar*. Not only does radar provide an important illustration of the application of the theory of Fourier transforms and matched filters, but it also serves to motivate several of the mathematical concepts we shall encounter in our discussion of wavelets. The connection between radar signal processing and wavelets is discussed in some detail in Kaiser's book [145].

21.2 Radar Problems

In radar a real-valued function $\psi(t)$ representing a time-varying voltage is converted by an antenna in transmission mode into a propagating electromagnetic wave. When this wave encounters a reflecting target an echo is produced. The antenna, now in receiving mode, picks up the echo $f(t)$, which is related to the original signal by

$$f(t) = A\psi(t - d(t)),$$

where $d(t)$ is the time required for the original signal to make the round trip from the antenna to the target and return back at time t. The amplitude A incorporates the reflectivity of the target as well as attenuation suffered by the signal. As we shall see shortly, the delay $d(t)$ depends on the distance from the antenna to the target and, if the target is moving, on its radial velocity. The main signal-processing problem here is to determine target range and radial velocity from knowledge of $f(t)$ and $\psi(t)$.

If the target is stationary, at a distance r_0 from the antenna, then $d(t) = 2r_0/c$, where c is the speed of light. In this case the original signal

and the received echo are related simply by

$$f(t) = A\psi(t - b),$$

for $b = 2r_0/c$. When the target is moving so that its distance to the antenna, $r(t)$, is time-dependent, the relationship between f and ψ is more complicated.

Exercise 21.1 *Suppose the target is at a distance $r_0 > 0$ from the antenna at time $t = 0$, and has radial velocity v, with $v > 0$ indicating away from the antenna. Show that the delay function $d(t)$ is now*

$$d(t) = 2\frac{r_0 + vt}{c + v}$$

and $f(t)$ is related to $\psi(t)$ according to

$$f(t) = A\psi(\frac{t - b}{a}), \tag{21.1}$$

for

$$a = \frac{c + v}{c - v}$$

and

$$b = \frac{2r_0}{c - v}.$$

Show also that if we select $A = (\frac{c-v}{c+v})^{1/2}$ then energy is preserved; that is, $||f|| = ||\psi||$.

Exercise 21.2 *Let $\Psi(\omega)$ be the Fourier transform of the signal $\psi(t)$. Show that the Fourier transform of the echo $f(t)$ in Equation (21.1) is then*

$$F(\omega) = Aae^{ib\omega}\Psi(a\omega). \tag{21.2}$$

The basic problem is to determine a and b, and therefore the range and radial velocity of the target, from knowledge of $f(t)$ and $\psi(t)$. An obvious approach is to do a matched filter.

21.3 The Wideband Cross-Ambiguity Function

Note that the received echo $f(t)$ is related to the original signal by the operations of rescaling and shifting. We therefore match the received echo

with all the shifted and rescaled versions of the original signal. For each $a > 0$ and real b, let

$$\psi_{a,b}(t) = \psi(\frac{t-b}{a}).$$

The *wideband cross-ambiguity function* (WCAF) is

$$(W_\psi f)(b, a) = \frac{1}{\sqrt{a}} \int_{-\infty}^{\infty} f(t)\psi_{a,b}(t)dt. \tag{21.3}$$

In the ideal case the values of a and b for which the WCAF takes on its largest absolute value should be the true values of a and b.

More generally, there will be many individual targets or sources of echos, each having their own values of a, b, and A. The resulting received echo function $f(t)$ is a superposition of the individual functions $\psi_{a,b}(t)$, which, for technical reasons, we write as

$$f(t) = \int_{-\infty}^{\infty} \int_{0}^{\infty} D(b, a)\psi_{a,b}(t)\frac{dadb}{a^2}. \tag{21.4}$$

We then have the inverse problem of determining $D(b, a)$ from $f(t)$.

Equation (21.4) provides a representation of the echo $f(t)$ as a superposition of rescaled translates of a single function, namely the original signal $\psi(t)$. We shall encounter this representation again in our discussion of wavelets, where the signal $\psi(t)$ is called the *mother wavelet* and the WCAF is called the *integral wavelet transform*. One reason for discussing radar and ambiguity functions now is to motivate some of the wavelet theory. Our discussion here follows closely the treatment in [145], where Kaiser emphasizes the important connections between wavelets and radar ambiguity functions.

As we shall see in the chapter on wavelets, we can recover the signal $f(t)$ from the WCAF using the following inversion formula: at points t where $f(t)$ is continuous we have

$$f(t) = \frac{1}{C_\psi} \int_{-\infty}^{\infty} \int_{-\infty}^{\infty} (W_\psi f)(b, a)\psi(\frac{t-b}{a})\frac{dadb}{a^2},$$

with

$$C_\psi = \int_{-\infty}^{\infty} \frac{|\Psi(\omega)|^2}{|\omega|}d\omega$$

for $\Psi(\omega)$ the Fourier transform of $\psi(t)$. The obvious conjecture is then that the distribution functon $D(b, a)$ is

$$D(b, a) = \frac{1}{C_\psi}(W_\psi f)(b, a).$$

However, this is not generally the case. Indeed, there is no particular reason why the physically meaningful function $D(b, a)$ must have the form

$(W_\psi g)(b, a)$ for some function g. So the inverse problem of estimating $D(b, a)$ from $f(t)$ is more complicated. One approach mentioned in [145] involves transmitting more than one signal $\psi(t)$ and estimating $D(b, a)$ from the echos corresponding to each of the several different transmitted signals.

21.4   The Narrowband Cross-Ambiguity Function

The real signal $\psi(t)$ with Fourier transform $\Psi(\omega)$ is said to be a *narrowband signal* if there are constants α and γ such that the conjugate-symmetric function $\Psi(\omega)$ is concentrated on $\alpha \leq |\omega| \leq \gamma$ and $\frac{\gamma - \alpha}{\gamma + \alpha}$ is nearly equal to zero, which means that α is very much greater than $\beta = \frac{\gamma - \alpha}{2}$. The center frequency is $\omega_c = \frac{\gamma + \alpha}{2}$.

Exercise 21.3 *Let $\phi = 2\omega_c v/c$. Show that $a\omega_c$ is approximately equal to $\omega_c + \phi$.*

It follows then that, for $\omega > 0$, $F(\omega)$, the Fourier transform of the echo $f(t)$, is approximately $Aae^{ib\omega}\Psi(\omega + \phi)$. Because the Doppler shift affects positive and negative frequencies differently, it is convenient to construct a related signal having only positive frequency components.

Let $G(\omega) = 2F(\omega)$ for $\omega > 0$ and $G(\omega) = 0$ otherwise. Let $g(t)$ be the inverse Fourier transform of $G(\omega)$. Then, the complex-valued function $g(t)$ is called the *analytic signal* associated with $f(t)$. The function $f(t)$ is the real part of $g(t)$; the imaginary part of $g(t)$ is the *Hilbert transform* of $f(t)$. Then, the *demodulated analytic signal* associated with $f(t)$ is $h(t)$ with Fourier transform $H(\omega) = G(\omega + \omega_c)$. Similarly, let $\gamma(t)$ be the demodulated analytic signal associated with $\psi(t)$.

Exercise 21.4 *Show that the demodulated analytic signals $h(t)$ and $\gamma(t)$ are related by*
$$h(t) = Be^{i\phi t}\gamma(t - b) = B\gamma_{\phi,b}(t),$$
for B a time-independent constant.

Hint: Use the fact that $\Psi(\omega) = 0$ for $0 \leq \omega < \alpha$ and $\phi < \alpha$.

To determine the range and radial velocity in the narrowband case we again use the matched filter, forming the *narrowband cross-ambiguity function* (NCAF)

$$N_h(\phi, b) = \langle h, \gamma_{\phi,b} \rangle = \int_{-\infty}^{\infty} h(t)e^{-i\phi t}\overline{\gamma(t - b)}dt. \qquad (21.5)$$

Ideally, the values of ϕ and b corresponding to the largest absolute value of $N_h(\phi, b)$ will be the true ones, from which the range and radial velocity can be determined. For each fixed value of b, the NCAF is the Fourier transform of the function $h(t)\overline{\gamma(t-b)}$, evaluated at $\omega = -\phi$; so the NCAF contains complete information about the function $h(t)$. In the chapter on wavelets we shall consider the NCAF in a different light, with γ playing the role of a window function and the NCAF the short-time Fourier transform of $h(t)$, describing the frequency content of $h(t)$ near the time b.

In the more general case in which the narrowband echo function $f(t)$ is a superposition of narrowband reflections,

$$f(t) = \int_{-\infty}^{\infty} \int_{0}^{\infty} D(b,a)\psi_{a,b}(t)\frac{dadb}{a^2},$$

we have

$$h(t) = \int_{-\infty}^{\infty} \int_{0}^{\infty} D_{NB}(b,\phi)e^{i\phi t}\gamma(t-b)d\phi db,$$

where $D_{NB}(b,\phi)$ is the narrowband distribution of reflecting target points, as a function of b and $\phi = 2\omega_c v/c$. The inverse problem now is to estimate this distribution, given $h(t)$.

21.5 Range Estimation

If the transmitted signal is $\psi(t) = e^{i\omega t}$ and the target is stationary at range r, then the echo received is $f(t) = Ae^{i\omega(t-b)}$, where $b = 2r/c$. So our information about r is that we know the value $e^{2i\omega r/c}$. Because of the periodicity of the complex exponential function, this is not enough information to determine r; we need $e^{2i\omega r/c}$ for a variety of values of ω. To obtain these values we can transmit a signal whose frequency changes with time, such as a *chirp* of the form

$$\psi(t) = e^{i\omega t^2}$$

with the frequency $2\omega t$ at time t.

Chapter 22

Time-Frequency Analysis

22.1 Chapter Summary

There are applications in which the frequency composition of the signal of interest will change over time. A good analogy is a piece of music, where notes at certain frequencies are heard for a while and then are replaced by notes at other frequencies. We do not usually care what the overall contribution of, say, middle C is to the song, but do want to know which notes are to be sounded when and for how long. Analyzing such non-stationary signals requires tools other than the Fourier transform: the short-time Fourier transform is one such tool; wavelet expansion is another.

22.2 Non-stationary Signals

The inverse Fourier transform formula

$$f(t) = \frac{1}{2\pi} \int_{-\infty}^{\infty} F(\omega) e^{-i\omega t} d\omega$$

provides a representation of the function of time $f(t)$ as a superposition of sinusoids $e^{-i\omega t}$ with frequencies ω. The value at ω of the Fourier transform

$$F(\omega) = \int_{-\infty}^{\infty} f(t) e^{i\omega t} dt$$

is the complex amplitude associated with the sinusoidal component $e^{-i\omega t}$. It quantifies the contribution to $f(t)$ made by that sinusoid, over all of t. To determine each individual number $F(\omega)$ we need $f(t)$ for all t. It is implicit that the frequency content has not changed over time.

22.3   The Short-Time Fourier Transform

To estimate the frequency content of the signal $f(t)$ around the time $t = b$, we could proceed as follows. Multiply $f(t)$ by the function that is equal to $\frac{1}{2\epsilon}$ on the interval $[b - \epsilon, b + \epsilon]$ and zero otherwise. Then take the Fourier transform. The multiplication step is called *windowing*.

To see how well this works, consider the case in which $f(t) = \exp(-i\omega_0 t)$ for all t. The Fourier transform of the windowed signal is then

$$\exp(i(\omega - \omega_0)b)\frac{\sin(\epsilon(\omega - \omega_0))}{\epsilon(\omega - \omega_0)}.$$

This function attains its maximum value of one at $\omega = \omega_0$. But, the first zeros of the function are at $|\omega - \omega_0| = \frac{\pi}{\epsilon}$, which says that as ϵ gets smaller the windowed Fourier transform spreads out more and more around $\omega = \omega_0$; that is, better time localization comes at the price of worse frequency localization. To achieve a somewhat better result we can change the window function.

The standard normal (or Gaussian) curve is

$$g(t) = \frac{1}{\sqrt{2\pi}}\exp(-\frac{1}{2}t^2),$$

which has its peak at $t = 0$ and falls off to zero symmetrically on either side. For $\sigma > 0$, let

$$g_\sigma(t) = \frac{1}{\sigma}g(t/\sigma).$$

Then the function $g_\sigma(t - b)$ is centered at $t = b$ and falls off on either side, more slowly for large σ, faster for smaller σ. Also we have

$$\int_{-\infty}^{\infty} g_\sigma(t - b)dt = 1$$

for each b and $\sigma > 0$. Such functions were used by Gabor [115] for *windowing* signals and are called *Gabor windows*.

Gabor's idea was to multiply $f(t)$, the signal of interest, by the window $g_\sigma(t - b)$ and then to take the Fourier transform, obtaining the *short-time Fourier transform* (STFT)

$$G_b^\sigma(\omega) = \int_{-\infty}^{\infty} f(t)g_\sigma(t - b)e^{i\omega t}dt.$$

Since $g_\sigma(t - b)$ falls off to zero on either side of $t = b$, multiplying by this window essentially restricts the signal to a neighborhood of $t = b$. The STFT then measures the frequency content of the signal, near the time $t = b$. The STFT therefore performs a *time-frequency analysis* of the signal.

We focus more tightly around the time $t = b$ by choosing a small value for σ. Because of the uncertainty principle, the Fourier transform of the window $g_\sigma(t - b)$ grows wider as σ gets smaller; the *time-frequency window* remains constant [78]. This causes the STFT to involve greater blurring in the frequency domain. In short, to get good resolution in frequency, we need to observe for a longer time; if we focus on a small time interval, we pay the price of reduced frequency resolution. This is unfortunate because when we focus on a short interval of time, it is to uncover a part of the signal that is changing within that short interval, which means it must have high frequency components within that interval. There is no reason to believe that the spacing is larger between those high frequencies we wish to resolve than between lower frequencies associated with longer time intervals. We would like to have the same resolving capability when focusing on a short time interval that we have when focusing on a longer one.

22.4   The Wigner-Ville Distribution

In [171] Meyer describes Ville's approach to determining the instantaneous power spectrum of the signal, that is, the energy in the signal $f(t)$ that corresponds to time t and frequency ω. The goal is to find a function $W_f(t, \omega)$ having the properties

$$\int W_f(t, \omega)d\omega/2\pi = |f(t)|^2,$$

which is the total energy in the signal at time t, and

$$\int W_f(t, \omega)dt = |F(\omega)|^2,$$

which is the total energy in the Fourier transform at frequency ω. Because these two properties do not specify a unique $W_f(t, \omega)$, two additional properties are usually required:

$$\int \int W_f(t, \omega)\overline{W_g(t, \omega)}dtd\omega/2\pi = |\int f(t)\overline{g(t)}dt|^2$$

and, for $f(t) = g_\sigma(t - b) \exp(i\alpha t)$,

$$W_f(t, \omega) = 2 \exp(-\sigma^{-2}(t - b)^2) \exp(-\sigma^2(\omega - \alpha)^2).$$

The *Wigner-Ville distribution* of $f(t)$, given by

$$WV_f(t, \omega) = \int_{-\infty}^{\infty} f(t + \frac{\tau}{2})\overline{f(t - \frac{\tau}{2})} \exp(-i\omega\tau)d\tau,$$

has all four of the desired properties. The Wigner-Ville distribution is always real-valued, but its values need not be nonnegative.

In [95] De Bruijn defines the *score* of a signal $f(t)$ to be $H(x, y; f, f)$, where

$$H(x, y; f_1, f_2) = 2 \int_{-\infty}^{\infty} f_1(x + t)\overline{f_2(x - t)}e^{-4\pi i y t}dt.$$

Exercise 22.1 *Relate the narrowband cross-ambiguity function to the De Bruijn's score and the Wigner-Ville distribution.*

Chapter 23

Wavelets

23.1   Chapter Summary

In this chapter we present a short overview of wavelet signal processing.

23.2   Background

The fantastic increase in computer power over the last few decades has made possible, even routine, the use of digital procedures for solving problems that were believed earlier to be intractable, such as the modeling of large-scale systems. At the same time, it has created new applications unimagined previously, such as medical imaging. In some cases the mathematical formulation of the problem is known and progress has come with the introduction of efficient computational algorithms, as with the Fast Fourier Transform. In other cases, the mathematics is developed, or perhaps rediscovered, as needed by the people involved in the applications. Only later it is realized that the theory already existed, as with the development of computerized tomography without Radon's earlier work on reconstruction of functions from their line integrals.

It can happen that applications give a theoretical field of mathematics a rebirth; such seems to be the case with *wavelets* [138]. Sometime in the 1980s researchers working on various problems in electrical engineering, quantum mechanics, image processing, and other areas became aware that what the others were doing was related to their own work. As connections became established, similarities with the earlier mathematical theory of approximation in functional analysis were noticed. Meetings began to take place, and a common language began to emerge around this reborn area, now called wavelets. One of the most significant meetings took place in June of 1990, at the University of Massachusetts Lowell. The keynote

speaker was Ingrid Daubechies; the lectures she gave that week were subsequently published in the book [94].

There are a number of good books on wavelets, such as [145], [18], and [222]. A recent issue of the IEEE Signal Processing Magazine has an interesting article on using wavelet analysis of paintings for artist identification [143].

Fourier analysis and synthesis concerns the decomposition, filtering, compressing, and reconstruction of signals using complex exponential functions as the building blocks; wavelet theory provides a framework in which other building blocks, better suited to the problem at hand, can be used. As always, efficient algorithms provide the bridge between theory and practice.

Since their development in the 1980s wavelets have been used for many purposes. In the discussion to follow, we focus on the problem of analyzing a signal whose frequency composition is changing over time. As we saw in our discussion of the narrowband cross-ambiguity function in radar, the need for such time-frequency analysis has been known for quite a while. Other methods, such as Gabor's short time Fourier transform and the Wigner-Ville distribution, have also been considered for this purpose.

23.3   A Simple Example

Imagine that $f(t)$ is defined for all real t and we have sampled $f(t)$ every half-second. We focus on the time interval $[0, 2)$. Suppose that $f(0) = 1$, $f(0.5) = -3$, $f(1) = 2$ and $f(1.5) = 4$. We approximate $f(t)$ within the interval $[0, 2)$ by replacing $f(t)$ with the step function that is 1 on $[0, 0.5)$, -3 on $[0.5, 1)$, 2 on $[1, 1.5)$, and 4 on $[1.5, 2)$; for notational convenience, we represent this step function by $(1, -3, 2, 4)$. We can decompose $(1, -3, 2, 4)$ into a sum of step functions

$$(1, -3, 2, 4) = 1(1, 1, 1, 1) - 2(1, 1, -1, -1) + 2(1, -1, 0, 0) - 1(0, 0, 1, -1).$$

The first basis element, $(1, 1, 1, 1)$, does not vary over a two-second interval. The second one, $(1, 1, -1, -1)$, is orthogonal to the first, and does not vary over a one-second interval. The other two, both orthogonal to the previous two and to each other, vary over half-second intervals. We can think of these basis functions as corresponding to different frequency components and time locations; that is, they are giving us a time-frequency decomposition.

Suppose we let $\phi_0(t)$ be the function that is 1 on the interval $[0, 1)$ and 0 elsewhere, and $\psi_0(t)$ the function that is 1 on the interval $[0, 0.5)$ and -1 on the interval $[0.5, 1)$. Then we say that

$$\phi_0(t) = (1, 1, 0, 0),$$

and
$$\psi_0(t) = (1, -1, 0, 0).$$

Then we write
$$\phi_{-1}(t) = (1, 1, 1, 1) = \phi_0(0.5t),$$
$$\psi_0(t - 1) = (0, 0, 1, -1),$$

and
$$\psi_{-1}(t) = (1, 1, -1, -1) = \psi_0(0.5t).$$

So we have the decomposition of $(1, -3, 2, 4)$ as

$$(1, -3, 2, 4) = 1\phi_{-1}(t) - 2\psi_{-1}(t) + 2\psi_0(t) - 1\psi_0(t - 1).$$

It what follows we shall be interested in extending these ideas, to find other functions $\phi_0(t)$ and $\psi_0(t)$ that lead to bases consisting of functions of the form

$$\psi_{j,k}(t) = \psi_0(2^j t - k).$$

These will be our *wavelet bases*.

23.4 The Integral Wavelet Transform

For real numbers b and $a \neq 0$, the *integral wavelet transform* (IWT) of the signal $f(t)$ relative to the *basic wavelet* (or *mother* wavelet) $\psi(t)$ is

$$(W_\psi f)(b, a) = |a|^{-\frac{1}{2}} \int_{-\infty}^{\infty} f(t)\psi(\frac{t - b}{a})dt.$$

This function is also the wideband cross-ambiguity function in radar. The function $\psi(t)$ is also called a window function and, like Gaussian functions, it will be relatively localized in time. However, it must also have properties quite different from those of Gabor's Gaussian windows; in particular, we want

$$\int_{-\infty}^{\infty} \psi(t)dt = 0.$$

An example is the *Haar wavelet* $\psi_{Haar}(t)$ that has the value $+1$ for $0 \leq t < \frac{1}{2}$, -1 for $\frac{1}{2} \leq t < 1$ and zero otherwise.

As the scaling parameter a grows larger the wavelet $\psi(t)$ grows wider, so choosing a small value of the scaling parameter permits us to focus on a neighborhood of the time $t = b$. The IWT then registers the contribution to $f(t)$ made by components with features on the scale determined by a, in the neightborhood of $t = b$. Calculations involving the uncertainty principle reveal that the IWT provides a flexible time-frequency window that narrows when we observe high frequency components and widens for lower frequencies [78].

Given the integral wavelet transform $(W_\psi f)(b, a)$, it is natural to ask how we might recover the signal $f(t)$. The following inversion formula answers that question: at points t where $f(t)$ is continuous we have

$$f(t) = \frac{1}{C_\psi} \int_{-\infty}^{\infty} \int_{-\infty}^{\infty} (W_\psi f)(b, a)\psi(\frac{t - b}{a})\frac{da}{a^2}db,$$

with

$$C_\psi = \int_{-\infty}^{\infty} \frac{|\Psi(\omega)|^2}{|\omega|}d\omega$$

for $\Psi(\omega)$ the Fourier transform of $\psi(t)$.

23.5   Wavelet Series Expansions

The Fourier series expansion of a function $f(t)$ on a finite interval is a representation of $f(t)$ as a sum of orthogonal complex exponentials. Localized alterations in $f(t)$ affect every one of the components of this sum. Wavelets, on the other hand, can be used to represent $f(t)$ so that localized alterations in $f(t)$ affect only a few of the components of the wavelet expansion. The simplest example of a wavelet expansion is with respect to the Haar wavelets.

Exercise 23.1 *Let* $w(t) = \psi_{Haar}(t)$. *Show that the functions* $w_{jk}(t) = w(2^j t - k)$ *are mutually orthogonal on the interval* $[0, 1]$, *where* $j = 0, 1, ...$ *and* $k = 0, 1, ..., 2^j - 1$.

These functions $w_{jk}(t)$ are the *Haar wavelets*. Every continuous function $f(t)$ defined on $[0, 1]$ can be written as

$$f(t) = c_0 + \sum_{j=0}^{\infty} \sum_{k=0}^{2^j - 1} c_{jk} w_{jk}(t)$$

for some choice of c_0 and c_{jk}. Notice that the *support of the function* $w_{jk}(t)$, the interval on which it is nonzero, gets smaller as j increases. Therefore, the components corresponding to higher values of j in the Haar expansion of $f(t)$ come from features that are localized in the variable t; such features are transients that live for only a short time. Such transient components affect all of the Fourier coefficients but only those Haar wavelet coefficients corresponding to terms supported in the region of the disturbance. This ability to isolate localized features is the main reason for the popularity of wavelet expansions.

The orthogonal functions used in the Haar wavelet expansion are themselves discontinuous, which presents a bit of a problem when we represent continuous functions. Wavelets that are themselves continuous, or better still, differentiable, should do a better job representing smooth functions.

We can obtain other wavelet series expansions by selecting a basic wavelet $\psi(t)$ and defining $\psi_{jk}(t) = 2^{j/2}\psi(2^j t - k)$, for integers j and k. We then say that the function $\psi(t)$ is an *orthogonal wavelet* if the family $\{\psi_{jk}\}$ is an orthonormal basis for the space of square-integrable functions on the real line, the Hilbert space $L^2(R)$. This implies that for every such $f(t)$ there are coefficients c_{jk} so that

$$f(t) = \sum_{j=-\infty}^{\infty} \sum_{k=-\infty}^{\infty} c_{jk}\psi_{jk}(t),$$

with convergence in the mean-square sense. The coefficients c_{jk} are found using the IWT:

$$c_{jk} = (W_\psi f)(\frac{k}{2^j}, \frac{1}{2^j}).$$

It is also of interest to consider wavelets ψ for which $\{\psi_{jk}\}$ form a basis, but not an orthogonal one, or, more generally, form a *frame*, in which the series representations of $f(t)$ need not be unique.

As with Fourier series, wavelet series expansion permits the filtering of certain components, as well as signal compression. In the case of Fourier series, we might attribute high frequency components to noise and achieve a smoothing by setting to zero the coefficients associated with these high frequencies. In the case of wavelet series expansions, we might attribute to noise localized small-scale disturbances and remove them by setting to zero the coefficients corresponding to the appropriate j and k. For both Fourier and wavelet series expansions we can achieve compression by ignoring those components whose coefficients are below some chosen level.

23.6 Multiresolution Analysis

One way to study wavelet series expansions is through *multiresolution analysis* (MRA) [166]. Let us begin with an example involving band-limited functions. This example is called the *Shannon* MRA.

23.6.1 The Shannon Multiresolution Analysis

Let V_0 be the collection of functions $f(t)$ whose Fourier transform $F(\omega)$ is zero for $|\omega| > \pi$; so V_0 is the collection of π-band-limited functions. Let V_1 be the collection of functions $f(t)$ whose Fourier transform $F(\omega)$ is zero for $|\omega| > 2\pi$; so V_1 is the collection of 2π-band-limited functions. In

general, for each integer j, let V_j be the collection of functions $f(t)$ whose Fourier transform $F(\omega)$ is zero for $|\omega| > 2^j\pi$; so V_j is the collection of $2^j\pi$-band-limited functions.

Exercise 23.2 *Show that if the function $f(t)$ is in V_j then the function $g(t) = f(2t)$ is in V_{j+1}.*

We then have a nested sequence of sets of functions $\{V_j\}$, with $V_j \subseteq V_{j+1}$ for each integer j. The intersection of all the V_j is the set containing only the zero function. Every function in $L^2(R)$ is arbitrarily close to a function in at least one of the sets V_j; more mathematically, we say that the union of the V_j is dense in $L^2(R)$. In addition, we have $f(t)$ in V_j if and only if $g(t) = f(2t)$ is in V_{j+1}. In general, such a collection of sets of functions is called a *multiresolution analysis* for $L^2(R)$. Once we have a MRA for $L^2(R)$, how do we get a wavelet series expansion?

A function $\phi(t)$ is called a *scaling function* or sometimes the *father wavelet* for the MRA if the collection of integer translates $\{\phi(t-k)\}$ forms a basis for V_0 (more precisely, a Riesz basis). Then, for each fixed j, the functions $\phi_{jk}(t) = \phi(2^j t - k)$, for integer k, will form a basis for V_j. In the case of the Shannon MRA, the scaling function is $\phi(t) = \frac{\sin \pi t}{\pi t}$. But how do we get a basis for all of $L^2(R)$?

23.6.2   The Haar Multiresolution Analysis

To see how to proceed, it is helpful to return to the Haar wavelets. Let $\phi_{Haar}(t)$ be the function that has the value $+1$ for $0 \le t < 1$ and zero elsewhere. Let V_0 be the collection of all functions in $L^2(R)$ that are linear combinations of integer translates of $\phi(t)$; that is, all functions $f(t)$ that are constant on intervals of the form $[k, k+1)$, for all integers k. Now V_1 is the collection of all functions $g(t)$ of the form $g(t) = f(2t)$, for some $f(t)$ in V_0. Therefore, V_1 consists of all functions in $L^2(R)$ that are constant on intervals of the form $[k/2, (k+1)/2)$.

Every function in V_0 is also in V_1 and every function $g(t)$ in V_1 can be written uniquely as a sum of a function $f(t)$ in V_0 and a function $h(t)$ in V_1 that is orthogonal to every function in V_0. For example, the function $g(t)$ that takes the value $+3$ for $0 \le t < 1/2$, -1 for $1/2 \le t < 1$, and zero elsewhere can be written as $g(t) = f(t) + h(t)$, where $h(t)$ has the value $+2$ for $0 \le t < 1/2$, -2 for $1/2 \le t < 1$, and zero elsewhere, and $f(t)$ takes the value $+1$ for $0 \le t < 1$ and zero elsewhere. Clearly, $h(t)$, which is twice the Haar wavelet function, is orthogonal to all functions in V_0.

Exercise 23.3 *Show that the function $f(t)$ can be written uniquely as $f(t) = d(t) + e(t)$, where $d(t)$ in V_{-1} and $e(t)$ is in V_0 and is orthogonal to every function in V_{-1}. Relate the function $e(t)$ to the Haar wavelet function.*

23.6.3   Wavelets and Multiresolution Analysis

To get an orthogonal wavelet expansion from a general MRA, we write the set V_1 as the direct sum $V_1 = V_0 \oplus W_0$, so every function $g(t)$ in V_1 can be uniquely written as $g(t) = f(t) + h(t)$, where $f(t)$ is a function in V_0 and $h(t)$ is a function in W_0, with $f(t)$ and $h(t)$ orthogonal. Since the scaling function or father wavelet $\phi(t)$ is in V_1, it can be written as

$$\phi(t) = \sum_{k=-\infty}^{\infty} p_k \phi(2t - k), \tag{23.1}$$

for some sequence $\{p_k\}$ called the *two-scale sequence* for $\phi(t)$. This most important identity is the *scaling relation* for the father wavelet. The mother wavelet is defined using a similar expression

$$\psi(t) = \sum_{k} (-1)^k \overline{p_{1-k}} \phi(2t - k). \tag{23.2}$$

We define

$$\phi_{jk}(t) = 2^{j/2} \phi(2^j t - k) \tag{23.3}$$

and

$$\psi_{jk}(t) = 2^{j/2} \psi(2^j t - k). \tag{23.4}$$

The collection $\{\psi_{jk}(t), -\infty < j, k < \infty\}$ then forms an orthogonal wavelet basis for $L^2(R)$. For the Haar MRA, the two-scale sequence is $p_0 = p_1 = 1$ and $p_k = 0$ for the rest.

Exercise 23.4 *Show that the two-scale sequence $\{p_k\}$ has the properties*

$$p_k = 2 \int \phi(t) \overline{\phi(2t - k)} dt;$$

$$\sum_{k=-\infty}^{\infty} p_{k-2m} \overline{p_k} = 0,$$

for $m \neq 0$ and equals two when $m = 0$.

23.7   Signal Processing Using Wavelets

Once we have an orthogonal wavelet basis for $L^2(R)$, we can use the basis
to represent and process a signal $f(t)$. Suppose, for example, that $f(t)$ is
band-limited but essentially zero for t not in $[0,1]$ and we have samples
$f(\frac{k}{M})$, $k = 0, ..., M$. We assume that the sampling rate $\Delta = \frac{1}{M}$ is faster
than the Nyquist rate so that the Fourier transform of $f(t)$ is zero outside,
say, the interval $[0, 2\pi M]$. Roughly speaking, the W_j component of $f(t)$,
given by

$$g_j(t) = \sum_{k=0}^{2^j - 1} \beta_k^j \psi_{jk}(t),$$

with $\beta_k^j = \langle f(t), \psi_{jk}(t) \rangle$, corresponds to the components of $f(t)$ with fre-
quencies ω between 2^{j-1} and 2^j. For $2^j > 2\pi M$ we have $\beta_k^j = 0$, so
$g_j(t) = 0$. Let J be the smallest integer greater than $\log_2(2\pi) + \log_2(M)$.
Then, $f(t)$ is in the space V_J and has the expansion

$$f(t) = \sum_{k=0}^{2^J - 1} \alpha_k^J \phi_{Jk}(t),$$

for $\alpha_k^J = \langle f(t), \phi_{Jk}(t) \rangle$. It is common practice, but not universally ap-
proved, to take $M = 2^J$ and to estimate the α_k^J by the samples $f(\frac{k}{M})$.
Once we have the sequence $\{\alpha_k^J\}$, we can begin the decomposition of $f(t)$
into components in V_j and W_j for $j < J$. As we shall see, the algorithms
for the decomposition and subsequent reconstruction of the signal are quite
similar to the FFT.

23.7.1   Decomposition and Reconstruction

The decomposition and reconstruction algorithms both involve the equa-
tion

$$\sum_k a_k^j \phi_{jk} = \sum_m a_m^{j-1} \phi_{(j-1),m} + b_m^{j-1} \psi_{(j-1),m} ; \tag{23.5}$$

in the decomposition step we know the $\{a_k^j\}$ and want the $\{a_m^{j-1}\}$ and
$\{b_m^{j-1}\}$, while in the reconstruction step we know the $\{a_m^{j-1}\}$ and $\{b_m^{j-1}\}$
and want the $\{a_k^j\}$.

Using Equations (23.1) and (23.3), we obtain

$$\phi_{(j-1),l} = 2^{-1/2} \sum_k p_k \phi_{j,(k+2l)} = 2^{-1/2} \sum_k p_{k-2l} \phi_{jk}; \tag{23.6}$$

using Equations (23.2), (23.3) and (23.4), we get

$$\psi_{(j-1),l} = 2^{-1/2} \sum_k (-1)^k \overline{p_{1-k+2l}} \phi_{jk}. \tag{23.7}$$

Therefore,

$$\langle \phi_{jk}, \phi_{(j-1),l} \rangle = 2^{-1/2} \overline{p_{k-2l}}; \tag{23.8}$$

this comes from substituting $\phi_{(j-1),l}$ as in Equation (23.6) into the second term in the inner product. Similarly, we have

$$\langle \phi_{jk}, \psi_{(j-1),l} \rangle = 2^{-1/2} (-1)^k p_{1-k+2l}. \tag{23.9}$$

These relationships are then used to derive the decomposition and reconstruction algorithms.

The decomposition step:

To find a_l^{j-1} we take the inner product of both sides of Equation (23.5) with the function $\phi_{(j-1),l}$. Using Equation (23.8) and the fact that $\phi_{(j-1),l}$ is orthogonal to all the $\phi_{(j-1),m}$ except for $m = l$ and is orthogonal to all the $\psi_{(j-1),m}$, we obtain

$$2^{-1/2} \sum_k a_k^j \overline{p_{k-2l}} = a_l^{j-1};$$

similarly, using Equation (23.9), we get

$$2^{-1/2} \sum_k a_k^j (-1)^k p_{1-k+2l} = b_l^{j-1}.$$

The decomposition step is to apply these two equations to get the $\{a_l^{j-1}\}$ and $\{b_l^{j-1}\}$ from the $\{a_k^j\}$.

The reconstruction step:

Now we use Equations (23.6) and (23.7) to substitute into the right hand side of Equation (23.5). Combining terms, we get

$$a_k^j = 2^{-1/2} \sum_l a_l^{j-1} p_{k-2l} + b_l^{j-1} (-1)^k \overline{p_{1-k+2l}}.$$

This takes us from the $\{a_l^{j-1}\}$ and $\{b_l^{j-1}\}$ to the $\{a_k^j\}$.

We have assumed that we have already obtained the scaling function $\phi(t)$ with the property that $\{\phi(t-k)\}$ is an orthogonal basis for V_0. But how do we actually obtain such functions?

23.8   Generating the Scaling Function

The scaling function $\phi(t)$ is generated from the two-scale sequence $\{p_k\}$ using the following iterative procedure. Start with $\phi_0(t) = \phi_{Haar}(t)$, the Haar scaling function that is one on $[0, 1]$ and zero elsewhere. Now, for each $n = 1, 2, ...$, define

$$\phi_n(t) = \sum_{k=-\infty}^{\infty} p_k \phi_{n-1}(2t - k).$$

Provided that the sequence $\{p_k\}$ has certain properties to be discussed below, this sequence of functions converges and the limit is the desired scaling function.

The properties of $\{p_k\}$ that are needed can be expressed in terms of properties of the function

$$P(z) = \frac{1}{2} \sum_{k=-\infty}^{\infty} p_k z^k.$$

For the Haar MRA, this function is $P(z) = \frac{1}{2}(1 + z)$. We require that

- **1.** $P(1) = 1$,

- **2.** $|P(e^{i\theta})|^2 + |P(e^{i(\theta+\pi)})|^2 = 1$, for $0 \leq \theta \leq \pi$, and

- **3.** $|P(e^{i\theta})| > 0$ for $-\frac{\pi}{2} \leq \theta \leq \frac{\pi}{2}$.

23.9   Generating the Two-scale Sequence

The final piece of the puzzle is the generation of the sequence $\{p_k\}$ itself, or, equivalently, finding a function $P(z)$ with the properties listed above. The following example, also used in [18], illustrates Ingrid Daubechies' method [93].

We begin with the identity

$$\cos^2 \frac{\theta}{2} + \sin^2 \frac{\theta}{2} = 1$$

and then raise both sides to an odd power $n = 2N - 1$. Here we use $N = 2$, obtaining

$$1 = \cos^6 \frac{\theta}{2} + 3 \cos^4 \frac{\theta}{2} \sin^2 \frac{\theta}{2}$$

$$+ \cos^6 \frac{(\theta + \pi)}{2} + 3 \cos^4 \frac{(\theta + \pi)}{2} \sin^2 \frac{(\theta + \pi)}{2}.$$

We then let

$$|P(e^{i\theta})|^2 = \cos^6 \frac{\theta}{2} + 3\cos^4 \frac{\theta}{2} \sin^2 \frac{\theta}{2},$$

so that

$$|P(e^{i\theta})|^2 + |P(e^{i(\theta+\pi)})|^2 = 1$$

for $0 \le \theta \le \pi$. Now we have to find $P(e^{i\theta})$.
Writing

$$|P(e^{i\theta})|^2 = \cos^4 \frac{\theta}{2}[\cos^2 \frac{\theta}{2} + 3\sin^2 \frac{\theta}{2}],$$

we have

$$P(e^{i\theta}) = \cos^2 \frac{\theta}{2}[\cos \frac{\theta}{2} + \sqrt{3}i \sin \frac{\theta}{2}]e^{i\alpha(\theta)},$$

where the real function $\alpha(\theta)$ is arbitrary. Selecting $\alpha(\theta) = 3\frac{\theta}{2}$, we get

$$P(e^{i\theta}) = p_0 + p_1 e^{i\theta} + p_2 e^{2i\theta} + p_3 e^{3i\theta},$$

for

$$p_0 = \frac{1 + \sqrt{3}}{4},$$

$$p_1 = \frac{3 + \sqrt{3}}{4},$$

$$p_2 = \frac{3 - \sqrt{3}}{4},$$

$$p_3 = \frac{1 - \sqrt{3}}{4},$$

and all the other coefficients are zero. The resulting Daubechies' wavelet is compactly supported and continuous, but not differentiable [18, 93]. Figure 23.1 shows the scaling function and mother wavelet for $N = 2$. When larger values of N are used, the resulting wavelet, often denoted $\psi_N(t)$, which is again compactly supported, has approximately $N/5$ continuous derivatives.

These notions extend to nonorthogonal wavelet bases and to frames. Algorithms similar to the fast Fourier transform provide the wavelet decomposition and reconstruction of signals. The recent text by Boggess and Narcowich [18] is a nice introduction to this fast-growing area; the more advanced book by Chui [78] is also a good source. Wavelets in the context of Riesz bases and frames are discussed in Christensen's book [77]. Applications of wavelets to medical imaging are found in [187], as well as in the other papers in that special issue.

23.10   Wavelets and Filter Banks

In [212] Strang and Nguyen take a somewhat different approach to wavelets, emphasizing the role of filters and matrices. To illustrate one of their main points, we consider the two-point moving average filter.

The two-point moving average filter transforms an input sequence $x = \{x(n)\}$ to output $y = \{y(n)\}$, with $y(n) = \frac{1}{2}x(n) + \frac{1}{2}x(n-1)$. The filter $h = \{h(k)\}$ has $h(0) = h(1) = \frac{1}{2}$ and all the remaining $h(n)$ are zero. This filter is a *finite impulse response* (FIR) low-pass filter and is not invertible; the input sequence with $x(n) = (-1)^n$ has output zero. Similarly, the two-point moving difference filter $g = \{g(k)\}$, with $g(0) = \frac{1}{2}$, $g(1) = -\frac{1}{2}$, and the rest zero, is a FIR high-pass filter, also not invertible. However, if we perform these filters in parallel, as a filter bank, no information is lost and the input can be completely reconstructed, with a unit delay. In addition, the outputs of the two filters contain redundancy that can be removed by *decimation*, which is taken here to mean *downsampling*, that is, throwing away every other term of a sequence.

The authors treat the more general problem of obtaining perfect reconstruction of the input from the output of a filter bank of low- and high-pass filters followed by downsampling. The properties that must be required of the filters are those we encountered earlier with regard to the two-scale sequences for the father and mother wavelets. When the filter operations are construed as matrix multiplications, the decomposition and reconstruction algorithms become matrix factorizations.

23.11   Using Wavelets

We consider the Daubechies mother wavelet $\psi_N(t)$, for $N = 1, 2, ...,$ and $n = 2N - 1$. The two-scale sequence $\{p_k\}$ then has nonzero terms $p_0, ..., p_n$. For example, when $N = 1$, we get the Haar wavelet, with $p_0 = p_1 = 1/2$, and all the other $p_k = 0$.

The wavelet signal analysis usually begins by sampling the signal $f(t)$ closely enough so that we can approximate the a_k^{j+1} by the samples $f(k/2^{j+1})$.

An important aspect of the Daubechies wavelets is the vanishing of moments. For $k = 0, 1, ..., N - 1$ we have

$$\int t^k \psi_N(t)dt = 0;$$

for the Haar case we have only that $\int \psi_1(t)dt = 0$. We consider now the significance of vanishing moments for detection.

For an arbitrary signal $f(t)$ the wavelet coefficients b_k^j are given by

$$b_k^j = \int f(t)2^{j/2}\psi_N(2^j t - k)dt.$$

We focus on $N = 2$

The function $\psi_2(2^j t - k)$ is supported on the interval $[k/2^j, (k+3)/2^j]$ so we have

$$b_k^j = \int_0^{3/2^j} f(t + k/2^j)\psi_2(2^j t)dt.$$

If $f(t)$ is smooth near $t = k/2^j$, and j is large enough, then

$$f(t + k/2^j) = f(k/2^j) + f'(k/2^j)t + \frac{1}{2!}f''(k/2^j)t^2 + \cdots,$$

and so

$$b_k^j \simeq 2^{j/2}[f(k/2^j)\int_0^{3/2^j} \psi_2(2^j t)dt$$

$$+f'(k/2^j)\int_0^{3/2^j} t\psi_2(2^j t)dt + f''(k/2^j)\int_0^{3/2^j} t^2\psi_2(2^j t)dt].$$

Since

$$\int \psi_2(t)dt = \int t\psi_2(t)dt = 0$$

and

$$\int t^2\psi_2(t)dt \simeq -\frac{1}{8}\sqrt{\frac{3}{2\pi}},$$

we have

$$b_k^j \simeq -\frac{1}{16}\sqrt{\frac{3}{2\pi}}2^{-5j/2}f''(k/2^j).$$

On the other hand, if $f(t)$ is not smooth near $t = k/2^j$, we expect the b_k^j to have a larger magnitude.

Example 1 Suppose that $f(t)$ is piecewise linear. Then $f''(t) = 0$, except at the places where the lines meet. So we expect the b_k^j to be zero, except at the nodes.

Example 2 Let $f(t) = t(1-t)$, for $t \in [0, 1]$, and zero elsewhere. We might begin with the sample values $f(k/2^7)$ and then consider b_k^6. Again using $N = 2$, we find that $b_k^6 \simeq f''(k/2^6) = 2$, independent of k, except near the endpoints $t = 0$ and $t = 1$. The discontinuity of $f'(t)$ at the ends will make the b_k^6 there larger.

Example 3 Now let $g(t) = t^2(1 - t)^2$, for $t \in [0, 1]$, and zero elsewhere. The first derivative is continuous at the endpoints $t = 0$ and $t = 1$, but the second derivative is discontinuous there. Using $N = 2$, we won't be able to detect this discontinuity, but using $N = 3$ we will.

Example 4 Suppose that $f(t) = e^{i\omega t}$. Then we have

$$b_k^j = 2^{-j/2} e^{i\omega k/2^j} \Psi_N(\omega/2^j),$$

independent of k, where Ψ_N denotes the Fourier transform of ψ_N . If we plot these values for various j, the maximum is reached when

$$\omega/2^j = \operatorname{argmax} \Psi_N,$$

from which we can find ω.
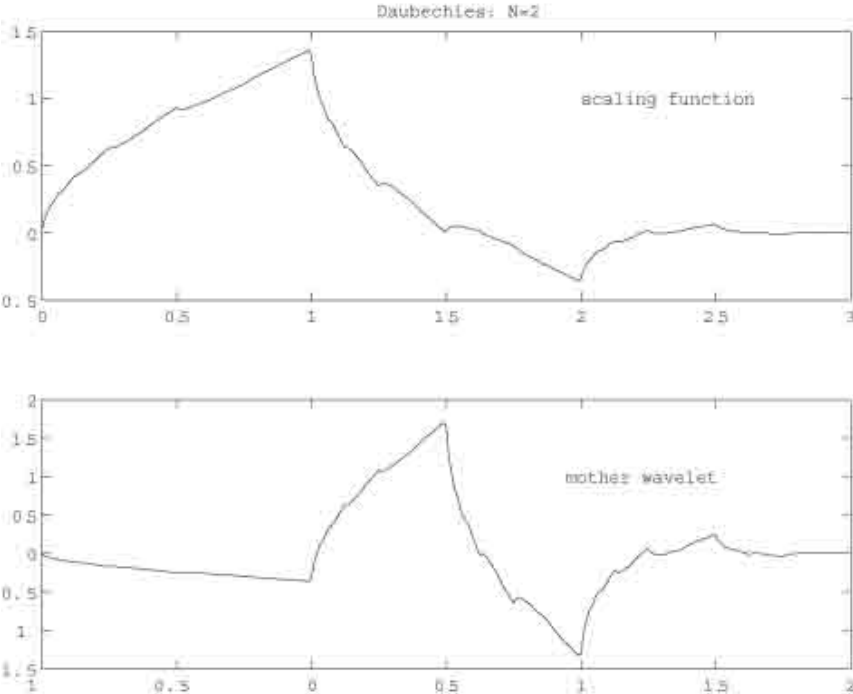
Figure 23.1: Daubechies' scaling function and mother wavelet for $N = 2$.

Part VII

Estimation and Detection

Chapter 24

The BLUE and The Kalman Filter

24.1 Chapter Summary

In most signal- and image-processing applications the measured data includes (or may include) a signal component we want and unwanted components called *noise*. Estimation involves determining the precise nature and strength of the signal component; deciding if that strength is zero or not is detection.

Noise often appears as an additive term, which we then try to remove. If we knew precisely the noisy part added to each data value we would simply subtract it; of course, we never have such information. How then do we remove something when we don't know what it is? Statistics provides a way out.

The basic idea in statistics is to use procedures that perform well on average, when applied to a class of problems. The procedures are built using properties of that class, usually involving probabilistic notions, and are evaluated by examining how they would have performed had they been applied to every problem in the class. To use such methods to remove additive noise, we need a description of the class of noises we expect to encounter, not specific values of the noise component in any one particular instance. We also need some idea about what signal components look like. In this chapter we discuss solving this noise removal problem using the *best linear unbiased estimation* (BLUE). We begin with the simplest case and then proceed to discuss increasingly complex scenarios.

An important application of the BLUE is in Kalman filtering. The connection between the BLUE and Kalman filtering is best understood by considering the case of the BLUE with a prior estimate of the signal com-

ponent, and mastering the various matrix manipulations that are involved in this problem. These calculations then carry over, almost unchanged, to the Kalman filtering.

Kalman filtering is usually presented in the context of estimating a sequence of vectors evolving in time. Kalman filtering for image processing is derived by analogy with the temporal case, with certain parts of the image considered to be in the "past" of a fixed pixel.

24.2   The Simplest Case

Suppose our data is $z_j = c + v_j$, for $j = 1, ..., J$, where c is an unknown constant to be estimated and the v_j are additive noise. We assume that $E(v_j) = 0, E(v_j \overline{v_k}) = 0$ for $j \neq k$, and $E(|v_j|^2) = \sigma_j^2$. So, the additive noises are assumed to have mean zero and to be independent (or at least uncorrelated). In order to estimate c, we adopt the following rules:

- **1.** The estimate $\hat{c}$ is *linear* in the data $\mathbf{z} = (z_1, ..., z_J)^T$; that is, $\hat{c} = \mathbf{k}^\dagger \mathbf{z}$, for some vector $\mathbf{k} = (k_1, ..., k_J)^T$.

- **2.** The estimate is *unbiased*; $E(\hat{c}) = c$. This means $\sum_{j=1}^{J} k_j = 1$.

- **3.** The estimate is best in the sense that it minimizes the expected error squared; that is, $E(|\hat{c} - c|^2)$ is minimized.

Exercise 24.1 *Show that the resulting vector* $\mathbf{k}$ *is*

$$k_i = \sigma_i^{-2} / (\sum_{j=1}^{J} \sigma_j^{-2}),$$

and the BLUE estimator of c *is then*

$$\hat{c} = \sum_{i=1}^{J} z_i \sigma_i^{-2} / (\sum_{j=1}^{J} \sigma_j^{-2}).$$

Exercise 24.2 *Suppose we have data* $z_1 = c + v_1$ *and* $z_2 = c + v_2$ *and we want to estimate the constant* c. *Assume that* $E(v_1) = E(v_2) = 0$ *and* $E(v_1 v_2) = \rho$, *with* $0 < |\rho| < 1$. *Find the BLUE estimate of* c.

Exercise 24.3 *The concentration of a substance in solution decreases exponentially during an experiment. Noisy measurements of the concentration are made at times* t_1 *and* t_2, *giving the data*

$$z_i = x_0 e^{-t_i} + v_i, \ i = 1, 2,$$

where the v_i *have mean zero, and are uncorrelated. Find the BLUE for the initial concentration* x_0.

24.3 A More General Case

Suppose now that our data vector is $\mathbf{z} = H\mathbf{x} + \mathbf{v}$. Here, $\mathbf{x}$ is an unknown vector whose value is to be estimated, the random vector $\mathbf{v}$ is additive noise whose mean is $E(\mathbf{v}) = 0$ and whose known covariance matrix is $Q = E(\mathbf{v}\mathbf{v}^\dagger)$, not necessarily diagonal, and the known matrix H is J by N, with $J > N$. Now we seek an estimate of the vector $\mathbf{x}$. We now use the following rules:

- **1.** The estimate $\hat{\mathbf{x}}$ must have the form $\hat{\mathbf{x}} = K^\dagger \mathbf{z}$, where the matrix K is to be determined.

- **2.** The estimate is unbiased; that is, $E(\hat{\mathbf{x}}) = \mathbf{x}$.

- **3.** The K is determined as the minimizer of the expected squared error; that is, once again we minimize $E(|\hat{\mathbf{x}} - \mathbf{x}|^2)$.

Exercise 24.4 *Show that for the estimator to be unbiased we need* $K^\dagger H = I$, *the identity matrix.*

Exercise 24.5 *Show that*

$$E(|\hat{\mathbf{x}} - \mathbf{x}|^2) = \operatorname{trace} K^\dagger Q K.$$

Hints: Write the left side as

$$E(\operatorname{trace}((\hat{\mathbf{x}} - \mathbf{x})(\hat{\mathbf{x}} - \mathbf{x})^\dagger)).$$

Also use the fact that the trace and expected-value operations commute.

The problem then is to minimize trace $K^\dagger Q K$ subject to the constraint equation $K^\dagger H = I$. We solve this problem using a technique known as *prewhitening*.

Since the noise covariance matrix Q is Hermitian and nonnegative definite, we have $Q = U D U^\dagger$, where the columns of U are the (mutually orthogonal) eigenvectors of Q and D is a diagonal matrix whose diagonal entries are the (necessarily nonnegative) eigenvalues of Q; therefore, $U^\dagger U = I$. We call $C = U D^{1/2} U^\dagger$ the Hermitian square root of Q, since $C^\dagger = C$ and $C^2 = Q$. We assume that Q is invertible, so that C is also. Given the system of equations

$$\mathbf{z} = H\mathbf{x} + \mathbf{v},$$

as before, we obtain a new system

$$\mathbf{y} = G\mathbf{x} + \mathbf{w}$$

by multiplying both sides by $C^{-1} = Q^{-1/2}$; here, $G = C^{-1}H$ and $\mathbf{w} = C^{-1}\mathbf{v}$. The new noise correlation matrix is

$$E(\mathbf{w}\mathbf{w}^\dagger) = C^{-1}QC^{-1} = I,$$

so the new noise is white. For this reason the step of multiplying by C^{-1} is called *prewhitening*.

With $J = CK$ and $M = C^{-1}H$, we have

$$K^\dagger QK = J^\dagger J$$

and

$$K^\dagger H = J^\dagger M.$$

Our problem then is to minimize trace $J^\dagger J$, subject to $J^\dagger M = I$. Recall that the trace of the matrix $A^\dagger A$ is simply the square of the 2-norm of the vectorization of A.

Our solution method is to transform the original problem into a simpler problem, where the answer is obvious.

First, for any given matrices L and M such that J and ML have the same dimensions, the minimum value of

$$f(J) = \text{trace}[(J^\dagger - L^\dagger M^\dagger)(J - ML)]$$

is zero and occurs when $J = ML$.

Now let $L = L^\dagger = (M^\dagger M)^{-1}$. The solution is again $J = ML$, but now this choice for J has the additional property that $J^\dagger M = I$. So, minimizing $f(J)$ is equivalent to minimizing $f(J)$ subject to the constraint $J^\dagger M = I$ and both problems have the solution $J = ML$.

Now using $J^\dagger M = I$, we expand $f(J)$ to get

$$f(J) = \text{trace}[J^\dagger J - J^\dagger ML - L^\dagger M^\dagger J + L^\dagger M^\dagger ML]$$

$$= \text{trace}[J^\dagger J - L - L^\dagger + L^\dagger M^\dagger ML].$$

The only term here that involves the unknown matrix J is the first one. Therefore, minimizing $f(J)$ subject to $J^\dagger M = I$ is equivalent to minimizing trace $J^\dagger J$ subject to $J^\dagger M = I$, which is our original problem. Therefore, the optimal choice for J is $J = ML$. Consequently, the optimal choice for K is

$$K = Q^{-1}HL = Q^{-1}H(H^\dagger Q^{-1}H)^{-1},$$

and the BLUE estimate of $\mathbf{x}$ is

$$\mathbf{x}_{BLUE} = \hat{\mathbf{x}} = K^\dagger \mathbf{z} = (H^\dagger Q^{-1}H)^{-1}H^\dagger Q^{-1}\mathbf{z}.$$

The simplest case can be obtained from this more general formula by taking $N = 1$, $H = (1, 1, ..., 1)^T$ and $\mathbf{x} = c$.

Note that if the noise is *white*, that is, $Q = \sigma^2 I$, then $\hat{\mathbf{x}} = (H^\dagger H)^{-1} H^\dagger \mathbf{z}$, which is the least-squares solution of the equation $\mathbf{z} = H\mathbf{x}$. The effect of requiring that the estimate be unbiased is that, in this case, we simply ignore the presence of the noise and calculate the least squares solution of the noise-free equation $\mathbf{z} = H\mathbf{x}$.

The BLUE estimator involves nested inversion, making it difficult to calculate, especially for large matrices. In the exercise that follows, we discover an approximation of the BLUE that is easier to calculate.

Exercise 24.6 *Show that for $\epsilon > 0$ we have*

$$(H^\dagger Q^{-1} H + \epsilon I)^{-1} H^\dagger Q^{-1} = H^\dagger (HH^\dagger + \epsilon Q)^{-1}. \tag{24.1}$$

Hint: Use the identity

$$H^\dagger Q^{-1}(HH^\dagger + \epsilon Q) = (H^\dagger Q^{-1} H + \epsilon I)H^\dagger.$$

It follows from Equation (24.1) that

$$\mathbf{x}_{BLUE} = \lim_{\epsilon \to 0} H^\dagger (HH^\dagger + \epsilon Q)^{-1} \mathbf{z}. \tag{24.2}$$

Therefore, we can get an approximation of the BLUE estimate by selecting $\epsilon > 0$ near zero, solving the system of linear equations

$$(HH^\dagger + \epsilon Q)\mathbf{a} = \mathbf{z}$$

for $\mathbf{a}$ and taking $\mathbf{x} = H^\dagger \mathbf{a}$.

24.4 Some Useful Matrix Identities

In the exercise that follows we consider several matrix identities that are useful in developing the Kalman filter.

Exercise 24.7 *Establish the following identities, assuming that all the products and inverses involved are defined:*

$$CDA^{-1}B(C^{-1} - DA^{-1}B)^{-1} = (C^{-1} - DA^{-1}B)^{-1} - C; \tag{24.3}$$

$$(A - BCD)^{-1} = A^{-1} + A^{-1}B(C^{-1} - DA^{-1}B)^{-1}DA^{-1}; \tag{24.4}$$

$$A^{-1}B(C^{-1} - DA^{-1}B)^{-1} = (A - BCD)^{-1}BC; \qquad (24.5)$$

$$(A - BCD)^{-1} = (I + GD)A^{-1}, \qquad (24.6)$$

for

$$G = A^{-1}B(C^{-1} - DA^{-1}B)^{-1}.$$

Hints: To get Equation (24.3) use

$$C(C^{-1} - DA^{-1}B) = I - CDA^{-1}B.$$

For the second identity, multiply both sides of Equation (24.4) on the left by $A - BCD$ and at the appropriate step use Equation (24.3). For Equation (24.5) show that

$$BC(C^{-1} - DA^{-1}B) = B - BCDA^{-1}B = (A - BCD)A^{-1}B.$$

For Equation (24.6), substitute what G is and use Equation (24.4).

24.5   The BLUE with a Prior Estimate

In Kalman filtering we have the situation in which we want to estimate an unknown vector $\mathbf{x}$ given measurements $\mathbf{z} = H\mathbf{x} + \mathbf{v}$, but also given a prior estimate $\mathbf{y}$ of $\mathbf{x}$. It is the case there that $E(\mathbf{y}) = E(\mathbf{x})$, so we write $\mathbf{y} = \mathbf{x} + \mathbf{w}$, with $\mathbf{w}$ independent of both $\mathbf{x}$ and $\mathbf{v}$ and $E(\mathbf{w}) = \mathbf{0}$. The covariance matrix for $\mathbf{w}$ we denote by $E(\mathbf{w}\mathbf{w}^\dagger) = R$. We now require that the estimate $\hat{\mathbf{x}}$ be linear in both $\mathbf{z}$ and $\mathbf{y}$; that is, the estimate has the form

$$\hat{\mathbf{x}} = C^\dagger \mathbf{z} + D^\dagger \mathbf{y},$$

for matrices C and D to be determined.

The approach is to apply the BLUE to the combined system of linear equations

$$\mathbf{z} = H\mathbf{x} + \mathbf{v} \quad \text{and}$$

$$\mathbf{y} = \mathbf{x} + \mathbf{w}.$$

In matrix language this combined system becomes $\mathbf{u} = J\mathbf{x} + \mathbf{n}$, with $\mathbf{u}^T = [\mathbf{z}^T \ \mathbf{y}^T]$, $J^T = [H^T \ I^T]$, and $\mathbf{n}^T = [\mathbf{v}^T \ \mathbf{w}^T]$. The noise covariance matrix becomes

$$P = \begin{bmatrix} Q & 0 \\ 0 & R \end{bmatrix}.$$

The BLUE estimate is $K^\dagger \mathbf{u}$, with $K^\dagger J = I$. Minimizing the variance, we find that the optimal $K^\dagger$ is

$$K^\dagger = (J^\dagger P^{-1} J)^{-1} J^\dagger P^{-1}.$$

The optimal estimate is then

$$\hat{\mathbf{x}} = (H^\dagger Q^{-1} H + R^{-1})^{-1} (H^\dagger Q^{-1} \mathbf{z} + R^{-1} \mathbf{y}).$$

Therefore,

$$C^\dagger = (H^\dagger Q^{-1} H + R^{-1})^{-1} H^\dagger Q^{-1}$$

and

$$D^\dagger = (H^\dagger Q^{-1} H + R^{-1})^{-1} R^{-1}.$$

Using the matrix identities in Equations (24.4) and (24.5) we can rewrite this estimate in the more useful form

$$\hat{\mathbf{x}} = \mathbf{y} + G(\mathbf{z} - H\mathbf{y}),$$

for

$$G = RH^\dagger (Q + HRH^\dagger)^{-1}. \tag{24.7}$$

The covariance matrix of the optimal estimator is $K^\dagger PK$, which can be written as

$$K^\dagger PK = (R^{-1} + H^\dagger Q^{-1} H)^{-1} = (I - GH)R.$$

In the context of the Kalman filter, R is the covariance of the prior estimate of the current state, G is the Kalman gain matrix, and $K^\dagger PK$ is the posterior covariance of the current state. The algorithm proceeds recursively from one state to the next in time.

24.6 Adaptive BLUE

We have assumed so far that we know the covariance matrix Q corresponding to the measurement noise. If we do not, then we may attempt to estimate Q from the measurements themselves; such methods are called *noise-adaptive*. To illustrate, let the *innovations* vector be $\mathbf{e} = \mathbf{z} - H\mathbf{y}$. Then the covariance matrix of $\mathbf{e}$ is $S = HRH^\dagger + Q$. Having obtained an estimate $\hat{S}$ of S from the data, we use $\hat{S} - HRH^\dagger$ in place of Q in Equation (24.7).

24.7 The Kalman Filter

So far in this chapter we have focused on the filtering problem: given the data vector $\mathbf{z}$, estimate $\mathbf{x}$, assuming that $\mathbf{z}$ consists of noisy measurements of $H\mathbf{x}$; that is, $\mathbf{z} = H\mathbf{x} + \mathbf{v}$. An important extension of this problem is that of stochastic prediction. Shortly, we discuss the Kalman-filter method

for solving this more general problem. One area in which prediction plays
an important role is the tracking of moving targets, such as ballistic mis-
siles, using radar. The range to the target, its angle of elevation, and its
azimuthal angle are all functions of time governed by linear differential
equations. The *state vector* of the system at time t might then be a vec-
tor with nine components, the three functions just mentioned, along with
their first and second derivatives. In theory, if we knew the initial state
perfectly and our differential equations model of the physics was perfect,
that would be enough to determine the future states. In practice neither
of these is true, and we need to assist the differential equation by taking
radar measurements of the state at various times. The problem then is to
estimate the state at time t using both the measurements taken prior to
time t and the estimate based on the physics.

When such tracking is performed digitally, the functions of time are
replaced by discrete sequences. Let the state vector at time $k\Delta t$ be de-
noted by $\mathbf{x}_k$, for k an integer and $\Delta t > 0$. Then, with the derivatives in
the differential equation approximated by divided differences, the physical
model for the evolution of the system in time becomes

$$\mathbf{x}_k = A_{k-1}\mathbf{x}_{k-1} + \mathbf{m}_{k-1}.$$

The matrix A_{k-1}, which we assume is known, is obtained from the differen-
tial equation, which may have nonconstant coefficients, as well as from the
divided difference approximations to the derivatives. The random vector
sequence $\mathbf{m}_{k-1}$ represents the error in the physical model due to the dis-
cretization and necessary simplification inherent in the original differential
equation itself. We assume that the expected value of $\mathbf{m_k}$ is zero for each
k. The covariance matrix is $E(\mathbf{m}_k\mathbf{m}_k^\dagger) = M_k$.

At time $k\Delta t$ we have the measurements

$$\mathbf{z}_k = H_k\mathbf{x}_k + \mathbf{v}_k,$$

where H_k is a known matrix describing the nature of the linear measure-
ments of the state vector and the random vector $\mathbf{v}_k$ is the noise in these
measurements. We assume that the mean value of $\mathbf{v}_k$ is zero for each k.
The covariance matrix is $E(\mathbf{v}_k\mathbf{v}_k^\dagger) = Q_k$. We assume that the initial state
vector $\mathbf{x}_0$ is arbitrary.

Given an unbiased estimate $\hat{\mathbf{x}}_{k-1}$ of the state vector $\mathbf{x}_{k-1}$, our prior
estimate of $\mathbf{x}_k$ based solely on the physics is

$$\mathbf{y}_k = A_{k-1}\hat{\mathbf{x}}_{k-1}.$$

Exercise 24.8 *Show that $E(\mathbf{y}_k - \mathbf{x}_k) = 0$, so the prior estimate of $\mathbf{x}_k$ is
unbiased. We can then write $\mathbf{y}_k = \mathbf{x}_k + \mathbf{w}_k$, with $E(\mathbf{w}_k) = \mathbf{0}$.*

24.8 Kalman Filtering and the BLUE

The *Kalman filter* [147, 117, 79] is a recursive algorithm to estimate the state vector $\mathbf{x}_k$ at time $k\Delta t$ as a linear combination of the vectors $\mathbf{z}_k$ and $\mathbf{y}_k$. The estimate $\hat{\mathbf{x}}_k$ will have the form

$$\hat{\mathbf{x}}_k = C_k^\dagger \mathbf{z}_k + D_k^\dagger \mathbf{y}_k, \tag{24.8}$$

for matrices C_k and D_k to be determined. As we shall see, this estimate can also be written as

$$\hat{\mathbf{x}}_k = \mathbf{y}_k + G_k(\mathbf{z}_k - H_k\mathbf{y}_k), \tag{24.9}$$

which shows that the estimate involves a prior prediction step, the $\mathbf{y}_k$, followed by a correction step, in which $H_k\mathbf{y}_k$ is compared to the measured data vector $\mathbf{z}_k$; such estimation methods are sometimes called *predictor-corrector methods*.

In our discussion of the BLUE, we saw how to incorporate a prior estimate of the vector to be estimated. The trick was to form a larger matrix equation and then to apply the BLUE to that system. The Kalman filter does just that.

The correction step in the Kalman filter uses the BLUE to solve the combined linear system

$$\mathbf{z}_k = H_k\mathbf{x}_k + \mathbf{v}_k$$

and

$$\mathbf{y}_k = \mathbf{x}_k + \mathbf{w}_k.$$

The covariance matrix of $\hat{\mathbf{x}}_{k-1} - \mathbf{x}_{k-1}$ is denoted by P_{k-1}, and we let $Q_k = E(\mathbf{w}_k\mathbf{w}_k^\dagger)$. The covariance matrix of $\mathbf{y}_k - \mathbf{x}_k$ is

$$\text{cov}(\mathbf{y}_k - \mathbf{x}_k) = R_k = M_{k-1} + A_{k-1}P_{k-1}A_{k-1}^\dagger.$$

It follows from our earlier discussion of the BLUE that the estimate of $\mathbf{x}_k$ is

$$\hat{\mathbf{x}}_k = \mathbf{y}_k + G_k(\mathbf{z}_k - H\mathbf{y}_k),$$

with

$$G_k = R_k H_k^\dagger (Q_k + H_k R_k H_k^\dagger)^{-1}.$$

Then, the covariance matrix of $\hat{\mathbf{x}}_k - \mathbf{x}_k$ is

$$P_k = (I - G_k H_k)R_k.$$

The recursive procedure is to go from P_{k-1} and M_{k-1} to R_k, then to G_k, from which $\hat{\mathbf{x}}_k$ is formed, and finally to P_k, which, along with the known matrix M_k, provides the input to the next step. The time-consuming part of this recursive algorithm is the matrix inversion in the calculation of G_k.

Simpler versions of the algorithm are based on the assumption that the matrices Q_k are diagonal, or on the convergence of the matrices G_k to a limiting matrix G [79].

There are many variants of the Kalman filter, corresponding to variations in the physical model, as well as in the statistical assumptions. The differential equation may be nonlinear, so that the matrices A_k depend on $\mathbf{x}_k$. The system noise sequence $\{\mathbf{w}_k\}$ and the measurement noise sequence $\{\mathbf{v}_k\}$ may be correlated. For computational convenience the various functions that describe the state may be treated separately. The model may include known external inputs to drive the differential system, as in the tracking of spacecraft capable of firing booster rockets. Finally, the noise covariance matrices may not be known *a priori* and adaptive filtering may be needed. We discuss this last issue briefly in the next section.

24.9   Adaptive Kalman Filtering

As in [79] we consider only the case in which the covariance matrix Q_k of the measurement noise $\mathbf{v}_k$ is unknown. As we saw in the discussion of adaptive BLUE, the covariance matrix of the innovations vector $\mathbf{e}_k = \mathbf{z}_k - H_k\mathbf{y}_k$ is

$$S_k = H_k R_k H_k^\dagger + Q_k.$$

Once we have an estimate for S_k, we estimate Q_k using

$$\hat{Q}_k = \hat{S}_k - H_k R_k H_k^\dagger.$$

We might assume that S_k is independent of k and estimate $S_k = S$ using past and present innovations; for example, we could use

$$\hat{S} = \frac{1}{k-1} \sum_{j=1}^{k} (\mathbf{z}_j - H_j\mathbf{y}_j)(\mathbf{z}_j - H_j\mathbf{y}_j)^\dagger.$$

Chapter 25

Signal Detection and Estimation

25.1 Chapter Summary

In this chapter we consider the problem of deciding whether or not a particular signal is present in the measured data; this is the *detection* problem. The underlying framework for the detection problem is optimal estimation and statistical hypothesis testing [117].

25.2 The Model of Signal in Additive Noise

The basic model used in detection is that of a signal in additive noise. The complex data vector is $\mathbf{x} = (x_1, x_2, ..., x_N)^T$. We assume that there are two possibilities:

Case 1: Noise only

$$x_n = z_n, \ n = 1, ..., N,$$

or

Case 2: Signal in noise

$$x_n = \gamma s_n + z_n,$$

where $\mathbf{z} = (z_1, z_2, ..., z_N)^T$ is a complex vector whose entries z_n are values of random variables that we call *noise*, about which we have only statistical information (that is to say, information about the average behavior), $\mathbf{s} = (s_1, s_2, ..., s_N)^T$ is a complex signal vector that we may known exactly, or at least for which we have a specific parametric model, and γ is a scalar that

271

may be viewed either as deterministic or random (but unknown, in either case). Unless otherwise stated, we shall assume that γ is deterministic.

The *detection problem* is to decide which case we are in, based on some calculation performed on the data $\mathbf{x}$. Since Case 1 can be viewed as a special case of Case 2 in which the value of γ is zero, the detection problem is closely related to the problem of estimating γ, which we discussed in the chapter dealing with the best linear unbiased estimator, the BLUE.

We shall assume throughout that the entries of $\mathbf{z}$ correspond to random variables with means equal to zero. What the variances are and whether or not these random variables are mutually correlated will be discussed next. In all cases we shall assume that this information has been determined previously and is available to us in the form of the covariance matrix $Q = E(\mathbf{z}\mathbf{z}^\dagger)$ of the vector $\mathbf{z}$; the symbol E denotes expected value, so the entries of Q are the quantities $Q_{mn} = E(z_m \bar{z}_n)$. The diagonal entries of Q are $Q_{nn} = \sigma_n^2$, the variance of z_n.

Note that we have adopted the common practice of using the same symbols, z_n, when speaking about the random variables and about the specific values of these random variables that are present in our data. The context should make it clear to which we are referring.

In Case 2 we say that the *signal power* is equal to $|\gamma|^2 \frac{1}{N} \sum_{n=1}^N |s_n|^2 = \frac{1}{N}|\gamma|^2 \mathbf{s}^\dagger \mathbf{s}$ and the *noise power* is $\frac{1}{N} \sum_{n=1}^N \sigma_n^2 = \frac{1}{N} tr(Q)$, where $tr(Q)$ is the trace of the matrix Q, that is, the sum of its diagonal terms; therefore, the noise power is the average of the variances σ_n^2. The *input signal-to-noise ratio* (SNR_{in}) is the ratio of the signal power to that of the noise, prior to processing the data; that is,

$$\text{SNR}_{in} = \frac{1}{N}|\gamma|^2 \mathbf{s}^\dagger \mathbf{s} / \frac{1}{N} tr(Q) = |\gamma|^2 \mathbf{s}^\dagger \mathbf{s} / tr(Q).$$

25.3 Optimal Linear Filtering for Detection

In each case to be considered next, our detector will take the form of a linear estimate of γ; that is, we shall compute the estimate $\hat{\gamma}$ given by

$$\hat{\gamma} = \sum_{n=1}^N \bar{b}_n x_n = \mathbf{b}^\dagger \mathbf{x},$$

where $\mathbf{b} = (b_1, b_2, ..., b_N)^T$ is a vector to be determined. The objective is to use what we know about the situation to select the optimal $\mathbf{b}$, which will depend on $\mathbf{s}$ and Q.

For any given vector $\mathbf{b}$, the quantity

$$\hat{\gamma} = \mathbf{b}^\dagger \mathbf{x} = \gamma \mathbf{b}^\dagger \mathbf{s} + \mathbf{b}^\dagger \mathbf{z}$$

is a random variable whose mean value is equal to $\gamma \mathbf{b}^\dagger \mathbf{s}$ and whose variance is

$$var(\hat{\gamma}) = E(|\mathbf{b}^\dagger \mathbf{z}|^2) = E(\mathbf{b}^\dagger \mathbf{z} \mathbf{z}^\dagger \mathbf{b}) = \mathbf{b}^\dagger E(\mathbf{z} \mathbf{z}^\dagger) \mathbf{b} = \mathbf{b}^\dagger Q \mathbf{b}.$$

Therefore, the *output signal-to-noise ratio* (SNR_{out}) is defined as

$$\mathrm{SNR}_{\mathrm{out}} = |\gamma \mathbf{b}^\dagger \mathbf{s}|^2 / \mathbf{b}^\dagger Q \mathbf{b}.$$

The advantage we obtain from processing the data is called the *gain* associated with $\mathbf{b}$ and is defined to be the ratio of the SNR_{out} to SNR_{in}; that is,

$$\mathrm{gain}(\mathbf{b}) = \frac{|\gamma \mathbf{b}^\dagger \mathbf{s}|^2 / (\mathbf{b}^\dagger Q \mathbf{b})}{|\gamma|^2 (\mathbf{s}^\dagger \mathbf{s}) / tr(Q)} = \frac{|\mathbf{b}^\dagger \mathbf{s}|^2 \, tr(Q)}{(\mathbf{b}^\dagger Q \mathbf{b})(\mathbf{s}^\dagger \mathbf{s})}.$$

The best $\mathbf{b}$ to use will be the one for which $\mathrm{gain}(\mathbf{b})$ is the largest. So, ignoring the terms in the gain formula that do not involve $\mathbf{b}$, we see that the problem becomes *maximize* $\frac{|\mathbf{b}^\dagger \mathbf{s}|^2}{\mathbf{b}^\dagger Q \mathbf{b}}$, *for fixed signal vector* $\mathbf{s}$ *and fixed noise covariance matrix* Q.

The Cauchy inequality plays a major role in optimal filtering and detection:

Cauchy's inequality: For any vectors $\mathbf{a}$ and $\mathbf{b}$ we have

$$|\mathbf{a}^\dagger \mathbf{b}|^2 \leq (\mathbf{a}^\dagger \mathbf{a})(\mathbf{b}^\dagger \mathbf{b}),$$

with equality if and only if $\mathbf{a}$ is proportional to $\mathbf{b}$; that is, there is a scalar β such that $\mathbf{b} = \beta \mathbf{a}$.

Exercise 25.1 *Use Cauchy's inequality to show that, for any fixed vector* $\mathbf{a}$, *the choice* $\mathbf{b} = \beta \mathbf{a}$ *maximizes the quantity* $|\mathbf{b}^\dagger \mathbf{a}|^2 / \mathbf{b}^\dagger \mathbf{b}$, *for any constant* β.

Exercise 25.2 *Use the definition of the covariance matrix* Q *to show that* Q *is Hermitian and that, for any vector* $\mathbf{y}$, $\mathbf{y}^\dagger Q \mathbf{y} \geq 0$. *Therefore,* Q *is a nonnegative definite matrix and, using its eigenvector decomposition, can be written as* $Q = CC^\dagger$, *for some invertible square matrix* C.

Exercise 25.3 *Consider now the problem of maximizing* $|\mathbf{b}^\dagger \mathbf{s}|^2 / \mathbf{b}^\dagger Q \mathbf{b}$. *Using the two previous exercises, show that the solution is* $\mathbf{b} = \beta Q^{-1} \mathbf{s}$, *for some arbitrary constant* β.

We can now use the results of these exercises to continue our discussion. We choose the constant $\beta = 1/(\mathbf{s}^\dagger Q^{-1}\mathbf{s})$ so that the optimal $\mathbf{b}$ has $\mathbf{b}^\dagger \mathbf{s} = 1$; that is, the *optimal filter* $\mathbf{b}$ is

$$\mathbf{b} = (1/(\mathbf{s}^\dagger Q^{-1}\mathbf{s}))Q^{-1}\mathbf{s},$$

and the *optimal estimate* of γ is

$$\hat{\gamma} = \mathbf{b}^\dagger \mathbf{x} = (1/(\mathbf{s}^\dagger Q^{-1}\mathbf{s}))(\mathbf{s}^\dagger Q^{-1}\mathbf{x}).$$

The mean of the random variable $\hat{\gamma}$ is equal to $\gamma \mathbf{b}^\dagger \mathbf{s} = \gamma$, and the variance is equal to $1/(\mathbf{s}^\dagger Q^{-1}\mathbf{s})$. Therefore, the output signal power is $|\gamma|^2$, the output noise power is $1/(\mathbf{s}^\dagger Q^{-1}\mathbf{s})$, and so the *output signal-to-noise ratio* (SNR$_{out}$) is

$$\text{SNR}_{\text{out}} = |\gamma|^2(\mathbf{s}^\dagger Q^{-1}\mathbf{s}).$$

The gain associated with the optimal vector $\mathbf{b}$ is then

$$\text{maximum gain} = \frac{(\mathbf{s}^\dagger Q^{-1}\mathbf{s})\, tr(Q)}{(\mathbf{s}^\dagger \mathbf{s})}.$$

The calculation of the vector $C^{-1}\mathbf{x}$ is sometimes called *prewhitening* since $C^{-1}\mathbf{x} = \gamma C^{-1}\mathbf{s} + C^{-1}\mathbf{z}$ and the new noise vector, $C^{-1}\mathbf{z}$, has the identity matrix for its covariance matrix. The new signal vector is $C^{-1}\mathbf{s}$. The filtering operation that gives $\hat{\gamma} = \mathbf{b}^\dagger \mathbf{x}$ can be written as

$$\hat{\gamma} = (1/(\mathbf{s}^\dagger Q^{-1}\mathbf{s}))(C^{-1}\mathbf{s})^\dagger C^{-1}\mathbf{x};$$

the term $(C^{-1}\mathbf{s})^\dagger C^{-1}\mathbf{x}$ is described by saying that we *prewhiten, then do a matched filter*. Now we consider some special cases of noise.

25.4   The Case of White Noise

We say that the noise is *white noise* if the covariance matrix is $Q = \sigma^2 I$, where I denotes the identity matrix that is one on the main diagonal and zero elsewhere and $\sigma > 0$ is the common standard deviation of the z_n. This means that the z_n are mutually uncorrelated (independent, in the Gaussian case) and share a common variance.

In this case the optimal vector $\mathbf{b}$ is $\mathbf{b} = \frac{1}{(\mathbf{s}^\dagger \mathbf{s})}\mathbf{s}$ and the gain is N. Notice that $\hat{\gamma}$ now involves only a matched filter. We consider now some special cases of the signal vectors $\mathbf{s}$.

25.4.1   Constant Signal

Suppose that the vector $\mathbf{s}$ is constant; that is, $\mathbf{s} = \mathbf{1} = (1, 1, ..., 1)^T$. Then, we have

$$\hat{\gamma} = \frac{1}{N}\sum_{n=1}^{N} x_n.$$

This is the same result we found in our discussion of the BLUE, when we estimated the mean value and the noise was white.

25.4.2 Sinusoidal Signal, Frequency Known

Suppose that

$$\mathbf{s} = \mathbf{e}(\omega_0) = (\exp(-i\omega_0), \exp(-2i\omega_0), ..., \exp(-Ni\omega_0))^T,$$

where ω_0 denotes a known frequency in $[-\pi, \pi)$. Then, $\mathbf{b} = \frac{1}{N}\mathbf{e}(\omega_0)$ and

$$\hat{\gamma} = \frac{1}{N}\sum_{n=1}^{N} x_n \exp(in\omega_0);$$

so, we see yet another occurrence of the DFT.

25.4.3 Sinusoidal Signal, Frequency Unknown

If we do not know the value of the signal frequency ω_0, a reasonable thing to do is to calculate the $\hat{\gamma}$ for each (actually, finitely many) of the possible frequencies within $[-\pi, \pi)$ and base the detection decision on the largest value; that is, we calculate the DFT as a function of the variable ω. If there is only a single ω_0 for which there is a sinusoidal signal present in the data, the values of $\hat{\gamma}$ obtained at frequencies other than ω_0 provide estimates of the noise power σ^2, against which the value of $\hat{\gamma}$ for ω_0 can be compared.

25.5 The Case of Correlated Noise

We say that the noise is *correlated* if the covariance matrix Q is not a multiple of the identity matrix. This means either that the z_n are mutually correlated (dependent, in the Gaussian case) or that they are uncorrelated, but have different variances.

In this case, as we saw previously, the optimal vector $\mathbf{b}$ is

$$\mathbf{b} = \frac{1}{(\mathbf{s}^\dagger Q^{-1}\mathbf{s})}Q^{-1}\mathbf{s}$$

and the gain is

$$\text{maximum gain} = \frac{(\mathbf{s}^\dagger Q^{-1}\mathbf{s})\, tr(Q)}{(\mathbf{s}^\dagger \mathbf{s})}.$$

How large or small the gain is depends on how the signal vector $\mathbf{s}$ relates to the matrix Q.

For sinusoidal signals, the quantity $\mathbf{s}^\dagger \mathbf{s}$ is the same, for all values of the parameter ω; this is not always the case, however. In passive detection of

sources in acoustic array processing, for example, the signal vectors arise from models of the acoustic medium involved. For far-field sources in an (acoustically) isotropic deep ocean, planewave models for $\mathbf{s}$ will have the property that $\mathbf{s}^\dagger \mathbf{s}$ does not change with source location. However, for near-field or shallow-water environments, this is usually no longer the case.

It follows from Exercise 25.3 that the quantity $\frac{\mathbf{s}^\dagger Q^{-1} \mathbf{s}}{\mathbf{s}^\dagger \mathbf{s}}$ achieves its maximum value when $\mathbf{s}$ is an eigenvector of Q associated with its smallest eigenvalue, λ_N; in this case, we are saying that the signal vector does not look very much like a typical noise vector. The maximum gain is then $\lambda_N^{-1} tr(Q)$. Since $tr(Q)$ equals the sum of its eigenvalues, multiplying by $tr(Q)$ serves to normalize the gain, so that we cannot get larger gain simply by having all the eigenvalues of Q small.

On the other hand, if $\mathbf{s}$ should be an eigenvector of Q associated with its largest eigenvalue, say λ_1, then the maximum gain is $\lambda_1^{-1} tr(Q)$. If the noise is signal-like, that is, has one dominant eigenvalue, then $tr(Q)$ is approximately λ_1 and the maximum gain is around one, so we have lost the maximum gain of N we were able to get in the white-noise case. This makes sense, in that it says that we cannot significantly improve our ability to discriminate between signal and noise by taking more samples, if the signal and noise are very similar.

25.5.1   Constant Signal with Unequal-Variance Uncorrelated Noise

Suppose that the vector $\mathbf{s}$ is constant; that is, $\mathbf{s} = \mathbf{1} = (1, 1, ..., 1)^T$. Suppose also that the noise covariance matrix is $Q = \text{diag}\{\sigma_1, ..., \sigma_N\}$.

In this case the optimal vector $\mathbf{b}$ has entries

$$b_m = \frac{1}{\left(\sum_{n=1}^N \sigma_n^{-1}\right)} \sigma_m^{-1},$$

for $m = 1, ..., N$, and we have

$$\hat{\gamma} = \frac{1}{\left(\sum_{n=1}^N \sigma_n^{-1}\right)} \sum_{m=1}^N \sigma_m^{-1} x_m.$$

This is the BLUE estimate of γ in this case.

25.5.2   Sinusoidal signal, Frequency Known, in Correlated Noise

Suppose that

$$\mathbf{s} = \mathbf{e}(\omega_0) = (\exp(-i\omega_0), \exp(-2i\omega_0), ..., \exp(-Ni\omega_0))^T,$$

where ω_0 denotes a known frequency in $[-\pi, \pi)$. In this case the optimal vector $\mathbf{b}$ is

$$\mathbf{b} = \frac{1}{\mathbf{e}(\omega_0)^\dagger Q^{-1} \mathbf{e}(\omega_0)} Q^{-1} \mathbf{e}(\omega_0)$$

and the gain is

$$\text{maximum gain} = \frac{1}{N} [\mathbf{e}(\omega_0)^\dagger Q^{-1} \mathbf{e}(\omega_0)] tr(Q).$$

How large or small the gain is depends on the quantity $q(\omega_0)$, where

$$q(\omega) = \mathbf{e}(\omega)^\dagger Q^{-1} \mathbf{e}(\omega).$$

The function $1/q(\omega)$ can be viewed as a sort of noise power spectrum, describing how the noise power appears when decomposed over the various frequencies in $[-\pi, \pi)$. The maximum gain will be large if this *noise power spectrum* is relatively small near $\omega = \omega_0$; however, when the noise is similar to the signal, that is, when the noise power spectrum is relatively large near $\omega = \omega_0$, the maximum gain can be small. In this case the noise power spectrum plays a role analogous to that played by the eigenvalues of Q earlier.

To see more clearly why it is that the function $1/q(\omega)$ can be viewed as a sort of noise power spectrum, consider what we get when we apply the optimal filter associated with ω to data containing only noise. The average output should tell us how much power there is in the component of the noise that resembles $\mathbf{e}(\omega)$; this is essentially what is meant by a noise power spectrum. The result is $\mathbf{b}^\dagger \mathbf{z} = (1/q(\omega)) \mathbf{e}(\omega)^\dagger Q^{-1} \mathbf{z}$. The expected value of $|\mathbf{b}^\dagger \mathbf{z}|^2$ is then $1/q(\omega)$.

25.5.3 Sinusoidal Signal, Frequency Unknown, in Correlated Noise

Again, if we do not know the value of the signal frequency ω_0, a reasonable thing to do is to calculate the $\hat{\gamma}$ for each (actually, finitely many) of the possible frequencies within $[-\pi, \pi)$ and base the detection decision on the largest value. For each ω the corresponding value of $\hat{\gamma}$ is

$$\hat{\gamma}(\omega) = [1/(\mathbf{e}(\omega)^\dagger Q^{-1} \mathbf{e}(\omega))] \sum_{n=1}^{N} a_n \exp(in\omega),$$

where $\mathbf{a} = (a_1, a_2, ..., a_N)^T$ satisfies the linear system $Q\mathbf{a} = \mathbf{x}$ or $\mathbf{a} = Q^{-1}\mathbf{x}$. It is interesting to note the similarity between this estimation procedure and the PDFT discussed earlier; to see the connection, view $[1/(\mathbf{e}(\omega)^\dagger Q^{-1} \mathbf{e}(\omega))]$ in the role of $P(\omega)$ and Q its corresponding matrix of Fourier-transform values. The analogy breaks down when we notice that Q need not be Toeplitz, as in the PDFT case; however, the similarity is intriguing.

25.6   Capon's Data-Adaptive Method

When the noise covariance matrix Q is not available, perhaps because we cannot observe the background noise in the absence of any signals that may also be present, we may use the signal-plus-noise covariance matrix R in place of Q.

Exercise 25.4 *Show that for*

$$R = |\gamma|^2 ss^\dagger + Q$$

maximizing the ratio

$$|b^\dagger s|^2/b^\dagger Rb$$

is equivalent to maximizing the ratio

$$|b^\dagger s|^2/b^\dagger Qb.$$

In [67] Capon offered a high-resolution method for detecting and resolving sinusoidal signals with unknown frequencies in noise. His estimator has the form

$$1/e(\omega)^\dagger R^{-1}e(\omega). \tag{25.1}$$

The idea here is to fix an arbitrary ω, and then to find the vector $b(\omega)$ that minimizes $b(\omega)^\dagger Rb(\omega)$, subject to $b(\omega)^\dagger e(\omega) = 1$. The vector $b(\omega)$ turns out to be

$$b(\omega) = \frac{1}{e(\omega)^\dagger R^{-1}e(\omega)} R^{-1}e(\omega). \tag{25.2}$$

Now we allow ω to vary and compute the expected output of the filter $b(\omega)$, operating on the signal plus noise input. This expected output is then

$$1/e(\omega)^\dagger R^{-1}e(\omega). \tag{25.3}$$

The reason that this estimator resolves closely spaced delta functions better than linear methods such as the DFT is that, when ω is fixed, we obtain an optimal filter using R as the noise covariance matrix, which then includes all sinusoids not at the frequency ω in the noise component. This is actually a good thing, since, when we are looking at a frequency ω that does not correspond to a frequency actually present in the data, we want the sinusoidal components present at nearby frequencies to be filtered out.

Part VIII

Appendices

Chapter 26

Appendix: Inner Products

26.1 Chapter Summary

Many methods for analyzing measured signals are based on the idea of matching the data against various potential signals to see which ones match best. The role of *inner products* in this matching approach is the topic of this chapter.

26.2 Cauchy's Inequality

The matching is done using the complex dot product, $\mathbf{e}_\omega^\dagger \mathbf{d}$. In the ideal case this dot product is large, for those values of ω that correspond to an actual component of the signal; otherwise it is small. Why this should be the case is the Cauchy-Schwarz inequality (or sometimes, depending on the context, just Cauchy's inequality, just Schwarz's inequality, or, in the Russian literature, Bunyakovsky's inequality). The proof of Cauchy's inequality rests on four basic properties of the complex dot product. These properties can then be used to obtain the more general notion of an inner product.

26.3 The Complex Vector Dot Product

Let $\mathbf{u} = (a, b)$ and $\mathbf{v} = (c, d)$ be two vectors in two-dimensional space. Let $\mathbf{u}$ make the angle $\alpha > 0$ with the positive x-axis and $\mathbf{v}$ the angle $\beta > 0$. Let $||\mathbf{u}|| = \sqrt{a^2 + b^2}$ denote the length of the vector $\mathbf{u}$. Then $a = ||\mathbf{u}|| \cos\alpha$, $b = ||\mathbf{u}|| \sin\alpha$, $c = ||\mathbf{v}|| \cos\beta$ and $d = ||\mathbf{v}|| \sin\beta$. So $\mathbf{u} \cdot \mathbf{v} = ac + bd =$

$||\mathbf{u}||||\mathbf{v}||(\cos\alpha\cos\beta + \sin\alpha\sin\beta = ||\mathbf{u}||\,||\mathbf{v}||\cos(\alpha - \beta)$. Therefore, we have

$$\mathbf{u} \cdot \mathbf{v} = ||\mathbf{u}||\,||\mathbf{v}||\cos\theta, \tag{26.1}$$

where $\theta = \alpha - \beta$ is the angle between $\mathbf{u}$ and $\mathbf{v}$. Cauchy's inequality is

$$|\mathbf{u} \cdot \mathbf{v}| \le ||\mathbf{u}||\,||\mathbf{v}||,$$

with equality if and only if $\mathbf{u}$ and $\mathbf{v}$ are parallel.

Cauchy's inequality extends to vectors of any size with complex entries. For example, the complex M-dimensional vectors $\mathbf{e}_\omega$ and $\mathbf{e}_\theta$ defined earlier both have length equal to $\sqrt{M}$ and

$$|\mathbf{e}_\omega^\dagger \mathbf{e}_\theta| \le M,$$

with equality if and only if ω and θ differ by an integer multiple of π.

From Equation (26.1) we know that the dot product $\mathbf{u} \cdot \mathbf{v}$ is zero if and only if the angle between these two vectors is a right angle; we say then that $\mathbf{u}$ and $\mathbf{v}$ are mutually *orthogonal*. Orthogonality was at the core of our first approach to signal analysis: the vectors $\mathbf{e}_j$ and $\mathbf{e}_k$ are orthogonal if $k \ne j$. The notion of orthogonality is fundamental in signal processing, and we shall return to it repeatedly in what follows. The idea of using the dot product to measure how similar two vectors are is called *matched filtering*; it is a popular method in signal detection and estimation of parameters.

Proof of Cauchy's inequality: To prove Cauchy's inequality for the complex vector dot product, we write $\mathbf{u} \cdot \mathbf{v} = |\mathbf{u} \cdot \mathbf{v}|e^{i\theta}$. Let t be a real variable and consider

$$0 \le ||e^{-i\theta}\mathbf{u} - t\mathbf{v}||^2 = (e^{-i\theta}\mathbf{u} - t\mathbf{v}) \cdot (e^{-i\theta}\mathbf{u} - t\mathbf{v})$$

$$= ||\mathbf{u}||^2 - t[(e^{-i\theta}\mathbf{u}) \cdot \mathbf{v} + \mathbf{v} \cdot (e^{-i\theta}\mathbf{u})] + t^2||\mathbf{v}||^2$$

$$= ||\mathbf{u}||^2 - t[(e^{-i\theta}\mathbf{u}) \cdot \mathbf{v} + \overline{(e^{-i\theta}\mathbf{u}) \cdot \mathbf{v}}] + t^2||\mathbf{v}||^2$$

$$= ||\mathbf{u}||^2 - 2Re(te^{-i\theta}(\mathbf{u} \cdot \mathbf{v})) + t^2||\mathbf{v}||^2$$

$$= ||\mathbf{u}||^2 - 2Re(t|\mathbf{u} \cdot \mathbf{v}|) + t^2||\mathbf{v}||^2 = ||\mathbf{u}||^2 - 2t|\mathbf{u} \cdot \mathbf{v}| + t^2||\mathbf{v}||^2.$$

This is a nonnegative quadratic polynomial in the variable t, so it cannot have two distinct real roots. Therefore, the discriminant $4|\mathbf{u} \cdot \mathbf{v}|^2 - 4||\mathbf{v}||^2||\mathbf{u}||^2$ must be non-positive; that is, $|\mathbf{u} \cdot \mathbf{v}|^2 \le ||\mathbf{u}||^2||\mathbf{v}||^2$. This is Cauchy's inequality. ∎

Exercise 26.1 *Use Cauchy's inequality to show that*

$$||\mathbf{u} + \mathbf{v}|| \le ||\mathbf{u}|| + ||\mathbf{v}||;$$

this is called the triangle inequality.

A careful examination of the proof just presented shows that we did not explicitly use the definition of the complex vector dot product, but only some of its properties. This suggested to mathematicians the possibility of abstracting these properties and using them to define a more general concept, an *inner product*, between objects more general than complex vectors, such as infinite sequences, random variables, and matrices. Such an inner product can then be used to define the *norm* of these objects and thereby a distance between such objects. Once we have an inner product defined, we also have available the notions of orthogonality and best approximation. We shall address all of these topics in a later chapter.

26.4 Orthogonality

Consider the problem of writing the two-dimensional real vector $(3, -2)$ as a linear combination of the vectors $(1, 1)$ and $(1, -1)$; that is, we want to find constants a and b so that $(3, -2) = a(1, 1) + b(1, -1)$. One way to do this, of course, is to compare the components: $3 = a + b$ and $-2 = a - b$; we can then solve this simple system for the a and b. In higher dimensions this way of doing it becomes harder, however. A second way is to make use of the dot product and orthogonality.

The dot product of two vectors (x, y) and (w, z) in R^2 is $(x, y) \cdot (w, z) = xw + yz$. If the dot product is zero then the vectors are said to be *orthogonal*; the two vectors $(1, 1)$ and $(1, -1)$ are orthogonal. We take the dot product of both sides of $(3, -2) = a(1, 1) + b(1, -1)$ with $(1, 1)$ to get

$$1 = (3, -2) \cdot (1, 1) = a(1, 1) \cdot (1, 1) + b(1, -1) \cdot (1, 1) = a(1, 1) \cdot (1, 1) + 0 = 2a,$$

so we see that $a = \frac{1}{2}$. Similarly, taking the dot product of both sides with $(1, -1)$ gives

$$5 = (3, -2) \cdot (1, -1) = a(1, 1) \cdot (1, -1) + b(1, -1) \cdot (1, -1) = 2b,$$

so $b = \frac{5}{2}$. Therefore, $(3, -2) = \frac{1}{2}(1, 1) + \frac{5}{2}(1, -1)$. The beauty of this approach is that it does not get much harder as we go to higher dimensions.

Since the cosine of the angle θ between vectors $\mathbf{u}$ and $\mathbf{v}$ is

$$\cos \theta = \mathbf{u} \cdot \mathbf{v} / \|\mathbf{u}\| \, \|\mathbf{v}\|,$$

where $\|\mathbf{u}\|^2 = \mathbf{u} \cdot \mathbf{u}$, the projection of vector $\mathbf{v}$ on to the line through the origin parallel to $\mathbf{u}$ is

$$\text{Proj}_{\mathbf{u}}(\mathbf{v}) = \frac{\mathbf{u} \cdot \mathbf{v}}{\mathbf{u} \cdot \mathbf{u}} \mathbf{u}.$$

Therefore, the vector $\mathbf{v}$ can be written as

$$\mathbf{v} = \text{Proj}_{\mathbf{u}}(\mathbf{v}) + (\mathbf{v} - \text{Proj}_{\mathbf{u}}(\mathbf{v})),$$

where the first term on the right is parallel to $\mathbf{u}$ and the second one is orthogonal to $\mathbf{u}$.

How do we find vectors that are mutually orthogonal? Suppose we begin with $(1, 1)$. Take a second vector, say $(1, 2)$, that is not parallel to $(1, 1)$ and write it as we did $\mathbf{v}$ earlier, that is, as a sum of two vectors, one parallel to $(1, 1)$ and the second orthogonal to $(1, 1)$. The projection of $(1, 2)$ onto the line parallel to $(1, 1)$ passing through the origin is

$$\frac{(1, 1) \cdot (1, 2)}{(1, 1) \cdot (1, 1)}(1, 1) = \frac{3}{2}(1, 1) = (\frac{3}{2}, \frac{3}{2})$$

so

$$(1, 2) = (\frac{3}{2}, \frac{3}{2}) + ((1, 2) - (\frac{3}{2}, \frac{3}{2})) = (\frac{3}{2}, \frac{3}{2}) + (-\frac{1}{2}, \frac{1}{2}).$$

The vectors $(-\frac{1}{2}, \frac{1}{2}) = -\frac{1}{2}(1, -1)$ and, therefore, $(1, -1)$ are then orthogonal to $(1, 1)$. This approach is the basis for the *Gram-Schmidt* method for constructing a set of mutually orthogonal vectors.

Exercise 26.2 *Use the Gram-Schmidt approach to find a third vector in R^3 orthogonal to both $(1, 1, 1)$ and $(1, 0, -1)$.*

Orthogonality is a convenient tool that can be exploited whenever we have an inner product defined.

26.5   Generalizing the Dot Product: Inner Products

The proof of Cauchy's inequality rests not on the actual definition of the complex vector dot product, but rather on four of its most basic properties. We use these properties to extend the concept of the complex vector dot product to that of *inner product*. Later in this chapter we shall give several examples of inner products, applied to a variety of mathematical objects, including infinite sequences, functions, random variables, and matrices. For now, let us denote our mathematical objects by $\mathbf{u}$ and $\mathbf{v}$ and the inner product between them as $\langle \mathbf{u}, \mathbf{v} \rangle$. The objects will then be said to be members of an *inner-product space*. We are interested in inner products because they provide a notion of orthogonality, which is fundamental to best approximation and optimal estimation.

Defining an inner product: The four basic properties that will serve to define an inner product are:

1: $\langle \mathbf{u}, \mathbf{u} \rangle \geq 0$, with equality if and only if $\mathbf{u} = \mathbf{0}$;

2. $\langle \mathbf{v}, \mathbf{u} \rangle = \overline{\langle \mathbf{u}, \mathbf{v} \rangle}$;

3. $\langle \mathbf{u}, \mathbf{v} + \mathbf{w} \rangle = \langle \mathbf{u}, \mathbf{v} \rangle + \langle \mathbf{u}, \mathbf{w} \rangle$;

4. $\langle c\mathbf{u}, \mathbf{v} \rangle = c\langle \mathbf{u}, \mathbf{v} \rangle$ for any complex number c.

The inner product is the basic ingredient in Hilbert space theory. Using the inner product, we define the *norm* of $\mathbf{u}$ to be

$$||\mathbf{u}|| = \sqrt{\langle \mathbf{u}, \mathbf{u} \rangle}$$

and the distance between $\mathbf{u}$ and $\mathbf{v}$ to be $||\mathbf{u} - \mathbf{v}||$.

The Cauchy-Schwarz inequality: Because these four properties were all we needed to prove the Cauchy inequality for the complex vector dot product, we obtain the same inequality whenever we have an inner product. This more general inequality is the Cauchy-Schwarz inequality:

$$|\langle \mathbf{u}, \mathbf{v} \rangle| \leq \sqrt{\langle \mathbf{u}, \mathbf{u} \rangle}\sqrt{\langle \mathbf{v}, \mathbf{v} \rangle}$$

or

$$|\langle \mathbf{u}, \mathbf{v} \rangle| \leq ||\mathbf{u}|| \, ||\mathbf{v}||,$$

with equality if and only if there is a scalar c such that $\mathbf{v} = c\mathbf{u}$. We say that the vectors $\mathbf{u}$ and $\mathbf{v}$ are *orthogonal* if $\langle \mathbf{u}, \mathbf{v} \rangle = 0$. We turn now to some examples.

Inner product of infinite sequences: Let $\mathbf{u} = \{u_n\}$ and $\mathbf{v} = \{v_n\}$ be infinite sequences of complex numbers. The inner product is then

$$\langle \mathbf{u}, \mathbf{v} \rangle = \sum u_n \overline{v_n},$$

and

$$||\mathbf{u}|| = \sqrt{\sum |u_n|^2}.$$

The sums are assumed to be finite; the index of summation n is singly or doubly infinite, depending on the context. The Cauchy-Schwarz inequality says that

$$|\sum u_n \overline{v_n}| \leq \sqrt{\sum |u_n|^2}\sqrt{\sum |v_n|^2}.$$

Inner product of functions: Now suppose that $\mathbf{u} = f(x)$ and $\mathbf{v} = g(x)$. Then,

$$\langle \mathbf{u}, \mathbf{v} \rangle = \int f(x)\overline{g(x)}dx$$

and

$$\|\mathbf{u}\| = \sqrt{\int |f(x)|^2 dx}.$$

The integrals are assumed to be finite; the limits of integration depend on the support of the functions involved. The Cauchy-Schwarz inequality now says that

$$|\int f(x)\overline{g(x)}dx| \leq \sqrt{\int |f(x)|^2 dx}\sqrt{\int |g(x)|^2 dx}.$$

Inner product of random variables: Now suppose that $\mathbf{u} = X$ and $\mathbf{v} = Y$ are random variables. Then,

$$\langle \mathbf{u}, \mathbf{v} \rangle = E(X\overline{Y})$$

and

$$\|\mathbf{u}\| = \sqrt{E(|X|^2)},$$

which is the standard deviation of X if the mean of X is zero. The expected values are assumed to be finite. The Cauchy-Schwarz inequality now says that

$$|E(X\overline{Y})| \leq \sqrt{E(|X|^2)}\sqrt{E(|Y|^2)}.$$

If $E(X) = 0$ and $E(Y) = 0$, the random variables X and Y are orthogonal if and only if they are *uncorrelated*.

Inner product of complex matrices: Now suppose that $\mathbf{u} = A$ and $\mathbf{v} = B$ are complex matrices. Then,

$$\langle \mathbf{u}, \mathbf{v} \rangle = \text{trace}(B^\dagger A)$$

and

$$\|\mathbf{u}\| = \sqrt{\text{trace}(A^\dagger A)},$$

where the trace of a square matrix is the sum of the entries on the main diagonal. As we shall see later, this inner product is simply the complex vector dot product of the vectorized versions of the matrices involved. The Cauchy-Schwarz inequality now says that

$$|\text{trace}(B^\dagger A)| \leq \sqrt{\text{trace}(A^\dagger A)}\sqrt{\text{trace}(B^\dagger B)}.$$

Weighted inner product of complex vectors: Let $\mathbf{u}$ and $\mathbf{v}$ be complex vectors and let Q be a Hermitian positive-definite matrix; that is, $Q^\dagger = Q$ and $\mathbf{u}^\dagger Q \mathbf{u} > 0$ for all nonzero vectors $\mathbf{u}$. The inner product is then

$$\langle \mathbf{u}, \mathbf{v} \rangle = \mathbf{v}^\dagger Q \mathbf{u}$$

and

$$\|\mathbf{u}\| = \sqrt{\mathbf{u}^\dagger Q \mathbf{u}}.$$

We know from the eigenvector decomposition of Q that $Q = C^\dagger C$ for some matrix C. Therefore, the inner product is simply the complex vector dot product of the vectors $C\mathbf{u}$ and $C\mathbf{v}$. The Cauchy-Schwarz inequality says that

$$|\mathbf{v}^\dagger Q \mathbf{u}| \leq \sqrt{\mathbf{u}^\dagger Q \mathbf{u}} \sqrt{\mathbf{v}^\dagger Q \mathbf{v}}.$$

Weighted inner product of functions: Now suppose that $\mathbf{u} = f(x)$ and $\mathbf{v} = g(x)$ and $w(x) > 0$. Then define

$$\langle \mathbf{u}, \mathbf{v} \rangle = \int f(x)\overline{g(x)}w(x)dx$$

and

$$\|\mathbf{u}\| = \sqrt{\int |f(x)|^2 w(x)dx}.$$

The integrals are assumed to be finite; the limits of integration depend on the support of the functions involved. This inner product is simply the inner product of the functions $f(x)\sqrt{w(x)}$ and $g(x)\sqrt{w(x)}$. The Cauchy-Schwarz inequality now says that

$$\left| \int f(x)\overline{g(x)}w(x)dx \right| \leq \sqrt{\int |f(x)|^2 w(x)dx} \sqrt{\int |g(x)|^2 w(x)dx}.$$

Once we have an inner product defined, we can speak about orthogonality and best approximation. Important in that regard is the orthogonality principle.

26.6   The Orthogonality Principle

Imagine that you are standing and looking down at the floor. The point B on the floor that is closest to N, the tip of your nose, is the unique point on the floor such that the vector from B to any other point A on the floor is perpendicular to the vector from N to B; that is, $\langle BN, BA \rangle = 0$. This is a simple illustration of the *orthogonality principle*. Whenever we

have an inner product defined we can speak of orthogonality and apply the orthogonality principle to find best approximations.

The orthogonality principle: Let $\mathbf{u}$ and $\mathbf{v}^1, ..., \mathbf{v}^N$ be members of an inner-product space. For all choices of scalars $a_1, ..., a_N$, we can compute the distance from $\mathbf{u}$ to the member $a_1\mathbf{v}^1 + ...a_N\mathbf{v}^N$. Then, we minimize this distance over all choices of the scalars; let $b_1, ..., b_N$ be this best choice. The *orthogonality principle* tells us that the member $\mathbf{u} - (b_1\mathbf{v}^1 + ...b_N\mathbf{v}^N)$ is orthogonal to the member $(a_1\mathbf{v}^1 + ... + a_N\mathbf{v}^N) - (b_1\mathbf{v}^1 + ...b_N\mathbf{v}^N)$, that is,

$$\langle \mathbf{u} - (b_1\mathbf{v}^1 + ...b_N\mathbf{v}^N), (a_1\mathbf{v}^1 + ... + a_N\mathbf{v}^N) - (b_1\mathbf{v}^1 + ...b_N\mathbf{v}^N) \rangle = 0,$$

for every choice of scalars a_n. We can then use the orthogonality principle to find the best choice $b_1., , , .b_N$.

For each fixed index value j in the set $\{1, ..., N\}$, let $a_n = b_n$ if j is not equal to n and $a_j = b_j + 1$. Then we have

$$0 = \langle \mathbf{u} - (b_1\mathbf{v}^1 + ...b_N\mathbf{v}^N), \mathbf{v}^j \rangle,$$

or

$$\langle \mathbf{u}, \mathbf{v}^j \rangle = \sum_{n=1}^{N} b_n \langle \mathbf{v}^n, \mathbf{v}^j \rangle,$$

for each j. The $\mathbf{v}^n$ are known, so we can calculate the inner products $\langle \mathbf{v}^n, \mathbf{v}^j \rangle$ and solve this system of equations for the best b_n.

We shall encounter a number of particular cases of the orthogonality principle in subsequent chapters. The example of the *least-squares* solution of a system of linear equations provides a good example of the use of this principle.

The least-squares solution: Let $V\mathbf{a} = \mathbf{u}$ be a system of M linear equations in N unknowns. For $n = 1, ..., N$ let $\mathbf{v}^n$ be the nth column of the matrix V. For any choice of the vector $\mathbf{a}$ with entries a_n, $n = 1, ..., N$, the vector $V\mathbf{a}$ is

$$V\mathbf{a} = \sum_{n=1}^{N} a_n \mathbf{v}^n.$$

Solving $V\mathbf{a} = \mathbf{u}$ amounts to representing the vector $\mathbf{u}$ as a linear combination of the columns of V.

If there is no solution of $V\mathbf{a} = \mathbf{u}$ then we can look for the best choice of coefficients so as to minimize the distance $||\mathbf{u} - (a_1\mathbf{v}^1 + ... + a_N\mathbf{v}^N)||$. The matrix with entries $\langle \mathbf{v}^n, \mathbf{v}^j \rangle$ is $V^\dagger V$, and the vector with entries $\langle \mathbf{u}, \mathbf{v}^j \rangle$ is $V^\dagger \mathbf{u}$. According to the orthogonality principle, we must solve the system of equations $V^\dagger \mathbf{u} = V^\dagger V\mathbf{a}$, which leads to the least-squares solution.

Exercise 26.3 *Find polynomial functions $f(x)$, $g(x)$ and $h(x)$ that are orthogonal on the interval $[0, 1]$ and have the property that every polynomial of degree two or less can be written as a linear combination of these three functions.*

Exercise 26.4 *Show that the functions e^{inx}, n an integer, are orthogonal on the interval $[-\pi, \pi]$. Let $f(x)$ have the Fourier expansion*

$$f(x) = \sum_{n=-\infty}^{\infty} a_n e^{inx}, \ |x| \leq \pi.$$

Use orthogonality to find the coefficients a_n.

We have seen that orthogonality can be used to determine the coefficients in the Fourier series representation of a function. There are other useful representations in which orthogonality also plays a role; wavelets is one example. Let $f(x)$ be defined on the closed interval $[0, X]$. Suppose that we change the function $f(x)$ to a new function $g(x)$ by altering the values for x within a small interval, keeping the remaining values the same: then all of the Fourier coefficients change. Looked at another way, a localized disturbance in the function $f(x)$ affects all of its Fourier coefficients. It would be helpful to be able to represent $f(x)$ as a sum of orthogonal functions in such a way that localized changes in $f(x)$ affect only a small number of the components in the sum. One way to do this is with wavelets, as we shall see shortly.

Chapter 27

Appendix: Reverberation and Echo Cancellation

27.1 Chapter Summary

A nice application of Dirac delta function models is the problem of reverberation and echo cancellation, as discussed in [168]. The received signal is viewed as a filtered version of the original and we want to remove the effects of the filter, thereby removing the echo. This leads to the problem of finding the inverse filter. A version of the echo cancellation problem arises in telecommunications, as discussed in [208] and [207].

27.2 The Echo Model

Suppose that $x(t)$ is the original transmitted signal and the received signal is

$$y(t) = x(t) + \alpha x(t - d), \tag{27.1}$$

where $d > 0$ is the delay present in the echo term. We assume that the echo term is weaker than the original signal, so we make $0 < \alpha < 1$. With the filter function $h(t)$ defined by

$$h(t) = \delta(t) + \alpha \delta(t - d) = \delta(t) + \alpha \delta_d(t), \tag{27.2}$$

where $\delta_d(t) = \delta(t - d)$, we can write $y(t)$ as the convolution of $x(t)$ and $h(t)$; that is,

$$y(t) = x(t) * h(t). \tag{27.3}$$

A more general model is used to describe reverberation:

$$h(t) = \sum_{k=0}^{K} \alpha_k \delta(t - d_k), \qquad (27.4)$$

with $\alpha_0 = 1$, $d_0 = 0$, and $d_k > 0$ and $0 < \alpha_k < 1$ for $k = 1, 2, ..., K$.

Our goal is to find a second filter, denoted $h_i(t)$, the inverse of $h(t)$ in Equation (27.2), such that

$$h(t) * h_i(t) = \delta(t), \qquad (27.5)$$

and therefore

$$x(t) = y(t) * h_i(t). \qquad (27.6)$$

For now, we use trial and error to find $h_i(t)$; later we shall use the Fourier transform.

27.3   Finding the Inverse Filter

As a first guess, let us try

$$g_1(t) = \delta(t) - \alpha\delta_d(t). \qquad (27.7)$$

Convolving $g_1(t)$ with $h(t)$, we get

$$h(t) * g_1(t) = \delta(t) * \delta(t) - \alpha^2 \delta_d(t) * \delta_d(t). \qquad (27.8)$$

We need to find out what $\delta_d(t) * \delta_d(t)$ is.

Exercise 27.1 *Use the sifting property of the Dirac delta and the definition of convolution to show that*

$$\delta_d(t) * \delta_d(t) = \delta_{2d}(t).$$

The Fourier transform of $\delta_d(t)$ is the function $\exp(id\omega)$, so that the Fourier transform of the convolution of $\delta_d(t)$ with itself is the square of $\exp(id\omega)$, or $\exp(i(2d)\omega)$. This tells us again that the convolution of $\delta_d(t)$ with itself is $\delta_{2d}(t)$. Therefore,

$$h(t) * g_1(t) = \delta(t) - \alpha^2 \delta_{2d}(t). \qquad (27.9)$$

We do not quite have what we want, but since $0 < \alpha < 1$, the α^2 is much smaller than α.

Suppose that we continue down this path, and take for our next guess the filter function $g_2(t)$ given by

$$g_2(t) = \delta(t) - \alpha\delta_d(t) + \alpha^2\delta_{2d}(t). \qquad (27.10)$$

We then find that

$$h(t) * g_2(t) = \delta(t) + \alpha^3 \delta_{3d}(t); \tag{27.11}$$

the coefficient is α^3 now, which is even smaller, and the delay in the echo term has moved to $3d$. We could continue along this path, but a final solution is beginning to suggest itself.

Suppose that we define

$$g_N(t) = \sum_{n=0}^{N} (-1)^n \alpha^n \delta_{nd}(t). \tag{27.12}$$

It would then follow that

$$h(t) * g_N(t) = \delta(t) - (-1)^{N+1} \alpha^{N+1} \delta_{(N+1)d}(t). \tag{27.13}$$

The coefficient α^{N+1} goes to zero and the delay goes to infinity, as $N \to \infty$. This suggests that the inverse filter should be the infinite sum

$$h_i(t) = \sum_{n=0}^{\infty} (-1)^n \alpha^n \delta_{nd}(t). \tag{27.14}$$

Then Equation (27.6) becomes

$$x(t) = y(t) - \alpha y(t-d) + \alpha^2 y(t-2d) - \alpha^3 y(t-3d) + \dots \tag{27.15}$$

Obviously, to remove the echo completely in this manner we need infinite memory.

Exercise 27.2 *Assume that $x(t) = 0$ for $t < 0$. Show that the problem of removing the echo is simpler now.*

27.4   Using the Fourier Transform

The Fourier transform of the filter function $h(t)$ in Equation (27.2) is

$$H(\omega) = 1 + \alpha \exp(id\omega). \tag{27.16}$$

If we are to have

$$h(t) * h_i(t) = \delta(t), \tag{27.17}$$

we must have

$$H(\omega) H_i(\omega) = 1, \tag{27.18}$$

where $H_i(\omega)$ is the Fourier transform of the inverse filter function $h_i(t)$ that we seek. It follows that

$$H_i(\omega) = (1 + \alpha \exp(id\omega))^{-1}. \qquad (27.19)$$

Recalling the formula for the sum of a geometric progression,

$$1 - r + r^2 - r^3 + ... = \frac{1}{1+r}, \qquad (27.20)$$

for $|r| < 1$, we find that we can write

$$H_i(\omega) = 1 - \alpha \exp(id\omega) + \alpha^2 \exp(i(2d)\omega) - \alpha^3 \exp(i(3d)\omega) + ..., \qquad (27.21)$$

which tells us that $h_i(t)$ is precisely as given in Equation (27.14).

27.5 The Teleconferencing Problem

In teleconferencing, each separate room is equipped with microphones for transmitting to the other rooms and loudspeakers for broadcasting what the people in the other rooms are saying. For simplicity, consider two rooms, the transmitting room (TR), in which people are currently speaking, and the receiving room (RR), where the people are currently listening to the broadcast from the TR. The RR also has microphones and the problem arises when the signal broadcast into the RR from the TR reaches the microphones in the RR and is broadcast back into the TR. If it reaches the microphones in the TR, it will be re-broadcast to the RR, creating an echo, or worse.

The signal that reaches a microphone in the RR will depend on the signals broadcast into the RR from the TR, as well as on the acoustics of the RR and on the placement of the microphone in the RR; that is, it will be a filtered version of what is broadcast into the RR. The hope is to be able to estimate the filter, generate an approximation of what is about to be re-broadcast, and subtract the estimate prior to re-broadcasting, thereby reducing to near zero what is re-broadcast back to the TR.

In practice, all signals are viewed as discrete time series, and all filters are taken to be *finite impulse response* (FIR) filters. Because the acoustics of the RR are not known a priori, the filter that the RR imposes must be estimated. This is done adaptively, by comparing vectors of samples of the original transmissions with the filtered version that is about to be re-broadcast, as described in [208].

Chapter 28

Appendix: Using Prior Knowledge to Estimate the Fourier Transform

28.1 Chapter Summary

A basic problem in signal processing is the estimation of the function $F(\omega)$ from finitely many values of its inverse Fourier transform $f(x)$. The DFT is one such estimator. As we shall see in this chapter, there are other estimators that are able to make better use of prior information about $F(\omega)$ and thereby provide a better estimate.

28.2 Over-sampling

In our discussions above, we assumed that $F(\omega) = 0$ for $|\omega| > \Omega$ and that $\Delta = \frac{\pi}{\Omega}$. In Figure 28.1 below, we show the DFT estimate for $F(\omega)$ for a case in which $\Omega = \frac{\pi}{30}$. This would tell us that the proper sampling spacing is $\Delta = 30$. However, it is not uncommon to have situations in which x is time and we can take as many samples of $f(x)$ as we wish, but must take the samples at points x within some limited time interval, say $[0, A]$. In the case considered in the figure, $A = 130$. If we had used $\Delta = 30$, we would have obtained only four data points, which is not sufficient information. Instead, we used $\Delta = 1$ and took $N = 129$ data points; we *over-sampled*. There is a price to be paid for over-sampling, however.

   The DFT estimation procedure does not "know" about the true value of Ω; it only "sees" Δ. It "assumes" incorrectly that Ω must be π, since $\Delta = 1$. Consequently, it "thinks" that we want it to estimate $F(\omega)$ on

the interval $[-\pi, \pi]$. It doesn't "know" that we know that $F(\omega)$ is zero on most of this interval. Therefore, the DFT spends a lot of its energy trying to describe the part of the graph of $F(\omega)$ where it is zero, and relatively little of its energy describing what is happening within the interval $[-\Omega, \Omega]$, which is all that we are interested in. This is why the bottom graph in the figure shows the DFT to be poor within $[-\Omega, \Omega]$. There is a second graph in the figure. It looks quite a bit better. How was that graph obtained?
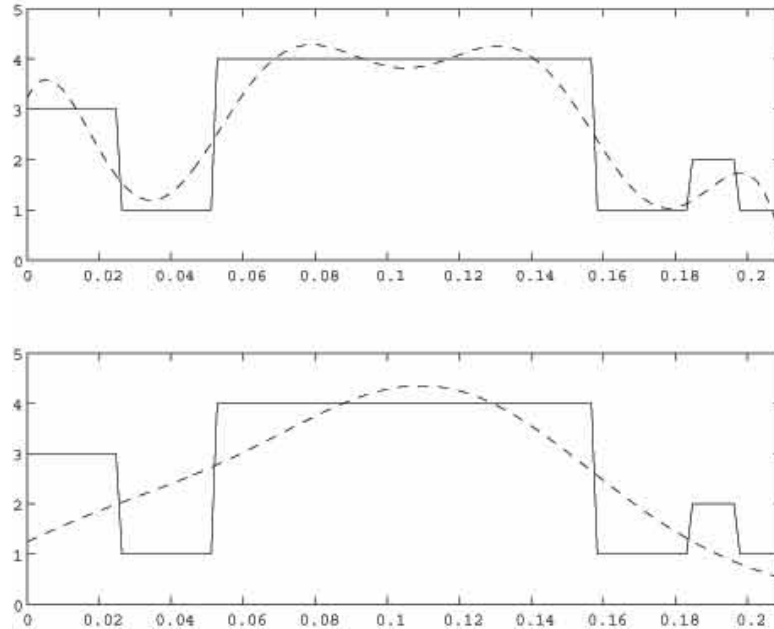
Figure 28.1:   The non-iterative band-limited extrapolation method (MDFT) (top) and the DFT (bottom) for $N = 129$, $\Delta = 1$ and $\Omega = \pi/30$.

We know that $F(\omega) = 0$ outside the interval $[-\Omega, \Omega]$. Can we somehow let the estimation process know that we know this, so that it doesn't waste its energy outside this interval? Yes, we can.

The *characteristic function* of the interval $[-\Omega, \Omega]$ is

$$\chi_\Omega(\omega) = \begin{cases} 1, \text{if } |\omega| \leq \Omega \,; \\ 0, \text{if } |\omega| > \Omega \,. \end{cases}$$

We take as our estimator of $F(\omega)$ a function called the *modified* DFT, (MDFT) having the form

$$MDFT(\omega) = \chi_\Omega(\omega) \sum_{m=0}^{N-1} a_m e^{im\Delta\omega}. \tag{28.1}$$

We determine the coefficients a_m by making $MDFT(\omega)$ consistent with the data. Inserting $MDFT(\omega)$ into the integral in Equation (8.2) and setting $x = n\Delta$, for each $n = 0, 1, ..., N-1$, in turn, we find that we must have

$$f(n\Delta) = \frac{1}{2\pi} \sum_{m=0}^{N-1} a_m \int_{-\Omega}^{\Omega} e^{i(m-n)\Delta\omega} d\omega.$$

Performing the integration, we find that we need

$$f(n\Delta) = \sum_{m=0}^{N-1} a_m \frac{\sin(\Omega(n-m)\Delta)}{\pi(n-m)\Delta}, \tag{28.2}$$

for $n = 0, 1, ..., N-1$. We solve for the a_m and insert these coefficients into the formula for the MDFT. The graph of the MDFT is the top graph in the figure.

The main idea in the MDFT is to use a form of the estimator that already includes whatever important features of $F(\omega)$ we may know a priori. In the case of the MDFT, we knew that $F(\omega) = 0$ outside the interval $[-\Omega, \Omega]$, so we introduced a factor of $\chi_\Omega(\omega)$ in the estimator. Now, whatever coefficients we use, any estimator of the form given in Equation (28.1) will automatically be zero outside $[-\Omega, \Omega]$. We are then free to select the coefficients so as to make the MDFT consistent with the data. This involves solving the system of linear equations in (28.2).

28.3 Using Other Prior Information

The approach that led to the MDFT estimate suggests that we can introduce other prior information besides the support of $F(\omega)$. For example, if we have some idea of the overall shape of the function $F(\omega)$, we could choose $P(\omega) > 0$ to indicate this shape and use it instead of $\chi_\Omega(\omega)$ in our estimator. This leads to the PDFT estimator, which has the form

$$PDFT(\omega) = P(\omega) \sum_{n=0}^{N-1} b_m e^{im\Delta\omega}. \tag{28.3}$$

Now we find the b_m by forcing the right side of Equation (28.3) to be consistent with the data. Inserting the function $PDFT(\omega)$ into the integral in Equation (8.2), we find that we must have

$$f(n\Delta) = \frac{1}{2\pi} \sum_{m=0}^{N-1} b_m \int_{-\infty}^{\infty} P(\omega) e^{i(m-n)\Delta\omega} d\omega. \tag{28.4}$$

Using $p(x)$, the inverse Fourier transform of $P(\omega)$, given by

$$p(x) = \frac{1}{2\pi} \int_{-\infty}^{\infty} P(\omega) e^{-ix\omega} d\omega,$$

we find that we must have

$$f(n\Delta) = \sum_{m=0}^{N-1} b_m p((n-m)\Delta), \qquad (28.5)$$

for $n = 0, 1, ..., N-1$. We solve this system of equations for the b_m and insert them into the PDFT estimator in Equation (28.3).

In Figure 28.2 we have the function $F(\omega)$ in the upper left corner. It consists of one large bump in the center and one smaller bump toward the right side. The DFT on the upper right side gives only slight indication that the smaller bump exists. The data here is somewhat over-sampled, so we can try the MDFT. The prior for the MDFT is $P(\omega) = \chi_\Omega(\omega)$, which is pictured in the center left frame; it is shown only over $[-\Omega, \Omega]$, where it is just one. The MDFT estimate is in the center right frame; it shows only slight improvement over the DFT. Now, suppose we know that there is a large bump in the center. Both the DFT and the MDFT tell us clearly that this is the case, so even if we did not know it at the start, we know it now. Let's select as our prior a function $P(\omega)$ that includes the big bump in the center, as shown in the lower left. The PDFT on the lower right now shows the smaller bump more clearly.

A more dramatic illustration of the use of the PDFT is shown in Figure 28.3. The function $F(\omega)$ is a function of two variables simulating a slice of a head. It has been approximated by a discrete image, called here the "original". The data was obtained by taking the two-dimensional vector DFT of the discrete image and replacing most of its values with zeros. When we formed the inverse vector DFT, we obtained the estimate in the lower right. This is essentially the DFT estimate, and it tells us nothing about the inside of the head. From prior information, or even from the DFT estimate itself, we know that the true $F(\omega)$ includes a skull. We therefore select as our prior the (discretized) function of two variables shown in the upper left. The PDFT estimate is the image in the lower left. The important point to remember here is that the same data was used to generate both pictures.

We saw previously how the MDFT can improve the estimate of $F(\omega)$, by incorporating the prior information about its support. Precisely why the improvement occurs is the subject of the next section.

28.4 Analysis of the MDFT

Let our data be $f(x_m)$, $m = 1, ..., M$, where the x_m are arbitrary values of the variable x. If $F(\omega)$ is zero outside $[-\Omega, \Omega]$, then minimizing the energy

over $[-\Omega, \Omega]$ subject to data consistency produces an estimate of the form

$$F_\Omega(\omega) = \chi_\Omega(\omega) \sum_{m=1}^{M} b_m \exp(ix_m\omega),$$

with the b_m satisfying the equations

$$f(x_n) = \sum_{m=1}^{M} b_m \frac{\sin(\Omega(x_m - x_n))}{\pi(x_m - x_n)},$$

for $n = 1, ..., M$. The matrix S_Ω with entries $\frac{\sin(\Omega(x_m - x_n))}{\pi(x_m - x_n)}$ we call a *sinc* matrix.

28.4.1   Eigenvector Analysis of the MDFT

Although it seems reasonable that incorporating the additional information about the support of $F(\omega)$ should improve the estimation, it would be more convincing if we had a more mathematical argument to make. For that we turn to an analysis of the eigenvectors of the sinc matrix. Throughout this subsection we make the simplification that $x_n = n$.

Exercise 28.1 *The purpose of this exercise is to show that, for an Hermitian nonnegative-definite M by M matrix Q, a norm-one eigenvector $\mathbf{u}^1$ of Q associated with its largest eigenvalue, λ_1, maximizes the quadratic form $\mathbf{a}^\dagger Q \mathbf{a}$ over all vectors $\mathbf{a}$ with norm one. Let $Q = ULU^\dagger$ be the eigenvector decomposition of Q, where the columns of U are mutually orthogonal eigenvectors $\mathbf{u}^n$ with norms equal to one, so that $U^\dagger U = I$, and $L = diag\{\lambda_1, ..., \lambda_M\}$ is the diagonal matrix with the eigenvalues of Q as its entries along the main diagonal. Assume that $\lambda_1 \geq \lambda_2 \geq ... \geq \lambda_M$. Then maximize*

$$\mathbf{a}^\dagger Q \mathbf{a} = \sum_{n=1}^{M} \lambda_n |\mathbf{a}^\dagger \mathbf{u}^n|^2,$$

subject to the constraint

$$\mathbf{a}^\dagger \mathbf{a} = \mathbf{a}^\dagger U^\dagger U \mathbf{a} = \sum_{n=1}^{M} |\mathbf{a}^\dagger \mathbf{u}^n|^2 = 1.$$

Hint: Show $\mathbf{a}^\dagger Q \mathbf{a}$ is a convex combination of the eigenvalues of Q.

Exercise 28.2 *Show that, for the sinc matrix $Q = S_\Omega$, the quadratic form $\mathbf{a}^\dagger Q \mathbf{a}$ in the previous exercise becomes*

$$\mathbf{a}^\dagger S_\Omega \mathbf{a} = \frac{1}{2\pi} \int_{-\Omega}^{\Omega} |\sum_{n=1}^{M} a_n e^{in\omega}|^2 d\omega.$$

Show that the norm of the vector $\mathbf{a}$ is the integral

$$\frac{1}{2\pi} \int_{-\pi}^{\pi} |\sum_{n=1}^{M} a_n e^{in\omega}|^2 d\omega.$$

Exercise 28.3 *For $M = 30$ compute the eigenvalues of the matrix S_Ω for various choices of Ω, such as $\Omega = \frac{\pi}{k}$, for $k = 2, 3, ..., 10$. For each k arrange the set of eigenvalues in decreasing order and note the proportion of them that are not near zero. The set of eigenvalues of a matrix is sometimes called its eigenspectrum and the nonnegative function $\chi_\Omega(\omega)$ is a power spectrum; here is one time in which different notions of a spectrum are related.*

28.4.2 The Eigenfunctions of S_Ω

Suppose that the vector $\mathbf{u}^1 = (u_1^1, ..., u_M^1)^T$ is an eigenvector of S_Ω corresponding to the largest eigenvalue, λ_1. Associate with $\mathbf{u}^1$ the *eigenfunction*

$$U^1(\omega) = \sum_{n=1}^{M} u_n^1 e^{in\omega}.$$

Then

$$\lambda_1 = \int_{-\Omega}^{\Omega} |U^1(\omega)|^2 d\omega / \int_{-\pi}^{\pi} |U^1(\omega)|^2 d\omega$$

and $U^1(\omega)$ is the function of its form that is most concentrated within the interval $[-\Omega, \Omega]$.

Similarly, if $\mathbf{u}^M$ is an eigenvector of S_Ω associated with the smallest eigenvalue λ_M, then the corresponding eigenfunction $U^M(\omega)$ is the function of its form least concentrated in the interval $[-\Omega, \Omega]$.

Exercise 28.4 *Plot for $|\omega| \leq \pi$ the functions $|U^m(\omega)|$ corresponding to each of the eigenvectors of the sinc matrix S_Ω. Pay particular attention to the places where each of these functions is zero.*

The eigenvectors of S_Ω corresponding to different eigenvalues are orthogonal, that is $(\mathbf{u}^m)^\dagger \mathbf{u}^n = 0$ if m is not n. We can write this in terms of integrals:

$$\int_{-\pi}^{\pi} U^n(\omega)\overline{U^m(\omega)}d\omega = 0$$

if m is not n. The mutual orthogonality of these eigenfunctions is related to the locations of their roots, which were studied in the previous exercise.

Any Hermitian matrix Q is invertible if and only if none of its eigenvalues is zero. With λ_m and $\mathbf{u}^m$, $m = 1, ..., M$, the eigenvalues and eigenvectors of Q, the inverse of Q can then be written as

$$Q^{-1} = (1/\lambda_1)\mathbf{u}^1(\mathbf{u}^1)^\dagger + ... + (1/\lambda_M)\mathbf{u}^M(\mathbf{u}^M)^\dagger.$$

Exercise 28.5 *Show that the MDFT estimator given by Equation (28.1) $F_\Omega(\omega)$ can be written as*

$$F_\Omega(\omega) = \chi_\Omega(\omega) \sum_{m=1}^{M} \frac{1}{\lambda_m}(\mathbf{u}^m)^\dagger \mathbf{d}\, U^m(\omega),$$

where $\mathbf{d} = (f(1), f(2), ..., f(M))^T$ is the data vector.

Exercise 28.6 *Show that the DFT estimate of $F(\omega)$, restricted to the interval $[-\Omega, \Omega]$, is*

$$F_{DFT}(\omega) = \chi_\Omega(\omega) \sum_{m=1}^{M} (\mathbf{u}^m)^\dagger \mathbf{d}\, U^m(\omega).$$

From these two exercises we can learn why it is that the estimate $F_\Omega(\omega)$ resolves better than the DFT. The former makes more use of the eigenfunctions $U^m(\omega)$ for higher values of m, since these are the ones for which λ_m is closer to zero. Since those eigenfunctions are the ones having most of their roots within the interval $[-\Omega, \Omega]$, they have the most flexibility within that region and are better able to describe those features in $F(\omega)$ that are not resolved by the DFT.
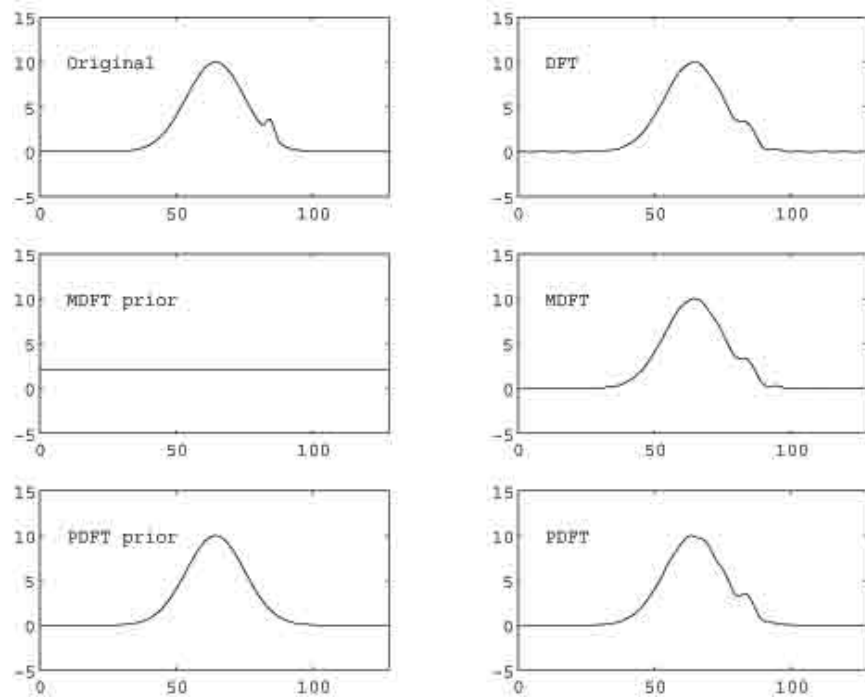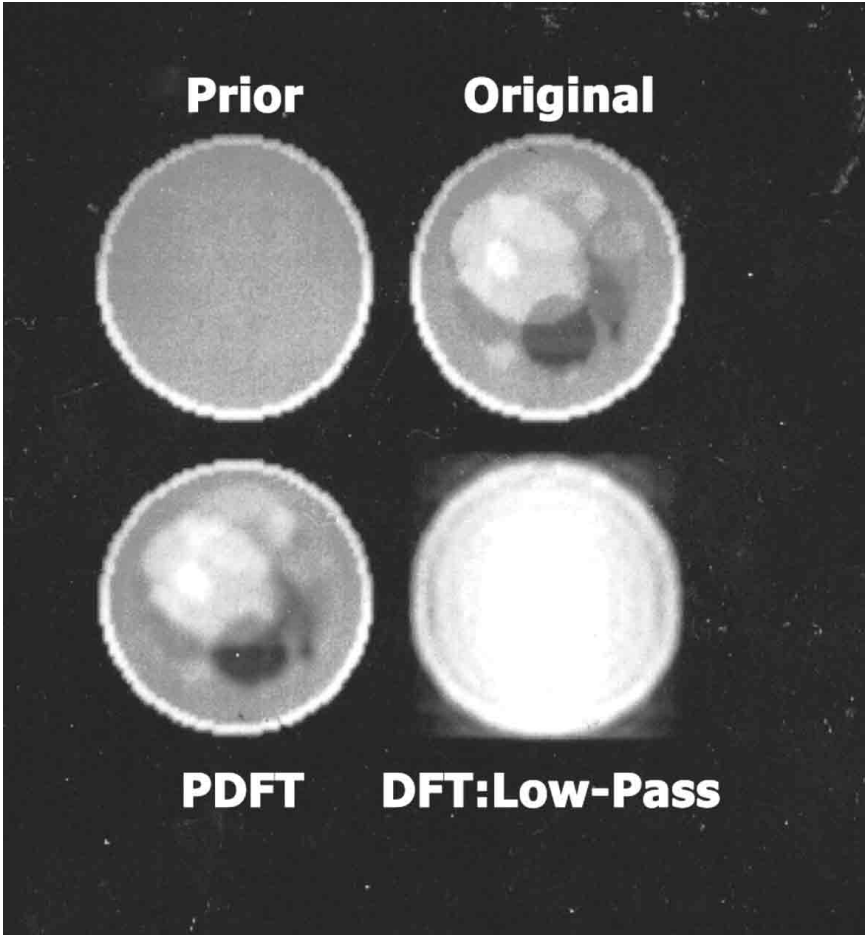
Figure 28.2: The DFT, the MDFT, and the PDFT.

Figure 28.3: The PDFT in image reconstruction.

Chapter 29

Appendix: The Vector Wiener Filter

29.1 Chapter Summary

The vector Wiener filter (VWF) provides another method for estimating the vector $\mathbf{x}$ given noisy measurements $\mathbf{z}$, where

$$\mathbf{z} = H\mathbf{x} + \mathbf{v},$$

with $\mathbf{x}$ and $\mathbf{v}$ independent random vectors and H a known matrix. We shall assume throughout this chapter that $E(\mathbf{v}) = \mathbf{0}$ and let $Q = E(\mathbf{v}\mathbf{v}^\dagger)$.

29.2 The Vector Wiener Filter in Estimation

It is common to formulate the VWF in the context of filtering a signal vector $\mathbf{s}$ from signal plus noise. The data is the vector

$$\mathbf{z} = \mathbf{s} + \mathbf{v},$$

and we want to estimate $\mathbf{s}$. Each entry of our estimate of the vector $\mathbf{s}$ will be a linear combination of the data values; that is, our estimate is $\hat{\mathbf{s}} = B^\dagger \mathbf{z}$ for some matrix B to be determined. This B will be called the *vector Wiener filter*. To extract the signal from the noise, we must know something about possible signals and possible noises. We consider several stages of increasing complexity and correspondence with reality.

29.3   The Simplest Case

Suppose, initially, that all signals must have the form $\mathbf{s} = a\mathbf{u}$, where a is an unknown scalar and $\mathbf{u}$ is a known vector. Suppose that all noises must have the form $\mathbf{v} = b\mathbf{w}$, where b is an unknown scalar and $\mathbf{w}$ is a known vector. Then, to estimate $\mathbf{s}$, we must find a. So long as $J \geq 2$, we should be able to solve for a and b. We form the two equations

$$\mathbf{u}^\dagger \mathbf{z} = a\mathbf{u}^\dagger \mathbf{u} + b\mathbf{u}^\dagger \mathbf{w}$$

and

$$\mathbf{w}^\dagger \mathbf{z} = a\mathbf{w}^\dagger \mathbf{u} + b\mathbf{w}^\dagger \mathbf{w}.$$

This system of two equations in two unknowns will have a unique solution unless $\mathbf{u}$ and $\mathbf{w}$ are proportional, in which case we cannot expect to distinguish signal from noise.

29.4   A More General Case

We move now to a somewhat more complicated model. Suppose that all signals must have the form

$$\mathbf{s} = \sum_{n=1}^{N} a_n \mathbf{u}^n,$$

where the a_n are unknown scalars and the $\mathbf{u}^n$ are known vectors. Suppose that all noises must have the form

$$\mathbf{v} = \sum_{m=1}^{M} b_m \mathbf{w}^m,$$

where the b_m are unknown scalars and $\mathbf{w}^m$ are known vectors. Then, to estimate $\mathbf{s}$, we must find the a_n. So long as $J \geq N + M$, we should be able to solve for the unique a_n and b_m. However, we usually do not know a great deal about the signal and the noise, so we find ourselves in the situation in which the N and M are large. Let U be the J by N matrix whose nth column is $\mathbf{u}^n$ and W the J by M matrix whose mth column is $\mathbf{w}^m$. Let V be the J by $N + M$ matrix whose first N columns contain U and whose last M columns contain W; so, $V = [U \quad W]$. Let $\mathbf{c}$ be the $N + M$ by 1 column vector whose first N entries are the a_n and whose last M entries are the b_m. We want to solve $\mathbf{z} = V\mathbf{c}$. But this system of linear equations has too many unknowns when $N + M > J$, so we seek the minimum norm solution. In closed form this solution is

$$\hat{\mathbf{c}} = V^\dagger (VV^\dagger)^{-1}\mathbf{z}.$$

The matrix $VV^\dagger = (UU^\dagger + WW^\dagger)$ involves the *signal correlation matrix* $UU^\dagger$ and the *noise correlation matrix* $WW^\dagger$. Consider $UU^\dagger$. The matrix $UU^\dagger$ is J by J and the (i,j) entry of $UU^\dagger$ is given by

$$UU^\dagger_{ij} = \sum_{n=1}^{N} u_i^n \overline{u_j^n},$$

so the matrix $\frac{1}{N} UU^\dagger$ has for its entries the average, over all the $n = 1, ..., N$, of the product of the ith and jth entries of the vectors $\mathbf{u}^n$. Therefore, $\frac{1}{N} UU^\dagger$ is statistical information about the signal; it tells us how these products look, on average, over all members of the family $\{\mathbf{u}^n\}$, the *ensemble*, to use the statistical word.

29.5   The Stochastic Case

To pass to a more formal statistical framework, we let the coefficient vectors $\mathbf{a} = (a_1, a_2, ..., a_N)^T$ and $\mathbf{b} = (b_1, b_2, ..., b_M)^T$ be independent random white-noise vectors, both with mean zero and covariance matrices $E(\mathbf{aa}^\dagger) = I$ and $E(\mathbf{bb}^\dagger) = I$. Then,

$$UU^\dagger = E(\mathbf{ss}^\dagger) = R_s$$

and

$$WW^\dagger = E(\mathbf{vv}^\dagger) = Q = R_v.$$

The estimate of $\mathbf{s}$ is the result of applying the vector Wiener filter to the vector $\mathbf{z}$ and is given by

$$\hat{\mathbf{s}} = UU^\dagger (UU^\dagger + WW^\dagger)^{-1} \mathbf{z}.$$

Exercise 29.1 *Apply the vector Wiener filter to the simplest problem discussed earlier in the chapter on the BLUE; let $N = 1$ and assume that c is a random variable with mean zero and variance one. It will help to use the matrix-inversion identity*

$$(Q + \mathbf{uu}^\dagger)^{-1} = Q^{-1} - (1 + \mathbf{u}^\dagger Q^{-1} \mathbf{u})^{-1} Q^{-1} \mathbf{uu}^\dagger Q^{-1}. \qquad (29.1)$$

29.6   The VWF and the BLUE

To apply the VWF to the problem considered in the discussion of the BLUE, let the vector $\mathbf{s}$ be $H\mathbf{x}$. We assume, in addition, that the vector $\mathbf{x}$ is a white-noise vector; that is, $E(\mathbf{xx}^\dagger) = \sigma^2 I$. Then, $R_s = \sigma^2 H H^\dagger$.

In the VWF approach we estimate $\mathbf{s}$ using

$$\hat{\mathbf{s}} = B^\dagger \mathbf{z},$$

where the matrix B is chosen so as to minimize the mean squared error, $E||\hat{\mathbf{s}} - \mathbf{s}||^2$. This is equivalent to minimizing

$$\text{trace}\, E((B^\dagger \mathbf{z} - \mathbf{s})(B^\dagger \mathbf{z} - \mathbf{s})^\dagger).$$

Expanding the matrix products and using the previous definitions, we see that we must minimize

$$\text{trace}\, (B^\dagger(R_s + R_v)B - R_s B - B^\dagger R_s + R_s).$$

Differentiating with respect to the matrix B using Equations (34.1) and (34.3), we find

$$(R_s + R_v)B - R_s = 0,$$

so that

$$B = (R_s + R_v)^{-1} R_s.$$

Our estimate of the signal component is then

$$\hat{\mathbf{s}} = R_s(R_s + R_v)^{-1}\mathbf{z}.$$

With $\mathbf{s} = H\mathbf{x}$, our estimate of $\mathbf{s}$ is

$$\hat{\mathbf{s}} = \sigma^2 H H^\dagger (\sigma^2 H H^\dagger + Q)^{-1}\mathbf{z},$$

and the VWF estimate of $\mathbf{x}$ is

$$\hat{\mathbf{x}} = \sigma^2 H^\dagger (\sigma^2 H H^\dagger + Q)^{-1}\mathbf{z}.$$

How does this estimate relate to the one we got from the BLUE?

The BLUE estimate of $\mathbf{x}$ is

$$\hat{\mathbf{x}} = (H^\dagger Q^{-1} H)^{-1} H^\dagger Q^{-1}\mathbf{z}.$$

From the matrix identity in Equation (24.5), we know that

$$(H^\dagger Q^{-1} H + \sigma^{-2} I)^{-1} H^\dagger Q^{-1} = \sigma^2 H^\dagger (\sigma^2 H H^\dagger + Q)^{-1}.$$

Therefore, the VWF estimate of $\mathbf{x}$ is

$$\hat{\mathbf{x}} = (H^\dagger Q^{-1} H + \sigma^{-2} I)^{-1} H^\dagger Q^{-1}\mathbf{z}.$$

Note that the BLUE estimate is unbiased and unaffected by changes in the signal strength or the noise strength. In contrast, the VWF is not unbiased and does depend on the signal-to-noise ratio; that is, it depends on the ratio $\sigma^2/\text{trace}\,(Q)$. The BLUE estimate is the limiting case of the VWF estimate, as the signal-to-noise ratio goes to infinity.

The BLUE estimates $\mathbf{s} = H\mathbf{x}$ by first finding the BLUE estimate of $\mathbf{x}$ and then multiplying it by H to get the estimate of the signal $\mathbf{s}$.

Exercise 29.2 *Show that the mean-squared error in the estimation of* **s** *is*

$$E(||\hat{\mathbf{s}} - \mathbf{s}||^2) = \text{trace}\,(H(H^\dagger Q^{-1}H)^{-1}H^\dagger).$$

The VWF finds the linear estimate of $\mathbf{s} = H\mathbf{x}$ that minimizes the mean-squared error $E(||\hat{\mathbf{s}} - \mathbf{s}||^2)$. Consequently, the mean squared error in the VWF is less than that in the BLUE.

Exercise 29.3 *Assume that* $E(\mathbf{x}\mathbf{x}^\dagger) = \sigma^2 I$. *Show that the mean squared error for the VWF estimate is*

$$E(||\hat{\mathbf{s}} - \mathbf{s}||^2) = \text{trace}\,(H(H^\dagger Q^{-1}H + \sigma^{-2}I)^{-1}H^\dagger).$$

29.7 Wiener Filtering of Functions

The Wiener filter is often presented in the context of random functions of, say, time. In this model the signal is $s(t)$ and the noise is $q(t)$, where these functions of time are viewed as random functions (stochastic processes). The data is taken to be $z(t)$, a function of t, so that the matrices $UU^\dagger$ and $WW^\dagger$ are now *infinite matrices*; the discrete index $j = 1, ..., J$ is now replaced by the continuous index variable t. Instead of the finite family $\{\mathbf{u}^n, n = 1..., N\}$, we now have an infinite family of functions $u(t)$ in $\mathcal{U}$. The entries of $UU^\dagger$ are essentially the average values of the products $u(t_1)\overline{u(t_2)}$ over all the members of $\mathcal{U}$. It is often assumed that this average of products is a function not of t_1 and t_2 separately, but only of their difference $t_1 - t_2$; this is called *stationarity*. So, $aver\{u(t_1)\overline{u(t_2)}\} = r_s(t_1 - t_2)$ comes from a function $r_s(\tau)$ of a single variable. The Fourier transform of $r_s(\tau)$ is $R_s(\omega)$, the signal power spectrum. The matrix $UU^\dagger$ is then an infinite Toeplitz matrix, constant on each diagonal. The Wiener filtering can actually be achieved by taking Fourier transforms and multiplying and dividing by power spectra, instead of inverting infinite matrices. It is also common to discretize the time variable and to consider the Wiener filter operating on infinite sequences, as we see in the next chapter.

Chapter 30

Appendix: Wiener Filter Approximation

30.1 Chapter Summary

As we saw in the chapter on the vector Wiener filter, when the data is a finite vector composed of signal plus noise the vector Wiener filter can be used to estimate the signal component, provided we know something about the possible signals and possible noises. In theoretical discussion of filtering signal from signal plus noise, it is traditional to assume that both components are doubly infinite sequences of random variables. In this case the Wiener filter is a convolution filter that operates on the input signal plus noise sequence to produce the output estimate of the signal-only sequence. The derivation of the Wiener filter is in terms of the autocorrelation sequences of the two components, as well as their respective power spectra.

30.2 The Discrete Stationary Case

Suppose now that the discrete stationary random process to be filtered is the doubly infinite sequence $\{z_n = s_n + q_n\}_{n=-\infty}^{\infty}$, where $\{s_n\}$ is the signal component with autocorrelation function $r_s(k) = E(s_{n+k}\overline{s_n})$ and power spectrum $R_s(\omega)$ defined for ω in the interval $[-\pi, \pi]$, and $\{q_n\}$ is the noise component with autocorrelation function $r_q(k)$ and power spectrum $R_q(\omega)$ defined for ω in $[-\pi, \pi]$. We assume that for each n the random variables s_n and q_n have mean zero and that the signal and noise are independent of one another. Then the autocorrelation function for the signal-plus-noise sequence $\{z_n\}$ is

$$r_z(n) = r_s(n) + r_q(n)$$

311

for all n and

$$R_z(\omega) = R_s(\omega) + R_q(\omega).$$

is the signal-plus-noise power spectrum.

Let $h = \{h_k\}_{k=-\infty}^{\infty}$ be a linear filter with *transfer function*

$$H(\omega) = \sum_{k=-\infty}^{\infty} h_k e^{ik\omega},$$

for ω in $[-\pi, \pi]$. Given the sequence $\{z_n\}$ as input to this filter, the output is the sequence

$$y_n = \sum_{k=-\infty}^{\infty} h_k z_{n-k}. \tag{30.1}$$

The goal of Wiener filtering is to select the filter h so that the output sequence y_n approximates the signal s_n sequence as well as possible. Specifically, we seek h so as to minimize the expected squared error, $E(|y_n - s_n|^2)$, which, because of stationarity, is independent of n. We have

$$E(|y_n|^2) = \sum_{k=-\infty}^{\infty} h_k \left(\sum_{j=-\infty}^{\infty} \overline{h_j}(r_s(j-k) + r_q(j-k)) \right)$$

$$= \sum_{k=-\infty}^{\infty} h_k \overline{(r_z * \overline{h})_k}$$

which, by the Parseval equation, equals

$$\frac{1}{2\pi} \int H(\omega) R_z(\omega) \overline{H(\omega)} d\omega = \frac{1}{2\pi} \int |H(\omega)|^2 R_z(\omega) d\omega.$$

Similarly,

$$E(s_n \overline{y_n}) = \sum_{j=-\infty}^{\infty} \overline{h_j} r_s(j),$$

which equals

$$\frac{1}{2\pi} \int R_s(\omega) \overline{H(\omega)} d\omega,$$

and

$$E(|s_n|^2) = \frac{1}{2\pi} \int R_s(\omega) d\omega.$$

Therefore,

$$E(|y_n - s_n|^2) = \frac{1}{2\pi} \int |H(\omega)|^2 R_z(\omega)d\omega - \frac{1}{2\pi} \int R_s(\omega)\overline{H(\omega)}d\omega$$

$$-\frac{1}{2\pi} \int R_s(\omega)H(\omega)d\omega + \frac{1}{2\pi} \int R_s(\omega)d\omega.$$

As we shall see shortly, minimizing $E(|y_n - s_n|^2)$ with respect to the function $H(\omega)$ leads to the equation

$$R_z(\omega)H(\omega) = R_s(\omega),$$

so that the transfer function of the optimal filter is

$$H(\omega) = R_s(\omega)/R_z(\omega).$$

The *Wiener filter* is then the sequence $\{h_k\}$ of the Fourier coefficients of this function $H(\omega)$.

To prove that this choice of $H(\omega)$ minimizes $E(|y_n - s_n|^2)$, we note that

$$|H(\omega)|^2 R_z(\omega) - R_s(\omega)\overline{H(\omega)} - R_s(\omega)H(\omega) + R_s(\omega)$$

$$= R_z|H(\omega) - R_s(\omega)/R_z(\omega)|^2 + R_s(\omega) - R_s(\omega)^2/R_z(\omega).$$

Only the first term involves the function $H(\omega)$.

30.3   Approximating the Wiener Filter

Since $H(\omega)$ is a nonnegative function of ω, therefore real-valued, its Fourier coefficients h_k will be *conjugate symmetric*; that is, $h_{-k} = \overline{h_k}$. This poses a problem when the random process z_n is a discrete time series, with z_n denoting the measurement recorded at time n. From Equation (30.1) we see that to produce the output y_n corresponding to time n we need the input for every time, past and future. To remedy this we can obtain the best causal approximation of the Wiener filter h.

A filter $g = \{g_k\}_{k=-\infty}^{\infty}$ is said to be *causal* if $g_k = 0$ for $k < 0$; this means that given the input sequence $\{z_n\}$, the output

$$w_n = \sum_{k=-\infty}^{\infty} g_k z_{n-k} = \sum_{k=0}^{\infty} g_k z_{n-k}$$

requires only values of z_m up to $m = n$. To obtain the causal filter g that best approximates the Wiener filter, we find the coefficients g_k that minimize the quantity $E(|y_n - w_n|^2)$, or, equivalently,

$$\int_{-\pi}^{\pi} |H(\omega) - \sum_{k=0}^{+\infty} g_k e^{ik\omega}|^2 R_z(\omega)d\omega. \tag{30.2}$$

The orthogonality principle tells us that the optimal coefficients must satisfy the equations

$$r_s(m) = \sum_{k=0}^{+\infty} g_k r_z(m-k),$$

(30.3)

for all m. These are the *Wiener-Hopf equations* [181].

Even having a causal filter does not completely solve the problem, since we would have to record and store the infinite past. Instead, we can decide to use a filter $f = \{f_k\}_{k=-\infty}^{\infty}$ for which $f_k = 0$ unless $-K \leq k \leq L$ for some positive integers K and L. This means we must store L values and wait until time $n + K$ to obtain the output for time n. Such a linear filter is a *finite memory, finite delay* filter, also called a *finite impulse response* (FIR) filter. Given the input sequence $\{z_n\}$ the output of the FIR filter is

$$v_n = \sum_{k=-K}^{L} f_k z_{n-k}.$$

To obtain such an FIR filter f that best approximates the Wiener filter, we find the coefficients f_k that minimize the quantity $E(|y_n - v_n|^2)$, or, equivalently,

$$\int_{-\pi}^{\pi} |H(\omega) - \sum_{k=-K}^{L} f_k e^{ik\omega}|^2 R_z(\omega) d\omega.$$

(30.4)

The orthogonality principle tells us that the optimal coefficients must satisfy the equations

$$r_s(m) = \sum_{k=-K}^{L} f_k r_z(m-k),$$

(30.5)

for $-K \leq m \leq L$.

In [52] it was pointed out that the linear equations that arise in Wiener-filter approximation also occur in image reconstruction from projections, with the image to be reconstructed playing the role of the power spectrum to be approximated. The methods of Wiener-filter approximation were then used to derive linear and nonlinear image-reconstruction procedures.

30.4   Adaptive Wiener Filters

Once again, we consider a stationary random process $z_n = s_n + v_n$ with autocorrelation function $E(z_n \overline{z_{n-m}}) = r_z(m) = r_s(m) + r_v(m)$. The finite

causal Wiener filter (FCWF) $\mathbf{f} = (f_0, f_1, ..., f_L)^T$ is convolved with $\{z_n\}$ to produce an estimate of s_n given by

$$\hat{s}_n = \sum_{k=0}^{L} f_k z_{n-k}.$$

With $\mathbf{y}_n^{\dagger} = (z_n, z_{n-1}, ..., z_{n-L})$ we can write $\hat{s}_n = \mathbf{y}_n^{\dagger} \mathbf{f}$. The FCWF $\mathbf{f}$ minimizes the expected squared error

$$J(\mathbf{f}) = E(|s_n - \hat{s}_n|^2)$$

and is obtained as the solution of the equations

$$r_s(m) = \sum_{k=0}^{L} f_k r_z(m - k),$$

for $0 \leq m \leq L$. Therefore, to use the FCWF we need the values $r_s(m)$ and $r_z(m - k)$ for m and k in the set $\{0, 1, ..., L\}$. When these autocorrelation values are not known, we can use adaptive methods to approximate the FCWF.

30.4.1 An Adaptive Least-Mean-Square Approach

We assume now that we have $z_0, z_1, ..., z_N$ and $p_0, p_1, ..., p_N$, where p_n is a prior estimate of s_n, but that we do not know the correlation functions r_z and r_s.

The gradient of the function $J(\mathbf{f})$ is

$$\nabla J(\mathbf{f}) = R_{zz}\mathbf{f} - \mathbf{r}_s,$$

where R_{zz} is the square matrix with entries $r_z(m - n)$ and $\mathbf{r}_s$ is the vector with entries $r_s(m)$. An iterative gradient descent method for solving the system of equations $R_{zz}\mathbf{f} = \mathbf{r}_s$ is

$$\mathbf{f}_\tau = \mathbf{f}_{\tau-1} - \mu_\tau \nabla J(\mathbf{f}_{\tau-1}),$$

for some step-size parameters $\mu_\tau > 0$.

The adaptive *least-mean-square* (LMS) approach [66] replaces the gradient of $J(\mathbf{f})$ with an approximation of the gradient of the function $G(\mathbf{f}) = |s_n - \hat{s}_n|^2$, which is $-2(s_n - \hat{s}_n)\mathbf{y}_n$. Since we do not know s_n, we replace that term with the estimate p_n. The iterative step of the LMS method is

$$\mathbf{f}_\tau = \mathbf{f}_{\tau-1} + \mu_\tau (p_\tau - \mathbf{y}_\tau^{\dagger} \mathbf{f}_{\tau-1}) \mathbf{y}_\tau, \tag{30.6}$$

for $L \leq \tau \leq N$. Notice that it is the approximate gradient of the function $|s_\tau - \hat{s}_\tau|^2$ that is used at this step, in order to involve all the data $z_0, ..., z_N$ as we iterate from $\tau = L$ to $\tau = N$. We illustrate the use of this method in adaptive interference cancellation.

30.4.2 Adaptive Interference Cancellation (AIC)

Adaptive interference cancellation (AIC) [224] is used to suppress a dominant noise component v_n in the discrete sequence $z_n = s_n + v_n$. It is assumed that we have available a good estimate q_n of v_n. The main idea is to switch the roles of signal and noise in the adaptive LMS method and design a filter to estimate v_n. Once we have that estimate, we subtract it from z_n to get our estimate of s_n.

In the role of z_n we use

$$q_n = v_n + \epsilon_n,$$

where ϵ_n denotes a low-level error component. In the role of p_n, we take z_n, which is approximately v_n, since the signal s_n is much lower than the noise v_n. Then, $\mathbf{y}_n^\dagger = (q_n, q_{n-1}, ..., q_{n-L})$. The iterative step used to find the filter $\mathbf{f}$ is then

$$\mathbf{f}_\tau = \mathbf{f}_{\tau-1} + \mu_\tau(z_\tau - \mathbf{y}_\tau^\dagger \mathbf{f}_{\tau-1})\mathbf{y}_\tau,$$

for $L \leq \tau \leq N$. When the iterative process has converged to $\mathbf{f}$, we take as our estimate of s_n

$$\hat{s}_n = z_n - \sum_{k=0}^{L} f_k q_{n-k}.$$

It has been suggested that this procedure be used in computerized tomography to correct artifacts due to patient motion [99].

30.4.3 Recursive Least Squares (RLS)

An alternative to the LMS method is to find the least squares solution of the system of $N - L + 1$ linear equations

$$p_n = \sum_{k=0}^{L} f_k z_{n-k},$$

for $L \leq n \leq N$. The *recursive least squares* (RLS) method is a recursive approach to solving this system.

For $L \leq \tau \leq N$ let Z_τ be the matrix whose rows are $\mathbf{y}_n^\dagger$ for $n = L, ..., \tau$, $\mathbf{p}_\tau^T = (p_L, p_{L+1}, ..., p_\tau)$ and $Q_\tau = Z_\tau^\dagger Z_\tau$. The least squares solution we seek is

$$\mathbf{f} = Q_N^{-1} Z_N^\dagger \mathbf{p}_N.$$

Exercise 30.1 *Show that $Q_\tau = Q_{\tau-1} + \mathbf{y}_\tau \mathbf{y}_\tau^\dagger$, for $L < \tau \leq N$.*

Exercise 30.2 *Use the matrix-inversion identity in Equation (29.1) to write Q_τ^{-1} in terms of $Q_{\tau-1}^{-1}$.*

Exercise 30.3 *Using the previous exercise, show that the desired least squares solution $\mathbf{f}$ is $\mathbf{f} = \mathbf{f}_N$, where, for $L \le \tau \le N$ we let*

$$\mathbf{f}_\tau = \mathbf{f}_{\tau-1} + \left(\frac{p_\tau - \mathbf{y}_\tau^\dagger \mathbf{f}_{\tau-1}}{1 + \mathbf{y}_\tau^\dagger Q_{\tau-1}^{-1} \mathbf{y}_\tau}\right) Q_{\tau-1}^{-1} \mathbf{y}_\tau.$$

Comparing this iterative step with that given by Equation (30.6), we see that the former gives an explicit value for μ_τ and uses $Q_{\tau-1}^{-1}\mathbf{y}_\tau$ instead of $\mathbf{y}_\tau$ as the direction vector for the iterative step. The RMS iteration produces a more accurate estimate of the FCWF than does the LMS method, but requires more computation.

Chapter 31

Appendix: Fourier Series and Analytic Functions

31.1 Chapter Summary

We first encounter infinite series expansions for functions in calculus when we study Maclaurin and Taylor series. Fourier series are usually first met in different contexts, such as partial differential equations and boundary value problems. Laurent expansions come later when we study functions of a complex variable. There are, nevertheless, important connections among these different types of infinite series expansions, which provide the subject for this chapter.

31.2 Laurent Series

Suppose that $f(z)$ is analytic in an annulus containing the unit circle $C = \{z \,|\, |z| = 1\}$. Then $f(z)$ has a Laurent series expansion

$$f(z) = \sum_{n=-\infty}^{\infty} f_n z^n$$

valid for z within that annulus. Substituting $z = e^{i\theta}$, we get $f(e^{i\theta})$, also written as $f(\theta)$, defined for θ in the interval $[-\pi, \pi]$ by

$$f(\theta) = f(e^{i\theta}) = \sum_{n=-\infty}^{\infty} f_n e^{in\theta};$$

here the Fourier series for $f(\theta)$ is derived from the Laurent series for the analytic function $f(z)$. If $f(z)$ is actually analytic in $(1 + \epsilon)D$, where

319

$D = \{z | |z| < 1\}$ is the open unit disk, then $f(z)$ has a Taylor series expansion and the Fourier series for $f(\theta)$ contains only terms corresponding to nonnegative n.

31.3 An Example

As an example, consider the rational function

$$f(z) = \frac{1}{z - \frac{1}{2}} - \frac{1}{z - 3} = -\frac{5}{2}/(z - \frac{1}{2})(z - 3).$$

In an annulus containing the unit circle this function has the Laurent series expansion

$$f(z) = \sum_{n=-\infty}^{-1} 2^{n+1} z^n + \sum_{n=0}^{\infty} (\frac{1}{3})^{n+1} z^n;$$

replacing z with $e^{i\theta}$, we obtain the Fourier series for the function $f(\theta) = f(e^{i\theta})$ defined for θ in the interval $[-\pi, \pi]$.

The function $F(z) = 1/f(z)$ is analytic for all complex z, but because it has a root inside the unit circle, its reciprocal, $f(z)$, is not analytic in a disk containing the unit circle. Consequently, the Fourier series for $f(\theta)$ is doubly infinite. We saw in the chapter on complex varables that the function $G(z) = \frac{z - \bar{a}}{1 - az}$ has $|G(e^{i\theta})| = 1$. With $a = 2$ and $H(z) = F(z)G(z)$, we have

$$H(z) = \frac{1}{5}(z - 3)(z - 2),$$

and its reciprocal has the form

$$1/H(z) = \sum_{n=0}^{\infty} a_n z^n.$$

Because

$$G(e^{i\theta})/H(e^{i\theta}) = 1/F(e^{i\theta}),$$

it follows that

$$|1/H(e^{i\theta})| = |1/F(e^{i\theta})| = |f(\theta)|$$

and so

$$|f(\theta)| = |\sum_{n=0}^{\infty} a_n e^{in\theta}|.$$

Multiplication by $G(z)$ permits us to move a root from inside C to outside C without altering the magnitude of the function's values on C.

The relationships between functions defined on C and functions analytic (or harmonic) in D form the core of *harmonic analysis* [135]. The factorization $F(z) = H(z)/G(z)$ above is a special case of the *inner-outer factorization* for functions in Hardy spaces; the function $H(z)$ is an *outer function*, and the functions $G(z)$ and $1/G(z)$ are *inner functions*.

31.4 Fejér-Riesz Factorization

Sometimes we start with an analytic function and restrict it to the unit circle. Other times we start with a function $f(e^{i\theta})$ defined on the unit circle, or, equivalently, a function of the form $f(\theta)$ for θ in $[-\pi, \pi]$, and view this function as the restriction to the unit circle of a function that is analytic in a region containing the unit circle. One application of this idea is the Fejér-Riesz factorization theorem:

Theorem 31.1 *Let $h(e^{i\theta})$ be a finite trigonometric polynomial*

$$h(e^{i\theta}) = \sum_{n=-N}^{N} h_n e^{in\theta},$$

such that $h(e^{i\theta}) \geq 0$ for all θ in the interval $[-\pi, \pi]$. Then there is

$$y(z) = \sum_{n=0}^{N} y_n z^n$$

with $h(e^{i\theta}) = |y(e^{i\theta})|^2$. The function $y(z)$ is unique if we require, in addition, that all its roots be outside D.

To prove this theorem we consider the function

$$h(z) = \sum_{n=-N}^{N} h_n z^n,$$

which is analytic in an annulus containing the unit circle. The rest of the proof is contained in the following exercise.

Exercise 31.1 *Use the fact that $h_{-n} = \overline{h}_n$ to show that z_j is a root of $h(z)$ if and only if $1/\overline{z}_j$ is also a root. From the nonnegativity of $h(e^{i\theta})$, conclude that if $h(z)$ has a root on the unit circle then it has even multiplicity. Take $y(z)$ to be proportional to the product of factors $z - z_j$ for all the z_j outside D; for roots on C, include them with half their multiplicities.*

31.5 Burg Entropy

The Fejér-Riesz theorem is used in the derivation of Burg's maximum entropy method for spectrum estimation. The problem there is to estimate a function $R(\theta) > 0$ knowing only the values

$$r_n = \frac{1}{2\pi} \int_{-\pi}^{\pi} R(\theta) e^{-in\theta} d\theta,$$

for $|n| \leq N$. The approach is to estimate $R(\theta)$ by the function $S(\theta) > 0$ that maximizes the so-called Burg entropy, $\int_{-\pi}^{\pi} \log S(\theta) d\theta$, subject to the data constraints.

The Euler-Lagrange equation from the calculus of variations allows us to conclude that $S(\theta)$ has the form

$$S(\theta) = 1 / \sum_{n=-N}^{N} h_n e^{in\theta}.$$

The function

$$h(\theta) = \sum_{n=-N}^{N} h_n e^{in\theta}$$

is nonnegative, so, by the Fejér-Riesz theorem, it factors as $h(\theta) = |y(\theta)|^2$. We then have $S(\theta)\overline{y(\theta)} = 1/y(\theta)$. Since all the roots of $y(z)$ lie outside D and none are on C, the function $1/y(z)$ is analytic in a region containing C and D so it has a Taylor series expansion in that region. Restricting this Taylor series to C, we obtain a one-sided Fourier series having zero terms for the negative indices.

Exercise 31.2 *Show that the coefficients y_n in $y(z)$ satisfy a system of linear equations whose coefficients are the r_n.*

Hint: Compare the coefficients of the terms on both sides of the equation $S(\theta)\overline{y}(\theta) = 1/y(\theta)$ that correspond to negative indices.

Chapter 32

Appendix: Inverse Problems and the Laplace Transform

32.1 Chapter Summary

In the farfield propagation examples considered previously, we found the measured data to be related to the desired object function by a Fourier transformation. The image reconstruction problem then became one of estimating a function from finitely many noisy values of its Fourier transform. In this chapter we consider two inverse problems involving the Laplace transform.

32.2 The Laplace Transform and the Ozone Layer

The example is taken from Twomey's book [218].

32.2.1 The Laplace Transform

The Laplace transform of the function $f(x)$ defined for $0 \leq x < +\infty$ is the function

$$\mathcal{F}(s) = \int_0^{+\infty} f(x)e^{-sx}dx. \qquad (32.1)$$

32.2.2 Scattering of Ultraviolet Radiation

The sun emits ultraviolet (UV) radiation that enters the Earth's atmosphere at an angle θ_0 that depends on the sun's position, and with intensity $I(0)$. Let the x-axis be vertical, with $x = 0$ at the top of the atmosphere and x increasing as we move down to the Earth's surface, at $x = X$. The intensity at x is given by

$$I(x) = I(0)e^{-kx/\cos\theta_0}. \tag{32.2}$$

Within the ozone layer, the amount of UV radiation scattered in the direction θ is given by

$$S(\theta, \theta_0)I(0)e^{-kx/\cos\theta_0}\Delta p, \tag{32.3}$$

where $S(\theta, \theta_0)$ is a known parameter, and Δp is the change in the pressure of the ozone within the infinitesimal layer $[x, x + \Delta x]$, and so is proportional to the concentration of ozone within that layer.

32.2.3 Measuring the Scattered Intensity

The radiation scattered at the angle θ then travels to the ground, a distance of $X - x$, weakened along the way, and reaches the ground with intensity

$$S(\theta, \theta_0)I(0)e^{-kx/\cos\theta_0}e^{-k(X-x)/\cos\theta}\Delta p. \tag{32.4}$$

The total scattered intensity at angle θ is then a superposition of the intensities due to scattering at each of the thin layers, and is then

$$S(\theta, \theta_0)I(0)e^{-kX/\cos\theta_0}\int_0^X e^{-x\beta}dp, \tag{32.5}$$

where

$$\beta = k[\frac{1}{\cos\theta_0} - \frac{1}{\cos\theta}]. \tag{32.6}$$

This superposition of intensity can then be written as

$$S(\theta, \theta_0)I(0)e^{-kX/\cos\theta_0}\int_0^X e^{-x\beta}p'(x)dx. \tag{32.7}$$

32.2.4 The Laplace Transform Data

Using integration by parts, we get

$$\int_0^X e^{-x\beta}p'(x)dx = p(X)e^{-\beta X} - p(0) + \beta\int_0^X e^{-\beta x}p(x)dx. \tag{32.8}$$

Since $p(0) = 0$ and $p(X)$ can be measured, our data is then the Laplace transform value

$$\int_0^{+\infty} e^{-\beta x} p(x) dx; \tag{32.9}$$

note that we can replace the upper limit X with $+\infty$ if we extend $p(x)$ as zero beyond $x = X$.

The variable β depends on the two angles θ and θ_0. We can alter θ as we measure and θ_0 changes as the sun moves relative to the earth. In this way we get values of the Laplace transform of $p(x)$ for various values of β. The problem then is to recover $p(x)$ from these values. Because the Laplace transform involves a smoothing of the function $p(x)$, recovering $p(x)$ from its Laplace transform is more ill-conditioned than is the Fourier transform inversion problem.

32.3 The Laplace Transform and Energy Spectral Estimation

In x-ray transmission tomography, x-ray beams are sent through the object and the drop in intensity is measured. These measurements are then used to estimate the distribution of attenuating material within the object. A typical x-ray beam contains components with different energy levels. Because components at different energy levels will be attenuated differently, it is important to know the relative contribution of each energy level to the entering beam. The energy spectrum is the function $f(E)$ that describes the intensity of the components at each energy level $E > 0$.

32.3.1 The Attenuation Coefficient Function

Each specific material, say aluminum, for example, is associated with attenuation coefficients, which is a function of energy, which we shall denote by $\mu(E)$. A beam with the single energy E passing through a thickness x of the material will be weakened by the factor $e^{-\mu(E)x}$. By passing the beam through various thicknesses x of aluminum and registering the intensity drops, one obtains values of the absorption function

$$R(x) = \int_0^\infty f(E) e^{-\mu(E)x} dE. \tag{32.10}$$

Using a change of variable, we can write $R(x)$ as a Laplace transform.

32.3.2 The Absorption Function as a Laplace Transform

For each material, the attenuation function $\mu(E)$ is a strictly decreasing function of E, so $\mu(E)$ has an inverse, which we denote by g; that is, $g(t) = E$, for $t = \mu(E)$. Equation (32.10) can then be rewritten as

$$R(x) = \int_0^\infty f(g(t))e^{-tx}g'(t)dt. \tag{32.11}$$

We see then that $R(x)$ is the Laplace transform of the function $r(t) = f(g(t))g'(t)$. Our measurements of the intensity drops provide values of $R(x)$, for various values of x, from which we must estimate the functions $r(t)$, and, ultimately, $f(E)$.

Chapter 33

Appendix: Matrix Theory

33.1 Chapter Summary

Matrices and their algebraic properties play an ever-increasing role in signal processing. In this chapter we outline the most important of these properties.

33.2 Matrix Inverses

A square matrix A is said to have inverse A^{-1} provided that

$$AA^{-1} = A^{-1}A = I,$$

where I is the identity matrix. The 2 by 2 matrix $A = \begin{bmatrix} a & b \\ c & d \end{bmatrix}$ has an inverse

$$A^{-1} = \frac{1}{ad - bc} \begin{bmatrix} d & -b \\ -c & a \end{bmatrix}$$

whenever the *determinant* of A, $\det(A) = ad - bc$ is not zero. More generally, associated with every complex square matrix is the complex number called its determinant, which is obtained from the entries of the matrix using formulas that can be found in any text on linear algebra. The significance of the determinant is that the matrix is invertible if and only if its determinant is not zero. This is of more theoretical than practical importance, since no computer can tell when a number is precisely zero. A matrix A that is not square cannot have an inverse, but does have a *pseudo-inverse*, which is found using the singular-value decomposition.

33.3   Basic Linear Algebra

In this section we discuss systems of linear equations, Gaussian elimination, and the notions of basic and non-basic variables.

33.3.1   Bases and Dimension

The notions of a basis and of linear independence are fundamental in linear algebra. Let $\mathcal{V}$ be a vector space.

Definition 33.1 *A collection of vectors $\{u^1, ..., u^N\}$ in $\mathcal{V}$ is* linearly independent *if there is no choice of scalars $\alpha_1, ..., \alpha_N$, not all zero, such that*

$$0 = \alpha_1 u^1 + ... + \alpha_N u^N. \tag{33.1}$$

Definition 33.2 *The* span *of a collection of vectors $\{u^1, ..., u^N\}$ in $\mathcal{V}$ is the set of all vectors x that can be written as linear combinations of the u^n; that is, for which there are scalars $c_1, ..., c_N$, such that*

$$x = c_1 u^1 + ... + c_N u^N. \tag{33.2}$$

Definition 33.3 *A collection of vectors $\{w^1, ..., w^N\}$ in $\mathcal{V}$ is called a* spanning set *for a subspace S if the set S is their span.*

Definition 33.4 *A collection of vectors $\{u^1, ..., u^N\}$ in $\mathcal{V}$ is called a* basis *for a subspace S if the collection is linearly independent and S is their span.*

Definition 33.5 *A collection of vectors $\{u^1, ..., u^N\}$ in an inner product space $\mathcal{V}$ is called* orthonormal *if $||u^n||_2 = 1$, for all n, and $\langle u^m, u^n \rangle = 0$, for $m \neq n$.*

   Suppose that S is a subspace of $\mathcal{V}$, that $\{w^1, ..., w^N\}$ is a spanning set for S, and $\{u^1, ..., u^M\}$ is a linearly independent subset of S. Beginning with w^1, we augment the set $\{u^1, ..., u^M\}$ with w^j if w^j is not in the span of the u^m and the w^k previously included. At the end of this process, we have a linearly independent spanning set, and therefore, a basis, for S (Why?). Similarly, beginning with w^1, we remove w^j from the set $\{w^1, ..., w^N\}$ if w^j is a linear combination of the w^k, $k = 1, ..., j - 1$. In this way we obtain a linearly independent set that spans S, hence another basis for S. The following lemma will allow us to prove that all bases for a subspace S have the same number of elements.

Lemma 33.1 *Let $W = \{w^1, ..., w^N\}$ be a spanning set for a subspace S in R^I, and $V = \{v^1, ..., v^M\}$ a linearly independent subset of S. Then $M \leq N$.*

Proof: Suppose that $M > N$. Let $B_0 = \{w^1, ..., w^N\}$. To obtain the set B_1, form the set $C_1 = \{v^1, w^1, ..., w^N\}$ and remove the first member of C_1 that is a linear combination of members of C_1 that occur to its left in the listing; since v^1 has no members to its left, it is not removed. Since W is a spanning set, v^1 is a linear combination of the members of W, so that some member of W is a linear combination of v^1 and the members of W that precede it in the list; remove the first member of W for which this is true.

We note that the set B_1 is a spanning set for S and has N members. Having obtained the spanning set B_k, with N members and whose first k members are $v^k, ..., v^1$, we form the set $C_{k+1} = B_k \cup \{v^{k+1}\}$, listing the members so that the first $k+1$ of them are $\{v^{k+1}, v^k, ..., v^1\}$. To get the set B_{k+1} we remove the first member of C_{k+1} that is a linear combination of the members to its left; there must be one, since B_k is a spanning set, and so v^{k+1} is a linear combination of the members of B_k. Since the set V is linearly independent, the member removed is from the set W. Continuing in this fashion, we obtain a sequence of spanning sets $B_1, ..., B_N$, each with N members. The set B_N is $B_N = \{v^1, ..., v^N\}$ and v^{N+1} must then be a linear combination of the members of B_N, which contradicts the linear independence of V. ∎

Corollary 33.1 *Every basis for a subspace S has the same number of elements.*

Exercise 33.1 *Let $W = \{w^1, ..., w^N\}$ be a spanning set for a subspace S in R^I, and $V = \{v^1, ..., v^M\}$ a linearly independent subset of S. Let A be the matrix whose columns are the v^m, B the matrix whose columns are the w^n. Show that there is an N by M matrix C such that $A = BC$. Prove Lemma 33.1 by showing that, if $M > N$, then there is a non-zero vector x with $Cx = Ax = 0$.*

Definition 33.6 *The* dimension *of a subspace S is the number of elements in any basis.*

Lemma 33.2 *For any matrix A, the maximum number of linearly independent rows equals the maximum number of linearly independent columns.*

Proof: Suppose that A is an I by J matrix, and that $K \leq J$ is the maximum number of linearly independent columns of A. Select K linearly independent columns of A and use them as the K columns of an I by K matrix U. Since every column of A must be a linear combination of these K selected ones, there is a K by J matrix M such that $A = UM$. From $A^T = M^T U^T$ we conclude that every column of A^T is a linear combination of the K columns of the matrix M^T. Therefore, there can be at most K linearly independent columns of A^T. ∎

Definition 33.7 *The* rank *of A is the maximum number of linearly independent rows or of linearly independent columns of A.*

33.3.2   Systems of Linear Equations

Consider the system of three linear equations in five unknowns given by

$$
\begin{array}{rrrrrl}
x_1 & +2x_2 & & +2x_4 & +x_5 & = 0 \\
-x_1 & -x_2 & +x_3 & +x_4 & & = 0 \, . \\
x_1 & +2x_2 & -3x_3 & -x_4 & -2x_5 & = 0
\end{array}
\tag{33.3}
$$

This system can be written in matrix form as $Ax = 0$, with A the coefficient matrix

$$
A = \begin{bmatrix}
1 & 2 & 0 & 2 & 1 \\
-1 & -1 & 1 & 1 & 0 \\
1 & 2 & -3 & -1 & -2
\end{bmatrix},
\tag{33.4}
$$

and $x = (x_1, x_2, x_3, x_4, x_5)^T$. Applying Gaussian elimination to this system, we obtain a second, simpler, system with the same solutions:

$$
\begin{array}{rrrrl}
x_1 & & -2x_4 & +x_5 & = 0 \\
& x_2 & +2x_4 & & = 0 \, . \\
& & x_3 & +x_4 & +x_5 & = 0
\end{array}
\tag{33.5}
$$

From this simpler system we see that the variables x_4 and x_5 can be freely chosen, with the other three variables then determined by this system of equations. The variables x_4 and x_5 are then independent, the others dependent. The variables x_1, x_2 and x_3 are then called *basic variables*. To obtain a basis of solutions we can let $x_4 = 1$ and $x_5 = 0$, obtaining the solution $x = (2, -2, -1, 1, 0)^T$, and then choose $x_4 = 0$ and $x_5 = 1$ to get the solution $x = (-1, 0, -1, 0, 1)^T$. Every solution to $Ax = 0$ is then a linear combination of these two solutions. Notice that which variables are basic and which are non-basic is somewhat arbitrary, in that we could have chosen as the non-basic variables any two whose columns are independent.

Having decided that x_4 and x_5 are the non-basic variables, we can write the original matrix A as $A = \begin{bmatrix} B & N \end{bmatrix}$, where B is the square invertible matrix

$$
B = \begin{bmatrix}
1 & 2 & 0 \\
-1 & -1 & 1 \\
1 & 2 & -3
\end{bmatrix},
\tag{33.6}
$$

and N is the matrix

$$
N = \begin{bmatrix}
2 & 1 \\
1 & 0 \\
-1 & -2
\end{bmatrix}.
\tag{33.7}
$$

With $x_B = (x_1, x_2, x_3)^T$ and $x_N = (x_4, x_5)^T$ we can write

$$Ax = Bx_B + Nx_N = 0, \qquad (33.8)$$

so that

$$x_B = -B^{-1} N x_N. \qquad (33.9)$$

33.3.3 Real and Complex Systems of Linear Equations

A system $Ax = b$ of linear equations is called a *complex system*, or a *real system* if the entries of A, x and b are complex, or real, respectively. For any matrix A, we denote by A^T and $A^\dagger$ the transpose and conjugate transpose of A, respectively.

Any complex system can be converted to a real system in the following way. A complex matrix A can be written as $A = A_1 + iA_2$, where A_1 and A_2 are real matrices and $i = \sqrt{-1}$. Similarly, $x = x^1 + ix^2$ and $b = b^1 + ib^2$, where x^1, x^2, b^1 and b^2 are real vectors. Denote by $\tilde{A}$ the real matrix

$$\tilde{A} = \begin{bmatrix} A_1 & -A_2 \\ A_2 & A_1 \end{bmatrix}, \qquad (33.10)$$

by $\tilde{x}$ the real vector

$$\tilde{x} = \begin{bmatrix} x^1 \\ x^2 \end{bmatrix}, \qquad (33.11)$$

and by $\tilde{b}$ the real vector

$$\tilde{b} = \begin{bmatrix} b^1 \\ b^2 \end{bmatrix}. \qquad (33.12)$$

Then x satisfies the system $Ax = b$ if and only if $\tilde{x}$ satisfies the system $\tilde{A}\tilde{x} = \tilde{b}$.

Definition 33.8 *A square matrix A is* symmetric *if $A^T = A$ and* Hermitian *if $A^\dagger = A$.*

Definition 33.9 *A non-zero vector x is said to be an* eigenvector *of the square matrix A if there is a scalar λ such that $Ax = \lambda x$. Then λ is said to be an* eigenvalue *of A.*

If x is an eigenvector of A with eigenvalue λ, then the matrix $A - \lambda I$ has no inverse, so its determinant is zero; here I is the identity matrix with ones on the main diagonal and zeros elsewhere. Solving for the roots of the

determinant is one way to calculate the eigenvalues of A. For example, the eigenvalues of the Hermitian matrix

$$B = \begin{bmatrix} 1 & 2+i \\ 2-i & 1 \end{bmatrix} \tag{33.13}$$

are $\lambda = 1 + \sqrt{5}$ and $\lambda = 1 - \sqrt{5}$, with corresponding eigenvectors $u = (\sqrt{5}, 2 - i)^T$ and $v = (\sqrt{5}, i - 2)^T$, respectively. Then $\tilde{B}$ has the same eigenvalues, but both with multiplicity two. Finally, the associated eigenvectors of $\tilde{B}$ are

$$\begin{bmatrix} u^1 \\ u^2 \end{bmatrix}, \tag{33.14}$$

and

$$\begin{bmatrix} -u^2 \\ u^1 \end{bmatrix}, \tag{33.15}$$

for $\lambda = 1 + \sqrt{5}$, and

$$\begin{bmatrix} v^1 \\ v^2 \end{bmatrix}, \tag{33.16}$$

and

$$\begin{bmatrix} -v^2 \\ v^1 \end{bmatrix}, \tag{33.17}$$

for $\lambda = 1 - \sqrt{5}$.

33.4   Solutions of Under-determined Systems of Linear Equations

Suppose that $A\mathbf{x} = \mathbf{b}$ is a consistent linear system of M equations in N unknowns, where $M < N$. Then there are infinitely many solutions. A standard procedure in such cases is to find that solution $\mathbf{x}$ having the smallest norm

$$||\mathbf{x}|| = \sqrt{\sum_{n=1}^{N} |x_n|^2}.$$

As we shall see shortly, the *minimum norm* solution of $A\mathbf{x} = \mathbf{b}$ is a vector of the form $\mathbf{x} = A^\dagger \mathbf{z}$, where $A^\dagger$ denotes the conjugate transpose of the matrix A. Then $A\mathbf{x} = \mathbf{b}$ becomes $AA^\dagger \mathbf{z} = \mathbf{b}$. Typically, $(AA^\dagger)^{-1}$ will exist, and we get $\mathbf{z} = (AA^\dagger)^{-1}\mathbf{b}$, from which it follows that the minimum

norm solution is $\mathbf{x} = A^\dagger (AA^\dagger)^{-1}\mathbf{b}$. When M and N are not too large, forming the matrix $AA^\dagger$ and solving for $\mathbf{z}$ is not prohibitively expensive and time-consuming. However, in image processing the vector $\mathbf{x}$ is often a vectorization of a two-dimensional (or even three-dimensional) image and M and N can be on the order of tens of thousands or more. The ART algorithm gives us a fast method for finding the minimum norm solution without computing $AA^\dagger$.

We begin by proving that the minimum norm solution of $A\mathbf{x} = \mathbf{b}$ has the form $\mathbf{x} = A^\dagger \mathbf{z}$ for some M-dimensional complex vector $\mathbf{z}$.

Let the *null space* of the matrix A be all N-dimensional complex vectors $\mathbf{w}$ with $A\mathbf{w} = \mathbf{0}$. If $A\mathbf{x} = \mathbf{b}$ then $A(\mathbf{x} + \mathbf{w}) = \mathbf{b}$ for all $\mathbf{w}$ in the null space of A. If $\mathbf{x} = A^\dagger \mathbf{z}$ and $\mathbf{w}$ is in the null space of A, then

$$||\mathbf{x} + \mathbf{w}||^2 = ||A^\dagger \mathbf{z} + \mathbf{w}||^2 = (A^\dagger \mathbf{z} + \mathbf{w})^\dagger (A^\dagger \mathbf{z} + \mathbf{w})$$

$$= (A^\dagger \mathbf{z})^\dagger (A^\dagger \mathbf{z}) + (A^\dagger \mathbf{z})^\dagger \mathbf{w} + \mathbf{w}^\dagger (A^\dagger \mathbf{z}) + \mathbf{w}^\dagger \mathbf{w}$$

$$= ||A^\dagger \mathbf{z}||^2 + (A^\dagger \mathbf{z})^\dagger \mathbf{w} + \mathbf{w}^\dagger (A^\dagger \mathbf{z}) + ||\mathbf{w}||^2$$

$$= ||A^\dagger \mathbf{z}||^2 + ||\mathbf{w}||^2,$$

since

$$\mathbf{w}^\dagger (A^\dagger \mathbf{z}) = (A\mathbf{w})^\dagger \mathbf{z} = \mathbf{0}^\dagger \mathbf{z} = 0$$

and

$$(A^\dagger \mathbf{z})^\dagger \mathbf{w} = \mathbf{z}^\dagger A\mathbf{w} = \mathbf{z}^\dagger \mathbf{0} = 0.$$

Therefore, $||\mathbf{x} + \mathbf{w}|| = ||A^\dagger \mathbf{z} + \mathbf{w}|| > ||A^\dagger \mathbf{z}|| = ||\mathbf{x}||$ unless $\mathbf{w} = \mathbf{0}$. This completes the proof.

Exercise 33.2 *Show that if $\mathbf{z} = (z_1, ..., z_N)^T$ is a column vector with complex entries and $H = H^\dagger$ is an N by N Hermitian matrix with complex entries then the quadratic form $\mathbf{z}^\dagger H\mathbf{z}$ is a real number. Show that the quadratic form $\mathbf{z}^\dagger H\mathbf{z}$ can be calculated using only real numbers. Let $\mathbf{z} = \mathbf{x} + i\mathbf{y}$, with $\mathbf{x}$ and $\mathbf{y}$ real vectors and let $H = A + iB$, where A and B are real matrices. Then show that $A^T = A$, $B^T = -B$, $\mathbf{x}^T B\mathbf{x} = 0$ and finally,*

$$\mathbf{z}^\dagger H\mathbf{z} = [\,\mathbf{x}^T \quad \mathbf{y}^T\,] \begin{bmatrix} A & -B \\ B & A \end{bmatrix} \begin{bmatrix} \mathbf{x} \\ \mathbf{y} \end{bmatrix}.$$

Use the fact that $\mathbf{z}^\dagger H\mathbf{z}$ is real for every vector $\mathbf{z}$ to conclude that the eigenvalues of H are real.

33.5   Eigenvalues and Eigenvectors

Given N by N complex matrix A, we say that a complex number λ is an *eigenvalue* of A if there is a nonzero vector $\mathbf{u}$ with $A\mathbf{u} = \lambda\mathbf{u}$. The column vector $\mathbf{u}$ is then called an *eigenvector* of A associated with eigenvalue λ; clearly, if $\mathbf{u}$ is an eigenvector of A, then so is $c\mathbf{u}$, for any constant $c \neq 0$. If λ is an eigenvalue of A, then the matrix $A - \lambda I$ fails to have an inverse, since $(A - \lambda I)\mathbf{u} = \mathbf{0}$ but $\mathbf{u} \neq \mathbf{0}$. If we treat λ as a variable and compute the determinant of $A - \lambda I$, we obtain a polynomial of degree N in λ. Its roots $\lambda_1, ..., \lambda_N$ are then the eigenvalues of A. If $||\mathbf{u}||^2 = \mathbf{u}^\dagger \mathbf{u} = 1$ then $\mathbf{u}^\dagger A\mathbf{u} = \lambda\mathbf{u}^\dagger\mathbf{u} = \lambda$.

It can be shown that it is possible to find a set of N mutually orthogonal eigenvectors of the Hermitian matrix H; call them $\{\mathbf{u}^1, ..., \mathbf{u}^N\}$. The matrix H can then be written as

$$H = \sum_{n=1}^{N} \lambda_n \mathbf{u}^n (\mathbf{u}^n)^\dagger,$$

a linear superposition of the *dyad* matrices $\mathbf{u}^n(\mathbf{u}^n)^\dagger$. We can also write $H = ULU^\dagger$, where U is the matrix whose nth column is the column vector $\mathbf{u}^n$ and L is the diagonal matrix with the eigenvalues down the main diagonal and zero elsewhere.

The matrix H is invertible if and only if none of the λ are zero and its inverse is

$$H^{-1} = \sum_{n=1}^{N} \lambda_n^{-1} \mathbf{u}^n (\mathbf{u}^n)^\dagger.$$

We also have $H^{-1} = UL^{-1}U^\dagger$.

A Hermitian matrix Q is said to be nonnegative-definite (positive-definite) if all the eigenvalues of Q are nonnegative (positive). The matrix Q is a nonnegative-definite matrix if and only if there is another matrix C such that $Q = C^\dagger C$. Since the eigenvalues of Q are nonnegative, the diagonal matrix L has a square root, $\sqrt{L}$. Using the fact that $U^\dagger U = I$, we have

$$Q = ULU^\dagger = U\sqrt{L}U^\dagger U\sqrt{L}U^\dagger;$$

we then take $C = U\sqrt{L}U^\dagger$, so $C^\dagger = C$. Then $\mathbf{z}^\dagger Q\mathbf{z} = \mathbf{z}^\dagger C^\dagger C\mathbf{z} = ||C\mathbf{z}||^2$, so that Q is positive-definite if and only if C is invertible.

Exercise 33.3 *Let A be an M by N matrix with complex entries. View A as a linear function with domain C^N, the space of all N-dimensional complex column vectors, and range contained within C^M, via the expression $A(\mathbf{x}) = A\mathbf{x}$. Suppose that $M > N$. The range of A, denoted $R(A)$, cannot be all of C^M. Show that every vector $\mathbf{z}$ in C^M can be written uniquely in*

the form $\mathbf{z} = A\mathbf{x} + \mathbf{w}$, *where* $A^\dagger \mathbf{w} = \mathbf{0}$. *Show that* $\|\mathbf{z}\|^2 = \|A\mathbf{x}\|^2 + \|\mathbf{w}\|^2$, *where* $\|\mathbf{z}\|^2$ *denotes the square of the norm of* $\mathbf{z}$.

Hint: If $\mathbf{z} = A\mathbf{x} + \mathbf{w}$ then consider $A^\dagger \mathbf{z}$. Assume $A^\dagger A$ is invertible.

33.6   Vectorization of a Matrix

When the complex M by N matrix A is stored in the computer it is usually *vectorized*; that is, the matrix

$$A = \begin{bmatrix} A_{11} & A_{12} & \ldots & A_{1N} \\ A_{21} & A_{22} & \ldots & A_{2N} \\ . & & & \\ . & & & \\ . & & & \\ A_{M1} & A_{M2} & \ldots & A_{MN} \end{bmatrix}$$

becomes

$$\mathbf{vec}(A) = (A_{11}, A_{21}, ..., A_{M1}, A_{12}, A_{22}, ..., A_{M2}, ..., A_{MN})^T.$$

Exercise 33.4 (a) *Show that the complex dot product* $\mathbf{vec}(A) \cdot \mathbf{vec}(B) = \mathbf{vec}(B)^\dagger \mathbf{vec}(A)$ *can be obtained by*

$$\mathbf{vec}(A) \cdot \mathbf{vec}(B) = \text{trace}\,(AB^\dagger) = tr(AB^\dagger),$$

where, for a square matrix C, *trace*$\,(C)$ *means the sum of the entries along the main diagonal of* C. *We can therefore use the trace to define an inner product between matrices:* $< A, B >= \text{trace}\,(AB^\dagger)$.

(b) *Show that* $\text{trace}\,(AA^\dagger) \geq 0$ *for all* A, *so that we can use the trace to define a norm on matrices:* $||A||^2 = \text{trace}\,(AA^\dagger)$.

Exercise 33.5 *Let* $B = ULD^\dagger$ *be an* M *by* N *matrix in diagonalized form; that is,* L *is an* M *by* N *diagonal matrix with entries* $\lambda_1, ..., \lambda_K$ *on its main diagonal, where* $K = \min(M, N)$, *and* U *and* V *are square matrices. Let the n-th column of* U *be denoted* $\mathbf{u}^n$ *and similarly for the columns of* V. *Such a diagonal decomposition occurs in the singular value decomposition (SVD). Show that we can write*

$$B = \lambda_1 \mathbf{u}^1 (\mathbf{v}^1)^\dagger + ... + \lambda_K \mathbf{u}^K (\mathbf{v}^K)^\dagger.$$

If B is an N by N Hermitian matrix, then we can take $U = V$ and $K = M = N$, with the columns of U the eigenvectors of B, normalized to have Euclidean norm equal to one, and the λ_n to be the eigenvalues of B. In this case we may also assume that U is a *unitary* matrix; that is, $UU^\dagger = U^\dagger U = I$, where I denotes the identity matrix.

33.7   The Singular Value Decomposition (SVD)

We have just seen that an N by N Hermitian matrix H can be written in terms of its eigenvalues and eigenvectors as $H = ULU^\dagger$ or as

$$H = \sum_{n=1}^{N} \lambda_n \mathbf{u}^n (\mathbf{u}^n)^\dagger.$$

The *singular value decomposition* (SVD) is a similar result that applies to any rectangular matrix. It is an important tool in image compression and pseudo-inversion.

33.7.1   The SVD

Let C be any N by K complex matrix. In presenting the SVD of C we shall assume that $K \geq N$; the SVD of $C^\dagger$ will come from that of C. Let $A = C^\dagger C$ and $B = CC^\dagger$; we assume, reasonably, that B, the smaller of the two matrices, is invertible, so all the eigenvalues $\lambda_1, ..., \lambda_N$ of B are positive. Then, write the eigenvalue/eigenvector decomposition of B as $B = ULU^\dagger$.

Exercise 33.6 *Show that the nonzero eigenvalues of A and B are the same.*

Let V be the K by K matrix whose first N columns are those of the matrix $C^\dagger U L^{-1/2}$ and whose remaining $K - N$ columns are any mutually orthogonal norm-one vectors that are all orthogonal to each of the first N columns. Let M be the N by K matrix with diagonal entries $M_{nn} = \sqrt{\lambda_n}$ for $n = 1, ..., N$ and whose remaining entries are zero. The nonzero entries of M, $\sqrt{\lambda_n}$, are called the *singular values* of C. The *singular value decomposition* (SVD) of C is $C = UMV^\dagger$. The SVD of $C^\dagger$ is $C^\dagger = VM^T U^\dagger$.

Exercise 33.7 *Show that $UMV^\dagger$ equals C.*

Using the SVD of C we can write

$$C = \sum_{n=1}^{N} \sqrt{\lambda_n} \mathbf{u}^n (\mathbf{v}^n)^{\dagger}, \tag{33.18}$$

where $\mathbf{v}^n$ denotes the nth column of the matrix V.

33.7.2 Using the SVD in Image Compression

In image processing, matrices such as C are used to represent discrete two-dimensional images, with the entries of C corresponding to the grey level or color at each pixel. It is common to find that most of the N singular values of C are nearly zero, so that C can be written approximately as a sum of far fewer than N dyads; this is SVD image compression.

Figures 33.1 and 33.2 illustrate what can be achieved with SVD compression. In both Figure the original is in the upper left. It is a 128 by 128 digitized image, so $M = 128$. In the images that follow, the number of terms retained in the sum in Equation (33.18) is, first, 2, then 4, 6, 8, 10, 20 and finally 30. The full sum has 128 terms, remember. In Figure 33.1 the text is nearly readable using only 10 terms, and certainly could be made perfectly readable with suitable software, so storing just this compressed image would be acceptable. In Figure 33.2, an image of a satellite, we get a fairly good idea of the general shape of the object from the beginning, with only two terms.

33.7.3 An Application in Space Exploration

The *Galileo* was deployed from the space shuttle *Atlantis* on October 18, 1989. After a detour around Venus and back past Earth to pick up gravity-assisted speed, *Galileo* headed for Jupiter. Its mission included a study of Jupiter's moon Europa, and the plan was to send back one high-resolution photo per minute, at a rate of 134 KB per second, via a huge high-gain antenna. When the time came to open the antenna, it stuck. Without the pictures, the mission would be a failure.

There was a much smaller *low-gain* antenna on board, but the best transmission rate was going to be ten bits per second. All that could be done from earth was to reprogram an old on-board computer to compress the pictures prior to transmission. The problem was that pictures could be taken much faster than they could be transmitted to earth; some way to store them prior to transmission was key. The original designers of the software had long since retired, but the engineers figured out a way to introduce state-of-the art image compression algorithms into the computer. It happened that there was an ancient reel-to-reel storage device on board that was there only to serve as a backup for storing atmospheric data.

Using this device and the compression methods, the engineers saved the mission [12].

33.7.4   Pseudo-Inversion

If $N \neq K$ then C cannot have an inverse; it does, however, have a *pseudo-inverse*, $C^* = V M^* U^\dagger$, where M^* is the matrix obtained from M by taking the inverse of each of its nonzero entries and leaving the remaining zeros the same. The pseudo-inverse of $C^\dagger$ is

$$(C^\dagger)^* = (C^*)^\dagger = U(M^*)^T V^\dagger = U(M^\dagger)^* V^\dagger.$$

Some important properties of the pseudo-inverse are the following:

1. $CC^*C = C$,

2. $C^*CC^* = C^*$,

3. $(C^*C)^\dagger = C^*C$,

4. $(CC^*)^\dagger = CC^*$.

The pseudo-inverse of an arbitrary I by J matrix G can be used in much the same way as the inverse of nonsingular matrices to find approximate or exact solutions of systems of equations $G\mathbf{x} = \mathbf{d}$. The following examples illustrate this point.

Exercise 33.8 *If $I > J$ the system $G\mathbf{x} = \mathbf{d}$ probably has no exact solution. Show that whenever $G^\dagger G$ is invertible the pseudo-inverse of G is $G^* = (G^\dagger G)^{-1} G^\dagger$ so that the vector $\mathbf{x} = G^*\mathbf{d}$ is the least squares approximate solution.*

Exercise 33.9 *If $I < J$ the system $G\mathbf{x} = \mathbf{d}$ probably has infinitely many solutions. Show that whenever the matrix $GG^\dagger$ is invertible the pseudo-inverse of G is $G^* = G^\dagger (GG^\dagger)^{-1}$, so that the vector $\mathbf{x} = G^*\mathbf{d}$ is the exact solution of $G\mathbf{x} = \mathbf{d}$ closest to the origin; that is, it is the minimum norm solution.*

33.8 Singular Values of Sparse Matrices

In image reconstruction from projections the M by N matrix A is usually quite large and often ϵ-sparse; that is, most of its elements do not exceed ϵ in absolute value, where ϵ denotes a small positive quantity. In transmission tomography each column of A corresponds to a single pixel in the digitized image, while each row of A corresponds to a line segment through the object, along which an x-ray beam has traveled. The entries of a given row of A are nonzero only for those columns whose associated pixel lies on that line segment; clearly, most of the entries of any given row of A will then be zero. In emission tomography the I by J nonnegative matrix P has entries $P_{ij} \geq 0$; for each detector i and pixel j, P_{ij} is the probability that an emission at the jth pixel will be detected at the ith detector. When a detection is recorded at the ith detector, we want the likely source of the emission to be one of only a small number of pixels. For single photon emission tomography (SPECT), a lead collimator is used to permit detection of only those photons approaching the detector straight on. In positron emission tomography (PET), coincidence detection serves much the same purpose. In both cases the probabilities P_{ij} will be zero (or nearly zero) for most combinations of i and j. Such matrices are called *sparse* (or *almost sparse*). We discuss now a convenient estimate for the largest singular value of an almost sparse matrix A, which, for notational convenience only, we take to be real.

In [44] it was shown that if A is normalized so that each row has length one, then the spectral radius of $A^T A$, which is the square of the largest singular value of A itself, does not exceed the maximum number of nonzero elements in any column of A. A similar upper bound on $\rho(A^T A)$ can be obtained for non-normalized, ϵ-sparse A.

Let A be an M by N matrix. For each $n = 1, ..., N$, let $s_n > 0$ be the number of nonzero entries in the nth column of A, and let s be the maximum of the s_n. Let G be the M by N matrix with entries

$$G_{mn} = A_{mn}/(\sum_{l=1}^{N} s_l A_{ml}^2)^{1/2}.$$

Lent has shown that the eigenvalues of the matrix $G^T G$ do not exceed one [159]. This result suggested the following proposition, whose proof was given in [44].

Proposition 33.1 *Let A be an M by N matrix. For each $m = 1, ..., M$ let $\nu_m = \sum_{n=1}^{N} A_{mn}^2 > 0$. For each $n = 1, ..., N$ let $\sigma_n = \sum_{m=1}^{M} e_{mn}\nu_m$, where $e_{mn} = 1$ if $A_{mn} \neq 0$ and $e_{mn} = 0$ otherwise. Let σ denote the maximum of the σ_n. Then the eigenvalues of the matrix $A^T A$ do not exceed σ. If A is normalized so that the Euclidean length of each of its rows is one, then*

the eigenvalues of $A^T A$ do not exceed s, the maximum number of nonzero elements in any column of A.

Proof: For simplicity, we consider only the normalized case; the proof for the more general case is similar.

Let $A^T A\mathbf{v} = c\mathbf{v}$ for some nonzero vector $\mathbf{v}$. We show that $c \leq s$. We have $AA^T A\mathbf{v} = cA\mathbf{v}$ and so $\mathbf{w}^T AA^T\mathbf{w} = \mathbf{v}^T A^T AA^T A\mathbf{v} = c\mathbf{v}^T A^T A\mathbf{v} = c\mathbf{w}^T\mathbf{w}$, for $\mathbf{w} = A\mathbf{v}$. Then, with $e_{mn} = 1$ if $A_{mn} \neq 0$ and $e_{mn} = 0$ otherwise, we have

$$(\sum_{m=1}^{M} A_{mn}w_m)^2 = (\sum_{m=1}^{M} A_{mn}e_{mn}w_m)^2$$

$$\leq (\sum_{m=1}^{M} A_{mn}^2 w_m^2)(\sum_{m=1}^{M} e_{mn}^2) =$$

$$(\sum_{m=1}^{M} A_{mn}^2 w_m^2)s_j \leq (\sum_{m=1}^{M} A_{mn}^2 w_m^2)s.$$

Therefore,

$$\mathbf{w}^T AA^T\mathbf{w} = \sum_{n=1}^{N}(\sum_{m=1}^{M} A_{mn}w_m)^2 \leq \sum_{n=1}^{N}(\sum_{m=1}^{M} A_{mn}^2 w_m^2)s,$$

and

$$\mathbf{w}^T AA^T\mathbf{w} = c\sum_{m=1}^{M} w_m^2 = c\sum_{m=1}^{M} w_m^2(\sum_{n=1}^{N} A_{mn}^2)$$

$$= c\sum_{m=1}^{M}\sum_{n=1}^{N} w_m^2 A_{mn}^2.$$

The result follows immediately. ∎

If we normalize A so that its rows have length one, then the trace of the matrix AA^T is $\text{tr}(AA^T) = M$, which is also the sum of the eigenvalues of $A^T A$. Consequently, the maximum eigenvalue of $A^T A$ does not exceed M; this result improves that upper bound considerably, if A is sparse and so $s << M$.

In image reconstruction from projection data that includes scattering we often encounter matrices A most of whose entries are small, if not exactly zero. A slight modification of the proof provides us with a useful upper bound for L, the largest eigenvalue of $A^T A$, in such cases. Assume that the rows of A have length one. For $\epsilon > 0$ let s be the largest number of entries in any column of A whose magnitudes exceed ϵ. Then we have

$$L \leq s + MN\epsilon^2 + 2\epsilon(MNs)^{1/2}.$$

The proof of this result is similar to that for Proposition 33.1.
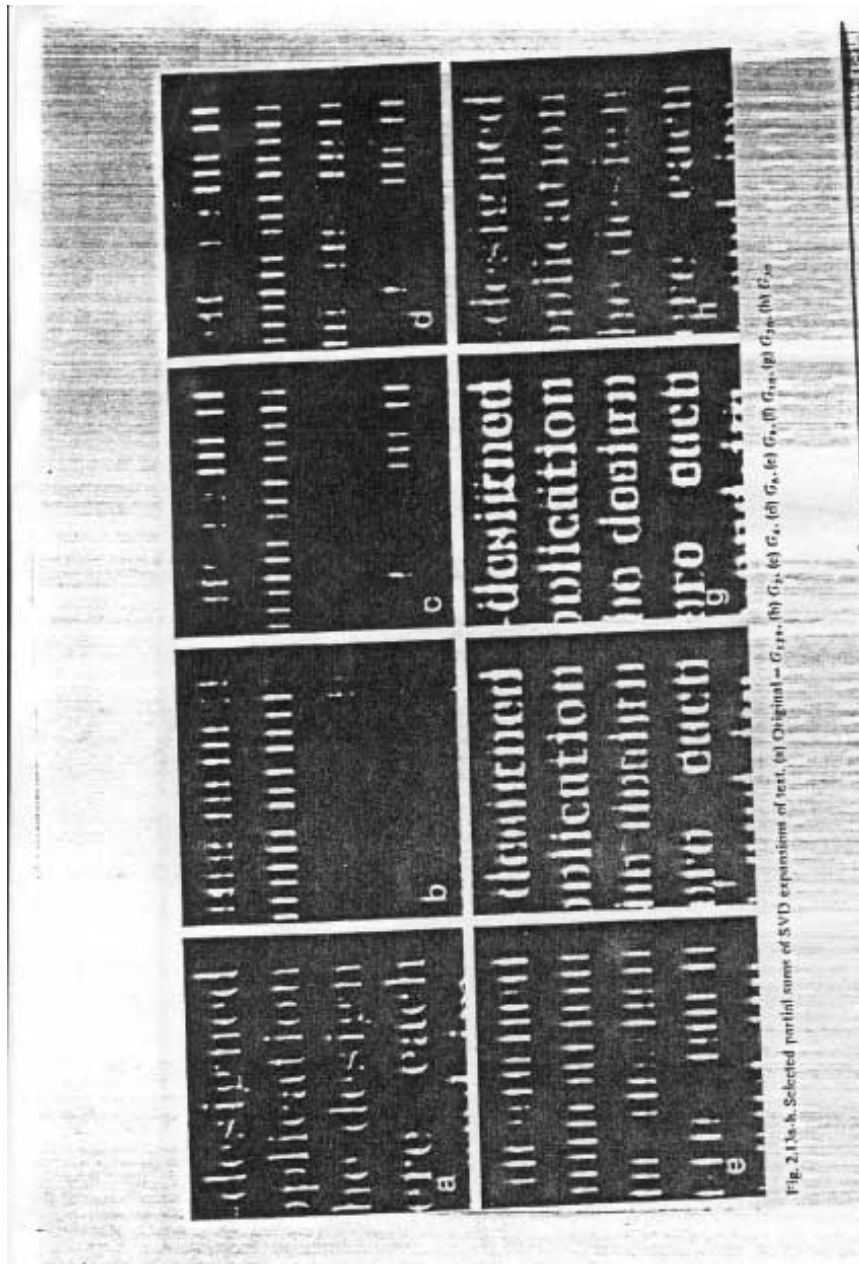
Figure 33.1: Compressing text with the SVD.
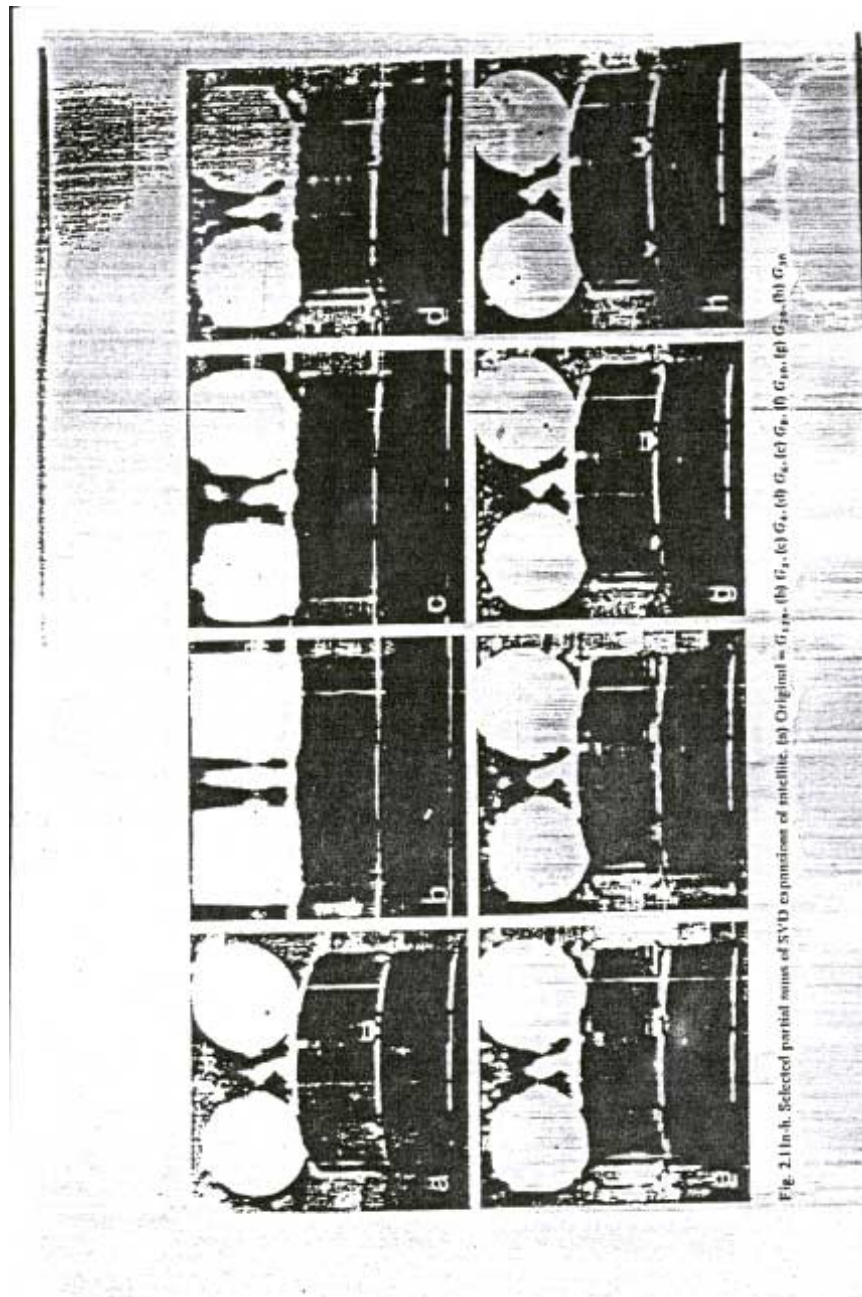
Figure 33.2: Compressing an image with the SVD.

Chapter 34

Appendix: Matrix and Vector Differentiation

34.1 Chapter Summary

The notation associated with matrix and vector algebra is designed to reduce the number of things we have to think about as we perform our calculations. This notation can be extended to multi-variable calculus, as we show in this chapter.

34.2 Functions of Vectors and Matrices

As we saw in the previous chapter, the least squares approximate solution of $A\mathbf{x} = \mathbf{b}$ is a vector $\hat{\mathbf{x}}$ that minimizes the function $||A\mathbf{x} - \mathbf{b}||$. In our discussion of band-limited extrapolation we showed that, for any nonnegative definite matrix Q, the vector having norm one that maximizes the quadratic form $\mathbf{x}^\dagger Q\mathbf{x}$ is an eigenvector of Q associated with the largest eigenvalue. In the chapter on best linear unbiased optimization we seek a matrix that minimizes a certain function. All of these examples involve what we can call *matrix-vector differentiation*, that is, the differentiation of a function with respect to a matrix or a vector. The gradient of a function of several variables is a well-known example and we begin there. Since there is some possibility of confusion, we adopt the notational convention that boldfaced symbols, such as $\mathbf{x}$, indicate a column vector, while x denotes a scalar.

34.3 Differentiation with Respect to a Vector

Let $\mathbf{x} = (x_1, ..., x_N)^T$ be an N-dimensional real column vector. Let $z = f(\mathbf{x})$ be a real-valued function of the entries of $\mathbf{x}$. The derivative of z with respect to $\mathbf{x}$, also called the *gradient* of z, is the column vector

$$\frac{\partial z}{\partial \mathbf{x}} = \mathbf{a} = (a_1, ..., a_N)^T$$

with entries

$$a_n = \frac{\partial z}{\partial x_n}.$$

Exercise 34.1 *Let* $\mathbf{y}$ *be a fixed real column vector and* $z = f(\mathbf{x}) = \mathbf{y}^T \mathbf{x}$. *Show that*

$$\frac{\partial z}{\partial \mathbf{x}} = \mathbf{y}.$$

Exercise 34.2 *Let* Q *be a real symmetric nonnegative definite matrix, and let* $z = f(\mathbf{x}) = \mathbf{x}^T Q \mathbf{x}$. *Show that the gradient of this quadratic form is*

$$\frac{\partial z}{\partial \mathbf{x}} = 2Q\mathbf{x}.$$

Hint: Write Q as a linear combination of dyads involving the eigenvectors.

Exercise 34.3 *Let* $z = ||A\mathbf{x} - \mathbf{b}||^2$. *Show that*

$$\frac{\partial z}{\partial \mathbf{x}} = 2A^T A\mathbf{x} - 2A^T \mathbf{b}.$$

Hint: Use $z = (A\mathbf{x} - \mathbf{b})^T (A\mathbf{x} - \mathbf{b})$.

We can also consider the second derivative of $z = f(\mathbf{x})$, which is the *Hessian matrix* of z

$$H = \frac{\partial^2 z}{\partial \mathbf{x}^2} = \nabla^2 f(x)$$

with entries

$$H_{mn} = \frac{\partial^2 z}{\partial x_m \partial x_n}.$$

If the entries of the vector $\mathbf{z} = (z_1, ..., z_M)^T$ are real-valued functions of the vector $\mathbf{x}$, the derivative of $\mathbf{z}$ is the matrix whose mth column is the derivative of the real-valued function z_m. This matrix is usually called the *Jacobian matrix* of $\mathbf{z}$. If $M = N$ the determinant of the Jacobian matrix is the *Jacobian*.

Exercise 34.4 *Suppose $(u, v) = (u(x, y), v(x, y))$ is a change of variables from the Cartesian (x, y) coordinate system to some other (u, v) coordinate system. Let $\mathbf{x} = (x, y)^T$ and $\mathbf{z} = (u(\mathbf{x}), v(\mathbf{x}))^T$.*

- **(a)** *Calculate the Jacobian for the rectangular coordinate system obtained by rotating the (x, y) system through an angle of θ.*

- **(b)** *Calculate the Jacobian for the transformation from the (x, y) system to polar coordinates.*

34.4   Differentiation with Respect to a Matrix

Now we consider real-valued functions $z = f(A)$ of a real matrix A. As an example, for square matrices A we have

$$z = f(A) = \operatorname{trace}(A) = \sum_{n=1}^{N} A_{nn},$$

the sum of the entries along the main diagonal of A.

The derivative of $z = f(A)$ is the matrix

$$\frac{\partial z}{\partial A} = B$$

whose entries are

$$B_{mn} = \frac{\partial z}{\partial A_{mn}}.$$

Exercise 34.5 *Show that the derivative of $\operatorname{trace}(A)$ is $B = I$, the identity matrix.*

Exercise 34.6 *Show that the derivative of $z = \operatorname{trace}(DAC)$ with respect to A is*

$$\frac{\partial z}{\partial A} = D^T C^T. \tag{34.1}$$

Consider the function f defined for all J by J positive-definite symmetric matrices by

$$f(Q) = -\log \det(Q). \tag{34.2}$$

Proposition 34.1 *The gradient of $f(Q)$ is $g(Q) = -Q^{-1}$.*

Proof: Let ΔQ be symmetric. Let γ_j, for $j = 1, 2, ..., J$, be the eigenvalues of the symmetric matrix $Q^{-1/2}(\Delta Q)Q^{-1/2}$. These γ_j are then real and are also the eigenvalues of the matrix $Q^{-1}(\Delta Q)$. We shall consider $\|\Delta Q\|$ small, so we may safely assume that $1 + \gamma_j > 0$.

Note that

$$\langle Q^{-1}, \Delta Q \rangle = \sum_{j=1}^{J} \gamma_j,$$

since the trace of any square matrix is the sum of its eigenvalues. Then we have

$$f(Q + \Delta Q) - f(Q) = -\log \det(Q + \Delta Q) + \log \det(Q)$$

$$= -\log \det(I + Q^{-1}(\Delta Q)) = -\sum_{j=1}^{J} \log(1 + \gamma_j).$$

From the submultiplicativity of the Frobenius norm we have

$$\|Q^{-1}(\Delta Q)\|/\|Q^{-1}\| \leq \|\Delta Q\| \leq \|Q^{-1}(\Delta Q)\|\|Q\|.$$

Therefore, taking the limit as $\|\Delta Q\|$ goes to zero is equivalent to taking the limit as $\|\gamma\|$ goes to zero, where γ is the vector whose entries are the γ_j.

To show that $g(Q) = -Q^{-1}$ note that

$$\limsup_{\|\Delta Q\| \to 0} \frac{f(Q + \Delta Q) - f(Q) - \langle -Q^{-1}, \Delta Q \rangle}{\|\Delta Q\|}$$

$$= \limsup_{\|\Delta Q\| \to 0} \frac{|-\log \det(Q + \Delta Q) + \log \det(Q) + \langle Q^{-1}, \Delta Q \rangle|}{\|\Delta Q\|}$$

$$\leq \limsup_{\|\gamma\| \to 0} \frac{\sum_{j=1}^{J} |\log(1 + \gamma_j) - \gamma_j|}{\|\gamma\|/\|Q^{-1}\|}$$

$$\leq \|Q^{-1}\| \sum_{j=1}^{J} \lim_{\gamma_j \to 0} \frac{\gamma_j - \log(1 + \gamma_j)}{|\gamma_j|} = 0.$$

∎

We note in passing that the derivative of $\det(DAC)$ with respect to A is the matrix $\det(DAC)(A^{-1})^T$.

Although the trace is not independent of the order of the matrices in a product, it is independent of cyclic permutation of the factors:

$$\text{trace}\,(ABC) = \text{trace}\,(CAB) = \text{trace}\,(BCA).$$

Therefore, the trace is independent of the order for the product of two matrices:

$$\text{trace}\,(AB) = \text{trace}\,(BA).$$

From this fact we conclude that

$$\mathbf{x}^T\mathbf{x} = \text{trace}\,(\mathbf{x}^T\mathbf{x}) = \text{trace}\,(\mathbf{x}\mathbf{x}^T).$$

If $\mathbf{x}$ is a random vector with correlation matrix

$$R = E(\mathbf{x}\mathbf{x}^T),$$

then

$$E(\mathbf{x}^T\mathbf{x}) = E(\text{trace}\,(\mathbf{x}\mathbf{x}^T)) = \text{trace}\,(E(\mathbf{x}\mathbf{x}^T)) = \text{trace}\,(R).$$

We shall use this trick in the chapter on detection.

Exercise 34.7 *Let $z = \text{trace}\,(A^T C A)$. Show that the derivative of z with respect to the matrix A is*

$$\frac{\partial z}{\partial A} = CA + C^T A. \tag{34.3}$$

Therefore, if $C = Q$ is symmetric, then the derivative is $2QA$.

We have restricted the discussion here to real matrices and vectors. It often happens that we want to optimize a real quantity with respect to a complex vector. We can rewrite such quantities in terms of the real and imaginary parts of the complex values involved, to reduce everything to the real case just considered. For example, let Q be a hermitian matrix; then the quadratic form $\mathbf{k}^\dagger Q\mathbf{k}$ is real, for any complex vector $\mathbf{k}$. As we saw in Exercise 33.2, we can write the quadratic form entirely in terms of real matrices and vectors.

If $w = u + iv$ is a complex number with real part u and imaginary part v, the function $z = f(w) = |w|^2$ is real-valued. The derivative of $z = f(w)$ with respect to the complex variable w does not exist. When we write $z = u^2 + v^2$, we consider z as a function of the real vector $\mathbf{x} = (u, v)^T$. The derivative of z with respect to $\mathbf{x}$ is the vector $(2u, 2v)^T$.

Similarly, when we consider the real quadratic form $\mathbf{k}^\dagger Q\mathbf{k}$, we view each of the complex entries of the N by 1 vector $\mathbf{k}$ as two real numbers forming a two-dimensional real vector. We then differentiate the quadratic form with respect to the $2N$ by 1 real vector formed from these real and imaginary parts. If we turn the resulting $2N$ by 1 real vector back into an N by 1 complex vector, we get $2Q\mathbf{k}$ as the derivative; so, it appears as if the formula for differentiating in the real case carries over to the complex case.

34.5 Eigenvectors and Optimization

We can use these results concerning differentiation with respect to a vector to show that eigenvectors solve certain optimization problems.

Consider the problem of maximizing the quadratic form $\mathbf{x}^\dagger Q\mathbf{x}$, subject to $\mathbf{x}^\dagger \mathbf{x} = 1$; here the matrix Q is Hermitian, positive-definite, so that all of its eigenvalues are positive. We use the Lagrange-multiplier approach, with the Lagrangian

$$L(\mathbf{x}, \lambda) = \mathbf{x}^\dagger Q\mathbf{x} - \lambda \mathbf{x}^\dagger \mathbf{x},$$

where the scalar variable λ is the Lagrange multiplier. We differentiate $L(\mathbf{x}, \lambda)$ with respect to $\mathbf{x}$ and set the result equal to zero, obtaining

$$2Q\mathbf{x} - 2\lambda \mathbf{x} = 0,$$

or

$$Q\mathbf{x} = \lambda \mathbf{x}.$$

Therefore, $\mathbf{x}$ is an eigenvector of Q and λ is its eigenvalue. Since

$$\mathbf{x}^\dagger Q\mathbf{x} = \lambda \mathbf{x}^\dagger \mathbf{x} = \lambda,$$

we conclude that $\lambda = \lambda_1$, the largest eigenvalue of Q, and $\mathbf{x} = \mathbf{u}^1$, a norm-one eigenvector associated with λ_1.

Now consider the problem of maximizing $\mathbf{x}^\dagger Q\mathbf{x}$, subject to $\mathbf{x}^\dagger \mathbf{x} = 1$, and $\mathbf{x}^\dagger \mathbf{u}^1 = 0$. The Lagrangian is now

$$L(\mathbf{x}, \lambda, \alpha) = \mathbf{x}^\dagger Q\mathbf{x} - \lambda \mathbf{x}^\dagger \mathbf{x} - \alpha \mathbf{x}^\dagger \mathbf{u}^1.$$

Differentiating with respect to the vector $\mathbf{x}$ and setting the result equal to zero, we find that

$$2Q\mathbf{x} - 2\lambda \mathbf{x} - \alpha \mathbf{u}^1 = 0,$$

or

$$Q\mathbf{x} = \lambda \mathbf{x} + \beta \mathbf{u}^1,$$

for $\beta = \alpha/2$. But, we know that

$$(\mathbf{u}^1)^\dagger Q\mathbf{x} = \lambda (\mathbf{u}^1)^\dagger \mathbf{x} + \beta (\mathbf{u}^1)^\dagger \mathbf{u}^1 = \beta,$$

and

$$(\mathbf{u}^1)^\dagger Q\mathbf{x} = (Q\mathbf{u}^1)^\dagger \mathbf{x} = \lambda_1 (\mathbf{u}^1)^\dagger \mathbf{x} = 0,$$

so $\beta = 0$ and we have

$$Q\mathbf{x} = \lambda \mathbf{x}.$$

Since

$$\mathbf{x}^\dagger Q\mathbf{x} = \lambda,$$

we conclude that $\mathbf{x}$ is a norm-one eigenvector of Q associated with the second-largest eigenvalue, $\lambda = \lambda_2$.

Continuing in this fashion, we can show that the norm-one eigenvector of Q associated with the nth largest eigenvalue λ_n maximizes the quadratic form $\mathbf{x}^{\dagger}Q\mathbf{x}$, subject to the constraints $\mathbf{x}^{\dagger}\mathbf{x} = 1$ and $\mathbf{x}^{\dagger}\mathbf{u}^m = 0$, for $m = 1, 2, ..., n - 1$.

Chapter 35

Appendix: Compressed Sensing

35.1   Chapter Summary

One area that has attracted much attention lately is *compressed sensing* or *compressed sampling* (CS) [101]. For applications such as medical imaging, CS may provide a means of reducing radiation dosage to the patient without sacrificing image quality. An important aspect of CS is finding sparse solutions of under-determined systems of linear equations, which can often be accomplished by one-norm minimization. The best reference to date is probably [27].

35.2   Compressed Sensing

The objective in CS is exploit sparseness to reconstruct a vector f in R^J from relatively few linear functional measurements [101].

Let $U = \{u^1, u^2, ..., u^J\}$ and $V = \{v^1, v^2, ..., v^J\}$ be two orthonormal bases for R^J, with all members of R^J represented as column vectors. For $i = 1, 2, ..., J$, let

$$\mu_i = \max_{1 \leq j \leq J} \{|\langle u^i, v^j \rangle|\}$$

and

$$\mu(U, V) = \max_{1 \leq i \leq J} \mu_i.$$

We know from Cauchy's Inequality that

$$|\langle u^i, v^j \rangle| \leq 1,$$

and from Parseval's Equation

$$\sum_{j=1}^{J} |\langle u^i, v^j \rangle|^2 = ||u^i||^2 = 1.$$

Therefore, we have

$$\frac{1}{\sqrt{J}} \leq \mu(U, V) \leq 1.$$

The quantity $\mu(U, V)$ is the *coherence* measure of the two bases; the closer $\mu(U, V)$ is to the lower bound of $\frac{1}{\sqrt{J}}$, the more *incoherent* the two bases are.

Let f be a fixed member of R^J; we expand f in the V basis as

$$f = x_1 v^1 + x_2 v^2 + ... + x_J v^J.$$

We say that the coefficient vector $x = (x_1, ..., x_J)$ is S-sparse if S is the number of non-zero x_j.

If S is small, most of the x_j are zero, but since we do not know which ones these are, we would have to compute all the linear functional values

$$x_j = \langle f, v^j \rangle$$

to recover f exactly. In fact, the smaller S is, the harder it would be to learn anything from randomly selected x_j, since most would be zero. The idea in CS is to obtain measurements of f with members of a different orthonormal basis, which we call the U basis. If the members of U are very much like the members of V, then nothing is gained. But, if the members of U are quite unlike the members of V, then each inner product measurement

$$y_i = \langle f, u^i \rangle = f^T u^i$$

should tell us something about f. If the two bases are sufficiently incoherent, then relatively few y_i values should tell us quite a bit about f. Specifically, we have the following result due to Candès and Romberg [64]: suppose the coefficient vector x for representing f in the V basis is S-sparse. Select uniformly randomly $M \leq J$ members of the U basis and compute the measurements $y_i = \langle f, u^i \rangle$. Then, if M is sufficiently large, it is highly probable that $z = x$ also solves the problem of minimizing the one-norm

$$||z||_1 = |z_1| + |z_2| + ... + |z_J|,$$

subject to the conditions

$$y_i = \langle g, u^i \rangle = g^T u^i,$$

for those M randomly selected u^i, where

$$g = z_1 v^1 + z_2 v^2 + ... + z_J v^J.$$

The smaller $\mu(U, V)$ is, the smaller the M is permitted to be without reducing the probability of perfect reconstruction.

35.3 Sparse Solutions

Suppose that A is a real M by N matrix, with $M < N$, and that the linear system $Ax = b$ has infinitely many solutions. For any vector x, we define the *support* of x to be the subset S of $\{1, 2, ..., N\}$ consisting of those n for which the entries $x_n \neq 0$. For any under-determined system $Ax = b$, there will, of course, be at least one solution of minimum support, that is, for which $|S|$, the size of the support set S, is minimum. However, finding such a maximally sparse solution requires combinatorial optimization, and is known to be computationally difficult. It is important, therefore, to have a computationally tractable method for finding maximally sparse solutions.

35.3.1 Maximally Sparse Solutions

Consider the problem P_0: among all solutions x of the consistent system $b = Ax$, find one, call it $\hat{x}$, that is maximally sparse, that is, has the minimum number of non-zero entries. Obviously, there will be at least one such solution having minimal support, but finding one, however, is a combinatorial optimization problem and is generally NP-hard.

35.3.2 Minimum One-Norm Solutions

Instead, we can seek a *minimum one-norm* solution, that is, we can solve the problem P_1: minimize

$$||x||_1 = \sum_{n=1}^{N} |x_n|,$$

subject to $Ax = b$. Denote the solution by x^*. Problem P_1 can be formulated as a linear programming problem, so is more easily solved. The big questions are: when does P_1 have a unique solution x^*, and when is $x^* = \hat{x}$? The problem P_1 will have a unique solution if and only if A is such that the one-norm satisfies

$$||x^*||_1 < ||x^* + v||_1,$$

for all non-zero v in the null space of A.

35.3.3 Minimum One-Norm as an LP Problem

The entries of x need not be non-negative, so the problem is not yet a linear programming problem. Let

$$B = [\, A \quad -A \,],$$

and consider the linear programming problem of minimizing the function

$$c^T z = \sum_{j=1}^{2J} z_j,$$

subject to the constraints $z \geq 0$, and $Bz = b$. Let z^* be the solution. We write

$$z^* = \begin{bmatrix} u^* \\ v^* \end{bmatrix}.$$

Then, as we shall see, $x^* = u^* - v^*$ minimizes the one-norm, subject to $Ax = b$.

First, we show that $u_j^* v_j^* = 0$, for each j. If, say, there is a j such that $0 < v_j^* < u_j^*$, then we can create a new vector z by replacing the old u_j^* with $u_j^* - v_j^*$ and the old v_j^* with zero, while maintaining $Bz = b$. But then, since $u_j^* - v_j^* < u_j^* + v_j^*$, it follows that $c^T z < c^T z^*$, which is a contradiction. Consequently, we have $\|x^*\|_1 = c^T z^*$.

Now we select any x with $Ax = b$. Write $u_j = x_j$, if $x_j \geq 0$, and $u_j = 0$, otherwise. Let $v_j = u_j - x_j$, so that $x = u - v$. Then let

$$z = \begin{bmatrix} u \\ v \end{bmatrix}.$$

Then $b = Ax = Bz$, and $c^T z = \|x\|_1$. Consequently,

$$\|x^*\|_1 = c^T z^* \leq c^T z = \|x\|_1,$$

and x^* must be a minimum one-norm solution.

35.3.4   Why the One-Norm?

When a system of linear equations $Ax = b$ is under-determined, we can find the *minimum-two-norm solution* that minimizes the square of the two-norm,

$$\|x\|_2^2 = \sum_{n=1}^{N} x_n^2,$$

subject to $Ax = b$. One drawback to this approach is that the two-norm penalizes relatively large values of x_n much more than the smaller ones, so tends to provide non-sparse solutions. Alternatively, we may seek the solution for which the one-norm,

$$\|x\|_1 = \sum_{n=1}^{N} |x_n|,$$

is minimized. The one-norm still penalizes relatively large entries x_n more than the smaller ones, but much less than the two-norm does. As a result, it often happens that the minimum one-norm solution actually solves P_0 as well.

35.3.5 Comparison with the PDFT

The PDFT approach to solving the under-determined system $Ax = b$ is to select weights $w_n > 0$ and then to find the solution $\tilde{x}$ that minimizes the weighted two-norm given by

$$\sum_{n=1}^{N} |x_n|^2 w_n.$$

Our intention is to select weights w_n so that w_n^{-1} is reasonably close to $|x_n^*|$; consider, therefore, what happens when $w_n^{-1} = |x_n^*|$. We claim that $\tilde{x}$ is also a minimum-one-norm solution.

To see why this is true, note that, for any x, we have

$$\sum_{n=1}^{N} |x_n| = \sum_{n=1}^{N} \frac{|x_n|}{\sqrt{|x_n^*|}} \sqrt{|x_n^*|}$$

$$\leq \sqrt{\sum_{n=1}^{N} \frac{|x_n|^2}{|x_n^*|}} \sqrt{\sum_{n=1}^{N} |x_n^*|}.$$

Therefore,

$$\sum_{n=1}^{N} |\tilde{x}_n| \leq \sqrt{\sum_{n=1}^{N} \frac{|\tilde{x}_n|^2}{|x_n^*|}} \sqrt{\sum_{n=1}^{N} |x_n^*|}$$

$$\leq \sqrt{\sum_{n=1}^{N} \frac{|x_n^*|^2}{|x_n^*|}} \sqrt{\sum_{n=1}^{N} |x_n^*|} = \sum_{n=1}^{N} |x_n^*|.$$

Therefore, $\tilde{x}$ also minimizes the one-norm.

35.3.6 Iterative Reweighting

Let x be the truth. Generally, we want each weight w_n to be a good prior estimate of the reciprocal of $|x_n|$. Because we do not yet know x, we may take a sequential-optimization approach, beginning with weights $w_n^0 > 0$, finding the PDFT solution using these weights, then using this PDFT solution to get a (we hope!) better choice for the weights, and so on. This sequential approach was successfully implemented in the early 1980's by Michael Fiddy and his students [111].

In [65], the same approach is taken, but with respect to the one-norm. Since the one-norm still penalizes larger values disproportionately, balance can be achieved by minimizing a weighted-one-norm, with weights close to the reciprocals of the $|x_n|$. Again, not yet knowing x, they employ a sequential approach, using the previous minimum-weighted-one-norm solution to obtain the new set of weights for the next minimization. At each step of the sequential procedure, the previous reconstruction is used to estimate the true support of the desired solution.

It is interesting to note that an on-going debate among users of the PDFT concerns the nature of the prior weighting. Does w_n approximate $|x_n|^{-1}$ or $|x_n|^{-2}$? This is close to the issue treated in [65], the use of a weight in the minimum-one-norm approach.

It should be noted again that finding a sparse solution is not usually the goal in the use of the PDFT, but the use of the weights has much the same effect as using the one-norm to find sparse solutions: to the extent that the weights approximate the entries of $\hat{x}$, their use reduces the penalty associated with the larger entries of an estimated solution.

35.4   Why Sparseness?

One obvious reason for wanting sparse solutions of $Ax = b$ is that we have prior knowledge that the desired solution is sparse. Such a problem arises in signal analysis from Fourier-transform data. In other cases, such as in the reconstruction of locally constant signals, it is not the signal itself, but its discrete derivative, that is sparse.

35.4.1   Signal Analysis

Suppose that our signal $f(t)$ is known to consist of a small number of complex exponentials, so that $f(t)$ has the form

$$f(t) = \sum_{j=1}^{J} a_j e^{i\omega_j t},$$

for some small number of frequencies ω_j in the interval $[0, 2\pi)$. For $n = 0, 1, ..., N-1$, let $f_n = f(n)$, and let f be the N-vector with entries f_n; we assume that J is much smaller than N. The discrete (vector) Fourier transform of f is the vector $\hat{f}$ having the entries

$$\hat{f}_k = \frac{1}{\sqrt{N}} \sum_{n=0}^{N-1} f_n e^{2\pi i k n/N},$$

for $k = 0, 1, ..., N-1$; we write $\hat{f} = Ef$, where E is the N by N matrix with entries $E_{kn} = \frac{1}{\sqrt{N}} e^{2\pi i k n/N}$. If N is large enough, we may safely assume

that each of the ω_j is equal to one of the frequencies $2\pi ik$ and that the vector $\hat{f}$ is J-sparse. The question now is: How many values of $f(n)$ do we need to calculate in order to be sure that we can recapture $f(t)$ exactly? We have the following theorem [63]:

Theorem 35.1 *Let N be prime. Let S be any subset of $\{0, 1, ..., N-1\}$ with $|S| \geq 2J$. Then the vector $\hat{f}$ can be uniquely determined from the measurements f_n for n in S.*

We know that
$$f = E^\dagger \hat{f},$$

where $E^\dagger$ is the conjugate transpose of the matrix E. The point here is that, for any matrix R obtained from the identity matrix I by deleting $N - |S|$ rows, we can recover the vector $\hat{f}$ from the measurements Rf.

If N is not prime, then the assertion of the theorem may not hold, since we can have $n = 0 \bmod N$, without $n = 0$. However, the assertion remains valid for most sets of J frequencies and most subsets S of indices; therefore, with high probability, we can recover the vector $\hat{f}$ from Rf.

Note that the matrix E is *unitary*, that is, $E^\dagger E = I$, and, equivalently, the columns of E form an orthonormal basis for C^N. The data vector is

$$b = Rf = RE^\dagger \hat{f}.$$

In this example, the vector f is not sparse, but can be represented sparsely in a particular orthonormal basis, namely as $f = E^\dagger \hat{f}$, using a sparse vector $\hat{f}$ of coefficients. The *representing basis* then consists of the columns of the matrix $E^\dagger$. The measurements pertaining to the vector f are the values f_n, for n in S. Since f_n can be viewed as the inner product of f with δ^n, the nth column of the identity matrix I, that is,

$$f_n = \langle \delta^n, f \rangle,$$

the columns of I provide the so-called *sampling basis*. With $A = RE^\dagger$ and $x = \hat{f}$, we then have

$$Ax = b,$$

with the vector x sparse. It is important for what follows to note that the matrix A is random, in the sense that we choose which rows of I to use to form R.

35.4.2 Locally Constant Signals

Suppose now that the function $f(t)$ is locally constant, consisting of some number of horizontal lines. We discretize the function $f(t)$ to get the

vector $f = (f(0), f(1), ..., f(N))^T$. The discrete derivative vector is $g = (g_1, g_2, ..., g_N)^T$, with

$$g_n = f(n) - f(n-1).$$

Since $f(t)$ is locally constant, the vector g is sparse. The data we will have will not typically be values $f(n)$. The goal will be to recover f from M linear functional values pertaining to f, where M is much smaller than N. We shall assume, from now on, that we have measured, or can estimate, the value $f(0)$.

Our M by 1 data vector d consists of measurements pertaining to the vector f:

$$d_m = \sum_{n=0}^{N} H_{mn} f_n,$$

for $m = 1, ..., M$, where the H_{mn} are known. We can then write

$$d_m = f(0)\Big(\sum_{n=0}^{N} H_{mn}\Big) + \sum_{k=1}^{N}\Big(\sum_{j=k}^{N} H_{mj}\Big)g_k.$$

Since $f(0)$ is known, we can write

$$b_m = d_m - f(0)\Big(\sum_{n=0}^{N} H_{mn}\Big) = \sum_{k=1}^{N} A_{mk} g_k,$$

where

$$A_{mk} = \sum_{j=k}^{N} H_{mj}.$$

The problem is then to find a sparse solution of $Ax = g$. As in the previous example, we often have the freedom to select the linear functions, that is, the values H_{mn}, so the matrix A can be viewed as random.

35.4.3   Tomographic Imaging

The reconstruction of tomographic images is an important aspect of medical diagnosis, and one that combines aspects of both of the previous examples. The data one obtains from the scanning process can often be interpreted as values of the Fourier transform of the desired image; this is precisely the case in magnetic-resonance imaging, and approximately true for x-ray transmission tomography, positron-emission tomography (PET) and single-photon emission tomography (SPECT). The images one encounters in medical diagnosis are often approximately locally constant, so the associated array of discrete partial derivatives will be sparse. If this sparse derivative array can be recovered from relatively few Fourier-transform values, then the scanning time can be reduced.

We turn now to the more general problem of compressed sampling.

35.5   Compressed Sampling

Our goal is to recover the vector $f = (f_1, ..., f_N)^T$ from M linear functional values of f, where M is much less than N. In general, this is not possible without prior information about the vector f. In compressed sampling, the prior information concerns the sparseness of either f itself, or another vector linearly related to f.

Let U and V be unitary N by N matrices, so that the column vectors of both U and V form orthonormal bases for C^N. We shall refer to the bases associated with U and V as the *sampling basis* and the *representing basis*, respectively. The first objective is to find a unitary matrix V so that $f = Vx$, where x is sparse. Then we want to find a second unitary matrix U such that, when an M by N matrix R is obtained from U by deleting rows, the sparse vector x can be determined from the data $b = RVx = Ax$. Theorems in compressed sensing describe properties of the matrices U and V such that, when R is obtained from U by a random selection of the rows of U, the vector x will be uniquely determined, with high probability, as the unique solution that minimizes the one-norm.

Chapter 36

Appendix: Transmission Tomography I

36.1 Chapter Summary

Our topic is now transmission tomography. This chapter will provide a detailed description of how the data is gathered, the mathematical model of the scanning process, and the problem to be solved. In the next chapter we shall study the various mathematical techniques needed to solve this problem and the manner in which these techniques are applied, including filtering methods for inverting the two-dimensional Fourier transform.

36.2 X-ray Transmission Tomography

Although transmission tomography is not limited to scanning living beings, we shall concentrate here on the use of x-ray tomography in medical diagnosis and the issues that concern us in that application. The mathematical formulation will, of course, apply more generally.

   In x-ray tomography, x-rays are transmitted through the body along many lines. In some, but not all, cases, the lines will all lie in the same plane. The strength of the x-rays upon entering the body is assumed known, and the strength upon leaving the body is measured. This data can then be used to estimate the amount of attenuation the x-ray encountered along that line, which is taken to be the integral, along that line, of the attenuation function. On the basis of these line integrals, we estimate the attenuation function. This estimate is presented to the physician as one or more two-dimensional images.

36.3   The Exponential-Decay Model

As an x-ray beam passes through the body, it encounters various types of matter, such as soft tissue, bone, ligaments, air, each weakening the beam to a greater or lesser extent. If the intensity of the beam upon entry is I_{in} and I_{out} is its lower intensity after passing through the body, then

$$I_{out} = I_{in}e^{-\int_L f},$$

where $f = f(x, y) \geq 0$ is the *attenuation function* describing the two-dimensional distribution of matter within the slice of the body being scanned and $\int_L f$ is the integral of the function f over the line L along which the x-ray beam has passed. To see why this is the case, imagine the line L parameterized by the variable s and consider the intensity function $I(s)$ as a function of s. For small $\Delta s > 0$, the drop in intensity from the start to the end of the interval $[s, s + \Delta s]$ is approximately proportional to the intensity $I(s)$, to the attenuation $f(s)$ and to Δs, the length of the interval; that is,

$$I(s) - I(s + \Delta s) \approx f(s)I(s)\Delta s.$$

Dividing by Δs and letting Δs approach zero, we get

$$I'(s) = -f(s)I(s).$$

Exercise 36.1 *Show that the solution to this differential equation is*

$$I(s) = I(0) \exp(-\int_{u=0}^{u=s} f(u)du).$$

Hint: Use an integrating factor.

From knowledge of I_{in} and I_{out}, we can determine $\int_L f$. If we know $\int_L f$ for every line in the x, y-plane we can reconstruct the attenuation function f. In the real world we know line integrals only approximately and only for finitely many lines. The goal in x-ray transmission tomography is to estimate the attenuation function $f(x, y)$ in the slice, from finitely many noisy measurements of the line integrals. We usually have prior information about the values that $f(x, y)$ can take on. We also expect to find sharp boundaries separating regions where the function $f(x, y)$ varies only slightly. Therefore, we need algorithms capable of providing such images.

36.4   Difficulties to be Overcome

There are several problems associated with this model. X-ray beams are not exactly straight lines; the beams tend to spread out. The x-rays are not monochromatic, and their various frequency components are attenuated at

different rates, resulting in *beam hardening*, that is, changes in the spectrum of the beam as it passes through the object. The beams consist of photons obeying statistical laws, so our algorithms probably should be based on these laws. How we choose the line segments is determined by the nature of the problem; in certain cases we are somewhat limited in our choice of these segments. Patients move; they breathe, their hearts beat, and, occasionally, they shift position during the scan. Compensating for these motions is an important, and difficult, aspect of the image reconstruction process. Finally, to be practical in a clinical setting, the processing that leads to the reconstructed image must be completed in a short time, usually around fifteen minutes. This time constraint is what motivates viewing the three-dimensional attenuation function in terms of its two-dimensional slices.

As we shall see, the Fourier transform and the associated theory of convolution filters play important roles in the reconstruction of transmission tomographic images.

The data we actually obtain at the detectors are counts of detected photons. These counts are not the line integrals; they are random quantities whose means, or expected values, are related to the line integrals. The Fourier inversion methods for solving the problem ignore its statistical aspects; in contrast, other methods, such as likelihood maximization, are based on a statistical model that involves Poisson-distributed emissions.

36.5   Reconstruction from Line Integrals

We turn now to the underlying problem of reconstructing attenuation functions from line-integral data.

36.5.1   The Radon Transform

Our goal is to reconstruct the function $f(x, y) \geq 0$ from line-integral data. Let θ be a fixed angle in the interval $[0, \pi)$. Form the t, s-axis system with the positive t-axis making the angle θ with the positive x-axis, as shown in Figure 36.1. Each point (x, y) in the original coordinate system has coordinates (t, s) in the second system, where the t and s are given by

$$t = x \cos \theta + y \sin \theta,$$

and

$$s = -x \sin \theta + y \cos \theta.$$

If we have the new coordinates (t, s) of a point, the old coordinates are (x, y) given by

$$x = t \cos \theta - s \sin \theta,$$

and

$$y = t \sin \theta + s \cos \theta.$$

We can then write the function f as a function of the variables t and s. For each fixed value of t, we compute the integral

$$\int_L f(x, y) ds = \int f(t \cos \theta - s \sin \theta, t \sin \theta + s \cos \theta) ds$$

along the single line L corresponding to the fixed values of θ and t. We repeat this process for every value of t and then change the angle θ and repeat again. In this way we obtain the integrals of f over every line L in the plane. We denote by $r_f(\theta, t)$ the integral

$$r_f(\theta, t) = \int_L f(x, y) ds = \int f(t \cos \theta - s \sin \theta, t \sin \theta + s \cos \theta) ds. \quad (36.1)$$

The function $r_f(\theta, t)$ is called the *Radon transform* of f.

36.5.2   The Central Slice Theorem

For fixed θ the function $r_f(\theta, t)$ is a function of the single real variable t; let $R_f(\theta, \omega)$ be its Fourier transform. Then

$$R_f(\theta, \omega) = \int r_f(\theta, t) e^{i\omega t} dt$$

$$= \int \int f(t \cos \theta - s \sin \theta, t \sin \theta + s \cos \theta) e^{i\omega t} ds dt$$

$$= \int \int f(x, y) e^{i\omega(x \cos \theta + y \sin \theta)} dx dy = F(\omega \cos \theta, \omega \sin \theta),$$

where $F(\omega \cos \theta, \omega \sin \theta)$ is the two-dimensional Fourier transform of the function $f(x, y)$, evaluated at the point $(\omega \cos \theta, \omega \sin \theta)$; this relationship is called the *Central Slice Theorem*. For fixed θ, as we change the value of ω, we obtain the values of the function F along the points of the line making the angle θ with the horizontal axis. As θ varies in $[0, \pi)$, we get all the values of the function F. Once we have F, we can obtain f using the formula for the two-dimensional inverse Fourier transform. We conclude that we are able to determine f from its line integrals. As we shall see, inverting the Fourier transform can be implemented by combinations of frequency-domain filtering and back-projection.
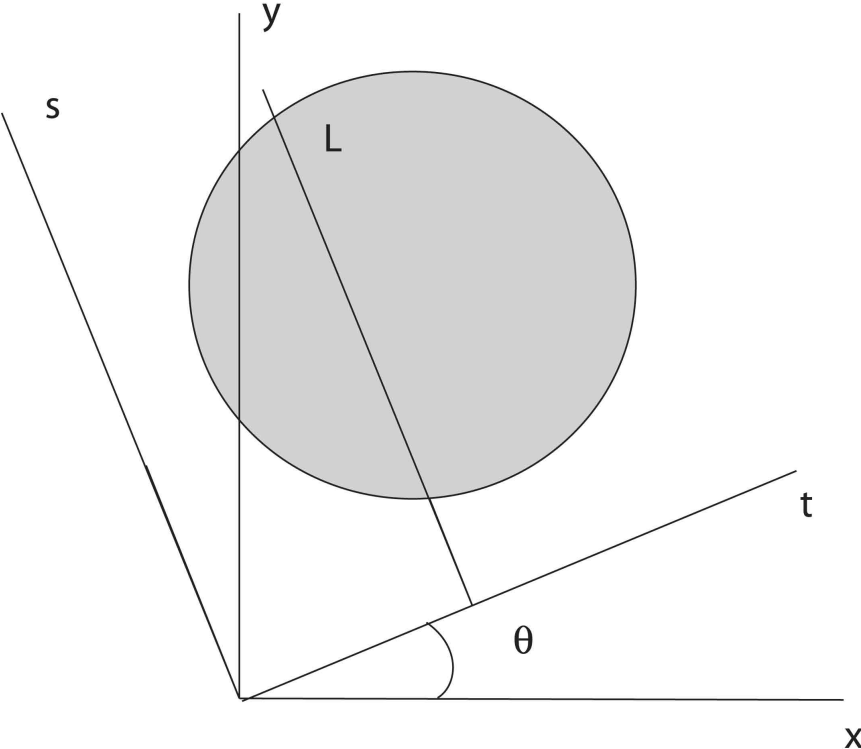
Figure 36.1: The Radon transform of f at (t, θ) is the line integral of f along line L.

Chapter 37

Appendix: Transmission Tomography II

37.1 Chapter Summary

According to the Central Slice Theorem, if we have all the line integrals through the attenuation function $f(x, y)$ then we have the two-dimensional Fourier transform of $f(x, y)$. To get $f(x, y)$ we need to invert the two-dimensional Fourier transform; that is the topic of this chapter.

37.2 Inverting the Fourier Transform

The Fourier-transform inversion formula for two-dimensional functions tells us that the function $f(x, y)$ can be obtained as

$$f(x, y) = \frac{1}{4\pi^2} \int \int F(u, v) e^{-i(xu+yv)} du dv. \qquad (37.1)$$

We now derive alternative inversion formulas.

37.2.1 Back-Projection

For $0 \leq \theta < \pi$ and all real t, let $h(\theta, t)$ be any function of the variables θ and t; for example, it could be the Radon transform. As with the Radon transform, we imagine that each pair (θ, t) corresponds to one line through the x, y-plane. For each fixed point (x, y) we assign to this point the average, over all θ, of the quantities $h(\theta, t)$ for every pair (θ, t) such that the point (x, y) lies on the associated line. The summing process is integration

367

and the *back-projection* function at (x, y) is

$$BP_h(x, y) = \int_0^\pi h(\theta, x\cos\theta + y\sin\theta)d\theta. \qquad (37.2)$$

The operation of back-projection will play an important role in what follows in this chapter.

37.2.2   Ramp Filter, then Back-project

Expressing the double integral in Equation (37.1) in polar coordinates (ω, θ), with $\omega \geq 0$, $u = \omega\cos\theta$, and $v = \omega\sin\theta$, we get

$$f(x, y) = \frac{1}{4\pi^2} \int_0^{2\pi} \int_0^\infty F(u, v)e^{-i(xu+yv)}\omega d\omega d\theta,$$

or

$$f(x, y) = \frac{1}{4\pi^2} \int_0^\pi \int_{-\infty}^\infty F(u, v)e^{-i(xu+yv)}|\omega|d\omega d\theta.$$

Now write

$$F(u, v) = F(\omega\cos\theta, \omega\sin\theta) = R_f(\theta, \omega),$$

where $R_f(\theta, \omega)$ is the FT with respect to t of $r_f(\theta, t)$, so that

$$\int_{-\infty}^\infty F(u, v)e^{-i(xu+yv)}|\omega|d\omega = \int_{-\infty}^\infty R_f(\theta, \omega)|\omega|e^{-i\omega t}d\omega.$$

The function $g_f(\theta, t)$ defined for $t = x\cos\theta + y\sin\theta$ by

$$g_f(\theta, x\cos\theta + y\sin\theta) = \frac{1}{2\pi} \int_{-\infty}^\infty R_f(\theta, \omega)|\omega|e^{-i\omega t}d\omega \qquad (37.3)$$

is the result of a linear filtering of $r_f(\theta, t)$ using a *ramp filter* with transfer function $H(\omega) = |\omega|$. Then,

$$f(x, y) = \frac{1}{2\pi}BP_{g_f}(x, y) = \frac{1}{2\pi} \int_0^\pi g_f(\theta, x\cos\theta + y\sin\theta)d\theta \qquad (37.4)$$

gives $f(x, y)$ as the result of a *back-projection operator*; for every fixed value of (θ, t) add $g_f(\theta, t)$ to the current value at the point (x, y) for all (x, y) lying on the straight line determined by θ and t by $t = x\cos\theta + y\sin\theta$. The final value at a fixed point (x, y) is then the average of all the values $g_f(\theta, t)$ for those (θ, t) for which (x, y) is on the line $t = x\cos\theta + y\sin\theta$. It is therefore said that $f(x, y)$ can be obtained by *filtered back-projection* (FBP) of the line-integral data.

Knowing that $f(x, y)$ is related to the complete set of line integrals by filtered back-projection suggests that, when only finitely many line integrals are available, a similar ramp filtering and back-projection can be used to estimate $f(x, y)$; in the clinic this is the most widely used method for the reconstruction of tomographic images.

37.2.3 Back-project, then Ramp Filter

There is a second way to recover $f(x, y)$ using back-projection and filtering, this time in the reverse order; that is, we back-project the Radon transform and then ramp filter the resulting function of two variables. We begin with the back-projection operation, as applied to the function $h(\theta, t) = r_f(\theta, t)$.

We have

$$BP_{r_f}(x, y) = \int_0^\pi r_f(\theta, x \cos \theta + y \sin \theta) d\theta. \tag{37.5}$$

Replacing $r_f(\theta, t)$ with

$$r_f(\theta, t) = \frac{1}{2\pi} \int_{-\infty}^{\infty} R_f(\theta, \omega) e^{-i\omega t} d\omega,$$

and inserting

$$R_f(\theta, \omega) = F(\omega \cos \theta, \omega \sin \theta),$$

and

$$t = x \cos \theta + y \sin \theta,$$

we get

$$BP_{r_f}(x, y) = \int_0^\pi \left(\frac{1}{2\pi} \int_{-\infty}^{\infty} F(\omega \cos \theta, \omega \sin \theta) e^{-i(x \cos \theta + y \sin \theta)} d\omega \right) d\theta.$$

With $u = \omega \cos \theta$ and $v = \omega \sin \theta$, this becomes

$$BP_{r_f}(x, y) = \int_0^\pi \left(\frac{1}{2\pi} \int_{-\infty}^{\infty} \frac{F(u, v)}{\sqrt{u^2 + v^2}} e^{-i(xu + yv)} |\omega| d\omega \right) d\theta,$$

$$= \int_0^\pi \left(\frac{1}{2\pi} \int_{-\infty}^{\infty} G(u, v) e^{-i(xu + yv)} |\omega| d\omega \right) d\theta$$

$$= \frac{1}{2\pi} \int_{-\infty}^{\infty} \int_{-\infty}^{\infty} G(u, v) e^{-i(xu + yv)} du dv.$$

This tells us that the back-projection of $r_f(\theta, t)$ is the function $g(x, y)$ whose two-dimensional Fourier transform is

$$G(u, v) = \frac{1}{2\pi} F(u, v) / \sqrt{u^2 + v^2}.$$

Therefore, we can obtain $f(x, y)$ from $r_f(\theta, t)$ by first back-projecting $r_f(\theta, t)$ to get $g(x, y)$ and then filtering $g(x, y)$ by forming $G(u, v)$, multiplying by $\sqrt{u^2 + v^2}$, and taking the inverse Fourier transform.

37.2.4 Radon's Inversion Formula

To get Radon's inversion formula, we need two basic properties of the Fourier transform. First, if $f(x)$ has Fourier transform $F(\gamma)$ then the derivative $f'(x)$ has Fourier transform $-i\gamma F(\gamma)$. Second, if $F(\gamma) = \text{sgn}(\gamma)$, the function that is $\frac{\gamma}{|\gamma|}$ for $\gamma \neq 0$, and equal to zero for $\gamma = 0$, then its inverse Fourier transform is $f(x) = \frac{1}{i\pi x}$.

Writing equation (37.3) as

$$g_f(\theta, t) = \frac{1}{2\pi} \int_{-\infty}^{\infty} \omega R_f(\theta, \omega) \text{sgn}(\omega) e^{-i\omega t} d\omega,$$

we see that g_f is the inverse Fourier transform of the product of the two functions $\omega R_f(\theta, \omega)$ and $\text{sgn}(\omega)$. Consequently, g_f is the convolution of their individual inverse Fourier transforms, $i\frac{\partial}{\partial t} r_f(\theta, t)$ and $\frac{1}{i\pi t}$; that is,

$$g_f(\theta, t) = \frac{1}{\pi} \int_{-\infty}^{\infty} \frac{\partial}{\partial t} r_f(\theta, s) \frac{1}{t - s} ds,$$

which is the Hilbert transform of the function $\frac{\partial}{\partial t} r_f(\theta, t)$, with respect to the variable t. Radon's inversion formula is then

$$f(x, y) = \frac{1}{2\pi} \int_0^{\pi} HT(\frac{\partial}{\partial t} r_f(\theta, t)) d\theta.$$

37.3 From Theory to Practice

What we have just described is the theory. What happens in practice?

37.3.1 The Practical Problems

Of course, in reality we never have the Radon transform $r_f(\theta, t)$ for all values of its variables. Only finitely many angles θ are used, and, for each θ, we will have (approximate) values of line integrals for only finitely many t. Therefore, taking the Fourier transform of $r_f(\theta, t)$, as a function of the single variable t, is not something we can actually do. At best, we can approximate $R_f(\theta, \omega)$ for finitely many θ. From the Central Slice Theorem, we can then say that we have approximate values of $F(\omega \cos\theta, \omega \sin\theta)$, for finitely many θ. This means that we have (approximate) Fourier transform values for $f(x, y)$ along finitely many lines through the origin, like the spokes of a wheel. The farther from the origin we get, the fewer values we have, so the *coverage* in Fourier space is quite uneven. The low-spatial-frequencies are much better estimated than higher ones, meaning that we have a low-pass version of the desired $f(x, y)$. The filtered back-projection approaches we have just discussed both involve ramp filtering, in which the

higher frequencies are increased, relative to the lower ones. This too can only be implemented approximately, since the data is noisy and careless ramp filtering will cause the reconstructed image to be unacceptably noisy.

37.3.2 A Practical Solution: Filtered Back-Projection

We assume, to begin with, that we have finitely many line integrals, that is, we have values $r_f(\theta, t)$ for finitely many θ and finitely many t. For each fixed θ we estimate the Fourier transform, $R_f(\theta, \omega)$. This step can be performed in various ways, and we can freely choose the values of ω at which we perform the estimation. The FFT will almost certainly be involved in calculating the estimates of $R_f(\theta, \omega)$.

For each fixed θ we multiply our estimated values of $R_f(\theta, \omega)$ by $|\omega|$ and then use the FFT again to inverse Fourier transform, to achieve a ramp filtering of $r_f(\theta, t)$ as a function of t. Note, however, that when $|\omega|$ is large, we may multiply by a smaller quantity, to avoid enhancing noise. We do this for each angle θ, to get a function of (θ, t), which we then back-project to get our final image. This is ramp-filtering, followed by back-projection, as applied to the finite data we have.

It is also possible to mimic the second approach to inversion, that is, to back-project onto the pixels each $r_f(\theta, t)$ that we have, and then to perform a ramp filtering of this two-dimensional array of numbers to obtain the final image. In this case, the two-dimensional ramp filtering involves many applications of the FFT.

There is a third approach. Invoking the Central Slice Theorem, we can say that we have finitely many approximate values of $F(u, v)$, the Fourier transform of the attenuation function $f(x, y)$, along finitely many lines through the origin. The first step is to use these values to estimate the values of $F(u, v)$ at the points of a rectangular grid. This step involves *interpolation* [215, 219]. Once we have (approximate) values of $F(u, v)$ on a rectangular grid, we perform a two-dimensional FFT to obtain our final estimate of the (discretized) $f(x, y)$.

37.4 Some Practical Concerns

As computer power increases and scanners become more sophisticated, there is pressure to include more dimensionality in the scans. This means going beyond slice-by-slice tomography to fully three-dimensional images, or even including time as the fourth dimension, to image dynamically. This increase in dimensionality comes at a cost, however [202]. Besides the increase in radiation to the patient, there are other drawbacks, such as longer acquisition time, storing large amounts of data, processing and analyzing

this data, displaying the results, reading and understanding the higher-dimensional images, and so on.

37.5 Summary

We have seen how the problem of reconstructing a function from line integrals arises in transmission tomography. The Central Slice Theorem connects the line integrals and the Radon transform to the Fourier transform of the desired attenuation function. Various approaches to implementing the Fourier Inversion Formula lead to filtered back-projection algorithms for the reconstruction. In x-ray tomography, as well as in PET, viewing the data as line integrals ignores the statistical aspects of the problem, and in SPECT, it ignores, as well, the important physical effects of attenuation. To incorporate more of the physics of the problem, iterative algorithms based on statistical models have been developed. We consider some of these algorithms in the books [46] and [48].

Bibliography

[1] Agmon, S. (1954) "The relaxation method for linear inequalities." *Canadian Journal of Mathematics* **6**, pp. 382–392.

[2] Anderson, T. (1972) "Efficient estimation of regression coefficients in time series." *Proc. of Sixth Berkeley Symposium on Mathematical Statistics and Probability, Volume 1: The Theory of Statistics* University of California Press, Berkeley, CA, pp. 471–482.

[3] Anderson, A. and Kak, A. (1984) "Simultaneous algebraic reconstruction technique (SART): a superior implementation of the ART algorithm." *Ultrasonic Imaging* **6**, pp. 81–94.

[4] Ash, R. and Gardner, M. (1975) *Topics in Stochastic Processes* Boston: Academic Press.

[5] Axelsson, O. (1994) *Iterative Solution Methods.* Cambridge, UK: Cambridge University Press.

[6] Baggeroer, A., Kuperman, W., and Schmidt, H. (1988) "Matched field processing: source localization in correlated noise as optimum parameter estimation." *Journal of the Acoustical Society of America* **83**, pp. 571–587.

[7] Baillon, J. and Haddad, G. (1977) "Quelques proprietes des operateurs angle-bornes et n-cycliquement monotones." *Israel J. of Mathematics* **26**, pp. 137–150.

[8] Barrett, H., White, T., and Parra, L. (1997) "List-mode likelihood." *J. Opt. Soc. Am. A* **14**, pp. 2914–2923.

[9] Bauschke, H. (2001) "Projection algorithms: results and open problems." in *Inherently Parallel Algorithms in Feasibility and Optimization and their Applications*, Butnariu, D., Censor, Y., and Reich, S., editors, Amsterdam: Elsevier Science. pp. 11–22.

[10] Bauschke, H. and Borwein, J. (1996) "On projection algorithms for solving convex feasibility problems."*SIAM Review* **38 (3)**, pp. 367–426.

[11] Bauschke, H., Borwein, J., and Lewis, A. (1997) "The method of cyclic projections for closed convex sets in Hilbert space."*Contemporary Mathematics: Recent Developments in Optimization Theory and Nonlinear Analysis* **204**, American Mathematical Society, pp. 1–38.

[12] Benson, M. (2003) "What *Galileo* Saw." in *The New Yorker*; reprinted in [81].

[13] Bertero, M. (1992) "Sampling theory, resolution limits and inversion methods."in [15], pp. 71–94.

[14] Bertero, M., and Boccacci, P. (1998) *Introduction to Inverse Problems in Imaging* Bristol, UK: Institute of Physics Publishing.

[15] Bertero, M. and Pike, E.R., editors (1992) *Inverse Problems in Scattering and Imaging* Malvern Physics Series, Adam Hilger, IOP Publishing, London.

[16] Bertsekas, D.P. (1997) "A new class of incremental gradient methods for least squares problems."*SIAM J. Optim.* **7**, pp. 913–926.

[17] Blackman, R. and Tukey, J. (1959) *The Measurement of Power Spectra.* New York: Dover Publications.

[18] Boggess, A. and Narcowich, F. (2001) *A First Course in Wavelets, with Fourier Analysis.* Englewood Cliffs, NJ: Prentice-Hall.

[19] Born, M. and Wolf, E. (1999) *Principles of Optics: 7th edition.* Cambridge, UK: Cambridge University Press.

[20] Bochner, S. and Chandrasekharan, K. (1949) *Fourier Transforms*, Annals of Mathematical Studies, No. 19. Princeton, NJ: Princeton University Press.

[21] Bolles, E.B. (1997) *Galileo's Commandment: 2,500 Years of Great Science Writing.* New York: W.H. Freeman.

[22] Borwein, J. and Lewis, A. (2000) *Convex Analysis and Nonlinear Optimization.* Canadian Mathematical Society Books in Mathematics, New York: Springer-Verlag.

[23] Bracewell, R.C. (1979) "Image reconstruction in radio astronomy." in [128], pp. 81–104.

[24] Bregman, L.M. (1967) "The relaxation method of finding the common point of convex sets and its application to the solution of problems in convex programming." *USSR Computational Mathematics and Mathematical Physics* **7**: pp. 200–217.

[25] Brodzik, A. and Mooney, J. (1999) "Convex projections algorithm for restoration of limited-angle chromotomographic images." *Journal of the Optical Society of America A* **16 (2)**, pp. 246–257.

[26] Browne, J. and A. DePierro, A. (1996) "A row-action alternative to the EM algorithm for maximizing likelihoods in emission tomography." *IEEE Trans. Med. Imag.* **15**, pp. 687–699.

[27] Bruckstein, A., Donoho, D., and Elad, M. (2009) "From sparse solutions of systems of equations to sparse modeling of signals and images." *SIAM Review*, **51(1)**, pp. 34–81.

[28] Bruyant, P., Sau, J., and Mallet, J.J. (1999) "Noise removal using factor analysis of dynamic structures: application to cardiac gated studies." *Journal of Nuclear Medicine* **40 (10)**, pp. 1676–1682.

[29] Bucker, H. (1976) "Use of calculated sound fields and matched field detection to locate sound sources in shallow water." *Journal of the Acoustical Society of America* **59**, pp. 368–373.

[30] Burg, J. (1967) "Maximum entropy spectral analysis." *paper presented at the 37th Annual SEG meeting, Oklahoma City, OK.*

[31] Burg, J. (1972) "The relationship between maximum entropy spectra and maximum likelihood spectra." *Geophysics* **37**, pp. 375–376.

[32] Burg, J. (1975) *Maximum Entropy Spectral Analysis*, Ph.D. dissertation, Stanford University.

[33] Byrne, C. (1992) "Effects of modal phase errors on eigenvector and nonlinear methods for source localization in matched field processing." *Journal of the Acoustical Society of America* **92(4)**, pp. 2159–2164.

[34] Byrne, C. (1993) "Iterative image reconstruction algorithms based on cross-entropy minimization." *IEEE Transactions on Image Processing* **IP-2**, pp. 96–103.

[35] Byrne, C. (1995) "Erratum and addendum to 'Iterative image reconstruction algorithms based on cross-entropy minimization'." *IEEE Transactions on Image Processing* **IP-4**, pp. 225–226.

[36] Byrne, C. (1996) "Iterative reconstruction algorithms based on cross-entropy minimization." in *Image Models (and their Speech Model Cousins)*, S.E. Levinson and L. Shepp, editors, IMA Volumes in Mathematics and its Applications, Volume 80, pp. 1–11. New York: Springer-Verlag.

[37] Byrne, C. (1996) "Block-iterative methods for image reconstruction from projections." *IEEE Transactions on Image Processing* **IP-5**, pp. 792–794.

[38] Byrne, C. (1997) "Convergent block-iterative algorithms for image reconstruction from inconsistent data." *IEEE Transactions on Image Processing* **IP-6**, pp. 1296–1304.

[39] Byrne, C. (1998) "Accelerating the EMML algorithm and related iterative algorithms by rescaled block-iterative (RBI) methods." *IEEE Transactions on Image Processing* **IP-7**, pp. 100–109.

[40] Byrne, C. (1999) "Iterative projection onto convex sets using multiple Bregman distances." *Inverse Problems* **15**, pp. 1295–1313.

[41] Byrne, C. (2000) "Block-iterative interior point optimization methods for image reconstruction from limited data." *Inverse Problems* **16**, pp. 1405–1419.

[42] Byrne, C. (2001) "Bregman-Legendre multidistance projection algorithms for convex feasibility and optimization." in *Inherently Parallel Algorithms in Feasibility and Optimization and their Applications*, Butnariu, D., Censor, Y., and Reich, S., editors, pp. 87–100. Amsterdam: Elsevier Publ.,

[43] Byrne, C. (2001) "Likelihood maximization for list-mode emission tomographic image reconstruction." *IEEE Transactions on Medical Imaging* **20(10)**, pp. 1084–1092.

[44] Byrne, C. (2002) "Iterative oblique projection onto convex sets and the split feasibility problem." *Inverse Problems* **18**, pp. 441–453.

[45] Byrne, C. (2004) "A unified treatment of some iterative algorithms in signal processing and image reconstruction." *Inverse Problems* **20**, pp. 103–120.

[46] Byrne, C. (2008) *Applied Iterative Methods*, Wellesley, MA: AK Peters, Publ.

[47] Byrne, C. (2009) *A First Course in Optimization*, unpublished text available at my web site.

[48] Byrne, C. (2009) *Applied and Computational Linear Algebra: A First Course*, unpublished text available at my web site.

[49] Byrne, C., Brent, R., Feuillade, C., and DelBalzo, D (1990) "A stable data-adaptive method for matched-field array processing in acoustic waveguides."*Journal of the Acoustical Society of America* **87(6)**, pp. 2493–2502.

[50] Byrne, C. and Censor, Y. (2001) "Proximity function minimization using multiple Bregman projections, with applications to split feasibility and Kullback-Leibler distance minimization."*Annals of Operations Research* **105**, pp. 77–98.

[51] Byrne, C. and Fiddy, M. (1987) "Estimation of continuous object distributions from Fourier magnitude measurements."*JOSA A* **4**, pp. 412–417.

[52] Byrne, C. and Fiddy, M. (1988) "Images as power spectra; reconstruction as Wiener filter approximation."*Inverse Problems* **4**, pp. 399–409.

[53] Byrne, C. and Fitzgerald, R. (1979) "A unifying model for spectrum estimation."in *Proceedings of the RADC Workshop on Spectrum Estimation- October 1979*, Griffiss AFB, Rome, NY.

[54] Byrne, C. and Fitzgerald, R. (1982) "Reconstruction from partial information, with applications to tomography."*SIAM J. Applied Math.* **42(4)**, pp. 933–940.

[55] Byrne, C., Fitzgerald, R., Fiddy, M., Hall, T. and Darling, A. (1983) "Image restoration and resolution enhancement."*J. Opt. Soc. Amer.* **73**, pp. 1481–1487.

[56] Byrne, C. and Fitzgerald, R. (1984) "Spectral estimators that extend the maximum entropy and maximum likelihood methods."*SIAM J. Applied Math.* **44(2)**, pp. 425–442.

[57] Byrne, C., Frichter, G., and Feuillade, C. (1990) "Sector-focused stability methods for robust source localization in matched-field processing."*Journal of the Acoustical Society of America* **88(6)**, pp. 2843–2851.

[58] Byrne, C., Haughton, D., and Jiang, T. (1993) "High-resolution inversion of the discrete Poisson and binomial transformations."*Inverse Problems* **9**, pp. 39–56.

[59] Byrne, C., Levine, B.M., and Dainty, J.C. (1984) "Stable estimation of the probability density function of intensity from photon frequency counts."*JOSA Communications* **1(11)**, pp. 1132–1135.

[60] Byrne, C., and Steele, A. (1985) "Stable nonlinear methods for sensor array processing." *IEEE Transactions on Oceanic Engineering* **OE-10(3)**, pp. 255–259.

[61] Byrne, C., and Wells, D. (1983) "Limit of continuous and discrete finite-band Gerchberg iterative spectrum extrapolation." *Optics Letters* **8 (10)**, pp. 526–527.

[62] Byrne, C., and Wells, D. (1985) "Optimality of certain iterative and non-iterative data extrapolation procedures." *Journal of Mathematical Analysis and Applications* **111 (1)**, pp. 26–34.

[63] Candès, E., Romberg, J., and Tao, T. (2006) "Robust uncertainty principles: Exact signal reconstruction from highly incomplete frequency information." *IEEE Transactions on Information Theory*, **52(2)**, pp. 489–509.

[64] Candès, E., and Romberg, J. (2007) "Sparsity and incoherence in compressive sampling." *Inverse Problems*, **23(3)**, pp. 969–985.

[65] Candès, E., Wakin, M., and Boyd, S. (2007) "Enhancing sparsity by reweighted l_1 minimization." preprint available at http://www.acm.caltech.edu/ emmanuel/publications.html .

[66] Candy, J. (1988) *Signal Processing: The Modern Approach* New York: McGraw-Hill Publ.

[67] Capon, J. (1969) "High-resolution frequency-wavenumber spectrum analysis." *Proc. of the IEEE* **57**, pp. 1408–1418.

[68] Cederquist, J., Fienup, J., Wackerman, C., Robinson, S., and Kryskowski, D. (1989) "Wave-front phase estimation from Fourier intensity measurements." *Journal of the Optical Society of America A* **6(7)**, pp. 1020–1026.

[69] Censor, Y. (1981) "Row-action methods for huge and sparse systems and their applications." *SIAM Review*, **23**: 444–464.

[70] Censor, Y. and Elfving, T. (1994) "A multiprojection algorithm using Bregman projections in a product space." *Numerical Algorithms* **8**, pp. 221–239.

[71] Censor, Y., Eggermont, P.P.B., and Gordon, D. (1983) "Strong underrelaxation in Kaczmarz's method for inconsistent systems." *Numerische Mathematik* **41**, pp. 83–92.

[72] Censor, Y., Iusem, A.N. and Zenios, S.A. (1998) "An interior point method with Bregman functions for the variational inequality problem with paramonotone operators."*Mathematical Programming*, **81**, pp. 373–400.

[73] Censor, Y. and Segman, J. (1987) "On block-iterative maximization."*J. of Information and Optimization Sciences* **8**, pp. 275–291.

[74] Censor, Y. and Zenios, S.A. (1997) *Parallel Optimization: Theory, Algorithms and Applications*. New York: Oxford University Press.

[75] Chang, J.-H., Anderson, J.M.M., and Votaw, J.R. (2004) "Regularized image reconstruction algorithms for positron emission tomography."*IEEE Transactions on Medical Imaging* **23(9)**, pp. 1165–1175.

[76] Childers, D., editor (1978) *Modern Spectral Analysis*. New York:IEEE Press.

[77] Christensen, O. (2003) *An Introduction to Frames and Riesz Bases*. Boston: Birkhäuser.

[78] Chui, C. (1992) *An Introduction to Wavelets*. Boston: Academic Press.

[79] Chui, C. and Chen, G. (1991) *Kalman Filtering*, second edition. Berlin: Springer-Verlag.

[80] Cimmino, G. (1938) "Calcolo approssimato per soluzioni dei sistemi di equazioni lineari."*La Ricerca Scientifica XVI, Series II, Anno IX* **1**, pp. 326–333.

[81] Cohen, J. (2010) (editor) *The Best of The Best American Science Writing*, Harper-Collins Publ.

[82] Combettes, P. (1993) "The foundations of set theoretic estimation."*Proceedings of the IEEE* **81 (2)**, pp. 182–208.

[83] Combettes, P. (1996) "The convex feasibility problem in image recovery."*Advances in Imaging and Electron Physics* **95**, pp. 155–270.

[84] Combettes, P. (2000) "Fejér monotonicity in convex optimization."in *Encyclopedia of Optimization*, C.A. Floudas and P. M. Pardalos, editors, Boston: Kluwer Publ.

[85] Combettes, P., and Trussell, J. (1990) "Method of successive projections for finding a common point of sets in a metric space."*Journal of Optimization Theory and Applications* **67 (3)**, pp. 487–507.

[86] Cooley, J. and Tukey, J. (1965) "An algorithm for the machine calculation of complex Fourier series."*Math. Comp.*, **19**, pp. 297–301.

[87] Cox, H. (1973) "Resolving power and sensitivity to mismatch of optimum array processors." *Journal of the Acoustical Society of America* **54**, pp. 771–785.

[88] Csiszár, I. and Tusnády, G. (1984) "Information geometry and alternating minimization procedures." *Statistics and Decisions* **Supp. 1**, pp. 205–237.

[89] Csiszár, I. (1989) "A geometric interpretation of Darroch and Ratcliff's generalized iterative scaling." *The Annals of Statistics* **17 (3)**, pp. 1409–1413.

[90] Csiszár, I. (1991) "Why least squares and maximum entropy? An axiomatic approach to inference for linear inverse problems." *The Annals of Statistics* **19 (4)**, pp. 2032–2066.

[91] Dainty, J. C. and Fiddy, M. (1984) "The essential role of prior knowledge in phase retrieval." *Optica Acta* **31**, pp. 325–330.

[92] Darroch, J. and Ratcliff, D. (1972) "Generalized iterative scaling for log-linear models." *Annals of Mathematical Statistics* **43**, pp. 1470–1480.

[93] Daubechies, I. (1988) "Orthogonal bases of compactly supported wavelets." *Commun. Pure Appl. Math.* **41**, pp. 909–996.

[94] Daubechies, I. (1992) *Ten Lectures on Wavelets*. Philadelphia: Society for Industrial and Applied Mathematics.

[95] De Bruijn, N. (1967) "Uncertainty principles in Fourier analysis." in *Inequalties*, O. Shisha, editor, pp. 57–71, Boston: Academic Press.

[96] Dempster, A.P., Laird, N.M. and Rubin, D.B. (1977) "Maximum likelihood from incomplete data via the EM algorithm." *Journal of the Royal Statistical Society, Series B* **37**, pp. 1–38.

[97] De Pierro, A. (1995) "A modified expectation maximization algorithm for penalized likelihood estimation in emission tomography." *IEEE Transactions on Medical Imaging* **14**, pp. 132–137.

[98] De Pierro, A. and Iusem, A. (1990) "On the asymptotic behaviour of some alternate smoothing series expansion iterative methods." *Linear Algebra and its Applications* **130**, pp. 3–24.

[99] Dhanantwari, A., Stergiopoulos, S., and Iakovidis, I. (2001) "Correcting organ motion artifacts in x-ray CT medical imaging systems by adaptive processing. I. Theory." *Med. Phys.* **28(8)**, pp. 1562–1576.

[100] Dolidze, Z.O. (1982) "Solution of variational inequalities associated with a class of monotone maps." *Ekonomika i Matem. Metody* **18 (5)**, pp. 925–927 (in Russian).

[101] Donoho, D. (2006) "Compressed sampling" *IEEE Transactions on Information Theory*, **52 (4)**. (download preprints at http://www.stat. stanford.edu/ donoho/Reports).

[102] Duda, R., Hart, P., and Stork, D. (2001) *Pattern Classification*, Wiley.

[103] Dugundji, J. (1970) *Topology* Boston: Allyn and Bacon, Inc.

[104] Eddington, A. (1927) "The story of Algol." *Stars and Atoms*; reprinted in [21].

[105] Eggermont, P.P.B., Herman, G.T., and Lent, A. (1981) "Iterative algorithms for large partitioned linear systems, with applications to image reconstruction." *Linear Algebra and its Applications* **40**, pp. 37–67.

[106] Everitt, B. and Hand, D. (1981) *Finite Mixture Distributions* London: Chapman and Hall.

[107] Feuillade, C., DelBalzo, D., and Rowe, M. (1989) "Environmental mismatch in shallow-water matched-field processing: geoacoustic parameter variability." *Journal of the Acoustical Society of America* **85**, pp. 2354–2364.

[108] Feynman, R. (1985) *QED: The Strange Theory of Light and Matter*. Princeton, NJ: Princeton University Press.

[109] Feynman, R., Leighton, R., and Sands, M. (1963) *The Feynman Lectures on Physics, Vol. 1*. Boston: Addison-Wesley.

[110] Fiddy, M. (1983) "The phase retrieval problem." in *Inverse Optics*, SPIE Proceedings 413 (A.J. Devaney, editor), pp. 176–181.

[111] Fiddy, M. (2008) *private communication*.

[112] Fienup, J. (1979) "Space object imaging through the turbulent atmosphere." *Optical Engineering* **18**, pp. 529–534.

[113] Fienup, J. (1987) "Reconstruction of a complex-valued object from the modulus of its Fourier transform using a support constraint." *Journal of the Optical Society of America A* **4(1)**, pp. 118–123.

[114] Frieden, B. R. (1982) *Probability, Statistical Optics and Data Testing.* Berlin: Springer-Verlag.

[115] Gabor, D. (1946) "Theory of communication." *Journal of the IEE (London)* **93**, pp. 429–457.

[116] Gasquet, C. and Witomski, F. (1998) *Fourier Analysis and Applications.* Berlin: Springer-Verlag.

[117] Gelb, A., editor, (1974) *Applied Optimal Estimation*, written by the technical staff of The Analytic Sciences Corporation, MIT Press, Cambridge, MA.

[118] Geman, S., and Geman, D. (1984) "Stochastic relaxation, Gibbs distributions and the Bayesian restoration of images." *IEEE Transactions on Pattern Analysis and Machine Intelligence* **PAMI-6**, pp. 721–741.

[119] Gerchberg, R. W. (1974) "Super-restoration through error energy reduction." *Optica Acta* **21**, pp. 709–720.

[120] Golshtein, E., and Tretyakov, N. (1996) *Modified Lagrangians and Monotone Maps in Optimization.* New York: John Wiley and Sons, Inc.

[121] Gordon, R., Bender, R., and Herman, G.T. (1970) "Algebraic reconstruction techniques (ART) for three-dimensional electron microscopy and x-ray photography." *J. Theoret. Biol.* **29**, pp. 471–481.

[122] Green, P. (1990) "Bayesian reconstructions from emission tomography data using a modified EM algorithm." *IEEE Transactions on Medical Imaging* **9**, pp. 84–93.

[123] Groetsch, C. (1999) *Inverse Problems: Activities for Undergraduates.* The Mathematical Association of America.

[124] Gubin, L.G., Polyak, B.T. and Raik, E.V. (1967) "The method of projections for finding the common point of convex sets." *USSR Computational Mathematics and Mathematical Physics* **7**, pp. 1–24.

[125] Haacke, E., Brown, R., Thompson, M., and Venkatesan, R. (1999) *Magnetic Resonance Imaging.* New York: Wiley-Liss.

[126] Haykin, S. (1985) *Array Signal Processing.* Englewood Cliffs, NJ: Prentice-Hall.

[127] Hebert, T. and Leahy, R. (1989) "A generalized EM algorithm for 3-D Bayesian reconstruction from Poisson data using Gibbs priors." *IEEE Transactions on Medical Imaging* **8**, pp. 194–202.

[128] Herman, G.T. (ed.) (1979) "Image Reconstruction from Projections" , *Topics in Applied Physics, Vol. 32*, Springer-Verlag, Berlin.

[129] Herman, G.T. (1999) *private communication.*

[130] Herman, G. T. and Meyer, L. (1993) "Algebraic reconstruction techniques can be made computationally efficient." *IEEE Transactions on Medical Imaging* **12**, pp. 600–609.

[131] Higbee, S. (2004) *private communication.*

[132] Hildreth, C. (1957) "A quadratic programming procedure." *Naval Research Logistics Quarterly* **4**, pp. 79–85. Erratum, p. 361.

[133] Hinich, M. (1973) "Maximum likelihood signal processing for a vertical array." *Journal of the Acoustical Society of America* **54**, pp. 499–503.

[134] Hinich, M. (1979) "Maximum likelihood estimation of the position of a radiating source in a waveguide." *Journal of the Acoustical Society of America* **66**, pp. 480–483.

[135] Hoffman, K. (1962) *Banach Spaces of Analytic Functions* Englewood Cliffs, NJ: Prentice-Hall.

[136] Hogg, R. and Craig, A. (1978) *Introduction to Mathematical Statistics* MacMillan, New York.

[137] Holte, S., Schmidlin, P., Linden, A., Rosenqvist, G. and Eriksson, L. (1990) "Iterative image reconstruction for positron emission tomography: a study of convergence and quantitation problems." *IEEE Transactions on Nuclear Science* **37**, pp. 629–635.

[138] Hubbard, B. (1998) *The World According to Wavelets.* Natick, MA: A K Peters, Inc.

[139] Hudson, H.M. and Larkin, R.S. (1994) "Accelerated image reconstruction using ordered subsets of projection data." *IEEE Transactions on Medical Imaging* **13**, pp. 601–609.

[140] Huesman, R., Klein, G., Moses, W., Qi, J., Ruetter, B., and Virador, P. (2000) "List-mode maximum likelihood reconstruction applied to positron emission mammography (PEM) with irregular sampling." *IEEE Transactions on Medical Imaging* **19 (5)**, pp. 532–537.

[141] Hutton, B., Kyme, A., Lau, Y., Skerrett, D., and Fulton, R. (2002) "A hybrid 3-D reconstruction/registration algorithm for correction of head motion in emission tomography." *IEEE Transactions on Nuclear Science* **49 (1)**, pp. 188–194.

[142] Johnson, R. (1960) *Advanced Euclidean Geometry.* New York: Dover Publ.

[143] Johnson, C., Hendriks, E., Berezhnoy, I., Brevdo, E., Hughes, S., Daubechies, I., Li, J., Postma, E., and Wang, J. (2008) "Image Processing for Artist Identification." *IEEE Signal Processing Magazine,* **25(4)**, pp. 37–48.

[144] Kaczmarz, S. (1937) "Angenäherte Auflösung von Systemen linearer Gleichungen."*Bulletin de l'Academie Polonaise des Sciences et Lettres* **A35**, pp. 355–357.

[145] Kaiser, G. (1994) *A Friendly Guide to Wavelets.* Boston: Birkhäuser.

[146] Kak, A., and Slaney, M. (2001) "Principles of Computerized Tomographic Imaging" , SIAM, Philadelphia, PA.

[147] Kalman, R. (1960) "A new approach to linear filtering and prediction problems."*Trans. ASME, J. Basic Eng.* **82**, pp. 35–45.

[148] Katznelson, Y. (1983) *An Introduction to Harmonic Analysis.* New York: John Wiley and Sons, Inc.

[149] Kheifets, A. (2004) *private communication.*

[150] Körner, T. (1988) *Fourier Analysis.* Cambridge, UK: Cambridge University Press.

[151] Körner, T. (1996) *The Pleasures of Counting.* Cambridge, UK: Cambridge University Press.

[152] Kullback, S. and Leibler, R. (1951) "On information and sufficiency."*Annals of Mathematical Statistics* **22**, pp. 79–86.

[153] Landweber, L. (1951) "An iterative formula for Fredholm integral equations of the first kind."*Amer. J. of Math.* **73**, pp. 615–624.

[154] Lane, R. (1987) "Recovery of complex images from Fourier magnitude."*Optics Communications* **63(1)**, pp. 6–10.

[155] Lange, K. and Carson, R. (1984) "EM reconstruction algorithms for emission and transmission tomography."*Journal of Computer Assisted Tomography* **8**, pp. 306–316.

[156] Lange, K., Bahn, M. and Little, R. (1987) "A theoretical study of some maximum likelihood algorithms for emission and transmission tomography."*IEEE Trans. Med. Imag.* **MI-6(2)**, pp. 106–114.

[157] Leahy, R., Hebert, T., and Lee, R. (1989) "Applications of Markov random field models in medical imaging."in *Proceedings of the Conference on Information Processing in Medical Imaging* Lawrence-Berkeley Laboratory, Berkeley, CA.

[158] Leahy, R. and Byrne, C. (2000) "Guest editorial: Recent development in iterative image reconstruction for PET and SPECT."*IEEE Trans. Med. Imag.* **19**, pp. 257–260.

[159] Lent, A. (1998) *private communication.*

[160] Levitan, E. and Herman, G. (1987) "A maximum *a posteriori* probability expectation maximization algorithm for image reconstruction in emission tomography."*IEEE Transactions on Medical Imaging* **6**, pp. 185–192.

[161] Liao, C.-W., Fiddy, M., and Byrne, C. (1997) "Imaging from the zero locations of far-field intensity data."*Journal of the Optical Society of America -A* **14 (12)**, pp. 3155–3161.

[162] Lindberg, D. (1992) *The Beginnings of Western Science*, University of Chicago Press.

[163] Luenberger, D. (1969) *Optimization by Vector Space Methods.* New York: John Wiley and Sons, Inc.

[164] Lustig, M., Donoho, D., and Pauly, J. (2008) *Magnetic Resonance in Medicine*, to appear.

[165] Magness, T., and McQuire, J. (1962) "Comparison of least squares and minimum variance estimates of regression parameters."*Annals of Mathematical Statistics* **33**, pp. 462–470.

[166] Mallat, S.G. (1989) "A theory of multiresolution signal decomposition: The wavelet representation."*IEEE Transactions on Pattern Analysis and Machine Intelligence* **PAMI-11**, pp. 674–693.

[167] Mann, W. (1953) "Mean value methods in iteration."*Proc. Amer. Math. Soc.* **4**, pp. 506–510.

[168] McClellan, J., Schafer, R., and Yoder, M. (2003) *Signal Processing First.* Upper Saddle River, New Jersey: Prentice Hall, Inc.

[169] McLachlan, G.J. and Krishnan, T. (1997) *The EM Algorithm and Extensions.* New York: John Wiley and Sons, Inc.

[170] Meidunas, E. (2001) *Re-scaled Block Iterative Expectation Maximization Maximum Likelihood (RBI-EMML) Abundance Estimation and Sub-pixel Material Identification in Hyperspectral Imagery*, MS thesis, Department of Electrical Engineering, University of Massachusetts Lowell.

[171] Meyer, Y. (1993) *Wavelets: Algorithms and Applications*. Philadelphia, PA: SIAM Publ.

[172] Mooney, J., Vickers, V., An, M., and Brodzik, A. (1997) "High-throughput hyperspectral infrared camera." *Journal of the Optical Society of America, A* **14 (11)**, pp. 2951–2961.

[173] Motzkin, T. and Schoenberg, I. (1954) "The relaxation method for linear inequalities." *Canadian Journal of Mathematics* **6**, pp. 393–404.

[174] Narayanan, M., Byrne, C. and King, M. (2001) "An interior point iterative maximum-likelihood reconstruction algorithm incorporating upper and lower bounds with application to SPECT transmission imaging." *IEEE Transactions on Medical Imaging* **TMI-20 (4)**, pp. 342–353.

[175] Nash, S. and Sofer, A. (1996) *Linear and Nonlinear Programming*. New York: McGraw-Hill.

[176] Natterer, F. (1986) *Mathematics of Computed Tomography*. New York: John Wiley and Sons, Inc.

[177] Natterer, F., and Wübbeling, F. (2001) *Mathematical Methods in Image Reconstruction*. Philadelphia, PA: SIAM Publ.

[178] Nelson, R. (2001) "Derivation of the missing cone." unpublished notes.

[179] Oppenheim, A. and Schafer, R. (1975) *Digital Signal Processing*. Englewood Cliffs, NJ: Prentice-Hall.

[180] Papoulis, A. (1975) "A new algorithm in spectral analysis and band-limited extrapolation." *IEEE Transactions on Circuits and Systems* **22**, pp. 735–742.

[181] Papoulis, A. (1977) *Signal Analysis*. New York: McGraw-Hill.

[182] Parra, L. and Barrett, H. (1998) "List-mode likelihood: EM algorithm and image quality estimation demonstrated on 2-D PET." *IEEE Transactions on Medical Imaging* **17**, pp. 228–235.

[183] Paulraj, A., Roy, R., and Kailath, T. (1986) "A subspace rotation approach to signal parameter estimation." *Proceedings of the IEEE* **74**, pp. 1044–1045.

[184] Peressini, A., Sullivan, F., and Uhl, J. (1988) *The Mathematics of Nonlinear Programming*. Berlin: Springer-Verlag.

[185] Pelagotti, A., Del Mastio, A., De Rosa, A., Piva, A. (2008) "Multispectral imaging of paintings." *IEEE Signal Processing Magazine*, **25(4)**, pp. 27–36.

[186] Pisarenko, V. (1973) "The retrieval of harmonics from a covariance function." *Geoph. J. R. Astrom. Soc.*, **30**.

[187] Pižurica, A., Philips, W., Lemahieu, I., and Acheroy, M. (2003) "A versatile wavelet domain noise filtration technique for medical imaging." *IEEE Transactions on Medical Imaging: Special Issue on Wavelets in Medical Imaging* **22**, pp. 323–331.

[188] Poggio, T. and Smale, S. (2003) "The mathematics of learning: dealing with data." *Notices of the American Mathematical Society* **50 (5)**, pp. 537–544.

[189] Priestley, M. B. (1981) *Spectral Analysis and Time Series*. Boston: Academic Press.

[190] Prony, G.R.B. (1795) "Essai expérimental et analytique sur les lois de la dilatabilité de fluides élastiques et sur celles de la force expansion de la vapeur de l'alcool, à différentes températures." *Journal de l'Ecole Polytechnique* (Paris) **1(2)**, pp. 24–76.

[191] Qian, H. (1990) "Inverse Poisson transformation and shot noise filtering." *Rev. Sci. Instrum.* **61**, pp. 2088–2091.

[192] Ribés, A., Pillay, R., Schmitt, F., and Lahanier,C. (2008) "Studying that smile." *IEEE Signal Processing Magazine*, **25(4)**, pp. 14–26.

[193] Rockafellar, R. (1970) *Convex Analysis*. Princeton, NJ: Princeton University Press.

[194] Rockmore, A., and Macovski, A. (1976) "A maximum likelihood approach to emission image reconstruction from projections." *IEEE Transactions on Nuclear Science*, **NS-23**, pp. 1428–1432.

[195] Schmidlin, P. (1972) "Iterative separation of sections in tomographic scintigrams." *Nucl. Med.* **15(1)**.

[196] Schmidt, R. (1981) *A Signal Subspace Approach to Multiple Emitter Location and Spectral Estimation*. PhD thesis, Stanford University.

[197] Schultz, L., Blanpied, G., Borozdin, K., *et al.* (2007) "Statistical reconstruction for cosmic ray muon tomography." *IEEE Transactions on Image Processing*, **16(8)**, pp. 1985–1993.

[198] Schuster, A. (1898) "On the investigation of hidden periodicities with application to a supposed 26 day period of meteorological phenomena." *Terrestrial Magnetism* **3**, pp. 13–41.

[199] Shang, E. (1985) "Source depth estimation in waveguides." *Journal of the Acoustical Society of America* **77**, pp. 1413–1418.

[200] Shang, E. (1985) "Passive harmonic source ranging in waveguides by using mode filter." *Journal of the Acoustical Society of America* **78**, pp. 172–175.

[201] Shang, E., Wang, H., and Huang, Z. (1988) "Waveguide characterization and source localization in shallow water waveguides using Prony's method." *Journal of the Acoustical Society of America* **83**, pp. 103–106.

[202] Shaw, C. (2010) "Dimensions in medical imaging: the more the better?" *Proceedings of the IEEE*, **98(1)**, pp. 2–5.

[203] Shepp, L., and Vardi, Y. (1982) "Maximum likelihood reconstruction for emission tomography." *IEEE Transactions on Medical Imaging*, **MI-1**, pp. 113–122.

[204] Shieh, M., Byrne, C., Testorf, M., and Fiddy, M. (2006) "Iterative image reconstruction using prior knowledge." *Journal of the Optical Society of America, A*, **23(6)**, pp. 1292–1300.

[205] Smith, C. Ray and Grandy, W.T., editors (1985) *Maximum-Entropy and Bayesian Methods in Inverse Problems*. Dordrecht: Reidel Publ.

[206] Smith, C. Ray and Erickson, G., editors (1987) *Maximum-Entropy and Bayesian Spectral Analysis and Estimation Problems*. Dordrecht: Reidel Publ.

[207] Sondhi, M. (2006) "The History of Echo Cancellation." *IEEE Signal Processing Magazine*, September 2006, pp. 95–102.

[208] Sondhi, M., Morgan, D., and Hall, J. (1995) "Stereophonic acoustic echo cancellation- an overview of the fundamental problem." *IEEE Signal Processing Letters*, **2(8)**, pp. 148–151.

[209] Stark, H., and Woods, J. (2002) *Probability and Random Processes, with Applications to Signal Processing*. Upper Saddle River, NJ: Prentice-Hall.

[210] Stark, H. and Yang, Y. (1998) *Vector Space Projections: A Numerical Approach to Signal and Image Processing, Neural Nets and Optics.* New York: John Wiley and Sons, Inc.

[211] Strang, G. (1980) *Linear Algebra and its Applications.* New York: Academic Press.

[212] Strang, G. and Nguyen, T. (1997) *Wavelets and Filter Banks.* Wellesley, MA: Wellesley-Cambridge Press.

[213] Tanabe, K. (1971) "Projection method for solving a singular system of linear equations and its applications."*Numer. Math.* **17**, pp. 203–214.

[214] Therrien, C. (1992) *Discrete Random Signals and Statistical Signal Processing.* Englewood Cliffs, NJ: Prentice-Hall.

[215] Thévenaz, P., Blu, T., and Unser, M. (2000) "Interpolation revisited." *IEEE Transactions on Medical Imaging*, **19**, pp.739–758.

[216] Tindle, C., Guthrie, K., Bold, G., Johns, M., Jones, D., Dixon, K., and Birdsall, T. (1978) "Measurements of the frequency dependence of normal modes."*Journal of the Acoustical Society of America* **64**, pp. 1178–1185.

[217] Tolstoy, A. (1993) *Matched Field Processing for Underwater Acoustics.* Signapore: World Scientific.

[218] Twomey, S. (1996) *Introduction to the Mathematics of Inversion in Remote Sensing and Indirect Measurement.* New York: Dover Publ.

[219] Unser, M. (1999) "Splines: A perfect fit for signal and image processing." *IEEE Signal Processing Magazine*, **16**, pp. 22–38.

[220] Van Trees, H. (1968) *Detection, Estimation and Modulation Theory.* New York: John Wiley and Sons, Inc.

[221] Vardi, Y., Shepp, L.A. and Kaufman, L. (1985) "A statistical model for positron emission tomography."*Journal of the American Statistical Association* **80**, pp. 8–20.

[222] Walnut, D. (2002) *An Introduction to Wavelets.* Boston: Birkhäuser.

[223] Wernick, M. and Aarsvold, J., editors (2004) *Emission Tomography: The Fundamentals of PET and SPECT.* San Diego: Elsevier Academic Press.

[224] Widrow, B. and Stearns, S. (1985) *Adaptive Signal Processing.* Englewood Cliffs, NJ: Prentice-Hall.

[225] Wiener, N. (1949) *Time Series.* Cambridge, MA: MIT Press.

[226] Wright, W., Pridham, R., and Kay, S. (1981) "Digital signal processing for sonar." *Proc. IEEE* **69**, pp. 1451–1506.

[227] Yang, T.C. (1987) "A method of range and depth estimation by modal decomposition." *Journal of the Acoustical Society of America* **82**, pp. 1736–1745.

[228] Yin, W., and Zhang, Y. (2008) "Extracting salient features from less data via l_1-minimization." *SIAG/OPT Views-and-News,* **19(1)**, pp. 11–19.

[229] Youla, D. (1978) "Generalized image restoration by the method of alternating projections." *IEEE Transactions on Circuits and Systems* **CAS-25 (9)**, pp. 694–702.

[230] Youla, D.C. (1987) "Mathematical theory of image restoration by the method of convex projections." in *Image Recovery: Theory and Applications*, pp. 29–78, Stark, H., editor (1987) Orlando FL: Academic Press.

[231] Young, R. (1980) *An Introduction to Nonharmonic Fourier Analysis.* Boston: Academic Press.

[232] Zeidler, E. (1990) *Nonlinear Functional Analysis and its Applications: II/B- Nonlinear Monotone Operators.* Berlin: Springer-Verlag.

Index